



HAL
open science

Hydrogen and lactic acid synthesis through capnophilic lactic fermentation by *Thermotoga neapolitana*

Nirakar Pradhan

► **To cite this version:**

Nirakar Pradhan. Hydrogen and lactic acid synthesis through capnophilic lactic fermentation by *Thermotoga neapolitana*. Materials. Université Paris-Est, 2016. English. NNT : 2016PESC1145 . tel-01557975

HAL Id: tel-01557975

<https://theses.hal.science/tel-01557975>

Submitted on 6 Jul 2017

HAL is a multi-disciplinary open access archive for the deposit and dissemination of scientific research documents, whether they are published or not. The documents may come from teaching and research institutions in France or abroad, or from public or private research centers.

L'archive ouverte pluridisciplinaire **HAL**, est destinée au dépôt et à la diffusion de documents scientifiques de niveau recherche, publiés ou non, émanant des établissements d'enseignement et de recherche français ou étrangers, des laboratoires publics ou privés.

**Hydrogen and lactic acid synthesis
through capnophilic lactic fermentation
by *Thermotoga neapolitana***

Joint PhD degree in Environmental Technology



Docteur de l'Université Paris-Est

Spécialité: Science et Technique de l'Environnement



Dottore di Ricerca in Tecnologie Ambientali



Degree of Doctor in Environmental Technology

Thèse – Tesi di Dottorato – PhD thesis

Nirakar PRADHAN

**Hydrogen and lactic acid synthesis through capnophilic lactic
fermentation by *Thermotoga neapolitana***

To be defended on 15th December 2016

In front of the PhD committee

Prof. Roberto DE PHILIPPIS	Reviewer
Prof. Katerina STAMATELATOU	Reviewer
Prof. Eric D. VAN HULLEBUSCH	Examiner
Prof. Giovanni ESPOSITO	Promoter
Prof. Piet N. L. LENS	Co-promoter
Prof. Michel MADON	Co-promoter
Dr. Giuliana D'IPPOLITO	Co-supervisor
Dr. Antonio PANICO	Co-supervisor



Erasmus Mundus Joint Doctorate program in Environmental Technologies for Contaminated Solids, Soils and Sediments (ETeCoS³)

Thesis committee

Thesis Promoter

Giovanni ESPOSITO, Professor
Department of Civil and Mechanical Engineering
University of Cassino and Southern Lazio
Cassino, Italy

Thesis Co-promoters

Piet N. L. LENS, Professor
Department of Environmental Engineering and Water Technology
UNESCO-IHE Institute for Water Education
Delft, The Netherlands

Michel MADON, Professor
Laboratoire Géomatériaux et Environnement
Université Paris-est
Paris, France

Thesis Co-supervisors

Giuliana D'IPPOLITO, PhD
Institute of Biomolecular Chemistry
Italian National Council of Research, Napoli, Italy

Angelo FONTANA, PhD
Institute of Biomolecular Chemistry
Italian National Council of Research, Napoli, Italy

Antonio PANICO, PhD
Department of Civil, Architectural and Environmental Engineering
University of Naples Federico II, Napoli, Italy

Table of Contents

Thesis committee	i
List of figures	vi
List of tables	xi
Acknowledgements	xiii
Summary	xv
Résumé.....	xvii
Sommario	xix
Samenvattig.....	xxi
Chapter 1: General introduction.....	2
1.1 Background of the study.....	2
1.2 Scope of the study.....	3
1.3 Structure of the thesis	4
References	7
Chapter 2: Literature review	10
Abstract	10
2.1 Introduction	11
2.2 Taxonomy of <i>Thermotoga neapolitana</i>	12
2.3 Dark fermentation pathway in <i>T. neapolitana</i>	13
2.4 Production of lactic acid and H ₂ by capnophilic lactic fermentation.....	16
2.5 Substrate metabolism by <i>T. neapolitana</i>	18
2.6 Systems integration.....	27
2.7 Bioreactor configuration.....	29
2.8 Operating conditions and kinetics of <i>T. neapolitana</i> fermentation.....	32
2.9 Conclusions	36
References	37
Chapter 3: Strain characterization	48
Abstract	48
3.1 Introduction	49
3.2 Materials and Methods	50

3.3	Results	53
3.4	Discussion.....	57
3.5	Conclusions	59
	References.....	59
	Chapter 4: Culture parameter optimization.....	64
	Abstract	64
4.1	Introduction	65
4.2	Materials and methods.....	66
4.3	Results	68
4.4	Discussion.....	75
4.5	Conclusions	78
	References.....	78
	Chapter 5: Dark fermentation model.....	82
	Abstract	82
5.1	Introduction	83
5.2	Materials and methods.....	85
5.3	Mathematical modeling	87
5.4	Results and discussion	92
5.5	Conclusions	100
	References.....	100
	Chapter 6: Capnophilic lactic fermentation model.....	104
	Abstract	104
6.1	Introduction	105
6.2	Materials and methods.....	106
6.3	Mathematical model design.....	107
6.4	Results and discussion.....	114
6.5	Conclusions	123
	References.....	123
	Chapter 7: Starch fermentation model.....	127
	Abstract	127
7.1	Introduction	128
7.2	Materials and methods.....	129
7.3	Results	133
7.4	Discussion.....	141

7.5	Conclusions	144
	References	144
7.6	System integration for downstream processing	148
	References	149
Chapter 8: Lactic acid recovery		151
	Abstract	151
8.1	Introduction	152
8.2	Materials and methods.....	154
8.3	Results	158
8.4	Discussion.....	166
8.5	Conclusions	172
	References	173
Chapter 9: General discussion and recommendations.....		178
9.1	General overview.....	178
9.2	Microbial fermentation: wet-lab experiments.....	179
9.3	Process modeling for <i>T. neapolitana</i> fermentation.....	182
9.4	Downstream processing of lactic acid	185
9.5	Outlook and recommendations for future work.....	187
	References	190
Curriculum Vitae.....		194

List of figures

Fig. 1. 1 Schematic outline of the thesis.....	5
Fig. 2. 1 Streamlined biochemical pathway for fermentative H ₂ production, adapted from Reference (Dipasquale et al., 2014), water is omitted for simplicity.	14
Fig. 2. 2 Proposed model of capnophilic lactic fermentation, adapted from (d'Ippolito et al., 2014), water is omitted for simplicity.....	17
Fig. 3. 1 Molecular comparison of <i>T. neapolitana</i> WT4359 (parent strain), TN-CMut (laboratory strain) and <i>T. neapolitana</i> 5068 (reference strain). (A) RiboPrint pattern for microbial characterization system of mutant and wild-type strains; (B) Cluster analysis of MALDI-TOF MS spectra. In the dendrogram, relative distance is displayed as arbitrary units. Zero indicates complete similarity and 1000 indicates the highest dissimilarity.....	54
Fig. 3. 2 Effect of temperature on cultures of TN-CMut and WT4359 supplemented with 28 mM glucose (5 g/L) and maintained under CLF condition for 72 h.	55
Fig. 3. 3 Effect of the salinity level (0–60 g/L) on cultures of TN-CMut and WT4359 supplemented with 28 mM glucose (5 g/L) and maintained under CLF condition at 80 °C for 72 h.	56
Fig. 3. 4 Fermentation of different substrates by cultures of TN-CMut and WT4359 under CLF condition at 80 °C for 72 h. Both strain cultures were supplemented with 33 mM of arabinose or xylose and 28 mM of fructose or lactose.	57
Fig. 3. 5 Schematic representation of the capnophilic lactic fermentation pathway with the catabolic (red) and biosynthetic (blue) branches.	58
Fig. 4. 1 Effect of salinity level on (a) the H ₂ production (mL/L culture) and (b) the biomass growth via the CLF pathway after 72 h of incubation ($n = 3$, error bars = standard error of mean).....	70
Fig. 4. 2 Effect of buffering agent on (a) the H ₂ production (mL/L culture) and (b) the biomass growth via CLF pathway after 72 h of incubation ($n = 3$, error bars = standard error of mean).....	71

Fig. 4. 3 Effect of carbon source on (a) the H ₂ production (mL/L culture) and (b) the biomass growth under CLF condition after 72 h of incubation ($n = 3$, error bars = standard error of mean).....	73
Fig. 4. 4 Effect of culture parameter optimization (serum bottles: SB) and process scale-up (CSTR) tests on (a) the H ₂ production (mL/L culture) and (b) the biomass growth via the CLF pathway after 72 h of incubation ($n = 3$, error bars = standard error of mean).....	74
Fig. 5. 1 Simplified biochemical pathway for fermentative hydrogen production by <i>T. neapolitana</i> (adapted and modified from Dipasquale et al. (2014)). Dashed arrow indicates the feedback cycle triggered by CO ₂ during CLF.....	87
Fig. 5. 2 Biomass growth, substrate consumption and product formation by <i>T. neapolitana</i> from tests A and B: (a) biomass growth, (b) residual glucose, (c) H ₂ yield, (d) acetate production, (e) lactate production and (f) pH (room temperature).	93
Fig. 5. 3 Model simulation for biomass growth and product formation by <i>T. neapolitana</i> for batch experiment A: predicted and measured results for (a) biomass growth (cell dry weight), (b) residual glucose, (c) H ₂ yield, (d) acetate production, (e) lactate production and (f) predicted CO ₂ production.	95
Fig. 5. 4 Absolute (or local) sensitivities of kinetic parameters during the fermentation time for (a) biomass growth, (b) substrate consumption, (c) H ₂ yield, (d) acetate production, (e) lactate production and (f) CO ₂ production.....	96
Fig. 5. 5 Model calibration for simultaneous changes in biomass yield coefficient (Y) and endogenous decay rate (k_d) with respect to ME for (a) substrate consumption (S) and (b) H ₂ production (H ₂); IA for (c) S and (d) H ₂ ; and RMSE for (e) S and (f) H ₂	97
Fig. 5. 6 Model validation for biomass growth and product formation by <i>T. neapolitana</i> from batch experiment C: predicted and measured data for (a) biomass growth (cell dry weight), (b) residual glucose, (c) H ₂ yield, (d) acetate production, (e) lactate production and (f) CO ₂ production.....	99

Fig. 6. 1 Simplified CLF-based biochemical pathway for fermentative H ₂ and lactic acid production by <i>T. neapolitana</i>	109
Fig. 6. 2 Simplified model simulation flow chart for sensitivity analysis, calibration and validation.	111
Fig. 6. 3 Model simulation for biomass growth, substrate consumption and products formation by <i>T. neapolitana</i> : predicted and measured results for (a) biomass growth in terms of cell dry weight, (b) residual glucose, (c) H ₂ yield, (d) acetate production, (e) lactate production and (f) CO ₂ production (Pradhan et al., 2016), error bars = standard error of mean (n = 3).	116
Fig. 6. 4 Absolute (or local) sensitivities of growth kinetic parameters during the simulation time for (a) biomass growth (X), (b) residual glucose (S), (c) H ₂ yield, (d) acetate (Ac), (e) lactate (Lac) and (f) CO ₂ production.....	117
Fig. 6. 5 Model calibration for simultaneous changes in biomass yield coefficient (Y) and endogenous decay rate (k_d) with respect to ME for (a) Acetate (Ac) production and (b) Lactate (Lac) production; IA for (c) Ac and (d) Lac; and RMSE for (e) Ac and (f) Lac.	119
Fig. 6. 6 Model validation for substrate consumption, biomass growth and products formation by <i>T. neapolitana</i> : predicted and measured data for (a) biomass growth in terms of cell dry weight, (b) residual glucose, (c) H ₂ yield, (d) acetate, (e) lactate and (f) CO ₂ production, error bars = standard error of mean (n = 3).	120
Fig. 6. 7 Model cross validation for substrate consumption, biomass growth and products formation by <i>T. neapolitana</i> using arabinose as substrate: predicted and measured data for (a) biomass growth in terms of cell dry weight, (b) residual arabinose, (c) H ₂ yield, (d) acetate, (e) lactate and (f) CO ₂ production, error bars = standard error of mean (n = 2).	121
Fig. 7. 1 CLF-based model simulation for catabolism and bioenergetics of the potato starch fermentation by <i>T. neapolitana</i> : predicted and measured results for (a) biomass growth in terms of cell dry weight, (b) residual sugar, (c) H ₂ yield, (d) acetic acid production, (e) lactic acid production and (f) ΔG^r values calculated from the measured concentrations of products and reactants. Error bars = standard error of mean (n = 4).	138

Fig. 7. 2 CLF-based model simulation for the catabolism and bioenergetics of wheat starch fermentation by *T. neapolitana*: predicted and measured results for (a) biomass growth in terms of cell dry weight, (b) residual sugar, (c) H₂ yield, (d) acetic acid production, (e) lactic acid production and (f) ΔG^r values calculated from measured concentrations of products and reactants. Error bars = standard error of mean (n = 2). 139

Fig. 7. 3 CLF-based model simulation for the catabolism and bioenergetics of potato starch fermentation supplemented with 35 g/L NaCl by *T. neapolitana*: predicted and measured results for (a) biomass growth in terms of cell dry weight, (b) residual sugar, (c) H₂ yield, (d) acetic acid production, (e) lactic acid production and (f) ΔG^r values calculated from measured concentrations of products and reactants. Error bars = standard error of mean (n = 2). 140

Fig. 8. 1 Effect of lactic acid adsorption onto GAC, RLX425 and AMB400 at 303.15 K. (a) contact time (0-24 h) with 4.5 g/L of lactic acid in the bulk solution without initial pH correction and an adsorbent dose of 10% (w/v), (b) different initial pH (2.0-6.5) with 4.5 g/L of lactic acid in the bulk solution and an adsorbent dose of 10% (w/v), (c) various adsorbent doses (5-30%) with 4.5 g/L of lactic acid in the bulk solution accompanied by initial pH corrections and (d) different initial lactic acid concentrations (1.5-36.3 g/L) accompanied by initial pH correction with an adsorbent dose of 10% (w/v). 160

Fig. 8. 2 (a) Effect of temperature (303.15-353.15 K) on the adsorption capacities of the adsorbents with 4.5 g/L of lactic acid in the bulk solution accompanied by initial pH corrections and 10% (w/v) adsorbent dose and (b) plot of $\ln K_L$ versus $1/T$ at a lactic acid concentration of 4.5 g/L in the temperature range of 303.15-353.15 K. 162

Fig. 8. 3 Linear fits of the (a) Langmuir, (b) Freundlich and (c) Temkin isotherm models for GAC and RLX425 at initial pH 2.0 and AMB400 at initial pH 5.0 with 4.5 g/L of lactic acid in the bulk solution at 303.15 K and an adsorbent dose of 10% (w/v). 164

Fig. 8. 4 Adsorption kinetics of lactic acid by the three adsorbents GAC, RLX425 and AMB400 at 303.15 K. (a) Pseudo-first order, (b) pseudo-second order and (c)

Elovich kinetic models at an initial lactic acid concentration of 4.5 g/L and an adsorbent dose of 10% (w/v).	165
Fig. 9. 1 Overview of the thesis structure and the aspects of CLF-based fermentation in a CSTR system.	179
Fig. 9. 2 Overview of the results of this thesis concerning <i>T. neapolitana</i> strain characterization and culture parameters optimization under CLF conditions.....	182
Fig. 9. 3 Overview of the results of this thesis concerning DF and CLF-based model for <i>T. neapolitana</i> fermentation.	185
Fig. 9. 4 Overview of the results of this thesis concerning lactic acid recovery from a model <i>T. neapolitana</i> fermentation broth by adsorption.	186

List of tables

Table 2. 1 H ₂ production from various substrates by hyperthermophilic eubacterium <i>T. neapolitana</i> . B = batch; FB = fed-batch; Ac = Acetic acid; Lac = Lactic acid; EtOH = Ethanol.	21
Table 2. 2 Continuous and fed-batch operation in CSTRs for <i>T. neapolitana</i>	31
Table 4. 1 Effect of varying salinity level (0–35 g/L NaCl) on H ₂ and organic acids production via the CLF pathway in tests supplemented with 28 mM glucose (72 h of incubation).....	69
Table 4. 2 Effect of the buffering agent (0.01 M) on H ₂ and organic acids production via CLF pathway in the tests supplemented with 28 mM glucose (72 h of incubation).	70
Table 4. 3 Effect of the different carbon source (5 g/L) on H ₂ and organic acids production under CLF conditions.....	72
Table 4. 4 Substrate consumption and major fermentation products via the CLF pathway with 35 g/L NaCl and 0.01 M phosphate buffer after 72 h of fermentation in serum bottles and 24 h of fermentation in a CSTR.	74
Table 5. 1 Kinetic expressions used for the simulation of the experimental data according to ADM1 model.....	88
Table 5. 2 Results from batch fermentation tests by <i>T. neapolitana</i> under CO ₂ or N ₂ atmosphere.....	93
Table 5. 3 Regression parameters for model validation.	99
Table 6. 1 Main possible metabolic reactions of glucose and xylose degradation via DF and CLF-based pathways in CSTR system.	108
Table 6. 2 The DF and CLF-based model pathway stoichiometries with glucose as the substrate.	109
Table 6. 3 The kinetic expressions included in the CLF-based model.	110
Table 6. 4 Experimental results of glucose and arabinose fermentation by <i>T. neapolitana</i> under CLF conditions.	115

Table 6. 5 Values of regression parameters for model simulation, validation and cross validation.	121
Table 7. 1 Metabolic reactions and Gibbs free energies for the key reactions under CLF conditions.	131
Table 7. 2 Effect of salinity level on batch fermentation of potato starch by <i>T. neapolitana</i> under CLF conditions.	134
Table 7. 3 Potato and wheat starch fermentation under CLF conditions by <i>T. neapolitana</i> in a CSTR system.	135
Table 7. 4 Stoichiometric yields of main metabolites after 48 h of starch fermentation by <i>T. neapolitana</i> under CLF conditions.	136
Table 7. 5 CLF-based model fitting parameters of the starch fermentation.	140
Table 7. 6 Comparative analysis of the present experimental results with the reported data on fermentative H ₂ and organic acids production under N ₂ and CO ₂ (~ 14 mM dissolved CO ₂) enriched atmosphere by <i>T. neapolitana</i> in a CSTR system supplemented with 5 g/L of carbon source.	142
Table 8. 1 List of non-linear and linear forms of adsorption isotherm model equations.	157
Table 8. 2 List of differential and linear forms of adsorption kinetic model equations.	158
Table 8. 3 Gibbs free energy for adsorption of lactic acid onto GAC, RLX425 and AMB400 at temperature ranges from 303.15 to 353.15 K ($\Delta H^0 = -16.7$ kJ/mol and $\Delta S^0 = -0.02$ kJ/ (mol K) for GAC; $\Delta H^0 = -19.9$ kJ/mol and $\Delta S^0 = -0.05$ kJ/ (mol K) for RLX425; $\Delta H^0 = 2.0$ kJ/mol and $\Delta S^0 = 0.02$ kJ/ (mol K) for AMB400)...	162
Table 8. 4 The Langmuir, Freundlich and Temkin isotherm model parameters obtained from the linear fitting for the three adsorbents (GAC, RLX425 and AMB400)..	164
Table 8. 5 Pseudo-second order model kinetic parameters for the three adsorbents (GAC, RLX452 and AMB400) at 303.15 K and with 4.5 g/L of lactic acid in the bulk solution.	165
Table 8. 6 Lactic acid recovery from the model fermentation broths using GAC, RLX425 and AMB400 in batch adsorption experiments (adsorbent dose 10% w/v).	168

Acknowledgements

First, I would like to express my gratitude to the European Union for supporting financially (grant agreement FPA No.: 2010-0009) to carry out the research work under the Erasmus Mundus Joint Doctorate program ETeCoS³ (Environmental Technologies for Contaminated Solids, Soils and Sediments). I would also like to thank the Italian Ministry of Education, University and Research (MIUR) for supporting through the Sfruttamento Integrato di Biomasse Algali in Filiera Energetica di Qualita (SIBAFEQ) project (grant agreement no.: PON01_02740) and by the CNR through the project Energia da FONti Rinnovabili (EFOR) to carry out the laboratory work. I would also like to thank all the ETeCoS³ PhD training board members and collaborating research institutes for giving me this wonderful opportunity.

There are many people I have to acknowledge and thank for the invaluable contribution in this research work over the last three years. It has been an honour and privilege to be working with each one of them.

I would like to extend gratefulness to my thesis promoter Prof. Giovanni Esposito for always believing in me and giving me complete freedom to carry the research work. I would like to express my sincere gratitude to Dr. Antonio Panico for his able guidance, constant support and cooperation. I would also like to thank both Prof. Giovanni Esposito and Dr. Antonio Panico for guiding me to develop and implement the mathematical model. I would like to express my sincere gratitude to Prof. Piet N. L. Lens for always encouraging me to think differently from a scientific point of view and privileged to have received his scientific suggestions and critical inputs throughout my PhD years. This research work would not have been possible without their able guidance and support.

I owe my deepest thanks to Dr. Angelo Fontan for giving me a wonderful opportunity to work on a completely new and novel research topic. I would also like to thank Dr. Giuliana d'ippolito for her kind support and encouragements throughout. I would like to express my sincere gratitude to Dr. Laura Dipasquale for mentoring me for all the research activities and patiently teaching me new methods and techniques on the day-to-day basis. Thanks for all the scientific discussions and guidance starting from planning of the experiments to implementation in a highly organized and professional manner. I am greatly indebted to Dr. Laura Dipasquale for all you have done for me.

This research work would not have been possible without the advice and support of the entire Bio-Organic Chemistry Unit members of Institute of Biomolecular Chemistry, CNR, Napoli, Italy.

I would like to offer my special thanks to Dr. Genoveffa Nuzzo, Dr. Angela Sardo, Mr. Luigi Leone and Ms. Juliette D. Melck for all you have done for me and making my stay worthwhile at CNR. I would also like to thank Dr. Ouacil Saouli for help in the mathematical model. I would like to extend my sincere thanks to Dr. Eldon Raj for guiding my research work at UNESCO-IHE and giving valuable inputs on how to write scientific papers. I owe my deepest thanks to Mr. Ludovic Pontoni, Prof. Francesco Pirozzi and Dr. Luigi Frunzo for their kind help and support during my stay at the University of Napoli Federico-II. I also would like to express my sincere thankfulness to the administrative staffs of University of Cassino and Southern Lazio, Italy and University of Paris-Est, France for all their support and cooperation. I also would like to express my gratitude to the administrative and the laboratory staff of UNESCO-IHE, Delft for all their kind support.

I would also like to acknowledge some important people who kindly guided me from time-to-time in shaping my career, including Dr. Oleg V. Shipin, Asian Institute of Technology; Prof. Bishnu Prasad Behera, Prof. Balram Panigrahi and Prof. Sanjay Kumar Dash of Orissa university of Agriculture Technology; Dr. Suryakumari Dasigi, Centre for People's Forestry; Dr. Zhiji Ding, SCELSE, NTU, Singapore; Mr. Tapas Kumar Chattopadhyay, Jawahar Navodaya Vidyalaya and Mr. Paul Jacob, Institut national des sciences appliquées de Toulouse.

I would like to thank all my PhD colleagues and friends from Napoli and Delft for always being standing up for me in the difficult times. Lastly, I would like to thank my family for their unconditional love, support and encouragements to pursue my dream and take decisions without fear or favour.

Sincerely,

Nirakar Pradhan

University of Cassino and Southern Lazio, Italy

Summary

The environmental impact of excessive exploitation of fossil fuel reserves has inspired the innovation of several sustainable neo-carbon-neutral technologies. To that end, the biological processes like fermentation may be leveraged to bioconvert carbohydrate-rich feedstocks to fuels like hydrogen (H₂) or commercially valuable organic acids like lactic acid. This research work investigated the engineering techniques for improving simultaneous synthesis of H₂ and lactic acid under capnophilic (CO₂-dependent) lactic fermentation (CLF) conditions by a lab strain of *Thermotoga neapolitana*.

Primarily, the genotypic comparison between the lab strain and the wild-type revealed DNA homology of 88.1 (\pm 2.4)%. Genotyping by RiboPrint[®] and matrix-assisted laser desorption/ionization time-of-flight mass spectrometry (MALDI-TOF MS) analyses showed a genetic differentiation beyond subspecies level, hence the lab strain was proposed as a new subspecies, *T. neapolitana* subsp. *lactica*. The lab strain produced 10-90% more lactic acid, based on the phenotypic characterization, than the wild-type strain under similar operating conditions without impairing the H₂ yield.

The lab strain was then studied to optimize the growth conditions as well as to estimate the growth kinetic parameters. A new kinetic model based on the dark fermentation (DF) principles and the Monod-like mathematical expressions were developed to enable the simulation of biomass growth, substrate consumption and product formation. The model failed to estimate acetic and lactic acid accurately, as the DF model did not consider the carboxylation of acetic acid to lactic acid by the pyruvate:ferredoxin oxidoreductase (PFOR) enzyme under CLF conditions. The model was then incorporated with the CLF mechanism and the kinetic parameters were recalibrated.

The kinetic parameters, i.e. maximum specific uptake rate (k), semi-saturation constant (k_s), biomass yield coefficient (Y) and endogenous decay rate (k_d) were 1.30 1/h, 1.42 g/L, 0.12 and 0.02 1/h, respectively, under CLF conditions. Interestingly, the new CLF-based model perfectly fitted the experimental results and estimated that about 40-80% of the lactic acid production is attributed to the recycling of acetic acid and CO₂.

In addition, the adsorption of lactic acid by activated carbon and anionic polymeric resins was successfully applied as a downstream processing technique for the recovery of lactic acid from a model *T. neapolitana* fermentation broth. This research work serves as a practical milestone in the field of microbial fermentation with a scope for wider scientific applications, including the development of bio-based renewable energy and industrial lactic acid production.

Résumé

Les énergies non-renouvelables ont été d'un apport capital dans l'industrialisation et l'urbanisation dans les derniers centenaires. L'exploitation excessive des réserves d'hydrocarbures et son impact environnemental ont contribué au développement de plusieurs technologies durables à caractère néo-carbone neutre. A cet effet, les processus biologiques comme la fermentation pourraient être exploités pour convertir biologiquement les hydrates de carbone en énergies comme l'hydrogène (H₂) ou des acides organiques commercialement rentables. Ce travail a étudié les techniques d'ingénierie pour améliorer la synthèse simultanée d'H₂ et d'acide lactique à travers des conditions de fermentation capnophile lactique (CLF) par une souche de labo de *Thermotoga neapolitana*.

En un premier temps, une comparaison génotypique entre la souche de labo et celle sauvage a révélé une ressemblance de 88,1 (±2,4) %. En plus, les analyses du génotypage par RiboPrint® et par spectroscopie de masse matrix-assisted laser desorption/ionization time-of-flight (MALDI-TOF MS) ont montré une différenciation génétique au-delà du niveau sous-espèce ; et par conséquent la souche de labo a été proposée comme sous-espèce, *T. neapolitana* subsp. *lactica*. Basé sur la caractérisation phénotypique, la souche de labo produisait 10-90% plus d'acide lactique que celle sauvage sous les mêmes conditions sans pour autant affecté le taux de production d'H₂.

La souche de labo a donc été étudiée pour aussi bien optimiser les conditions de croissance que pour estimer les paramètres cinétiques de croissance. Un nouveau modèle cinétique basé sur les principes de fermentation à l'obscurité (DF) et les expressions mathématiques Monod ont été développés pour permettre la simulation de la croissance en biomasse, la consommation de substrat, et la formation de produit. Le modèle n'a cependant pas pu faire une estimation des acides acétique et lactique avec précision du fait que le modèle DF n'a pas considéré la carboxylation de l'acide acétique en acide lactique par l'enzyme pyruvate ferrédoxine oxydoréductase (PFOR) sous les conditions CLF.

Le modèle a été associé avec le mécanisme CLF et les paramètres cinétiques ont été recalibrés. Les paramètres cinétiques qui sont le taux d'absorption spécifique maximum (k), la constante semi-saturation (k_s), le coefficient en rendement biomasse (Y), et le taux de décomposition interne (k_d) étaient de 1,30 l/h, 1,42 g/L, 0,12 et 0,02

l/h. Le nouveau modèle CLF s'est parfaitement adapté avec les résultats expérimentaux et a estimé que près de 40-80% de la production d'acide lactique est attribué au recyclage de l'acide acétique et le CO₂.

En plus, l'adsorption de l'acide lactique par le carbone actif et les résines polymères anioniques a été appliquée avec succès comme technique de transformation en aval dans la récupération et la purification de l'acide lactique à partir du modèle de fermentation type *T. neapolitana*. Pour ce faire, ce travail de recherche constitue une étape majeure dans le domaine de la fermentation bactérienne utilisable pour de vastes applications scientifiques prenant en compte le développement d'énergies renouvelables et la production industrielle d'acide lactique.

Sommario

Gli effetti negativi sull'ambiente prodotti dall'eccessivo sfruttamento dei combustibili fossili ha promosso lo sviluppo di nuove tecnologie, sostenibili, a zero emissioni di carbonio. In questo contesto, i processi biologici, quali la fermentazione, possono essere validamente utilizzati per convertire flussi di materia ricchi di carboidrati in combustibili quali l'idrogeno (H₂) e in acidi organici dal valore commerciale quali l'acido lattico. Il presente lavoro di ricerca ha avuto per oggetto uno studio sperimentale finalizzato a mettere a punto tecniche ingegneristiche per migliorare la produzione simultanea di H₂ e acido lattico mediante un processo di fermentazione lattica (CLF) condotto in un ambiente capnofilico (in presenza di CO₂) utilizzando ceppi del batterio *Thermotoga neapolitana* coltivati in laboratorio.

Un primo importante risultato è stato raggiunto confrontando il genotipo tra il ceppo coltivato in laboratorio e quello selezionato in natura. Dal confronto sulla base delle analisi di geotipizzazione condotte con RiboPrint® e spettrometria di massa a tecnologia MALDI-TOF (matrix assisted laser desorption/ionisation – time of flight mass spectrometry) sono emerse un'omologia del DNA pari al 88.1 (± 2.4)% e una differenziazione genetica oltre il livello di sottospecie. Pertanto il ceppo coltivato in laboratorio è stato proposto come una nuova sottospecie alla quale è stato dato il nome di *T. neapolitana* subsp. *lactica*. Il ceppo di laboratorio, sulla base di una caratterizzazione fenotipica, è in grado di produrre una quantità di acido lattico superiore del 10-90% rispetto alla specie isolata in natura, nelle medesime condizioni operative e senza penalizzare la produzione di H₂.

Il ceppo di laboratorio è stato successivamente oggetto di uno studio mirato a ottimizzarne le condizioni di crescita e a valutarne i parametri cinetici. I risultati ottenuti hanno permesso di sviluppare un modello matematico cinetico, basato sulla *dark fermentation* (DF) tradizionale e sull'espressione matematiche di Monod, in grado di simulare la crescita della biomassa, il consumo del substrato e la formazioni dei prodotti delle reazioni biochimiche. Il modello si è dimostrato non accurato nella stima della produzione di acido lattico e acido acetico dal momento che la DF tradizionale non prende in considerazione, in condizioni CLF, il fenomeno di carbossilazione dell'acido acetico ad acido lattico mediante l'enzima piruvato:ferredossina ossidoreduttasi (PFOR).

Il modello è stato pertanto rivisitato incorporando al suo interno il meccanismo della CLF e i parametri cinetici sono stati ricalibrati pervenendo ai seguenti valori: velocità massima di utilizzazione del substrato (k), costante di semisaturazione (k_s), coefficiente di resa cellulare (Y), velocità di scomparsa batterica (k_d) rispettivamente pari a 1.30 1/h, 1.42 g/L, 0.12 and 0.02 1/h. Il nuovo modello, basato sul meccanismo CLF, riproduce i dati sperimentali in maniera quasi perfetta e associa circa il 40-80% della produzione di acido lattico alla riconversione dell'acido acetico e della CO₂.

Infine, è stata testata con successo l'estrazione dell'acido lattico mediante carbone attivo e resina anionica polimerica per il recupero di questo acido dal brodo di fermentazione del *T. neapolitana*. Questo lavoro di ricerca ha il merito di gettare importanti basi nel campo della fermentazione microbica per applicazioni scientifiche più vaste, compreso lo sviluppo di energie rinnovabili basate su processi biologici e la produzione industriale di acido lattico.

Samenvattig

Door de impact van grootschalige exploitatie van fossiele brandstoffen op het milieu kwam er aandacht voor de ontwikkeling van verschillende duurzame, koolstof-neutrale, technologieën. Biologische processen, zoals fermentatie, kunnen worden gebruikt om koolhydraatrijke landbouwgewassen om te zetten tot brandstoffen zoals waterstof (H₂), of tot commercieel waardevolle organische zuren zoals melkzuur. In de studie in dit proefschrift werd technologie onderzocht om gelijktijdige synthese van H₂ en melkzuur te verbeteren, die verloopt via de capnofiele (CO₂ afhankelijke) melkzuur fermentatie route (CLF) in een labstam van *Thermotoga neapolitana*.

Vergelijking van het genotype van de labstam en een wildtype bacterie gaf een DNA homologie van 88.1 (± 2.4)%. RiboPrint® en matrix-assisted laser desorption/ionization time-of-flight mass spectrometry (MALDI-TOF MS) tests bevestigden een differentiatie op sub-species niveau. Daarom besloten we de labstam te hernoemen naar een nieuw sub-species *T. neapolitana* subsp. *lactica*. Bij de fenotypische karakterisering produceerde onder gelijke omstandigheden de labstam 10-90% meer azijnzuur dan de wildtype stam, zonder dat de H₂ opbrengst verminderde.

De groeiomstandigheden van de labstam werden verder geoptimaliseerd, en de groei-kinetische parameters werden bepaald. Een nieuw model werd ontwikkeld gebaseerd op dark fermentation (DF) principes, en Monod-achtige vergelijkingen werden ontwikkeld om biomassagroei, substraatgebruik en productvorming te simuleren. Het DF model kon echter niet voorspellen hoeveel azijnzuur en melkzuur werden gevormd, omdat het onder CLF omstandigheden geen rekening hield met de carboxylering van azijnzuur naar melkzuur door het enzym pyruvate:ferredoxin oxidoreductase (PFOR). Vervolgens werd het CLF mechanisme in het model opgenomen en werden de kinetische parameters opnieuw gekalibreerd.

Deze parameters waren: maximum specifieke opnamesnelheid (k), semi-verzadigings constante (k_s), biomassa opbrengst coëfficiënt (yield, Y) en endogene verval snelheid (k_d). Deze parameters waren onder CLF omstandigheden respectievelijk 1.30 1/h, 1.42 g/L, 0.12 en 0.02 1/h. Opvallend was dat het nieuwe op CLF gebaseerde model perfect paste op de experimentele data. 40-80% van de melkzuurproductie kan worden toegeschreven aan de recycling van azijnzuur en CO₂.

De adsorptie van melkzuur door geactiveerde kool en anionisch polymeerhars is succesvol toegepast als een downstream processing techniek voor de terugwinning en de zuivering van melkzuur uit een *T. neapolitana* fermentatie-extract. Het onderzoek kan worden beschouwd als een praktische mijlpaal op het gebied van microbiële fermentatie, gericht op bredere wetenschappelijke toepassingen, waaronder de ontwikkeling van duurzame energie en industriële melkzuurproductie.

Chapter 1

General introduction

Chapter 1: General introduction

1.1 Background of the study

The current global energy demand (~ 80%) largely depends on non-renewable energy resources. Their exploitation has led to the depletion of non-renewable energy reserves. As a consequence, the greenhouse gas (GHG) concentration in the atmosphere has escalated, posing a major threat for the global climate change. In the past years, there was a significant rise in interest in exploring alternative and renewable energy resources. There is an urgent need to accelerate the transition to equitable and sustainable post-fossil carbon energies (Huisingsh et al., 2015). To that end, the future energy should be based upon bio-based renewable energies in order to reduce dependence upon fossil fuels and reduce GHG emissions (Philp, 2015). Among them (i.e. hydroelectric, solar, wind, nuclear, hydrothermal and tidal energy), hydrogen (H₂) is one of the cleanest with a very high-energy content (120.7 kJ/g) and its combustion is free of emissions (Hallenbeck, 2009). At present, > 90% of the global H₂ is produced from the natural gas or light oil fractions by thermochemical process, i.e. pyrolysis and gasification (Anshuman et al., 2005; Manish & Banerjee, 2008). Recently, considerable attention is being paid to the biological way of H₂ production, which has clear environmental benefits (i.e. (i) organic waste valorisation, (ii) energy generation and (iii) organic acid recovery) compared to the physicochemical processes (Hallenbeck & Benemann, 2002).

The United States, countries in the European Union and Japan are front-runner for biological H₂ production technologies, however these technologies are still in the developmental stage and require further innovations before being scaled-up for the commercial applications (Brentner et al., 2010). Dark- and photo-fermentative H₂ production has enormous potential to replace the conventional H₂ production technologies using fossil fuels (Basak & Das, 2007; Uyar et al., 2009). The dark fermentation (DF) has additional benefits compared to photo-fermentation due to its operational flexibility, working independent of light energy and being able to use a wide range of organic feedstocks (Sinha & Pandey, 2014; Wukovits et al., 2013). Several studies have documented H₂ production at mesophilic, thermophilic and

hyperthermophilic conditions using pure or mixed cultures either in batch or continuous fermentation processes (Amend & Shock, 2001; Elsharnouby et al., 2013). The application of pure cultures is interesting as the H₂ production reaches its theoretical maximum value (4 mol H₂/mol of glucose), but at the same time the pure culture needs strict environmental conditions for fermentation unlike the mixed cultures (Munro et al., 2009; Thauer, 1977).

The present study used a hyperthermophilic marine eubacterium namely *Thermotoga neapolitana* for H₂ production from sugars (mono-, di- and polysaccharides) in a continuous stirred-tank reactor (CSTR) system. Based on the technological reviews, it is understood that the hyperthermophilic fermentation is suitable for H₂ production, but it is energy intensive based on the single usable product, i.e. H₂ (Brentner et al., 2010). To exploit the benefit and avoid the limitations with hyperthermophilic pure culture fermentation, the study was focused on the capnophilic (CO₂-requiring) lactic fermentation (CLF), which is a newly found metabolic pathway for *T. neapolitana* (Dipasquale et al., 2014). In the CLF-based fermentation, both H₂ and lactic acid are synthesized simultaneously, thus making the process more attractive and cost effective for large scale applications (d'Ippolito et al., 2014).

In addition to H₂ production, this PhD study also addresses another pertinent issue with respect to the synthetic polymers, which are neither biodegradable nor produced from renewable sources, thus their disposal has serious environmental impacts (Heydarifard et al., 2016). There is an increasing desire for biodegradable polymers like polylactic acid (PLA), which are renewable, cheap and recyclable compared to synthetic polymers (Hamad et al., 2011; Hamad et al., 2010). The CLF-based fermentation enables for the industrial scale lactic acid production using carbohydrate-rich feedstocks. However, the CLF-based fermentation needs all-round process optimization with respect to feedstocks, operational parameters, kinetic parameters, reactor design and downstream processing (Brentner et al., 2010; Dipasquale et al., 2014; Yu & Drapcho, 2011).

1.2 Scope of the study

The main objective of this PhD research was to investigate the engineering techniques for improving hydrogen and lactic acid production from organic substrates under CLF conditions. The information available about the *T. neapolitana* fermentation processes

under CLF conditions and the factors that influence the process is limited. The research presented here is focused on fermentative H₂ and lactic acid production under various operating conditions by using *T. neapolitana* as a model bacterium. For this purpose, the investigation of the culture parameters favouring the simultaneous H₂ and lactic acid production under CLF conditions were crucial. In order to design reactors, the biological growth kinetic parameters for the model bacterium were evaluated. Extraction and purification of lactic acid from the fermentation broth was also investigated. The specific objectives of the study were:

1. To perform genotypic and phenotypic characterization for *T. neapolitana* and its mutant strain under CLF conditions
2. To investigate the effect of varying culture parameters (i.e. salinity level, carbon source and buffering agent) on the H₂ and lactic acid production under CLF conditions
3. To determine the biological growth kinetic parameters for *T. neapolitana* and to develop a kinetic model for the *T. neapolitana* fermentation
4. To improve the kinetic model for the CLF-based pathway and to validate the model with different series of experimental results with mono- and poly-saccharide sugars
5. To perform batch adsorption studies for the lactic acid recovery using anionic resins and study the adsorption thermodynamics, isotherms and kinetics

1.3 Structure of the thesis

The chapters in this thesis are written as journal articles style with each chapter covering an explicit concept and can be read independently. Each chapter contains its own abstract, introduction and materials and methods section, which may have some similarities with the other chapters, as the chapters are related in one way or other. The chapters are arranged in the order of advancement of concepts and ideas as shown in [Fig.1.1](#). This thesis is composed of nine chapters:

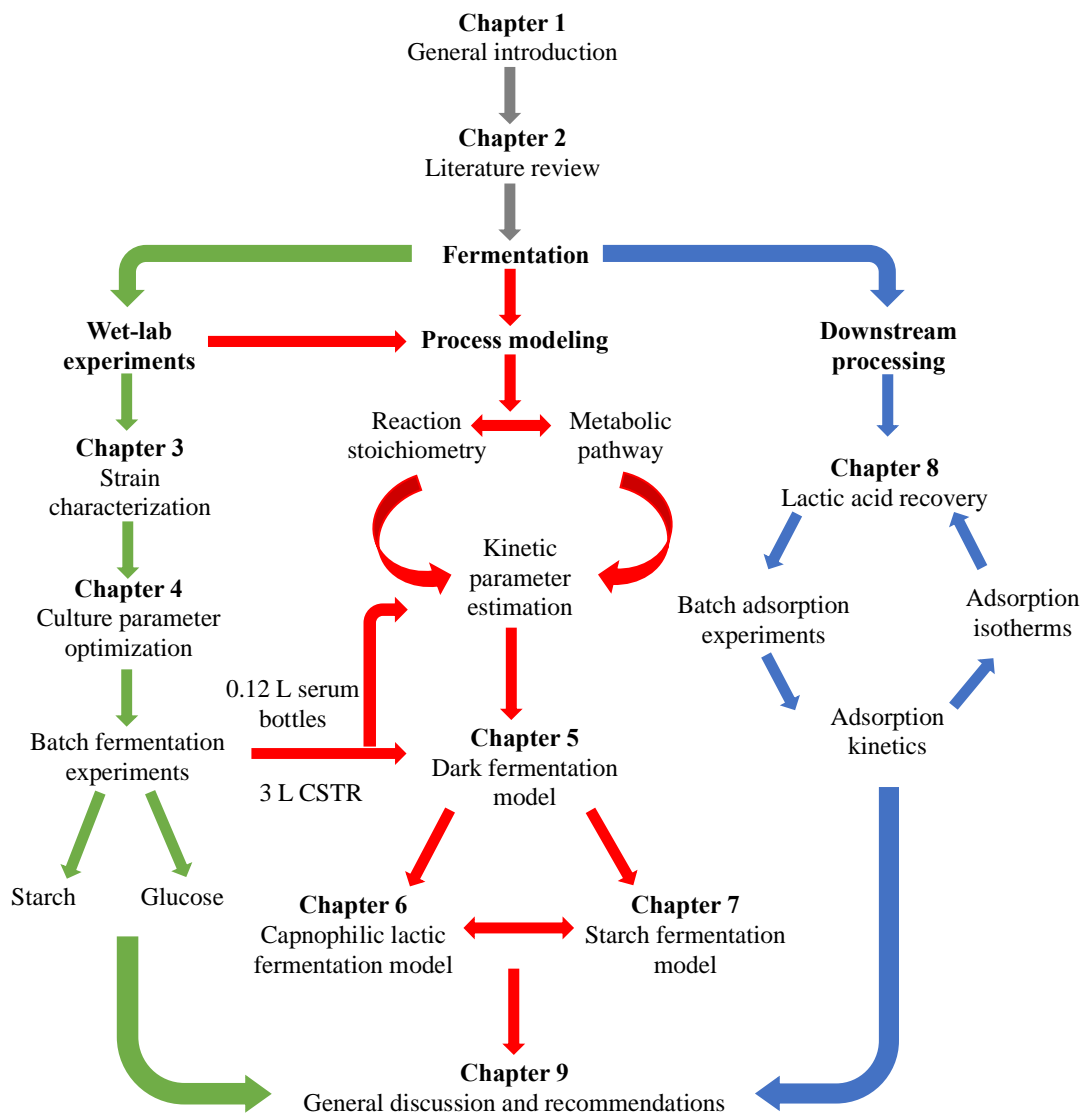


Fig. 1. 1 Schematic outline of the thesis.

Chapter 1: General introduction. The first chapter provides a brief overview and scope of the study for the fermentative H₂ and lactic acid production using *T. neapolitana* as model bacterium.

Chapter 2: Literature review. In this chapter, *Thermotoga neapolitana*, a hyperthermophilic marine bacterium for fermentative H₂ production, is reviewed. The main research gaps are identified with respect to feedstocks, fermentation by-products, operating conditions, capnophilic lactic fermentation (CLF) pathway and introduction to kinetic modeling.

Chapter 3: Strain characterization. In this chapter, the laboratory strain of *T. neapolitana* is compared with the parent *T. neapolitana* strain for lactic acid production. Various phenotypic (i.e. temperature, salinity, sugars and electron acceptor) and genotypic (DNA-DNA hybridization and Riboprint patterns) studies were performed to verify the sub-species level differentiation with respect to the parent strain under CLF conditions.

Chapter 4: Culture parameter optimization. The main aim of this chapter was to identify how the culture parameters in terms of salinity level, buffering agent and substrates affect the H₂ and lactic acid production under CLF conditions. In addition, scaled-up experiments (from 0.12 L serum bottles to 3.0 L CSTR) were performed to verify the efficiency of the CLF-based processes.

Chapter 5: Dark fermentation model. In this chapter, a kinetic model for fermentative H₂ production by *T. neapolitana* according to the DF conditions is developed. Batch fermentation tests were carried out in order to estimate the biological kinetic parameters for *T. neapolitana* fermentation and then the process was mathematically modeled (i.e. sensitivity analysis, model calibration and model validation) according to the DF principles.

Chapter 6: Capnophilic lactic fermentation model. In the chapter, the deficiency in the DF model (as in [Chapter 5](#)) are highlighted and overcome with a model for the CLF-based pathways. The previously estimated kinetic parameters (in [Chapter 5](#)) were recalibrated to fit the experimental results under CLF conditions. Furthermore, a new kinetic model with mass balance equations was used to describe the kinetics of product formation (i.e. H₂, lactic and acetic acid) under CLF conditions. In addition, the process of lactic acid production by the carboxylation of acetic acid was evaluated and integrated to the model.

Chapter 7: Starch fermentation model. In this chapter, the H₂ and lactic acid production potential of potato and wheat starches under CLF conditions are tested as well as the experimental results are simulated with a CLF-based kinetic model for a CSTR system ([Chapter 6](#)). In addition, reaction thermodynamics under hyperthermophilic conditions for the starch fermentation are discussed.

Chapter 8: Lactic acid recovery. In this chapter, the feasibility of lactic acid recovery by adsorption is studied. The effects of contact time, initial pH, adsorbent dose and

lactic acid concentration on the adsorption of lactic acid from a model fermentation broth by granular active carbon, as well as weakly-basic (Reillex[®] 425) and strongly-basic (Amberlite[®] IRA-400) anion exchange resins were investigated in batch equilibrium studies. In addition, a systematic investigation of varying temperature adsorption and thermodynamic characterization of lactic acid onto adsorbents. To understand the adsorbate-adsorbent mechanisms, the Langmuir, Freundlich and Temkin isotherms as well as the kinetic model to the experimental results of lactic acid adsorption were applied.

Chapter 9: General discussion and recommendations. This chapter critically analyses the results from the previous chapters and discusses the highlights of the research findings and their perspectives for large-scale applications. This chapter also makes specific recommendations that are required for further improvements to the CLF techniques as well as proposes several system integration methods, which will maximize energy recovery from the substrates used to feed to the system.

References

- Amend, J.P., Shock, E.L. 2001. Energetics of overall metabolic reactions of thermophilic and hyperthermophilic Archaea and Bacteria. *FEMS Microbiology Reviews*, **25**, 175-243.
- Anshuman, K., Mike, M., Brenda, J. 2005. Hydrogen: The energy source for the 21st century. *Technovation*, **25**, 569-585.
- Basak, N., Das, D. 2007. The prospect of purple non-sulfur (PNS) photosynthetic bacteria for hydrogen production: The present state of the art. *World Journal of Microbiology & Biotechnology*, **23**, 31-42.
- Brentner, L.B., Peccia, J., Zimmerman, J.B. 2010. Challenges in developing biohydrogen as a sustainable energy source: implications for a research agenda. *Environmental Science and Technology*, **44**, 2243-54.
- d'Ippolito, G., Dipasquale, L., Fontana, A. 2014. Recycling of carbon dioxide and acetate as lactic acid by the hydrogen-producing bacterium *Thermotoga neapolitana*. *ChemSusChem*, **7**, 2678-83.
- Dipasquale, L., d'Ippolito, G., Fontana, A. 2014. Capnophilic lactic fermentation and hydrogen synthesis by *Thermotoga neapolitana*: An unexpected deviation from the dark fermentation model. *International Journal of Hydrogen Energy*, **39**, 4857-4862.
- Elsharnouby, O., Hafez, H., Nakhla, G., el Naggar, M.H. 2013. A critical literature review on biohydrogen production by pure cultures. *International Journal of Hydrogen Energy*, **38**, 4945-4966.

- Hallenbeck, P.C. 2009. Fermentative hydrogen production: Principles, progress, and prognosis. *International Journal of Hydrogen Energy*, **34**, 7379-89.
- Hallenbeck, P.C., Benemann, J.R. 2002. Biological hydrogen production; fundamentals and limiting processes. *International Journal of Hydrogen Energy*, **27**, 1185-1193.
- Hamad, K., Kaseem, M., Deri, F. 2011. Melt rheology of poly(lactic acid)/low density polyethylene polymer blends. *Advances in Chemical Engineering and Science*, **1**, 208-214.
- Hamad, K., Kaseem, M., Deri, F. 2010. Rheological and mechanical properties of poly(lactic acid)/polystyrene polymer blend. *Polymer Bulletin*, **65**, 509–519.
- Heydarifard, S., Nazhad, M.M., Xiao, H., Shipin, O., Olson, J. 2016. Water-resistant cellulosic filter for aerosol entrapment and water purification, Part I: production of water-resistant cellulosic filter. *Environmental Technology* **37**, 1716-1722.
- Huisingh, D., Zhang, Z., Moore, J.C., Qiao, Q., Lif, Q. 2015. Recent advances in carbon emissions reduction: policies, technologies, monitoring, assessment and modeling. *Journal of Cleaner Production*, **103**, 1-12.
- Manish, S., Banerjee, R. 2008. Comparison of biohydrogen production processes. *International Journal of Hydrogen Energy*, **33**, 279-286.
- Munro, S.A., Zinder, S.H., Walker, L.P. 2009. The fermentation stoichiometry of *Thermotoga neapolitana* and influence of temperature, oxygen, and pH on hydrogen production. *Biotechnology Progress*, **25**, 1035-1042.
- Philp, J. 2015. Balancing the bioeconomy: supporting biofuels and bio-based materials in public policy. *Energy and Environmental Science*, **8**, 3063-3068.
- Sinha, P., Pandey, A. 2014. Biohydrogen production from various feedstocks by *Bacillus firmus* NMBL-03. *International Journal of Hydrogen Energy*, **39**, 7518-7525.
- Thauer, R. 1977. Limitation of microbial hydrogen formation via fermentatio. *Microbial Energy Conversion*, 201-204.
- Uyar, B., Eroglu, I., Yucel, M., Gunduz, U. 2009. Photofermentative hydrogen production from volatile fatty acids present in dark fermentation effluents. *International Journal of Hydrogen Energy*, **34**, 4517-23.
- Wukovits, W., Drljo, A., Hilby, E., Friedl, A. 2013. Integration of Biohydrogen Production with Heat and Power Generation from Biomass Residues. *16th International Conference on Process Integration, Modelling and Optimisation for Energy Saving and Pollution Reduction (Pres'13)*, **35**, 1003-1008.
- Yu, X., Drapcho, C. 2011. Hydrogen production by the hyperthermophilic bacterium *Thermotoga neapolitana* using agricultural-based carbon and nitrogen sources. *Biological Engineering Transactions*, **4**, 101-112.

Chapter 2

Literature review

This chapter has been published as:

Pradhan, N., Dipasquale, L., d'Ippolito, G., Panico, A., Lens, P.N.L., Esposito, G., Fontana, A. 2015. Hydrogen production by the thermophilic bacterium *Thermotoga neapolitana*. *International Journal of Molecular Sciences*, 16, 12578-12600.

Chapter 2: Literature review

Abstract

As the only fuel that is not chemically bound to carbon, hydrogen has gained interest as an energy carrier to face the current environmental issues of greenhouse gas emissions and to substitute the depleting non-renewable reserves. In the last years, there has been a significant increase in the number of publications about the bacterium *Thermotoga neapolitana* that is responsible for production yields of H₂ that are among the highest achievements reported in the literature. Here we present an extensive overview of the most recent studies on this hyperthermophilic bacterium together with a critical discussion of the potential of fermentative production by this bacterium. The review article is organized into sections focused on biochemical, microbiological and technical issues, including the effect of substrate, reactor type, gas sparging, temperature, pH, hydraulic retention time and organic loading parameters on rate and yield of gas production.

Keywords: thermophilic bacteria; fermentation; hydrogen; lactic acid; carbon dioxide; biomass; renewable energy; process kinetics; energy carrier; green-house gas.

2.1 Introduction

Anaerobic digestion of organic material is regarded as a potential method for hydrogen (H₂) production from biomass (Hallenbeck & Benemann, 2002; Nath & Das, 2004). Besides simple carbohydrates (e.g., glucose) or polymers such as starch and cellulose, the process utilizes a wide range of organic compounds as substrate, including organic wastes and agro-industrial matrices (Fan et al., 2006; Guo et al., 2010a; Guo et al., 2010b; Kotsopoulos et al., 2009; Sinha & Pandey, 2011; Vijayaraghavan & Ahmad, 2006; Wukovits et al., 2013). Considering that such residues are abundant, cheap, renewable and biodegradable, H₂ production by fermentation of this material is potentially competitive over conventional process (Guo et al., 2010a) and technically more feasible than other biological methods, including photofermentation and photobiolysis. Furthermore, production of H₂ from organic substrates is viewed as an environmentally friendly process because of its potential to yield clean energy while reducing waste and greenhouse gas emissions. Although a more detailed life cycle assessment of feedstock materials is required to fully understand the environmental impact of the whole process, the possible implications on climate change have prompted growing attention to the fermentative production of H₂ in recent years (Djomo & Blumberga, 2011).

Chemotrophic H₂ production can be operated at mesophilic (25-40 °C), thermophilic (40-65 °C) or hyperthermophilic (>80 °C) temperatures (Amend & Shock, 2001; Angenenta et al., 2004; Elsharnouby et al., 2013), but the process in heated cultures benefits from thermodynamically favorable reaction (Hafez et al., 2012; Krishna, 2013). Although metabolic activity sharply drops outside the optimum temperature range, increase of temperature accelerates reaction rates and offers a number of technical advantages including reduction of viscosity, improvement of mixing efficiency, reduced risk of contamination and no need for reactor cooling (Verhaart et al., 2010). In addition, the high operating temperature enhances hydrolysis rate of complex substrates and, generally speaking, thermophiles can more effectively utilize complex sugars, e.g., cellulose, than mesophiles (Islam et al., 2009; Zhang et al., 2003). Furthermore, hyperthermophilic conditions suffer less from inhibition due to H₂ partial pressure and, in the case of microbial consortia, are less sensitive to H₂ consumers like methanogens (Liu et al., 2008; van Niel et al., 2003).

In the last years, pure cultures of the hyperthermophilic eubacterium *Thermotoga neapolitana* has shown promising results for fermentative H₂ production from several organic substrates (Cappelletti et al., 2014). In a recent paper (Dipasquale et al., 2014), we have also shown that *T. neapolitana* can yield significant amounts of lactic acid without affecting H₂ synthesis, thus offering novel applications for the fermentative process. Here we critically review the most recent data on H₂ production by *T. neapolitana* and discuss the challenges and future prospects of H₂ production using this bacterium.

2.2 Taxonomy of *Thermotoga neapolitana*

Originally isolated from a shallow submarine hot spring near Lucrino in the Bay of Naples in 1986 (Belkin et al., 1986; Jannasch et al., 1988), *T. neapolitana* is a gram-negative bacterium that grows between 55 and 90 °C with an optimal growth temperature of 80 °C (Belkin et al., 1986; Jannasch et al., 1988). The species belongs to the order *Thermotogales* (Phylum *Thermotogae*, class *Thermotogae*) that have, until the recent report of *Mesotoga prima* (Nesbo et al., 2012), been exclusively comprised of thermophilic or hyperthermophilic organisms. The order includes an assembly of rod-shaped, non-sporulating bacteria that are characterized by an unconventional outer envelope called the “toga”, which forms a large periplasmic space at the poles of each rod (Angel et al., 1993; Huber et al., 1986; Rachel et al., 1990). Although it has been shown that these regions could be involved in the formation of multicellular rods (Kuwabara & Igarashi, 2012), the physiological role of the large periplasm remains unknown. *Thermotogales* also synthesizes many polysaccharide hydrolases, some exposed on the cell surface, that allow utilization of diverse sources of carbon (Choi et al., 2011; Choi et al., 2009; Dipasquale et al., 2009; Kang et al., 2011; Lama et al., 2014; Liebl et al., 2008; Okazaki et al., 2013; Pozzo et al., 2010; Schumann et al., 1991; Yun et al., 2011).

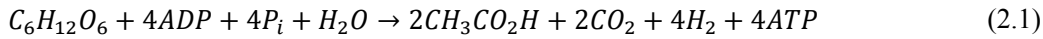
The phylogenetic position of *Thermotogae* is still unresolved, even if many studies agree to place members of this phylum among the deepest branches of bacteria, and, thus, as prime candidates for evolutionary studies (Cappelletti et al., 2014; Latif et al., 2013). Based upon different phylogenetic approaches, the class *Thermotogae* is divided into three orders (*Thermotogales*, *Kosmotogales* and *Petrotogales*) containing four families (*Thermotogaceae*, *Fervidobacteriaceae*, *Kosmotogaceae* and

Petrotogaceae) and 10 genera (*Thermotoga*, *Thermosipho*, *Fervidobacterium*, *Geotoga*, *Petrotoga*, *Marinitoga*, *Thermococcoides*, *Kosmotoga*, *Oceanotoga*, and *Defluviitoga*). The genus *Thermotoga* currently includes eleven species, i.e., *T. maritima*, *T. neapolitana*, *T. thermarum*, *T. elfii*, *T. subterranea*, *T. hypogea*, *T. petrophila*, *T. naphthophila*, *T. lettingae*, *T. caldifontis*, and *T. profunda*, that thrive in marine hydrothermal vents, oil reservoir sites and volcanic springs (Cappelletti et al., 2014). Recently, Bhandari and Gupta (2014) proposed to split the current genus *Thermotoga* into two evolutionary distinct groups. According to this last classification, the original genus *Thermotoga* retains only the species *T. maritima*, *T. neapolitana*, *T. petrophila*, *T. naphthophila*, *Thermotoga* sp. EMP, *Thermotoga* sp. A7A and *Thermotoga* sp. RQ2 while the other *Thermotoga* species (*T. lettingae*, *T. thermarum*, *T. elfii*, *T. subterranea* and *T. hypogea*) belong to the new genus *Pseudothermotoga* (Bhandari & Gupta, 2014).

2.3 Dark fermentation pathway in *T. neapolitana*

Chemotropic production of H₂ is a respiration process using H⁺ as electron acceptor. The biochemical synthesis by bacteria of the genus *Thermotoga* entails catabolism of carbohydrates even if different members of the genus have the ability to use a large variety of substrates that, for example in *T. elfii*, include also sulfur compounds (Ravot et al., 1995). As in the related species *T. maritima* (Schroder et al., 1994; Schut & Adams, 2009), *T. neapolitana* harvests energy mainly by glycolysis via the Embden-Meyerhoff pathway (EMP) (d'Ippolito et al., 2010). EMP is the most common route for oxidation of glucose (and other hexoses) and supplies energy (ATP), reducing equivalents (NADH) and pyruvate that undergoes terminal oxidation (acetate) or is used for biosynthesis (e.g., acetyl-CoA). According to the classical model of fermentation, generally referred to as Dark Fermentation (DF), 4 mol of H₂ can be theoretically produced per mol of consumed glucose (Thauer, 1977). This molar ratio between H₂ and glucose is usually referred to as the Thauer limit and represents the highest yield that can be achieved by a sugar-based fermentation by thermophilic bacteria. As fermentative H₂ production is a mean to dispose of electrons, there is a direct relationship between the biogas yield and the type of the organic products that are concurrently released during the process. Yield is optimized only when all glucose is converted to acetate because NADH and electrons are fully consumed to produce the

energy carrier (Eq. 2.1). On the other hand, in a redox neutral process, no H₂ is produced when lactic acid is the organic product released in the medium (Eq. 2.2).



As shown in Fig. 2.1, acetate production is driven by formation of additional ATP but, when H₂ accumulates and consumption of NADH stops, pyruvate is diverted away for the synthesis of other organic substrates, mostly lactate that is produced by lactate dehydrogenase (LDH) with the concomitant oxidation of NADH. Lactate levels reported during fermentation by *Thermotoga* species vary from trace amounts up to levels rivaling those of acetate (Anshuman et al., 2005; Khanna & Das, 2013; Schut & Adams, 2009; Wu et al., 2006). Low levels of alanine and ethanol have been also reported in *T. neapolitana* (Cappelletti et al., 2014; d'Ippolito et al., 2010; De Vrije et al., 2010).

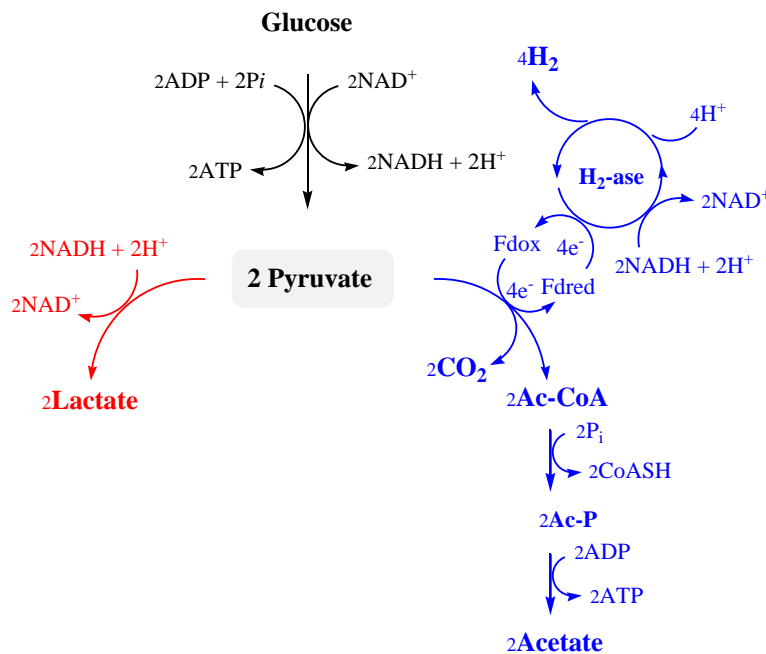


Fig. 2. 1 Streamlined biochemical pathway for fermentative H₂ production, adapted from Reference (Dipasquale et al., 2014), water is omitted for simplicity.

The mechanism behind the high H₂ yields achieved by *T. neapolitana* is likely related to the unique characteristic of the heterotrimeric [FeFe]-hydrogenase that is present in the bacterium. Hydrogenases (H₂ase) constitute a family of enzymes that efficiently reduce protons to H₂ in many anaerobic microorganisms. Sequence analysis on the three proteins that form the H₂ase of *T. maritima*, which has more than 90% homology with that of *T. neapolitana*, suggests that the β subunit is a flavoprotein that accepts electrons from NADH, and the γ subunit transfers electrons from the β subunit to the catalytic α subunit. The catalytic site (the so-called H cluster) shows the most complex Fe-S structure characterized to date and requires the specific action of three highly conserved proteins to be assembled (Albertini et al., 2014). Despite the detailed knowledge of the active site, how the endergonic reaction of H₂ production is accomplished under physiological conditions is not clear. In fact, the reduction of H₂ase by NADH is an energetically unfavorable reaction and the reaction is typically influenced by environmental conditions such as pH, cell growth rate and H₂ partial pressure. In many thermophilic bacteria and several *Clostridium* species, the transfer of electrons to proton ion by [FeFe]-H₂ase requires the presence of NADH-Ferredoxin oxidoreductase (NFOR). In this reaction, it is suggested that the oxidized ferredoxin (Fd) is reduced by NADH, which is formed during carbon metabolism. Then, the electrons in Fd are transferred to protons by [FeFe]-H₂ase to form molecular H₂ (Fig. 2.1) (Oh et al., 2011).

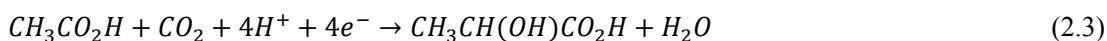
Recently Schut and Adams proposed a novel model for H₂ production for *Thermotoga* species based on the synergistic effect of NADH and reduced Fd (Schut & Adams, 2009). According to this study, H₂ase of *T. maritima* concurrently oxidizes reduced Fd and NADH in a 1:1 ratio in order to reduce the H⁺ ions. Ferredoxin is cyclically produced by pyruvate Fd oxidoreductase (POR) during oxidation of pyruvate to acetyl coenzyme A (Fig. 2.1). This mechanism that couples an exoergonic reduction with an endoergonic reduction has been called “bifurcating” (Li et al., 2008a) and it is proposed to correspond to a novel type of energy conservation. Thus, energy from the oxidation of Fd drives the unfavorable oxidation of NADH in *T. maritima* (Schut & Adams, 2009) and the hyperthermophilic bacterium has the ability to achieve H₂ yields close to the Thauer limit. According to this mechanism, H₂ production by H₂ase of *T. neapolitana* is influenced by factors that affect either NADH or reduced Fd.

Furthermore, the composite mechanism of this H₂ase is consistent with the complexity of the trimeric structure, which is much greater than that of the typical Fd-dependent, single subunit [Fe-Fe]-H₂ase found in *Clostridium* spp. (Schut & Adams, 2009).

2.4 Production of lactic acid and H₂ by capnophilic lactic fermentation

T. neapolitana and the other taxonomically-related species, such as *T. maritima*, *T. petrophila*, *T. naphthophila*, *T. caldifontis*, *T. profunda*, *Pseudothermotoga thermarum*, *P. elfii*, *P. subterranea*, *P. hypogea* and *P. lettingae* have been targeted for biological production of H₂ because of yields approaching the theoretical maximum value (Thauer limit) of 4 mol H₂/mol glucose (Thauer, 1977). According to Fig. 2.1, this result can be achieved only if all of the reducing equivalents from glucose oxidation are used to reduce protons to H₂. Nevertheless, as discussed above, in practice these reducing equivalents are also employed for biosynthetic purposes or formation of other fermentation products. Thus, the high H₂ yields and low production of biomass that have been reported for *T. neapolitana* suggest that pyruvate is only partially used in other metabolic transformations under standard operating conditions (Frock et al., 2010).

Inflow of gases is the most commonly reported method for removing oxygen and H₂ from bacterial cultures in closed reactors (Mizuno et al., 2000; Valdez et al., 2006). Use of CO₂ as gas sparging significantly increases the rate of both glucose consumption and hydrogen production even if there was no improvement of the overall productivity and molar yield that remained substantially unchanged in comparison with N₂ (Dipasquale et al., 2014). Paradoxically, CO₂ stimulated also synthesis of lactic acid. Feeding experiments with labeled precursors clearly proved that at least part of exogenous CO₂ is biologically coupled with acetyl-CoA to give lactic acid when the cultures are stripped by CO₂ gas or enriched in sodium bicarbonate. The process recycles glycolysis-derived acetyl-CoA or employs exogenous acetate with ATP consumption. In this latter case the overall outcome is a conversion of equimolar concentration of acetate and carbon dioxide into lactic acid according to reaction Eq. (2.3).



The fermentative CO₂-dependent synthesis of lactic acid and hydrogen was named capnophilic lactic fermentation (CLF) and, as suggested in Fig. 2.2, it put forward the possibility to fully convert sugar to lactic acid (or other reduced derivatives of pyruvate) without affecting hydrogen synthesis by means of an additional consumption of reducing equivalents deriving from other cellular processes (d'Ippolito et al., 2014).

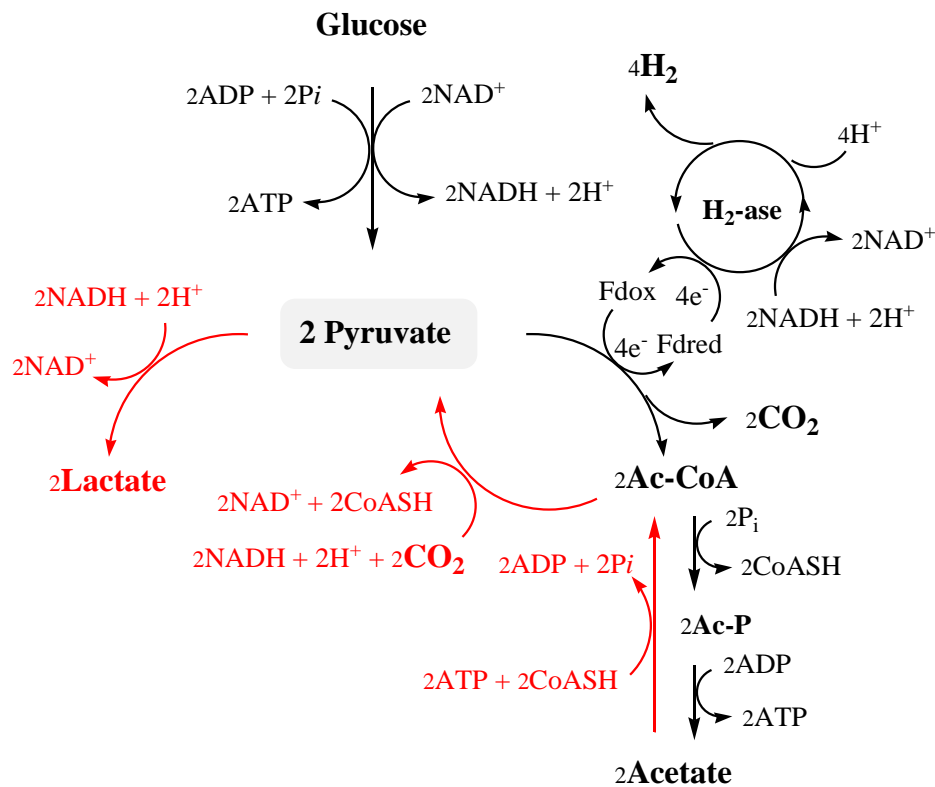


Fig. 2. 2 Proposed model of capnophilic lactic fermentation, adapted from (d'Ippolito et al., 2014), water is omitted for simplicity.

To date, CLF has been described only in *T. neapolitana* but the pathway is likely to occur in other species of the order *Thermotogales*. The key enzyme of the process is a Pyruvate Synthase (also named Pyruvate Oxido-Reductase) that utilizes reduced ferredoxin as source of electrons (d'Ippolito et al., 2014). In *Thermotogales* reductive carboxylation of Ac-CoA likely requires the pool of Fd that is also involved in hydrogen production. Role of Fd as efficient reductant in pyruvate synthesis has been demonstrated *in vitro* with *Clostridium thermoaceticum* (Furdui & Ragsdale, 2000) and

suggested *in vivo* for methanogenic archaea, such as *Methanosarcina barkeri* (Bock et al., 1996). It is noteworthy that the sequence of pyruvate oxido-reductase of this last organism has a good relation to those of *T. neapolitana* and *T. maritima* (d'Ippolito et al., 2014). CLF is an example of biological sequestration of carbon dioxide by coupling with an exogenous substrate (acetate, glucose, etc.) and release of the end-product (lactic acid) outside of the cell. Since *T. neapolitana* does not convert CO₂ to the reduced organic compounds required for cell metabolism, the above mechanism is not related to the autotrophic fixation known in other anaerobes. In fact, unlike known autotrophic (Berg et al., 2010; Braakman & Smith, 2010) and heterotrophic (Krebs, 1941; Werkman & Wood, 2006) pathways for carbon dioxide assimilation, the capnophilic metabolism of *T. neapolitana* implies complete excretion of CO₂ after fixation in lactic acid and no synthesis of reduced organic compounds required for cell metabolism.

2.5 Substrate metabolism by *T. neapolitana*

As discussed above, extreme thermophiles are capable of producing H₂ yields close to the theoretical Thauer limit of 4.0 mol H₂/mol of glucose. In addition, the theoretical maximum yield for xylose, sucrose and glycerol are 3.33 mol H₂/mol xylose, 8.0 mol H₂/mol sucrose and 3.0 mol H₂/mol glycerol under dark fermentation. Glucose is the substrate that gives the highest production of H₂ with *T. neapolitana*. In batch experiments with this sugar, independent studies have reported H₂ yield higher than 3.5 mol/mol and production rate ranging from 23 to 50 mL/L/h at pH of 7.5 and temperature of 80 °C (d'Ippolito et al., 2010; Ngo et al., 2011a). As already mentioned above, the bacterium can also efficiently use a wide range of other substrates ranging from simple to complex sugars including ribose, xylose, fructose, sucrose, maltose, lactose, galactose, starch, and glycogen (Table 2.1) (Cappelletti et al., 2012; Cappelletti et al., 2014; De Vrije et al., 2010; Dipasquale et al., 2012; Eriksen et al., 2011; Jannasch et al., 1988; Mars et al., 2010; Maru et al., 2012; Nguyen et al., 2010a; Nguyen et al., 2010b).

Waste glycerol from bio-diesel manufacturing is currently considered an attractive and abundant feedstock for fermentation process. Batch tests conducted by Maru et al. (2012) have demonstrated that 2.65 mol of H₂ can be produced per mol of glycerol by using the bacterium *T. neapolitana* at a glycerol concentration of 2.5 g/L.

Ngo and Sim (2012) also reported that the bacterium transforms pure glycerol and crude waste glycerol with approximately similar H₂ production (447 (± 22) and 437 (± 21) mL/L, respectively). According to these authors, these yields are better than those reported with mesophilic bacteria (Ito et al., 2005; Pott et al., 2013) and addition of itaconic acid to buffer the culture medium further increased this productivity with both substrates. It is notable that a prediction model built on comparative analysis of the genomes of *T. maritima* and *T. neapolitana* put forward that this latter species should not be able to metabolize a number of sugars, including cellotetraose. However, experimental assessment proved that the bacterium grows on this substrate despite that the model predicted an incomplete cellotetraose transport complex. Proteomic analysis of glucose and cellotetraose revealed two possible new gene clusters that may be associated with transport of these sugars (Munro et al., 2012).

Cappelletti et al. (2012) showed that *T. neapolitana*, *T. maritima*, *T. petrophila* and *T. naphthophila* produce about 2.95 mol of H₂ per mol of glucose equivalent from molasses and 2.5 mol of H₂ per mol of glucose equivalent from cheese whey, whereas 2.7–2.8 mol of H₂ per mol of glucose equivalent were produced on carrot pulp hydrolysates containing glucose, fructose and sucrose as main sugars (De Vrije et al., 2010). Enzymatic hydrolysis of the polysaccharide fraction prior to fermentation increased the H₂ yield of almost 10% to 2.3 g/kg of hydrolyzed carrot pulp. Lignocellulosic substrates (e.g., crop residues) were tested for H₂ production with some standard pretreatment to wash out lignin (De Vrije et al., 2009; Ngo et al., 2012; Nguyen et al., 2010a). Thermo-chemical pretreatment (*i.e.*, heat, ammonia soaking and dilute H₂SO₄ soaking) were found to be effective pretreatment techniques to remove lignin and enhance availability of simple sugars for H₂ production. According to Ngo et al. (2012) 2.8 mol of H₂ per mol of xylose equivalent are produced by *T. neapolitana* in a pH-controlled continuously stirred anaerobic bioreactor sparged with N₂ gas. Similar results have also been reported with rice straw pretreated with ammonia soaking and diluted sulfuric acid (Nguyen et al., 2010a). Algal biomass (*Chlamydomonas reinhardtii*) pretreated by heat-HCl or Termamyl[®] enzymatic hydrolysis has been also used as substrate of *T. neapolitana* to give 2.5 mol of H₂ per mol of glucose equivalent (Nguyen et al., 2010b). Without pretreatment, a slightly lower yield (2.2 mol H₂/mol of glucose

equivalent) was produced by fermentation of laminarans derived from the marine diatom *Thalassiosira weissflogii* ([Dipasquale et al., 2012](#)).

Table 2. 1 H₂ production from various substrates by hyperthermophilic eubacterium *T. neapolitana*. B = batch; FB = fed-batch; Ac = Acetic acid; Lac = Lactic acid; EtOH = Ethanol.

Carbon Source	Substrate Load (g/L)	Culture Type	T(°C)/Start pH	Mixing Speed (rpm)	Reactor Volume (mL)	Working Volume (mL)	H ₂ Yield	By-products	References
Glucose	5	B	80/7.5	250	3800	1000	2.8 mol H ₂ /mol glucose	Ac, Lac, CO ₂	(Dipasquale et al., 2014)
Glucose	5	B	80/7.1	250	2400	600	3.5 ± 0.1 mol H ₂ /mol glucose ^a	Ac, Lac, CO ₂	(d'Ippolito et al., 2010)
Glucose	10	B	72/7.0	350	2000	1000	3.5 mol H ₂ /mol glucose	Ac, Lac, CO ₂	(De Vrije et al., 2010)
Glucose	20	B	72/7.0	350	2000	1000	3.4 mol H ₂ /mol glucose	Ac, Lac, CO ₂	(De Vrije et al., 2010)
Glucose/Fructose 7:3	10	B	72/7.0	350	2000	1000	3.3 mol H ₂ /mol glucose	Ac, Lac, CO ₂	(De Vrije et al., 2010)
Glucose/Fructose 7:3	20	B	72/7.0	350	2000	1000	3.0 mol H ₂ /mol glucose	Ac, Lac, CO ₂	(De Vrije et al., 2010)
Fructose	10	B	72/7.0	350	2000	1000	3.4 mol H ₂ /mol fructose	Ac, Lac, CO ₂	(De Vrije et al., 2010)
Fructose	20	B	72/7.0	350	2000	1000	3.2 mol H ₂ /mol fructose	Ac, Lac, CO ₂	(De Vrije et al., 2010)

Carbon Source		Substrate Load (g/L)	Culture Type	T(°C)/Start pH	Mixing Speed (rpm)	Reactor Volume (mL)	Working Volume (mL)	H ₂ Yield	By-products	References
Carrot hydrolysate	pulp	10	B	72/7	350	2000	1000	2.7 mol H ₂ /mol glucose	Ac, Lac, CO ₂ , EtOH	(De Vrije et al., 2010)
Carrot hydrolysate	pulp	20	B	72/7	350	2000	1000	2.4 mol H ₂ /mol glucose	Ac, Lac, CO ₂ , EtOH	(De Vrije et al., 2010)
Glycerol		5	B	75/7.5	-	120	40	2.7 ± 0.1 mol H ₂ /mol glycerol	Ac, Lac, CO ₂	(Ngo et al., 2011a)
Molasses		20	B	77/8.5	100	116	40	2.6 ± 0.1 mol H ₂ /mol glucose	Ac, Lac, CO ₂	(Cappelletti et al., 2012)
Cheese whey		12.5	B	77/8.5	100	116	40	2.4 ± 0.1 mol H ₂ /mol glucose	Ac, Lac, CO ₂	(Cappelletti et al., 2012)
Diatom ^b water soluble sugars		2	B	80/7.5–8	250	3800	500	1.9 ± 0.1 mol H ₂ /mol glucose	Ac, Lac, CO ₂	(Dipasquale et al., 2012)
Glucose		5	B	80/8	200	120	60	3.8 ± 0.4 mol H ₂ /mol glucose	Ac, Lac, CO ₂	(Eriksen et al., 2011)

Carbon Source	Substrate Load (g/L)	Culture Type	T(°C)/Start pH	Mixing Speed (rpm)	Reactor Volume (mL)	Working Volume (mL)	H ₂ Yield	By-products	References
Arabinose	5	B	80/8	200	120	60	3.8 ± 0.5 mol H ₂ /mol arabinose	Ac, Lac, CO ₂	(Eriksen et al., 2011)
Xylose	5	B	80/8	200	120	60	3.4 ± 0.3 mol H ₂ /mol xylose	Ac, Lac, CO ₂	(Eriksen et al., 2011)
Potato steam peels	10	B	75/6.9	350	2000	1000	3.8 mol H ₂ /mol glucose	Ac, Lac, CO ₂	(Mars et al., 2010)
Glycerol	2.5	B	80/7.3	200	120/240	25/50	2.6 mol H ₂ /mol glycerol	Ac, Lac, CO ₂	(Maru et al., 2012)
Rice straw	10	B	75/7.5	150	120	40	2.7 mmol H ₂ /g straw	-	(Nguyen et al., 2010a)
Algal ^c starch	5	B	75/7–7.4	150	120	40	2.5 ± 0.3 mol H ₂ /mol glucose	-	(Nguyen et al., 2010b)
Glycerol	1–10	B	75/7.5	-	120	40	620 ± 30 mL H ₂ /L glycerol	Ac, Lac, CO ₂	(Ngo & Sim, 2012)
Xylose	5	B	75/7.5	300	3000	1000	2.8 ± 0.1 mol H ₂ /mol xylose	Ac, Lac, CO ₂	(Ngo et al., 2012)

Carbon Source	Substrate Load (g/L)	Culture Type	T(°C)/ Start pH	Mixing Speed (rpm)	Reactor Volume (mL)	Working Volume (mL)	H ₂ Yield	By-products	References
Glucose/Xylose 7:3	10–28	B	80/6.8	350	2000	1000	2.5–3.3 mol H ₂ /mol glucose	Ac, Lac, CO ₂	(De Vrije et al., 2009)
Cellulose	10–28	B	80/6.8	350	2000	1000	2.0–3.2 mol H ₂ /mol glucose	Ac, Lac, CO ₂	(De Vrije et al., 2009)
Xylose	5	B	75/7	300	3000	1000	1.8 ± 0.1 mol H ₂ /mol xylose	Ac, Lac, CO ₂	(Ngo & Bui, 2013)
Glucose	7.5	B	77/8.5	100	119	40	1.3 ± 0.1 mmol H ₂ /g glucose	Ac, Lac, CO ₂	(Frasconi et al., 2013)
Molasses	20	B	77/8.5	100	119	40	1.8 ± 0.1 mol H ₂ /g glucose	Ac, Lac, CO ₂	(Frasconi et al., 2013)
Cheese whey	12.5	B	77/8.5	100	119	40	1.04 ± 0.05 mol H ₂ /mol glucose	Ac, Lac, CO ₂	(Frasconi et al., 2013)
Glucose	5	FB	75/7.5	300	3000	1000	3.2 ± 0.2 mol H ₂ /mol glucose	Ac, Lac, CO ₂	(Ngo et al., 2011b)
Xylose	5	FB	75/7.5	300	3000	1000	2.2 ± 0.1 mol H ₂ /mol xylose	Ac, Lac, CO ₂	(Ngo et al., 2011b)

Carbon Source	Substrate Load (g/L)	Culture Type	T(°C)/Start pH	Mixing Speed (rpm)	Reactor Volume (mL)	Working Volume (mL)	H ₂ Yield	By-products	References
Sucrose	5	FB	75/7.5	300	3000	1000	4.9 ± 0.2 mol H ₂ /mol sucrose	Ac, Lac, CO ₂	(Ngo et al., 2011b)
Glucose	2.5	B	77/7.5	75	160	50	3.8 ± 0.3 mol H ₂ /mol glucose	Ac, Lac, CO ₂	(Munro et al., 2009)
Glucose	5	B	70/8.5	75	160	50	24% H ₂ (v/v) headspace ^d	CO ₂	(Van Ooteghem et al., 2004)
Glucose	7	B	77/7.5	150	120	40	3.2 ± 0.1 mol H ₂ /mol glucose	Ac, Lac, CO ₂	(Nguyen et al., 2008a)
Xylose	4	B	77/7.5	150	120	40	2.2 ± 0.1 mol H ₂ /mol xylose	Ac, Lac, CO ₂	(Nguyen et al., 2008a)
Glucose	5	B	70/8.5	-	160	50	25%–30% H ₂ (v/v) headspace ^d	Ac, Lac, CO ₂	(Van Ooteghem et al., 2002)

Carbon Source	Substrate Load (g/L)	Culture Type	T(°C)/ Start pH	Mixing Speed (rpm)	Reactor Volume (mL)	Working Volume (mL)	H ₂ Yield	By-products	References
Cellulose ^e	5	B	75– 80/7.5	150	120	50	0.25 ± 0.01 mol H ₂ /mol glucose	Ac, CO ₂	(Nguyen et al., 2008b)
Cellulose derivative	5	B	75– 80/7.5	150	120	50	0.77 ± 0.04 mol H ₂ /g glucose	Ac, CO ₂	(Nguyen et al., 2008b)
Cellulose	5	B	80/7.5	150	120	40	2.2 mol H ₂ /mol glucose	Ac, CO ₂	(Nguyen et al., 2008b)
Starch	5	B	75– 80/7.5	150	120	50	1.4 ± 0.1 mL H ₂ /g glucose	Ac, CO ₂	(Nguyen et al., 2008b)

^a excluding the estimated contribution from protein; ^b *Thalassiosira weissflogii*; ^c *Chlamydomonas reinhardtii*; ^d yield not reported; ^e *Miscanthus giganteus*.

There are conflicting reports on the effect of protein lysates on growth and H₂ production by *T. neapolitana*. Maru et al. (2012) noticed that reduced level of yeast extract (YE) negatively affects H₂ production but increasing concentration from 2 to 4 g/L did not induce significant change in gas evolution. On the contrary, increasing YE concentration from 1 to 4 g/L improved biomass and H₂ production in cultures of *T. neapolitana* on glycerol as reported by other independent studies (Ito et al., 2005; Ngo & Sim, 2012). No effect is reported through increasing the concentration of protein lysates above 5 g/L. Cappelletti et al. (2012) reported that partial production of H₂ can be due to metabolism of tryptone soy broth (TSB) whereas the contribution of YE is null. On the other hand, transformation of peptone, tryptone and YE yields 10–15% to the total H₂ production according to d'Ippolito et al. (2010) and (Eriksen et al., 2011).

2.6 Systems integration

According to Levin et al. (2004), H₂ production by dark fermentation is considered the most practically applicable process for production of the energy carrier. However, as shown in Fig. 2.1, only 2 mol of carbon from the substrate (*i.e.*, glucose) are fully oxidized to CO₂ and only 4 mol H₂ are formed. Thus, according to the dark fermentation model, a fermentative H₂ production can only convert, even in an optimal condition, less than 33% of the energy from the substrate (*e.g.*, glucose). On the other hand, the transformation efficiency can be significantly improved (theoretically up to 12 mol H₂ per mol of glucose) if a second biological process allows for the complete oxidation of the residual products released by the thermophilic process. In particular, photo-heterotrophic fermentation of organic acids produced by *T. neapolitana* is hypothetically entitled to produce a further 8 mol of H₂, thus reaching the maximum possible yield of 12 mol of H₂.

Purple nonsulphur (PNS) bacteria are a non-taxonomic group of microorganisms that are attractive for the biological production of H₂ from biomass (reviewed in (Basak & Das, 2007)). A few studies have also demonstrated that these microorganisms can be successfully integrated into a two-step process to produce H₂ in combination with dark fermentation. The first report of a two-stage process with *T. neapolitana* by Uyar et al. (2009) showed that *Rhodobacter capsulatus* effectively produces hydrogen when the concentration of acetate is lower than 60 mM in the spent medium of the thermophilic

bacterium. Interestingly these authors also noticed that addition of iron II in the range of 0–29 μM to the culture medium (*i.e.*, to the spent medium of thermophilic bacterium) of *R. capsulatus* increased the hydrogen production in a significant manner (1.37 L H_2 /L culture in effluent media supplemented with iron and vitamins; 0.30 L H_2 /L culture in effluent media supplemented only with vitamins). More recently, we have repeated the experiment with *T. neapolitana* and *Rhodospseudomonas palustris* by replacing the traditional conditions of DF (dark fermentation) with those of CLF (capnophilic lactic fermentation) (Dipasquale et al., 2015). To achieve photo-fermentation by a mutant strain of *R. palustris* (Adessi et al., 2012), *T. neapolitana* was grown under reduced level of NaCl and nitrogen-containing compounds. According to Uyar et al. (2009), the spent broths of the thermophilic bacterium were only supplemented with Fe-citrate and phosphate buffer. The combined microbial system gave 9.4 mol of hydrogen per mol of glucose consumed during the anaerobic process, which is the best production yield so far reported for conventional two-stage batch cultivations (Dipasquale et al., 2015). The results also proved that CLF can be used for inducing a metabolic switch in *T. neapolitana* that brings actual improvements of hydrogen yields in combination with photofermentation.

The advantages of using biomass for H_2 production range from the mitigation of CO_2 and other pollutant emissions, to reduction of environmental and economical costs for disposing wastes. Limitations in use of biomass are mainly due to the seasonal availability of agro wastes, costs of their collection and incomplete use of the organic matter. In this view, microalgal biomass is an attractive alternative since algal cultivation can theoretically run continuously with no restriction due to seasonal cycle and can yield large amounts of biomass of constant composition. Furthermore, fermentation of algal feedstock can be associated with production of biofuels or by-products of high value. *T. neapolitana* directly produces H_2 by fermentation of the biomass of the green alga *Chlamydomonas reinhardtii* with molar yields (1.8–2.2 mol/mol glucose equivalent) depending on pretreatment methods (Nguyen et al., 2010b). *T. neapolitana* possesses genes encoding both for a 1,3- β -glucosidase BglB (laminaribiase) and a 1,3- β -glucanase LamA (laminarinase) that are able to completely degrade chrysolaminarin, the storage polysaccharides of diatoms, to glucose with a synergic action (Zverlov et al., 1997a; Zverlov et al., 1997b). Accordingly, the

bacterium fermented the water-soluble fraction of the marine diatom *Thalassiosira weissflogii* without any pretreatment (Dipasquale et al., 2012). Production (434 mL/L in 24 h; 18.1 mL/L/h) and yield (2.2 mol H₂/mol glu. eq) of H₂ on diatom extracts containing 2 g/L of sugar equivalent were just slightly lower than those achieved by fermentation of glucose (809 mL/L in 24 h; 33.7 mL/L/h; 3.0 mol H₂/mol glu) and pure chrysolaminarin (643 mL/L in 24 h; 26.8 mL/L/h; 3.2 mol H₂/mol glu. eq).

2.7 Bioreactor configuration

Several bioreactor configurations such as continuously stirred tank reactors (CSTRs), fluidized bed reactors (FBRs), packed bed reactors (PBRs), up-flow anaerobic sludge blanket (UASB) reactors, anaerobic sequencing batch reactors (AnSBRs), high rate/hybrid reactors, and membrane biological reactors (MBRs) have promising prospects for dark fermentation processes (Krishna, 2013). Table 2.2 reports the CSTR used for fed-batch and continuous reactors studied for H₂ production by suspended and immobilized cells of *T. neapolitana*. CSTRs operate continuously and the bulk inside the reactor is mixed uniformly. However, the mixing rate depends on the reactor geometry and power input (Li et al., 2008b). CSTRs favor mass transfer among biomass, substrates and gases, and are effective in temperature and pH bulk control. However, CSTR can experience biomass washout, when the loading and the dilution rate increases.

The biomass washout is less probable in attached biomass reactors (e.g., FBRs, PBRs, UASB) where inert material is used to support and contain the bacteria, thus providing a high concentration of cells and, consequently high solids retention time, high organic load, high mass transfer efficiency and high tolerance for shock loads (Malina & Poland, 1992; Mohan et al., 2005; Ngo & Bui, 2013). Several inert materials have been used successfully as support for *T. neapolitana* growth, *i.e.*, coir, bagasse, loofah sponge, expanded clay, diatomaceous clay, activated carbon, polysaccharide gels (e.g., alginate, k-carrageenan, agar, chitosan), synthesized materials (e.g., polyvinyl alcohol (PVA), silicone, polyacrylamide, urethane foam and polymethyl methacrylate) (Angel et al., 1993; Basile et al., 2012a; Chang et al., 2002; Kumar & Das, 2001; Wu & Chang, 2007), ceramic porous carriers (*i.e.*, biomax) (Cappelletti et al., 2012; Frascari et al., 2013), and porous glass beads (Ngo & Bui, 2013). The batch fermentation tests conducted by Ngo and Bui have shown that the H₂ production rate and H₂ yield of the

immobilized cells reached the highest values of 5.64 ± 0.19 mmol H₂/L/h and 1.84 ± 0.1 mol H₂/mol xylose, respectively, which were 1.7- and 1.3-fold higher than those with free cells (Ngo & Bui, 2013). Synthetic hydrogels based on methacrylate derivatives with buffer capacity also effectively supported cell growth and hydrogen production (Basile et al., 2012a; Basile et al., 2012b). In particular, the use of hydrogel with positive charge and amine groups doubled hydrogen production rate compared with suspension cultures. Both sugar metabolism and hydrogen synthesis were affected positively by neutralization of the acidic side-products of the fermentation, *i.e.*, acetate and lactate. The presence of positively charged groups on the inert support proved to be critical to promote the colonization of the polymeric material by a great number of *T. neapolitana* cells laying in a biofilm-like arrangement.

Table 2. 2 Continuous and fed-batch operation in CSTRs for *T. neapolitana*.

Substrate	Reactor Volume (L)	Working Volume (L)	Temp. (°C)	Culture Type	Culture Condition	H ₂ Yield	References
Glucose/ Xylose/ Arabinose	3.0	2.75	80	Suspended cells	Fed-batch	3.8 ± 0.4 mol H ₂ /mol glucose; 3.4 ± 0.3 mol H ₂ /mol xylose; 3.8 ± 0.5 mol H ₂ /mol arabinose	(Eriksen et al., 2011)
Glucose/ Sucrose/ Xylose	3.0	1.0	75	Suspended cells	Fed-batch	3.2 ± 0.16 mol H ₂ /mol glucose; 4.95 ± 0.25 mol H ₂ /mol sucrose; 2.2 ± 0.11 mol H ₂ /mol xylose	(Ngo et al., 2011b)
Xylose	3.0	1.0	75	Immobilized cells	Fed-batch	1.84 ± 0.1 mol H ₂ /mol xylose	(Ngo & Bui, 2013)
Glucose/ Cheese whey/ Molasses	19.0	15.0	77	Suspended cells	Continuous	1.2 mmol H ₂ /L/h for glucose; 0.42 mmol/L/h for cheese whey; 1.3 mmol/L/h for molasses	(Frasconi et al., 2013)
Glucose	-	-	80	Immobilized cells	Fed-batch	3.3 mol H ₂ /mol glucose	(Basile et al., 2012a)

2.8 Operating conditions and kinetics of *T. neapolitana* fermentation

2.8.1 Hydraulic retention time

In the dark fermentative H₂ production, hydraulic retention time (HRT), organic loading rate (OLR) and pH are coupled variables since short HRT and high OLR generally correspond to low pH condition that affects the biomass metabolism. Both high OLR and low HRT represent favorable conditions for H₂ production as such operating conditions inhibits other slow growing bacteria, such as methanogens (Yang et al., 2007). A HRT in the range of 0.25–60 h (lower HRT for attached/immobilized biomass and higher HRT for suspended growth biomass) is proved to be suitable for hyperthermophilic dark fermentative H₂ production by *T. neapolitana* in batch, fed-batch and continuous bioreactors using a wide range of substrates such as glucose, sucrose, starch, lignocellulose, organic waste and algal starch (Kim et al., 2008). *T. neapolitana* is an exceptionally robust microorganism for H₂ production because of its efficient hydrolytic abilities and adaptability to different culture conditions. Nevertheless, production of H₂ is optimal only in very restricted range of operating conditions. In particular, the bacterium grows in a wide interval of temperatures (i.e., 55–90 °C) but the highest H₂ production occurs between 75 and 80 °C (Ngo et al., 2012).

2.8.2 Working pH

As reported above, culture pH is directly affected by the acidogenic activity. Consequently, pH control by base addition (e.g., NaOH) is critically important to maximize both H₂ production and substrate consumption (Khanna & Das, 2013; Munro et al., 2009; Ngo et al., 2011b). Growth of *T. neapolitana* is inhibited at pH of 4.5 (Van Ooteghem et al., 2004), whereas change from 4.0 to 5.5 induces an increase of H₂ content in the headspace from 42% to 64% (Fang & Liu, 2001). Nguyen et al. demonstrated that variation of pH in *T. neapolitana* cultures from 5.5 to 7.0 enhances cumulative H₂ production from 125 to 198 mL H₂/L medium, but further increase to 8.0–9.0 leads to total decline in the biogas evolution (Nguyen et al., 2008a). At laboratory scale, the strict control of pH has also suggested the use of compounds with increased buffer capacity such as diacid/monoacid phosphate (HPO₄²⁻/H₂PO₄⁻), tris (hydroxymethyl) aminomethane (TRIS), 3-(*N*-morpholino) propanesulfonic acid (MOPS), piperazine-*N,N'*-bis(2-ethanesulfonic) acid (PIPES), and 4-(2-hydroxyethyl)-1-piperazineethanesulfonic acid (HEPES) (De Vrije et al., 2009; Munro et al., 2009; Van Ooteghem et al., 2002;

Van Ooteghem et al., 2004). For large scale application the use of these chemicals is probably economically prohibitive but similar effects could be achieved by use of more convenient products (e.g., CO₂).

2.8.3 Temperature

The primary fermentation products for *T. neapolitana* across the permissive growth temperature range are H₂, CO₂, acetate and small amounts of lactate. Two independent studies on the influence of temperature on H₂ production of *T. neapolitana* and *T. maritima* support a direct correlation with H₂ production and bacterial growth (Munro et al., 2009; Nguyen et al., 2008b). Munro *et al.* reported that rate and amount of glucose consumption and H₂ formation increased by arising the operating temperature from 60 to 77 °C, but there was no significant difference from 77 to 85 °C (Munro et al., 2009). Although production of acetate and lactate indicated a difference between 77 and 85 °C, a comparison of the molar yields acetate/glucose and lactate/glucose for the operating temperatures between 65 and 85 °C suggested no significant change in molar yield for the two organic acids.

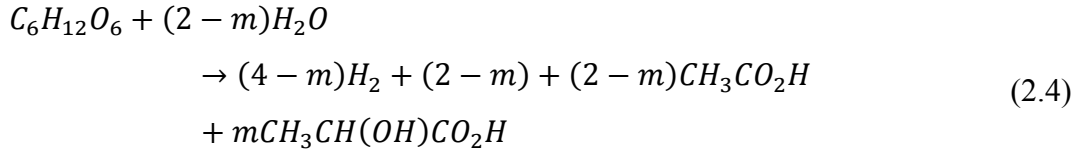
2.8.4 Partial pressure

The total and partial pressure of gas inside the reactor influences the biomass growth and product formation. According to Schonheit and Schafer (1995), H₂ itself inhibits the process in a batch reactor. van Niel et al. (2003) reported that H₂ partial pressure less than 20 kPa is required for reactor operating at high temperature (>70 °C). Partial pressure of H₂ above 20 kPa reverses the metabolic pathway, thereby facilitating the production of more reduced products such as acetone, ethanol, lactate, butanol and alanine (Angenenta et al., 2004; De Vrije et al., 2010; Hawkes et al., 2007). Experimental data show that use of pure nitrogen as gas sparging and high ratio between headspace volume/culture volume can contain the partial pressure of H₂ below the critical limit in cultures of *T. neapolitana* (Eriksen et al., 2011; Munro et al., 2009; Thauer, 1977). Increase in yield and production of H₂ are reported by N₂ sparging compared to no sparging condition (d'Ippolito et al., 2010; Nguyen et al., 2008a). The tolerance of *T. neapolitana* to oxygen is matter of debate. Van Ooteghem *et al.* described significant improvement of H₂ production under microaerobic condition (Van Ooteghem et al., 2002; Van Ooteghem et al., 2004), whereas Eriksen *et al.*, in line with other studies, reported that *T. neapolitana* can tolerate only low oxygen partial pressure

(1% or 1.2 kPa) and found that 6% O₂ (7.2 kPa) inside the reactor completely inhibits H₂ production and reduces glucose consumption from 12 to 4 μmol/h (Eriksen et al., 2008).

2.8.5 Mathematical modeling and kinetics

Metabolic transformation of glucose by *T. neapolitana* can be effectively described with the Eq. (2.4).



where m is a stoichiometric coefficient (Dipasquale et al., 2014). A majority of studies have either adapted or modified existing mathematical (or empirical) models to describe the experimental results (Gadhe et al., 2013). Gompertz empirical model (Eq. (2.5)) and International Water Association (IWA) anaerobic digestion model No. 1 (ADM1) are the most popular models to simulate dark fermentation. The Gompertz model is particularly used to estimate the maximum hydrogen production potential and to determine the lag phase for H₂ production (Gadhamshtetty et al., 2010) but it does not allow the process kinetics to be addressed because of the exclusion of operating conditions (e.g., substrate type and concentration, pH, temperature, and partial pressure of gas mixture) that regulate the fermentation reaction (Gadhamshtetty et al., 2010).

$$H(t) = P * \exp \left\{ - \exp \left[\frac{R_m e}{P} (\lambda - t) + 1 \right] \right\} \tag{2.5}$$

where

$H(t)$ = Cumulative H₂ production (mL/L)

P = H₂ production potential (mL H₂)

R_m = Maximum H₂ production rate (mL H₂/h)

t = Incubation/cultivation time (h)

λ = Duration of the lag phase (h)

On the other hand, ADM1 is a complete and comprehensive kinetic model based on Monod kinetic Eq. (2.6) (Batstone et al., 2002; Castello et al., 2009; Fuentes et al., 2011; Paulo et al., 2013; Wang & Wan, 2009) and has been used often to model DF reactions (Fracari et al., 2013; Wang & Wan, 2009; Yu & Drapcho, 2011).

$$\mu = \frac{\mu_{\max} S}{k_s + S} \quad (2.6)$$

where

μ = specific growth rate of biomass (h^{-1})

μ_{\max} = maximum specific growth rate of biomass (h^{-1})

k_s = semi saturation constant (g/L); k_s equals the substrate concentration at which μ equals $\frac{1}{2} \mu_{\max}$

S = substrate concentration (g/L)

The ADM1-based model and Gompertz empirical model have been extensively used to study H_2 production by fermentative process, but to date there are only two studies with *T. neapolitana*. In pure culture on glucose at 77 °C, Yu and Drapcho (2011) reported maximum specific maximum growth rate (μ_{\max}) of 0.94 1/h and semi saturation constant (k_s) of 0.57 g sugar/L when H_2 and biomass product yields were 0.0286 g H_2 /g glucose and 0.248 g biomass/g glucose, respectively. More recently, Frascari et al. (2013) have studied the kinetic parameters for *T. neapolitana* grown on glucose, molasses and cheese whey by suspended or immobilized cells. The μ_{\max} value with immobilized bacteria (0.09 ± 0.05 1/h for glucose, 0.19 ± 0.02 1/h for molasses and 0.042 ± 0.007 1/h for cheese whey) was found to be significantly higher than with suspended cells (0.024 ± 0.005 1/h for glucose, 0.055 ± 0.005 1/h for molasses and 0.033 ± 0.006 1/h for cheese whey). On the contrary, the semi saturation constant (k_s) was 0.09 ± 0.05 g sugar/L for glucose, 0.6 ± 0.2 g sugar/L for molasses and 1.2 ± 0.3 g sugar/L for cheese whey in the immobilized systems and 1.1 ± 0.3 g sugar/L for glucose, 0.2 ± 0.05 g sugar/L for molasses and 1.5 ± 0.5 g sugar/L for cheese whey with bacterial suspensions (Frascari et al., 2013).

2.9 Conclusions

Among the various technologies, fermentation has many advantages for the biological production of H₂ and is theoretically feasible for large-scale application particularly from the fermentation of solid wastes (Kovács et al., 2006; Munoz-Páez et al., 2012). Extensive research in the last decades has shown the promising prospect of using pure cultures of the bacterium *T. neapolitana*. Like other hyperthermophilic process, the technology is readily used at laboratory scale with high production rate, low energy demand, easy operation and sustainability. On the contrary little has been done in terms of comparison of cost and effectiveness between *T. neapolitana* and traditional processes that use fossil fuel for production of hydrogen.

T. neapolitana has also shown great potential for other applications such as recovery of byproducts with potential economic value in the market *i.e.*, lactic acid. Introduction of capnophilic process for the simultaneous production of H₂ and lactic acid is very promising and could significantly influence the future of agro-waste management. Clearly, further research is needed to optimize the operating parameters and reactor configurations and more experiments are needed to verify process kinetics and full-scale applicability. Nevertheless, fermentation of organic material by the thermophilic bacterium could be the beachhead of a complete conversion process that generates H₂ only as a first step.

Agro-food wastes and algal biomass seem to be attractive substrates for fermentation by *T. neapolitana* and thus are considered as feedstock for comprehensive development of biorefineries. Moreover, coupling of *T. neapolitana*-based transformation with other biological processes also seems very promising. In this view, chemotrophic production of hydrogen by hyperthermophilic bacteria has already shown great potential in association with both microalgal cultivations and photofermentation by purple nonsulphur bacteria. Finally, considerable enhancement of the fermentative capacity of *T. neapolitana* can be also expected by metabolic engineering and physiological manipulations of strains, as well as by improvement in reactor configurations (Hallenbeck & Benemann, 2002; Mathews & Wang). In fact, for example the unexpected success of CLF suggests that a huge unexplored gene pool available in nature, with great potential for H₂ production, is yet to be discovered (Show et al., 2012).

References

- Adessi, A., McKinlay, J.B., Harwood, C.S., de Philippis, R. 2012. A *Rhodospseudomonas palustris nifA** mutant produces hydrogen from NH₄⁺ containing vegetable wastes. *International Journal of Hydrogen Energy*, **37**, 15893-15900.
- Albertini, M., Vallese, F., Valentin, M., Berto, P., Giacometti, G.M., Costantini, P., Carbonera, D. 2014. The proton iron-sulfur cluster environment of the [FeFe]-hydrogenase maturation protein HydF from *Thermotoga neapolitana*. *International Journal of Hydrogen Energy*, **39**, 18574-18582.
- Amend, J.P., Shock, E.L. 2001. Energetics of overall metabolic reactions of thermophilic and hyperthermophilic Archaea and Bacteria. *FEMS Microbiology Reviews*, **25**, 175-243.
- Angel, A.M., Brunene, M., Baumeister, W. 1993. The functional properties of Omp β , the regularly arrayed porin of the hyperthermophilic bacterium *Thermotoga neapolitana*. *FEMS Microbiology Letters*, **109**, 231-236.
- Angenenta, L.T., Karima, K., Al-Dahhana, M.H., Brian, A., Wrennb, B.A., Domínguez-Espinosad, R. 2004. Production of bioengineering and biochemical's from industrial and agricultural wastewater. *Trends in Microbiology*, **22**, 477-485.
- Anshuman, K., Mike, M., Brenda, J. 2005. Hydrogen: The energy source for the 21st century. *Technovation*, **25**, 569-585.
- Basak, N., Das, D. 2007. The prospect of purple non-sulfur (PNS) photosynthetic bacteria for hydrogen production: The present state of the art. *World Journal of Microbiology & Biotechnology*, **23**, 31-42.
- Basile, M.A., Carfagna, C., Cerruti, P., d'Ayala, G.G., Fontana, A., Gambacorta, A., Malinconico, M., Dipasquale, L. 2012a. Continuous hydrogen production by immobilized cultures of *Thermotoga neapolitana* on an acrylic hydrogel with pH-buffering properties. *Rsc Advances*, **2**, 3611-14.
- Basile, M.A., Carfagna, C., Dipasquale, L., Fontana, A., Gambacorta, A., d'Ayala, G.G., Malinconico, M., Cerruti, P. 2012b. Development of novel immobilizing hydrogels for thermophilic hydrogen production. in: *Hydrogen Production: Prospects and Processes*, pp. 399-409.
- Batstone, D.J., Keller, J., Angelidaki, I., Kalyuzhnyi, S.V., Pavlostathis, S.G., Rozzi, A. 2002. Anaerobic digestion model No. 1. *IWA Scientific and Technical Report* **13**.
- Belkin, S., Wirsén, C.O., Jannasch, H.W. 1986. A new sulfur-reducing, extremely thermophilic eubacterium from a submarine thermal vent. *Appl. Environ. Microbiol.*, **51**, 1180-1185.
- Berg, I.A., Kockelkorn, D., Ramos-vera, W.H., Say, R.F., Zarzycki, J., Hugler, M., Alber, B.E., Fuchs, G. 2010. Autotrophic carbon fixation in archaea. *Nat. Rev. Microbiol.*, **8**, 447-460.
- Bhandari, V., Gupta, R.S. 2014. Molecular signatures for the phylum (class) Thermotogae and a proposal for its division into three orders (*Thermotogales*,

- Kosmotogales* ord. nov. and *Petrotogales* ord. nov.) containing four families (*Thermotogaceae*, *Fervidobacteriaceae* fam. nov., *Kosmotogaceae* fam. nov. and *Petrotogaceae* fam. nov.) and a new genus *Pseudothermotoga* gen. nov. with five new combinations. *Antonie van Leeuwenhoek, International Journal of General and Molecular Microbiology*, **105**, 143-168.
- Bock, A.K., Kunow, J., Glasemacher, J., Schönheit, P. 1996. Catalytic properties, molecular composition and sequence alignments of pyruvate: Ferredoxin oxidoreductase from the methanogenic archaeon *Methanosarcina barkeri* (strain Fusaro). *Eur. J. Biochem.*, **237**, 35-44.
- Braakman, R., Smith, E. 2010. The emergence and early evolution of biological carbon-fixation. *PLoS Comput. Biol.*, **8**, e1002455.
- Cappelletti, M., Bucchi, G., Mendes, J.D.S., Alberini, A., Fedi, S., Bertin, L., Frascari, D. 2012. Biohydrogen production from glucose, molasses and cheese whey by suspended and attached cells of four hyperthermophilic *Thermotoga* strains. *Journal of Chemical Technology and Biotechnology*, **87**, 1291-1301.
- Cappelletti, M., Zannoni, D., Postec, A., Ollivier, B. 2014. Members of the order *Thermotogales*: from microbiology to hydrogen production. in: *Microbial bioenergy: hydrogen production* (Eds.) D. Zannoni, R. DePhilippis, Vol. 38, pp. 197-224.
- Castello, E., Garcia y Santos, C., Iglesias, T., Paolino, G., Wenzel, J., Borzacconi, L., Etchebehere, C. 2009. Feasibility of biohydrogen production from cheese whey using a UASB reactor: Links between microbial community and reactor performance. *International Journal of Hydrogen Energy*, **34**, 5674-5682.
- Chang, J.S., Lee, K.S., Lin, P.J. 2002. Biohydrogen production with fixed-bed bioreactors. *International Journal of Hydrogen Energy*, **27**, 1167-1174.
- Choi, K.H., Hwang, S., Lee, H.S., Cha, J. 2011. Identification of an extracellular thermostable glycosyl hydrolase family 13 α -amylase from *Thermotoga neapolitana*. *Journal of Microbiology*, **49**, 628-634.
- Choi, K.W., Seo, J.Y., Park, K.M., Park, C.S., Cha, J. 2009. Characterization of glycosyl hydrolase family 3 β -N-acetylglucosaminidases from *Thermotoga maritima* and *Thermotoga neapolitana*. *J. Biosci. Bioeng.*, **108**, 455-459.
- d'Ippolito, G., Dipasquale, L., Fontana, A. 2014. Recycling of carbon dioxide and acetate as lactic acid by the hydrogen-producing bacterium *thermotoga neapolitana*. *ChemSusChem*.
- d'Ippolito, G., Dipasquale, L., Vella, F.M., Romano, I., Gambacorta, A., Cutignano, A., Fontana, A. 2010. Hydrogen metabolism in the extreme thermophile *Thermotoga neapolitana*. *International Journal of Hydrogen Energy*, **35**, 2290-2295.
- De Vrije, T., Bakker, R.R., Budde, M.A.W., Lai, M.H., Mars, A.E., Claassen, P.A.M. 2009. Efficient hydrogen production from the lignocellulosic energy crop miscanthus by the extreme thermophilic bacteria *Caldicellulosiruptor saccharolyticus* and *Thermotoga neapolitana*. *Biotechnol. Biofuels*, **2**, 12.

- De Vrije, T., Budde, M.A.W., Lips, S.J., Bakker, R.R., Mars, A.E., Claassen, P.A.M. 2010. Hydrogen production from carrot pulp by the extreme thermophiles *Caldicellulosiruptor saccharolyticus* and *Thermotoga neapolitana*. *Int. J. Hydrog. Energy*, **35**, 13206-13213.
- Dipasquale, L., Adessi, A., d'Ippolito, G., Rossi, F., Fontana, A., De Philippis, R. 2015. Introducing capnophilic lactic fermentation in a combined dark-photo fermentation process: a route to unparalleled hydrogen yields. *Applied Microbiology and Biotechnology*, **99**, 1001-10.
- Dipasquale, L., d'Ippolito, G., Fontana, A. 2014. Capnophilic lactic fermentation and hydrogen synthesis by *Thermotoga neapolitana*: An unexpected deviation from the dark fermentation model. *International Journal of Hydrogen Energy*, **39**, 4857-4862.
- Dipasquale, L., d'Ippolito, G., Gallo, C., Vella, F.M., Gambacorta, A., Picariello, G., Fontana, A. 2012. Hydrogen production by the thermophilic eubacterium *Thermotoga neapolitana* from storage polysaccharides of the carbon dioxide fixing diatom *Thalassiosira weissflogii*. *International Journal of Hydrogen Energy*, **37**, 12250-12257.
- Dipasquale, L., Gambacorta, A., Siciliano, R.A., Mazzeo, M.F., Lama, L. 2009. Purification and biochemical characterization of a native invertase from the hydrogen-producing *Thermotoga neapolitana*. *Extremophiles*, **13**, 345-354.
- Djomo, S.N., Blumberg, D. 2011. Comparative life cycle assessment of three biohydrogen pathways. *Bioresource Technology*, **102**(3), 2684-2694.
- Elsharnouby, O., Hafez, H., Nakhla, G., el Naggar, M.H. 2013. A critical literature review on biohydrogen production by pure cultures. *International Journal of Hydrogen Energy*, **38**, 4945-4966.
- Eriksen, N.T., Riis, M.L., Holm, N.K., Iversen, N. 2011. Hydrogen synthesis from pentoses and biomass in *Thermotoga* spp. *Biotechnology Letters*, **33**, 293-300.
- Eriksen, T.N., Niels, N.T., Iversen, N. 2008. Hydrogen production in anaerobic and microaerobic *Thermotoga neapolitana*. *Biotechnol. Lett.*, **30**, 103-109.
- Fan, Y.T., Zhang, Y.H., Zhang, S.F., Hou, H.W., Ren, B.Z. 2006. Efficient conversion of wheat straw wastes into biohydrogen gas by cow dung compost. *Bioresource Technology*, **97**, 500-505.
- Fang, H.H.P., Liu, H. 2001. Granulation of hydrogen producing acidogenic sludge. *9th World Congress Anaerobic Digestion*, **2**, 527-532.
- Frasconi, D., Cappelletti, M., Mendes, J.D.S., Alberini, A., Scimonelli, F., Manfreda, C., Longanesi, L., Zannoni, D., Pinelli, D., Fedi, S. 2013. A kinetic study of biohydrogen production from glucose, molasses and cheese whey by suspended and attached cells of *Thermotoga neapolitana*. *Bioresource Technology*, **147**, 553-61.
- Frock, A.D., Notey, J.S., Kelly, R.M. 2010. The genus *Thermotoga*: Recent developments. *Environ. Tech.*, **31**, 1169-1181.

- Fuentes, M., Scenna, N.J., Aguirre, P.A. 2011. Modeling of hydrogen production in biofilm reactors: Application of the Anaerobic Digestion Model 1. *Hyfusen*, 01-233.
- Furdui, C., Ragsdale, S.W. 2000. The role of pyruvate ferredoxin oxidoreductase in pyruvate synthesis during autotrophic growth by the Wood-Ljungdahl pathway. *J. Biol. Chem.* , **275**, 28494-99.
- Gadhamshetty, V., Arudchelvam, Y., Nirmalakhandan, N., Johnson, D.C. 2010. Modeling dark fermentation for biohydrogen production: ADM1-based model vs. Gompertz model. *International Journal of Hydrogen Energy*, **35**, 479-490.
- Gadhe, A., Sonawane, S., Varma, M. 2013. Kinetic modeling of biohydrogen production from complex wastewater by anaerobic cultures. *Research Journal of Chemistry and Environment*, **17**, 129-135.
- Guo, X.M., Trably, E., Latrille, E., Carrere, H., Steyer, J.-P. 2010a. Hydrogen production from agricultural waste by dark fermentation: A review. *International Journal of Hydrogen Energy*, **35**(19), 10660-10673.
- Hafez, H., Nakhla, G., el Naggar, H. 2012. Biological hydrogen production. *Handbook of Hydrogen Energy*.
- Hawkes, F.R., Hussy, I., Kyazza, G., Dinsdale, R., Hawkes, D.L. 2007. Continuous dark fermentative hydrogen production by mesophilic microflora: Principles and progress. *International Journal of Hydrogen Energy*, **32**, 172-184.
- Huber, R., Langworthy, T.A., Konig, H., Thomm, M., Woese, C.R., Sleytr, U.B., Stetter, K.O. 1986. *Thermotoga maritima* sp. nov. represents a new genus of unique extremely thermophilic eubacteria growing up to 90 °C. *Arch. Microbiol.*, **144**, 324-333.
- Islam, R., Cicek, N., Sparling, R., Levin, D. 2009. Influence of initial cellulose concentration on the carbon flow distribution during batch fermentation by *Clostridium thermocellum* ATCC 27405. *Appl. Microbiol. Biotechnol.* , **82**, 141-148.
- Ito, T., Nakashimada, Y., Senba, K., Matsui, T., Nishio, N. 2005. Hydrogen and ethanol production from Glycerol-containing wastes discharged after biodiesel manufacturing process. *J. Biosci. Bioeng.* , **100**, 260-265.
- Jannasch, H.W., Huber, R., Belkin, S., Stetter, K.O. 1988. *Thermotoga neapolitana* sp. nov. of the extremely thermophilic, eubacterial genus *Thermotoga*. *Archives of Microbiology*, **150**, 103-104.
- Kang, L., Park, K.M., Choi, K.H., Park, C.S., Kim, G.E., Kim, D., Cha, J. 2011. Molecular cloning and biochemical characterization of a heat-stable pullulanase type I from *Thermotoga neapolitana*. *Enzym. Microb. Technol.*, **48**, 260-266.
- Khanna, N., Das, D. 2013. Biohydrogen production by dark fermentation. *Wiley Interdisciplinary Reviews-Energy and Environment*, **2**, 401-421.
- Kim, S.H., Han, S.K., Shin, H.S. 2008. Optimization of continuous hydrogen fermentation of food waste as a function of solids retention time independent of hydraulic retention time. *Process Biochem.*, **43**, 213-218.

- Kotsopoulos, T.A., Fotidis, I.A., Tsolakis, N., Martzopoulos, G.G. 2009. Biohydrogen production from pig slurry in a CSTR reactor system with mixed cultures under hyper-thermophilic temperature (70 °C). *Biomass and Bioenergy*, **33**(9), 1168-1174.
- Kovács, K.L., Maróti, G., Rákhely, G. 2006. A novel approach for biohydrogen production. *International Journal of Hydrogen Energy*, **31**, 1460-68.
- Krebs, H.A. 1941. Carbon dioxide assimilation in heterotrophic organisms. *Nature*, **147**, 560-563.
- Krishna, R.H. 2013. Review of research on bioreactors used in wastewater treatment for production of biohydrogen: Future fuel. *Int. J. Sci. Invent. Today*, **2**, 302-310.
- Kumar, N., Das, D. 2001. Continuous hydrogen production by immobilized *Enterobacter cloacae* IIT-BT 08 using lignocellulosic materials as solid matrices. *Enzym. Microb. Technol.*, **29**, 280-287.
- Kuwabara, T., Igarashi, K. 2012. Microscopic studies on *Thermosipho globiformans* implicate a role of the large periplasm of *Thermotogales*. *Extremophiles*, **16**, 863-870.
- Lama, L., Tramice, A., Finore, I., Anzelmo, G., Calandrelli, V., Pagnotta, E., Tommonaro, G., Poli, A., Di Donato, P., Nicolaus, B., Fagnano, M., Mori, M., Impagliazzo, A., Trincone, A. 2014. Degradative actions of microbial xylanolytic activities on hemicelluloses from rhizome of *Arundo donax*. *AMB Express*, **4**.
- Latif, H., Lerman, J.A., Portnoy, V.A., Tarasova, Y., Nagarajan, H. 2013. The Genome Organization of *Thermotoga maritima* reflects its lifestyle. *PLoS Genet.*, **9**, e1003485.
- Levin, D.B., Pitt, L., Love, M. 2004. Biohydrogen production: Prospects and limitations to practical application. *International Journal of Hydrogen Energy*, **29**, 173-185.
- Li, F., Hinderberger, J., Seedorf, H., Zhang, J., Buckel, W., Thauer, R.K. 2008a. Coupled ferredoxin and crotonyl coenzyme A (CoA) reduction with NADH catalyzed by the butyryl-CoA deH₂ase/Etf complex from *Clostridium kluyveri*. *J. Bacteriol.*, **190**, 843-850.
- Li, R.Y., Zhang, T., Fang, H.H.P. 2008b. Characteristics of a phototrophic sludge producing hydrogen from acetate and butyrate. *International Journal of Hydrogen Energy*, **33**, 2147-55.
- Liebl, W.G., Winterhalter, C., Baumeister, W., Armbrech, M., Valdez, M. 2008. Xylanase attachment to the cell wall of the hyperthermophilic bacterium *Thermotoga maritima*. *J. Bacteriol*, **190**, 1350-1358.
- Liu, Y., Yu, P., Song, X., Qu, Y. 2008. Hydrogen production from cellulose by co-culture of *Clostridium thermocellum* JN4 and *Thermoanaerobacterium thermosaccharolyticum* GD17. *Int. J. Hydrog. Energy* **33**, 2927-2933.
- Malina, J.F., Poland, F.G. 1992. Design of anaerobic processes for treatment of industrial and municipal wastes. *Technomic Publishing Co., Inc.: Lanchester, UK*.

- Mars, A.E., Veuskens, T., Budde, M.A.W., van Doeveren, P.F.N.M., Lips, S.J., Bakker, R.R., de Vrije, T., Claassen, P.A.M. 2010. Biohydrogen production from untreated and hydrolyzed potato steam peels by the extreme thermophiles *Caldicellulosiruptor saccharolyticus* and *Thermotoga neapolitana*. *International Journal of Hydrogen Energy*, **35**, 7730–7737.
- Maru, B.T., Bielen, A.A.M., Kengen, S.W.M., Constanti, M., Medina, F. 2012. Biohydrogen production from glycerol using *Thermotoga* spp. *Energy Procedia*, **29**, 300-307.
- Mathews, J., Wang, G. Metabolic pathway engineering for enhanced biohydrogen production. *International Journal of Hydrogen Energy*, **34**, 7404-7416.
- Mizuno, O., Dinsdale, R., Hawkes, F., Hawkes, D., Noike, T. 2000. Enhancement of hydrogen production from glucose by nitrogen gas sparging. *Bioresour. Technol.*, **73**, 59-65.
- Mohan, S.V., Rao, N.C., Prasad, K.K., Madhavi, B.T.V., Sarma, P.N. 2005. Treatment of complex chemical effluents by sequencing batch reactor (SBR) with aerobic suspended growth configuration. *Process Biochem.*, **40**, 1501-1508.
- Munoz-Páez, K.M., Ríos-Leal, E., Valdez-Vazquez, I. 2012. Re-fermentation of washed spent solids from batch hydrogenogenic fermentation for additional production of biohydrogen from the organic fraction of municipal solid waste. *Journal of Environmental Management*, **95**, 355–359.
- Munro, S.A., Choe, L., Zinder, S.H., Lee, K.H., Walker, L.P. 2012. Proteomic and physiological experiments to test *Thermotoga neapolitana* constraint-based model hypotheses of carbon source utilization. *Biotechnol. Prog.*, **28**, 312-318.
- Munro, S.A., Zinder, S.H., Walker, L.P. 2009. The fermentation stoichiometry of *Thermotoga neapolitana* and influence of temperature, oxygen, and pH on hydrogen production. *Biotechnology Progress*, **25**, 1035-1042.
- Nath, K., Das, D. 2004. Improvement of fermentative hydrogen production: Various approaches. *Applied Microbiology and Biotechnology*, **65**, 520-529.
- Nesbo, C.L., Bradnan, D.N., Adebusuyi, A., Dlutek, M., Petrus, A.K., Foght, J., Doolittle, W.F., Noll, K.M. 2012. *Mesotoga prima* gen. nov., sp. nov., the first described mesophilic species of the *Thermotogales*. *Extremophiles*, **16**, 387-393.
- Ngo, T.A., Bui, H.T.V. 2013. Biohydrogen production using immobilized cells of hyperthermophilic eubacterium *Thermotoga neapolitana* on porous glass beads. *Journal of Technology Innovations in Renewable Energy*, **2**, 231-238.
- Ngo, T.A., Kim, M.S., Sim, S.J. 2011a. High-yield biohydrogen production from biodiesel manufacturing waste by *Thermotoga neapolitana*. *International Journal of Hydrogen Energy*, **36**, 5836-42.
- Ngo, T.A., Kim, M.S., Sim, S.J. 2011b. Thermophilic hydrogen fermentation using *Thermotoga neapolitana* DSM 4359 by fed-batch culture. *International Journal of Hydrogen Energy*, **36**, 14014-23.

- Ngo, T.A., Nguyen, T.H., Bui, H.T.V. 2012. Thermophilic fermentative hydrogen production from xylose by *Thermotoga neapolitana* DSM 4359. *Renewable Energy*, **37**, 174-179.
- Ngo, T.A., Sim, S.J. 2012. Dark fermentation of hydrogen from waste glycerol using hyperthermophilic eubacterium *Thermotoga neapolitana*. *Environmental Progress and Sustainable Energy*, **31**, 466-473.
- Nguyen, T.A.D., Han, S.J., Kim, J.P., Kim, M.S., Oh, Y.K., Sim, S.J. 2008a. Hydrogen production by the hyperthermophilic eubacterium, *Thermotoga neapolitana*, using cellulose pretreated by ionic liquid. *International Journal of Hydrogen Energy*, **33**, 5161-68.
- Nguyen, T.A.D., Kim, J.P., Kim, M.S., Oh, Y.K., Sim, S.J. 2008b. Optimization of hydrogen production by hyperthermophilic eubacteria, *Thermotoga maritima* and *Thermotoga neapolitana* in batch fermentation. *International Journal of Hydrogen Energy*, **33**, 1483-88.
- Nguyen, T.A.D., Kim, K.R., Kim, M.S., Sim, S.J. 2010a. Thermophilic hydrogen fermentation from Korean rice straw by *Thermotoga neapolitana*. *International Journal of Hydrogen Energy*, **35**, 13392-98.
- Nguyen, T.A.D., Kim, K.R., Nguyen, M.T., Kim, M.S., Kim, D., Sim, S.J. 2010b. Enhancement of fermentative hydrogen production from green algal biomass of *Thermotoga neapolitana* by various pretreatment methods. *International Journal of Hydrogen Energy*, **35**, 13035-40.
- Oh, Y.-K., Raj, S.M., Jung, G.Y., Park, S. 2011. Current status of the metabolic engineering of microorganisms for biohydrogen production. *Bioresource Technology*, **102**, 8357-67.
- Okazaki, F., Nakashima, N., Ogino, C., Tamaru, Y., Kondo, A. 2013. Biochemical characterization of a thermostable β -1,3-xylanase from the hyperthermophilic eubacterium, *Thermotoga neapolitana* strain DSM 4359. *Applied Microbiology and Biotechnology*, **97**, 6749-57.
- Paulo, C.I., Di Maggio, J.A., Soledad Diaz, M., Ruggeri, B. 2013. Modeling and Parameter Estimation in Biofuel Discontinuous Production by Hydrogen Forming Bacteria (HFB). *11th International Conference on Chemical and Process Engineering*, **32**, 1033-1038.
- Pott, R.W.M., Howe, C.J., Dennis, J.S. 2013. Photofermentation of crude glycerol from biodiesel using *Rhodospseudomonas palustris*: Comparison with organic acids and the identification of inhibitory compounds. *Bioresource Technology*, **130**, 725-730.
- Pozzo, T., Pasten, J.L., Karlsson, E.N., Logan, D.T. 2010. Structural and Functional Analyses of β -Glucosidase 3B from *Thermotoga neapolitana*: A Thermostable Three-Domain Representative of Glycoside Hydrolase 3. *Journal of Molecular Biology*, **397**, 724-739.

- Rachel, R., Engel, A.M., Huber, R., Stetter, K.O., Baumeister, W. 1990. A porin-type protein is the main constituent of the cell envelope of the ancestral bacterium *Thermotoga maritima*. *FEBS Letters*, **262**, 64-68.
- Ravot, G., Magot, M., Fardeau, M.L., Patel, B.K.C., Prensier, G., Egan, A., Garcia, J.L., Ollivier, B. 1995. *Thermotoga elfii* Sp-Nov, a novel thermophilic bacterium from an african oil-producing well. *Int. J. Syst. Bacteriol.*, **45**, 308-314.
- Schonheit, P., Schafer, T. 1995. Metabolism of hyperthermophiles. *World J. Microbiol. Biotechnol.*, **11**, 26-57.
- Schroder, C., Selig, M., Schonheit, P. 1994. Glucose fermentation to acetate, carbon dioxide and hydrogen in the anaerobic hyperthermophilic eubacterium *Thermotoga maritima*-involvement of the Embden-Meyerhof pathway. *Arch. Microbiol.*, **161**, 460-470.
- Schumann, J., Wrba, A., Jaenicke, R., Stetter, K.O. 1991. Topographical and enzymatic characterization of amylases from the extremely thermophilic eubacterium *Thermotoga maritima*. *FEBS Letters*, **282**, 122-126.
- Schut, G.J., Adams, M.W. 2009. The iron-H₂ase of *Thermotoga maritima* utilizes ferredoxin and NADH synergistically: A new perspective on anaerobic hydrogen production. *J. Bacteriol.*, **191**, 4451-4457.
- Show, K.Y., Lee, D.J., Tay, J.H., Lin, C.Y., Chang, J.S. 2012. Biohydrogen production: Current perspectives and the way forward. *International Journal of Hydrogen Energy*, **37**, 15616-31.
- Sinha, P., Pandey, A. 2011. An evaluative report and challenges for fermentative biohydrogen production. *International Journal of Hydrogen Energy*, **36**(13), 7460-7478.
- Thauer, R. 1977. Limitation of microbial hydrogen formation via fermentatio. *Microbial Energy Conversion*, 201-204.
- Uyar, B., Eroglu, I., Yucel, M., Gunduz, U. 2009. Photofermentative hydrogen production from volatile fatty acids present in dark fermentation effluents. *International Journal of Hydrogen Energy*, **34**, 4517-23.
- Valdez, I., Rios, E., Carmona, A., Muñoz, K., Poggi, H. 2006. Improvement of biohydrogen production from solid wastes by intermittent venting and gas flushing of batch reactors headspace. *Environ. Sci. Technol.*, **40**, 3409-3415.
- van Niel, E.W.J., Claassen, P.A.M., Stams, A.J.M. 2003. Substrate and product inhibition of hydrogen production by the extreme thermophile, *Caldicellulosiruptor saccharolyticus*. *Biotechnology and Bioengineering*, **81**, 255-262.
- Van Ooteghem, S.A., Beer, S.K., Yue, P.C. 2002. Hydrogen production by the thermophilic bacterium *Thermotoga neapolitana*. *Applied Biochemistry and Biotechnology - Part A Enzyme Engineering and Biotechnology*, **98-100**, 177-189.
- Van Ooteghem, S.A., Jones, A., Van Der Lelie, D., Dong, B., Mahajan, D. 2004. Hydrogen production and carbon utilization by *Thermotoga neapolitana* under

- anaerobic and microaerobic growth conditions. *Biotechnology Letters*, **26**, 1223-32.
- Verhaart, M.R., Bielen, A.A., Oost, J.V.D., Stams, A.J., Kengen, S.W. 2010. Hydrogen production by hyperthermophilic and extremely thermophilic bacteria and archaea: Mechanisms for reductant disposal. *Environmental Technology*, **31**, 993-1003.
- Vijayaraghavan, K., Ahmad, D. 2006. Biohydrogen generation from palm oil mill effluent using anaerobic contact filter. *International Journal of Hydrogen Energy*, **31**, 1284-1291.
- Wang, J., Wan, W. 2009. Kinetic models for fermentative hydrogen production: A review. *International Journal of Hydrogen Energy*, **34**, 3313.
- Werkman, C.H., Wood, H.G. 2006. Heterotrophic assimilation of carbon dioxide. *Adv. Enzymol. Relat. Areas Mol. Biol.*, **2**, 135-179.
- Wu, K.J., Chang, J.S. 2007. Batch and continuous fermentative production of hydrogen with anaerobic sludge entrapped in a composite polymeric matrix. *Process Biochemistry*, **42**, 279-284.
- Wu, S.Y., Hung, C.H., Lin, C.N., Chen, H.W., Lee, A.S., Chang, J.S. 2006. Fermentative hydrogen production and bacterial community structure in high-rate anaerobic bioreactors containing silicone immobilized and self-flocculated sludge. *Biotechnol. Bioeng.*, **93**, 934-946.
- Wukovits, W., Drljo, A., Hilby, E., Friedl, A. 2013. Integration of Biohydrogen Production with Heat and Power Generation from Biomass Residues. *16th International Conference on Process Integration, Modelling and Optimisation for Energy Saving and Pollution Reduction (Pres'13)*, **35**, 1003-1008.
- Yang, P., Zhang, R., McGarvey, J.A., Benemann, J.R. 2007. Biohydrogen production from cheese processing wastewater by anaerobic fermentation using mixed microbial communities. *International Journal of Hydrogen Energy*, **32**, 4761-71.
- Yu, X., Drapcho, C. 2011. Hydrogen production by the hyperthermophilic bacterium *Thermotoga neapolitana* using agricultural-based carbon and nitrogen sources. *Biological Engineering Transactions*, **4**, 101-112.
- Yun, B.Y., Jun, S.Y., Kim, N.A., Yoon, B.Y., Piao, S., Park, S.H., Jeong, S.H., Lee, H., Ha, N.C. 2011. Crystal structure and thermostability of a putative α -glucosidase from *Thermotoga neapolitana*. *Biochemical and Biophysical Research Communications*, **416**, 92-98.
- Zhang, T., Liu, H., Fang, H.H.P. 2003. Biohydrogen production from starch in wastewater under thermophilic condition. *J. Environ. Manag.*, **69**, 149-156.
- Zverlov, V.V., Volkov, I.Y., Velikodvorskaya, T.V., Schwarz, W.H. 1997a. Highly thermostable endo-1,3- β -glucanase (laminarinase) LamA from *Thermotoga neapolitana*: Nucleotide sequence of the gene and characterization of the recombinant gene product. *Microbiology*, **143**, 1701-08.

Zverlov, V.V., Volkov, I.Y., Velikodvorskaya, T.V., Schwarz, W.H. 1997b. *Thermotoga neapolitana* bglB gene, upstream of lamA, encodes a highly thermostable β -glucosidase that is a laminaribiase. *Microbiology*, **143**, 3537-42.

Chapter 3

Strain characterization

This chapter has been submitted as:

Pradhan, N., Dipasquale, L., d'Ippolito, G., Panico, A., Lens, P.N.L., Esposito, G., Fontana, A. 2016. Hydrogen and lactic acid synthesis by the wild-type and a laboratory strain of the hyperthermophilic bacterium *Thermotoga neapolitana* DSMZ 4359 under capnophilic lactic fermentation condition. *International Journal of Hydrogen Energy*.

Chapter 3: Strain characterization

Abstract

Thermotoga neapolitana is a hyperthermophilic eubacterium that produces hydrogen by fermentation of sugars. A lab strain of the *T. neapolitana* DSMZ 4359 maintained in CO₂-enriched atmosphere showed an atypical ability to produce lactic acid under capnophilic lactic fermentation (CLF) condition. The genotypic comparison between the putative mutant and the wild-type DSMZ 4359 revealed a DNA homology of 88.1 (\pm 2.4)%. Genotyping by RiboPrint[®] and MALDI-TOF MS analyses showed a genetic differentiation beyond subspecies level. The phenotypic characterization (growth temperature, growth rate, substrate preference, salinity, hydrogen rate and yield) supported the high correlation between the two strains, except for the lactic acid production. The lab isolate produced in the range of 10–90% more lactic acid than the parent strain under similar operating conditions. Interestingly, this occurred without impairing hydrogen yield. Based on these results, we propose the lab strain is a new subspecies of the genus *Thermotoga* and we named the new strain as *T. neapolitana* subsp. *lactica* with regards to its improved feature to produce lactic acid.

Keywords: *Thermotoga neapolitana*; hydrogen; lactic acid; capnophilic lactic fermentation; genotype; phenotype.

3.1 Introduction

The anaerobic digestion restricted to the acetogenic phase (also termed as dark fermentation) leads to the production of hydrogen (H₂) along with various other commercially valuable organic acids. The dark fermentation reaction can be performed by using a consortium or pure culture of microorganisms at mesophilic (25–40 °C), thermophilic (40–65 °C) or hyperthermophilic (> 65 °C) conditions (Elsharnouby et al., 2013). Particularly, the hyperthermophilic fermentation with pure cultures has shown a promising prospect to bioconvert various organic substrates into products with significant environmental, economic and commercial values, i.e. H₂, acetic acid, butyric acid, lactic acid and ethanol (Pradhan et al., 2016a; Pradhan et al., 2016b).

Thermotoga neapolitana is a hyperthermophilic gram-negative bacterium isolated from a shallow submarine hot spring in the Bay of Naples in 1986 (Huber et al., 1986). The microorganism grows between 55 and 90 °C with an optimal growth temperature of 80 °C (Pradhan et al., 2015) and produces H₂ close to the Thauer limit (d'Ippolito et al., 2010). *T. neapolitana* belongs to the order *Thermotogales* (phylum Thermotogae; class *Thermotogae*), whose taxonomy has been recently reviewed on the basis of different lines of evidence including branching in the 16S rRNA and concatenated protein trees, character compatibility analysis, species distribution of different conserved signature inserts and deletions of protein sequences (Bhandari & Gupta, 2014).

In the last years, we showed that *T. neapolitana* DSMZ 4359^T (hereafter referred to as WT4359) possesses a novel anaplerotic pathway to convert sugars into lactic acid under an atmosphere enriched in carbon dioxide (CO₂). The process does not affect H₂ production, thus leading to a high yield of both H₂ (usually around 3.6 mol/mol of glucose) and lactic acid (up to 0.6 mol/mol of glucose) (Pradhan et al., 2016a). We named the process as capnophilic (CO₂-requiring) lactic fermentation (CLF) with regards to the surprising feature to produce lactic acid more than one could expect from the classical dark fermentation model (d'Ippolito et al., 2014; Pradhan et al., 2016a). In order to carry out our experiments, WT4359 has been regularly maintained under CO₂ atmosphere in the last years. Recently, an additional increase in the lactic acid production under CLF conditions by the laboratory strain (hereafter referred to as TN-

CMut) led us to hypothesize a genetic modification or mutation of the original isolate has occurred.

The susceptibility of microorganisms to mutations has often been associated with the influence of natural environments on the DNA integrity (Clemente et al., 2007; Derrick et al., 2015). For *T. neapolitana*, unusually high levels of dissolved CO₂ could have induced an adaptation over a period of time. The purpose of the present work was to investigate if our laboratory strain (TN-CMut) has acquired a stable mutation that is responsible for the increased productivity of lactic acid in comparison with WT4359 under CLF conditions. To this aim, we performed genotypic and phenotypic study of TN-CMut in order to verify subspecies differentiation from the parent strain WT4359 and to evaluate the potential biotechnological advantage of the mutant.

3.2 Materials and Methods

3.2.1 Bacterial strains

Thermotoga neapolitana DSMZ 4359^T and 5068 were purchased from the Leibniz-Institut DSMZ - Deutsche Sammlung von Mikroorganismen und Zellkulturen (Braunschweig, Germany). TN-CMut was originally bought as *T. neapolitana* DSMZ 4359^T and maintained in our laboratory under saturating concentrations of CO₂ for several years.

3.2.2 Medium preparation

Bacteria were grown and maintained in the modified ATCC 1977 culture medium containing 10 mL/L of filter-sterilized vitamins and trace element solutions (DSM medium 141) together with the following components in g/L of distilled water: 10 NaCl; 0.1 KCl; 0.2 MgCl₂·6 H₂O; 1 NH₄Cl; 0.3 K₂HPO₄; 0.3 KH₂PO₄; 0.1 CaCl₂·2 H₂O; 1 cysteine-HCl; 2 yeast extract; 2 tryptone; 5 glucose; 0.001 resazurin (d'Ippolito et al., 2010). Aliquots (30 mL) of standard culture medium were distributed into 120 mL serum bottles. Excess oxygen was removed by heating until the solution was colorless. The serum bottles were immediately capped with butyl rubber stoppers and sterilized by autoclaving for 15 min at 110 °C (d'Ippolito et al., 2010).

3.2.3 Standard growth conditions

The culture medium was sparged with CO₂ gas for 3 min at 30 mL/min in order to create an anaerobic atmosphere. Bacterial cultures were inoculated with the pre-

culture inoculum of both *T. neapolitana* strains at 6% (v/v). The initial pH was adjusted to approximately 7.5 by 1M NaOH. The temperature of the medium was constantly maintained at 80 (\pm 1) °C in the oven without agitation. Approximately 3 mL fermentation mixture was withdrawn at the end of the incubation period (see below), centrifuged (at 13,000 rpm for 5 min) and stored (at -20 °C) for the biochemical assay.

3.2.4 DNA-DNA hybridization, RiboPrint and MALDI-TOF MS analyses

The biomass samples of *T. neapolitana* DSMZ 4359^T and TN-CMut were prepared as per the instruction of the DSMZ laboratory. The DNA-DNA hybridization, RiboPrint and MALDI-TOF MS analyses were performed by the Leibniz-Institut DSMZ - Deutsche Sammlung von Mikroorganismen und Zellkulturen (Braunschweig, Germany) and the results were compared with a reference strain (*T. neapolitana* DSMZ 5068).

For DNA-DNA hybridization, cells were disrupted by using a Constant Systems TS 0.75 KW (IUL Instruments, Germany). DNA in the crude lysate was purified by chromatography on hydroxyapatite as described by [Cashion et al. \(1977\)](#). DNA-DNA hybridization was carried out as described by [De Ley et al. \(1970\)](#) under consideration of the modifications described by [Huss et al. \(1983\)](#) using a model Cary 100 Bio UV/VIS-spectrophotometer equipped with a Peltier-thermostated 6x6 multicell changer and a temperature controller with *in-situ* temperature probe (Varian).

Postgenomic methods are routinely used for taxonomic purposes and strain typing. Riboprint analysis is a highly discriminatory technique that is effective in differentiating strains inter- and intraspecifically within genera ([Behrendt et al., 2003](#); [Clark et al., 2006](#); [Pantucek et al., 2013](#); [Sikorski et al., 2001](#)). In combination with MALDI-TOF MS analysis of ribosomal proteins, Riboprinting allows to reveal differentiation in closely related species ([Soro-Yao et al., 2014](#)). The number of bands visualized by traditional or automated ribotyping depends on the number of recognitions sites of the restriction enzyme selected for digestion of chromosomal DNA. For RiboPrinting analysis, DNA fragments were generated by digestion of microbial DNA with the restriction enzymes *EcoRI* and *PvuII*. Analysis of the digested material was carried out by the RiboPrinter microbial characterization system (DuPont Qualicon) according to [Schumann and Pukall \(2013\)](#).

For the MALDI-TOF MS analysis, a score oriented dendrogram was calculated by the BioTyper software (version 3.1, Bruker Daltonics) on the following parameters: basis of distance measure/correlation, linkage/average, score threshold for a single organism = 350 and score threshold for related organisms = 0. Sample preparation and instrumental conditions for the MALDI-TOF MS were applied as described in Protocol 3 of [Schumann and Maier \(Schumann & Maier, 2014\)](#).

3.2.5 Phenotypic evaluation

Three different series of experiments were conducted to verify the main possible differences between WT4359 and TN-CMut in terms of product formation. For both strains, the optimum operating conditions for biomass growth, substrate consumption, H₂ and organic acids production were determined after 72 h of incubation by varying either the temperature from 50 to 90 °C or the salt concentration from 0 to 60 g/L NaCl. Furthermore, the ability of both strains to utilize different carbon sources was investigated on 5 g/L of glucose (28 mM), arabinose (33 mM), xylose (33 mM), fructose (28 mM) or lactose (28 mM). All batch experiments were performed in duplicate.

3.2.6 Analytical methods

The gaseous metabolites (H₂ and CO₂) were measured by thermal conductivity detector-gas chromatography (TCD-GC) on a Focus GC (Thermo Scientific) ([Dipasquale et al., 2014](#)). The analyses for aqueous metabolites (i.e. acetic acid and lactic acid) were performed on the supernatants after centrifugation of the culture medium by ¹H Nuclear Magnetic Resonance (NMR) on an Avance 600 spectrometer (Bruker) ([Dipasquale et al., 2014](#)).

Glucose and fructose concentrations were measured by the dinitrosalicylic acid (DNS) method calibrated on a standard solution of 1 g/L of glucose ([Bernfeld, 1955](#)). Similarly, arabinose and xylose concentrations were measured by the DNS method calibrated on a standard solution of 1 g/L of xylose, whereas lactose was measured by the phenol/sulfuric acid method calibrated on a standard solution of 0.2 g/L of glucose ([Dubois et al., 1956](#)). Biomass growth was monitored as optical density (OD) at 540 nm on a V-650 spectrophotometer (Jasco).

3.3 Results

3.3.1 Comparison of *T. neapolitana* strains

Riboprint patterns for WT4359 and TN-CMut were recorded using the restriction enzyme *EcoRI* (Fig. 3.1A), while it was not possible to obtain an *EcoRI* analysis with the second strain of *T. neapolitana*, namely DSMZ 5068. No RiboPrint result could be generated with WT4359, TN-CMut and *T. neapolitana* DSMZ 5068 by using another restriction enzyme (*PvuII*) as additional protocol. As reported in Fig. 3.1A, the resulting genetic fingerprintings of WT4359 and TN-CMut showed a similarity of only 0.76. The pattern of the DNA fragments differed significantly at the lowest kbp for intensity and position, whereas two strong bands of similar intensity were present at approximately 8 kbp. The biggest and most intense band could be considered species-specific, while the other additional bands allowed more detailed differentiation.

Differentiation between WT4359 and TN-CMut was also supported in mass spectrometric fingerprints by MALDI-TOF MS (Schumann & Maier, 2014). In fact, Biotyper analysis of the MS spectral similarities indicated that the laboratory strain did not cluster with either WT4359 or the reference strain *T. neapolitana* DSMZ 5068, which instead cluster closely together. The score oriented dendrogram of MALDI TOF MS analysis is shown in Fig. 3.1B.

Finally, DNA-DNA hybridization homology of WT4359 and TN-CMut was 88.1 (\pm 2.4)%, well above the 70% similarity that is the gold standard threshold for species boundaries but lower than values obtained for *Lactobacillus* subspecies, for whose characterization also DNA-DNA hybridization was used (Soro-Yao et al., 2014).

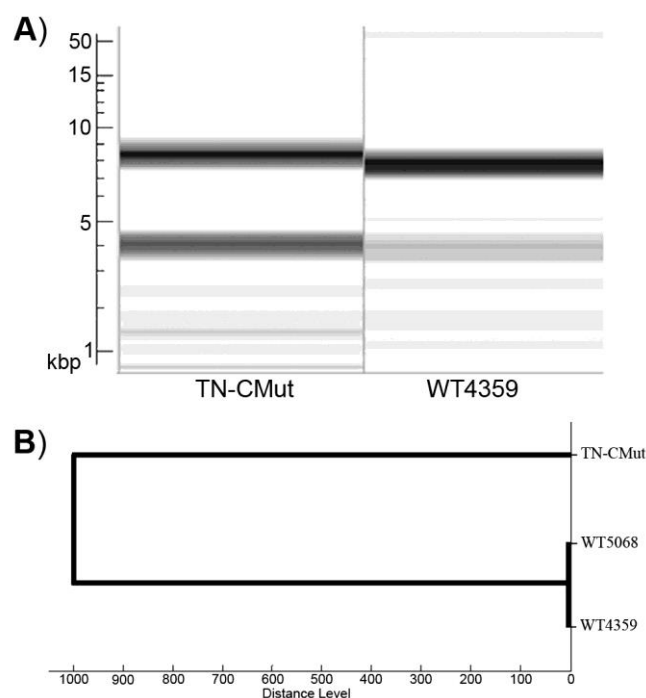


Fig. 3. 1 Molecular comparison of *T. neapolitana* WT4359 (parent strain), TN-CMut (laboratory strain) and *T. neapolitana* 5068 (reference strain). (A) RiboPrint pattern for microbial characterization system of mutant and wild-type strains; (B) Cluster analysis of MALDI-TOF MS spectra. In the dendrogram, relative distance is displayed as arbitrary units. Zero indicates complete similarity and 1000 indicates the highest dissimilarity.

3.3.2 Effect of growth temperature

Fig. 3.2 reports the effect of temperature on the cultures of TN-CMut and WT4359 supplemented with 28 mM glucose under CLF condition (Dipasquale et al., 2014). Both strains showed very similar growth rates with the best results recorded between 70 and 80 °C. Outside of this range, culture parameters dropped sharply and almost no growth was observed below 50 and above 90 °C. In the optimal temperature interval, H₂ production and substrate consumption were similar for both strains, but the mutant culture produced much more lactic acid. Maximum divergence was observed at 80 °C with 20.9 mM lactic acid produced by TN-CMut and 11.1 mM by WT4359. Interestingly, differences in lactic acid were independent of the acetic acid production that was comparable for both strains, thus determining an evident discrepancy in the

lactic acid/acetic acid ratio between the two strains (0.7 in TN-CMut and 0.3 in WT4359 at 80 °C).

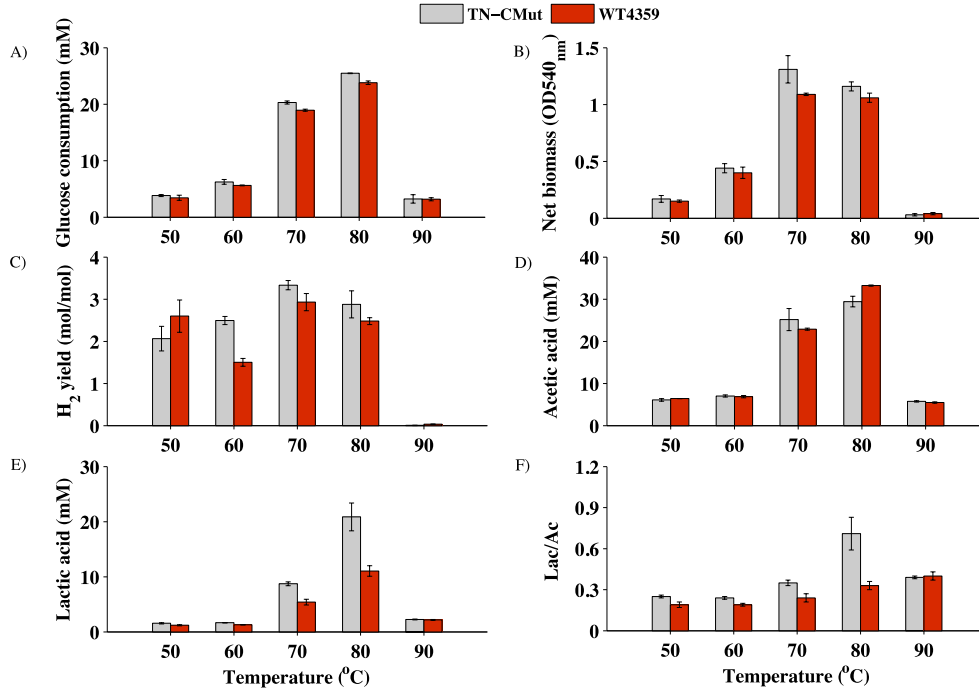


Fig. 3. 2 Effect of temperature on cultures of TN-CMut and WT4359 supplemented with 28 mM glucose (5 g/L) and maintained under CLF condition for 72 h.

3.3.3 Effect of salinity

Both strains could thrive from 0 to 50 g/L NaCl in the culture medium (Fig. 3.3). Bacterial growth and glucose consumption were consistent in this saline range and dropped only above this concentration (Fig. 3.3). Production of H₂ and acetic acid was the highest between 10 and 30 g/L NaCl with both strains, whereas the lactic acid level increased at higher salt concentrations in both cultures. In particular, the production of lactic acid raised regularly from about 10 mM to above 30 mM when raising the salinity level from 10 to 50 g/L. This response was similar with both strains, even if TN-CMut showed a slightly higher tendency to produce lactic acid.

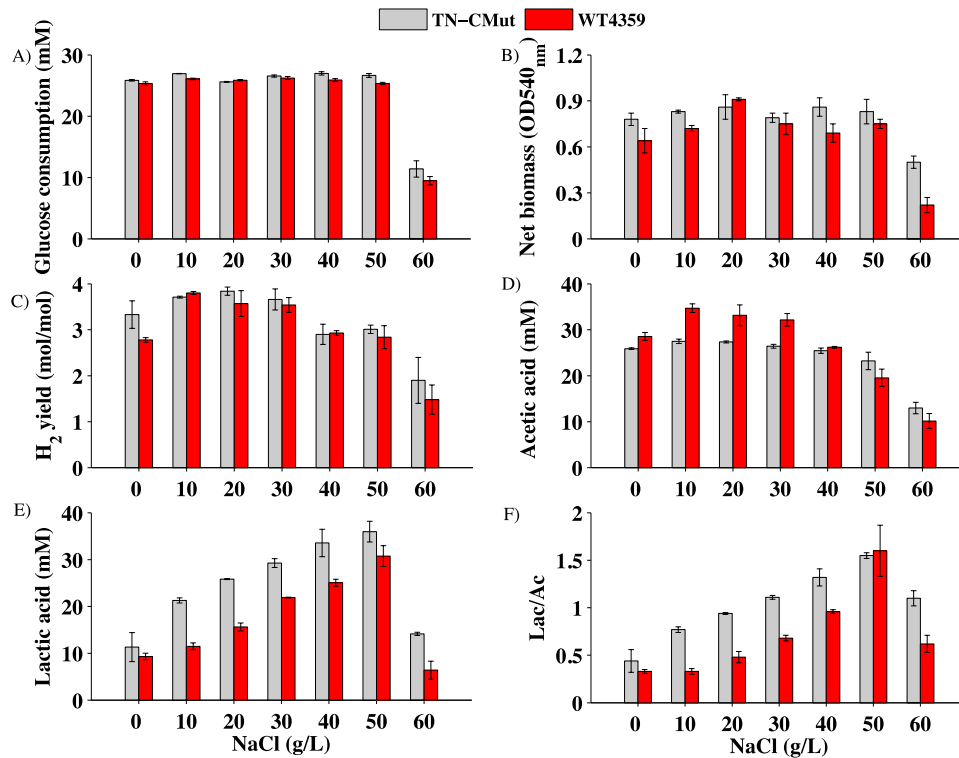


Fig. 3.3 Effect of the salinity level (0–60 g/L) on cultures of TN-CMut and WT4359 supplemented with 28 mM glucose (5 g/L) and maintained under CLF condition at 80 °C for 72 h.

3.3.4 Effect of carbon source

The effect of substrate change on TN-CMut and WT4359 is shown in Fig. 3.4. The strains did not show any preference or divergence in the consumption of arabinose, xylose, fructose and lactose after 72 h. The two cultures showed a parallel response also in terms of H₂ and acetic acid production, even if there were differences in the yields from one sugar to another. However, TN-CMut seemed to adapt better or more quickly to the change of the carbon source since the growth of this strain was appreciably higher than that of WT4359 (20–30% higher biomass). Significantly, the two strains revealed a major divergence in the production of lactic acid on arabinose and lactose. This finding is very evident from the comparison of the lactic acid/acetic acid ratio from the two cultures containing these substrates. It is to note that lactic acid levels from arabinose, xylose, fructose and lactose were generally very low in comparison to the amount produced by glucose fermentation at 80 °C (Fig. 3.2 and Fig. 3.4), whereas all the other culture parameters (sugar consumption, H₂ and acetic acid production) were not much

affected by the change of the sugar substrate under similar operating conditions (Fig. 3.2 and Fig. 3.4).

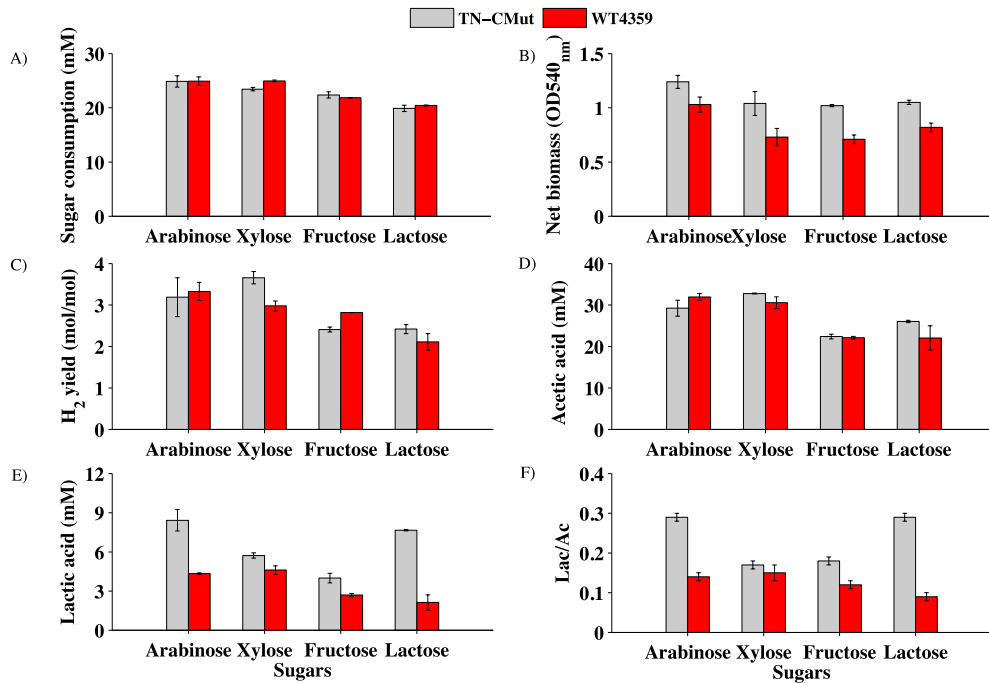


Fig. 3. 4 Fermentation of different substrates by cultures of TN-CMut and WT4359 under CLF condition at 80 °C for 72 h. Both strain cultures were supplemented with 33 mM of arabinose or xylose and 28 mM of fructose or lactose.

3.4 Discussion

The exposure of *T. neapolitana* WT4359 to high CO₂ concentrations over a long period of time has induced a stable mutation during the cultivation of the laboratory strain TN-CMut showing phenotypic and genotypic differences. In addition to a genetic similarity of about 88% as established by DNA-DNA hybridization, TN-CMut showed distinct characters from the parent WT4359 strain in RiboPrint and MALDI-TOF MS analyses. RiboPrinter, alone or in combination with MALDI-TOF MS analysis, has been proposed to support differentiation above species level (Soro-Yao et al., 2014). In our study, the two strains showed a similarity coefficient of 0.76, which is lower than 0.93 that is considered the limit value for the assignment of a species to an existing RiboGroup (Schumann & Pukall, 2013). The differentiation of the lab strain from the parent bacterium was also corroborated by ribosomal protein fingerprinting (Schumann & Maier, 2014). The MALDI-TOF MS spectra of TN-CMut showed characters

different from those of WT4359, while this latter species could not be differentiated by another *T. neapolitana* strain (DSMZ 5068) that was used as internal control (Fig. 3.1B).

Unlike the parent strain, the mutant TN-CMut showed a clear increase in the lactic acid synthesis. This response was evident in every phenotypic test that was performed to compare the production of the two strains under CLF (Figs. 3.2–3.4). Under these conditions, the use of CO₂ induces a metabolic shift that leads to recycling of acetate with synthesis of pyruvate and then lactic acid (Fig. 3.5) (d'Ippolito et al., 2014). Formally, this pathway is distinct from the catabolism of the sugars thus, if there is an appropriate surplus of reducing power, the bacterial cells are able to produce lactic acid without affecting the physiological progression and productivity of the culture (Dipasquale et al., 2014).

Recently, we showed that conversion of glucose to lactic acid instead of acetic acid increases H₂ production in a two-stage process based on photofermentation of CLF effluents (Dipasquale et al., 2015). The new subspecies of *T. neapolitana* here described seems to be the most favourable strain for this type of combined approaches that are widely recognized as the most effective method for biological production of H₂ from organic substrates (d'Ippolito et al., 2014; Dipasquale et al., 2014)]. Lactic acid has also a number of commercial applications and consequently the potential use of *T. neapolitana* subsp. *lactica* to achieve H₂ and lactic acid is a more attractive and potentially more profitable process than other traditional method for biological H₂ production.

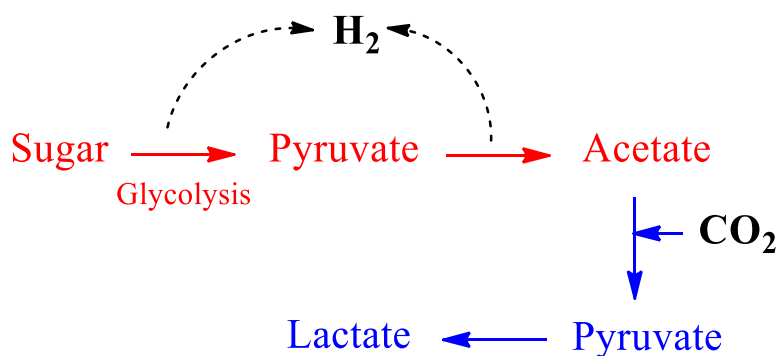


Fig. 3. 5 Schematic representation of the capnophilic lactic fermentation pathway with the catabolic (red) and biosynthetic (blue) branches.

TN-CMut and WT4359 did not show any apparent differences in the catabolic branch of CLF as the main parameters linked to sugar fermentation (growth, sugar consumption and H₂ production, Figs. 3.2 and 3.4A–C) remained unaltered in the two strain cultures. Consequently, the increase of lactic acid production in TN-CMut must depend on the up-regulation of the biosynthetic process starting from the recycling of acetate. The identification of the physiological changes leading to this response was beyond the aim of this study, nevertheless it is evident that the origin of the process involves adaptation of TN-CMut to the increased CO₂ concentrations in the culture medium. As stated above, CLF is triggered by CO₂ that activates the conversion of acetate to lactate. It is conceivable that the original *T. neapolitana* strain maintained under these high CO₂ conditions selected the ability to thrive in the CO₂-enriched environment by improving the biosynthetic activity, which likely led to the emergence of the mutation.

On the basis of the above results, we suggest that the strain TN-CMut is classified as a new subspecies of the genus *Thermotoga* and is named as *Thermotoga neapolitana* subsp. *lactica* owing to its potential to produce higher lactic acid concentrations compared to the original strain. Further genetic studies are required to determine the specific mutated site in the *Thermotoga* genome.

3.5 Conclusions

The phenotypic and genotypic comparisons support that the bacterial strain *T. neapolitana* subsp. *lactica* is a subspecies to *T. neapolitana* DSMZ 4359^T. The new subspecies consistently produced from 10 to 90% more lactic acid than the original strain under CLF condition. This increased lactic acid production did not affect other fermentation parameters, including substrate consumption and H₂ production. Thus, the new subspecies is a potentially more suitable candidate than the parent strain to be used in a CLF process to convert different types of sugars to lactic acid without reducing the H₂ yield.

References

- Behrendt, U., Ulrich, A., Schumann, P. 2003. Fluorescent pseudomonads associated with the phyllosphere of grasses; *Pseudomonas trivialis* sp. nov., *Pseudomonas poae* sp. nov. and *Pseudomonas congelans* sp. nov. *International Journal of Systematic and Evolutionary Microbiology*, **53**, 1461-1469.
- Bernfeld, P. 1955. Alpha and beta-amylases. *Methods in Enzymology*, **1**, 149-158.

- Bhandari, V., Gupta, R.S. 2014. Molecular signatures for the phylum (class) Thermotogae and a proposal for its division into three orders (*Thermotogales*, *Kosmotogales* ord. nov. and *Petrotogales* ord. nov.) containing four families (*Thermotogaceae*, *Fervidobacteriaceae* fam. nov., *Kosmotogaceae* fam. nov. and *Petrotogaceae* fam. nov.) and a new genus *Pseudothermotoga* gen. nov. with five new combinations. *Antonie van Leeuwenhoek, International Journal of General and Molecular Microbiology*, **105**, 143-168.
- Cashion, P., Hodler-Franklin, M.A., McCully, J., Franklin, M. 1977. A rapid method for base ratio determination of bacterial DNA. *Analytical Biochemistry*, **81**, 461-466.
- Clark, D.M., Ehlers, A., Hackmann, A., McManus, F., Fennell, M., Grey, N., Waddington, L., Wild, J. 2006. Cognitive therapy versus exposure and applied relaxation in social phobia: A randomized controlled trial. *Journal of Consulting and Clinical Psychology*, **74**, 568-578.
- Clemente, I.M., Matthew, R.J., Chung-Jung, C., Shannon, B.C., Sarah, G.G., Sabrina, T., Jason, D.N., Robert, M.K. 2007. Responses of wild-type and resistant strains of the hyperthermophilic bacterium *Thermotoga maritima* to chloramphenicol challenge. *Applied and Environment Microbiology*, **73**, 5058-5065.
- d'Ippolito, G., Dipasquale, L., Fontana, A. 2014. Recycling of carbon dioxide and acetate as lactic acid by the hydrogen-producing bacterium *Thermotoga neapolitana*. *ChemSusChem*, **7**, 2678-83.
- d'Ippolito, G., Dipasquale, L., Vella, F.M., Romano, I., Gambacorta, A., Cutignano, A., Fontana, A. 2010. Hydrogen metabolism in the extreme thermophile *Thermotoga neapolitana*. *International Journal of Hydrogen Energy*, **35**, 2290-2295.
- De Ley, J., Cattoir, H., Reynaerts, A. 1970. The quantitative measurement of DNA hybridization from renaturation rates. *European Journal of Biochemistry*, **12**, 133-142.
- Derrick, L.L., Jaspreet, S.N., Sanjeev, K.C., Andrew, J.L., Gina, L.L., Michael, W.W.A., Robert, M.K. 2015. A mutant ('lab strain') of the hyperthermophilic archaeon *Pyrococcus furiosus*, lacking agella, has unusual growth physiology. *Extremophiles*, **19**, 269-281.
- Dipasquale, L., Adessi, A., d'Ippolito, G., Rossi, F., Fontana, A., De Philippis, R. 2015. Introducing capnophilic lactic fermentation in a combined dark-photo fermentation process: a route to unparalleled hydrogen yields. *Applied Microbiology and Biotechnology*, **99**, 1001-10.
- Dipasquale, L., d'Ippolito, G., Fontana, A. 2014. Capnophilic lactic fermentation and hydrogen synthesis by *Thermotoga neapolitana*: An unexpected deviation from the dark fermentation model. *International Journal of Hydrogen Energy*, **39**, 4857-4862.

- Dubois, M., Gilles, K.A., Hamilton, J.K., Rebers, P.A., Smith, F. 1956. Colorimetric method for determination of sugars and related substances. *Analytical Chemistry*, **28**, 350-6.
- Elsharnouby, O., Hafez, H., Nakhla, G., el Naggar, M.H. 2013. A critical literature review on biohydrogen production by pure cultures. *International Journal of Hydrogen Energy*, **38**, 4945-4966.
- Huber, R., Langworthy, T.A., Konig, H., Thomm, M., Woese, C.R., Sleytr, U.B., Stetter, K.O. 1986. *Thermotoga maritima* sp. nov. represents a new genus of unique extremely thermophilic eubacteria growing up to 90 °C. *Arch. Microbiol.*, **144**, 324-333.
- Huss, V.A.R., Festl, H., Schleifer, K.H. 1983. Studies on the spectrophotometric determination of DNA hybridization from renaturation rates. *Systematic and Applied Microbiology*, **4**, 184-192.
- Pantucek, R., Svec, P., Dajcs, J.J., Machova, I., Cernohlavkova, J., Sedo, O., Gelbicova, T., Maslanova, I., Doskar, J., Zdrahal, Z., Ruzickova, V., Sedlacek, I. 2013. *Staphylococcus petrasii* sp. nov. including *S. petrasii* subsp. *petrasii* subsp. nov. and *S. petrasii* subsp. *croceilyticus* subsp. nov., isolated from human clinical specimens and human ear infections. *Systematic and Applied Microbiology*, **36**, 90-95.
- Pradhan, N., Dipasquale, L., d'Ippolito, G., Fontana, A., Panico, A., Pirozzi, F., Lens, P.N.L., Esposito, G. 2016a. Model development and experimental validation of capnophilic lactic fermentation and hydrogen synthesis by *Thermotoga neapolitana*. *Water Research*, **99**, 225-234.
- Pradhan, N., Dipasquale, L., d'Ippolito, G., Fontana, A., Panico, A., Lens, P.N.L., Pirozzi, F., Esposito, G. 2016b. Kinetic modeling of fermentative hydrogen production by *Thermotoga neapolitana*. *International Journal of Hydrogen Energy*, **41**, 4931-4940.
- Pradhan, N., Dipasquale, L., d'Ippolito, G., Panico, A., Lens, P.N.L., Esposito, G., Fontana, A. 2015. Hydrogen production by the thermophilic bacterium *Thermotoga neapolitana*. *International Journal of Molecular Sciences*, **16**, 12578-12600.
- Schumann, P., Maier, T. 2014. MALDI-TOF mass spectrometry applied to classification and identification of bacteria. *Methods Microbiol*, **41**, 275-306.
- Schumann, P., Pukall, R. 2013. The discriminatory power of ribotyping as automatable technique for differentiation of bacteria. *Systematic and Applied Microbiology*, **36**, 369-375.
- Sikorski, J., Stackebrandt, E., Wackernagel, W. 2001. *Pseudomonas kilonensis* sp. nov., a bacterium isolated from agricultural soil. *International Journal of Systematic and Evolutionary Microbiology*, **51**, 1549-1555.
- Soro-Yao, A.A., Schumann, P., Thonart, P., Dje, K.M., Pukall, R. 2014. The use of MALDI-TOF mass spectrometry, ribotyping and phenotypic tests to identify

lactic acid bacteria from fermented cereal foods in Abidjan (Côte d'Ivoire). *The Open Microbiology Journal*, **8**, 78-86.

Chapter 4

Culture parameter optimization

Chapter 4: Culture parameter optimization

Abstract

This study investigated the effect of the salinity level, buffering agent and carbon source on the hydrogen (H₂) and lactic acid production under capnophilic (CO₂-led) lactic fermentation (CLF) by *Thermotoga neapolitana*. Fermentation experiments were conducted either in 0.12 L serum bottles or in a 3 L continuously stirred tank reactor (CSTR). Increasing the salinity level in the culture medium from 0 to 35 g/L NaCl increased the lactic acid production increased by 750% without affecting H₂ yield. A stable H₂ yield (i.e. 3.0 mol H₂/mol of glucose) and lactic acid (i.e. 13.7 mM) synthesis were observed when the culture medium was co-buffered with 0.01 M of diacid/monoacid phosphate, 3-(*N*-morpholino) propanesulfonic acid (MOPS), tris (hydroxymethyl) aminomethane (TRIS), 4-(2-hydroxyethyl)-1-piperazineethanesulfonic acid (HEPES) and exogenous CO₂ as the source of bicarbonate. When applying the optimized culture parameters obtained in the 0.12 L serum bottle experiments about 230% higher lactic acid was produced in the process scale-up using a 3 L CSTR. This study unravels a novel strategy to valorize carbohydrate rich organic substrates with different salinity level for cost-effective generation of H₂ and lactic acid by applying CLF-based fermentation techniques.

Keywords: hydrogen; lactic acid; capnophilic lactic fermentation; salinity level; buffering agent.

4.1 Introduction

Research efforts are currently focused on finding sustainable, clean and alternative energy sources, which are of urgent need for the ever increasing energy demand and growing concerns about greenhouse gases emissions. Hydrogen (H₂) is such a clean energy source, as it does not produce any greenhouse gases upon its combustion. Currently, over 90% of the global H₂ is produced through physico-chemical processes, such as pyrolysis and gasification, thereby emitting huge amounts of greenhouse gases (i.e. SO_x, NO_x, CO and CO₂) to the atmosphere (Johnston et al., 2005; Nath & Das, 2004). Therefore, biological routes, and especially dark fermentation (DF), have generated tremendous interest among the scientific community thanks to its benefits such as reasonably high H₂ production rates, low energy demand, low cost feedstock and simple operational techniques with reliable process stability (Pradhan et al., 2015).

With the introduction of the hyperthermophilic marine bacterium *Thermotoga neapolitana* for biological H₂ production, there has been a significant achievement in the field of bioenergy development (Pradhan et al., 2015). With further advancement, a new metabolic pathway was introduced in the *T. neapolitana* fermentation process, which is termed as capnophilic (CO₂-assisted) lactic fermentation (CLF) (d'Ippolito et al., 2014; Dipasquale et al., 2014). The CLF pathway recycles CO₂ and acetic acid produced by the glycolytic fermentation of sugar to lactic acid without affecting the H₂ yield (Dipasquale et al., 2014; Pradhan et al., 2016a; Pradhan et al., 2016b). This new CLF pathway is considered as an important invention in the field of biotechnology that, unlike the DF pathway, provides robust process stability and reliability. The CLF pathway can be used for simultaneous synthesis of H₂ and lactic acid, which is not possible in the DF pathway where lactic acid production is inversely proportional to H₂ production.

Lactic acid is an important chemical of wide commercial use in the food, pharmaceutical, cosmetic and chemical industries. Currently, lactic acid is used in limited applications due to its modest production and lack of cost effective extraction and purification techniques (Joglekar et al., 2006). Due to the increasing demand for lactic acid, the CLF-based fermentation could play a significant role in the large-scale industrial production of lactic acid. Moreover, various kinds of carbohydrate rich

organic waste/substrate can be treated through CLF-based processes and in addition this process sequestrates CO₂ to produce lactic acid (Pradhan et al., 2015). The main aim of this study was to identify how the culture parameters in terms of salinity level, buffering agent and substrates affect the H₂ and lactic acid production under CLF conditions. In addition, the efficiency of CLF-based process scale-up experiments were performed from a 0.12 L micro fermenter (serum bottle) to a laboratory scale 3.0 L continuously stirred tank reactor (CSTR) system.

4.2 Materials and methods

4.2.1 Bacterial strain

Thermotoga neapolitana strain was purchased from the Deutsche Sammlung von Mikroorganismen und Zellkulturen (DSMZ) (Braunschweig, Germany).

4.2.2 Experimental set-up

The effects of culture parameters on the H₂ yield and lactic acid production by *T. neapolitana* (Pradhan et al., 2016a; Pradhan et al., 2016b) were investigated under CLF conditions by systematically varying three key culture components in the culture medium, i.e. salinity level, buffering agent and carbon source. The culture medium was prepared according to d'Ippolito et al. (2010). Batch tests were conducted in 120 mL serum bottles with 30 mL culture medium. All the batch fermentation experiments were conducted in serum bottles with a working volume to headspace ratio maintained at 1:3 (approx.). The culture medium was sparged with pure CO₂ for 3 min at 30 mL/min and then inoculated with wet biomass (6%, v/v), previously washed twice in 10 g/L NaCl solution. The serum bottles were kept in the incubator at 80 °C without agitation. The initial pH (t = 0 h) was corrected to about 7.5 for all the serum bottles with 1 M NaOH, except for the buffering agent and optimization experiments. The successive pH corrections were done every 24 h except, for the buffering agent and optimization experiments. All the fermentation experiments were triplicated and incubated for 72 h.

The effect of the salinity level was studied by varying NaCl concentrations between 0–35 g/L (i.e. 0, 5, 10, 20 and 35 g/L) in the culture medium as done for the standard medium (d'Ippolito et al., 2010). The effect of a buffering agent was investigated by using 0.01 M for each of the following chemicals: (i) diacid/monoacid phosphate; (ii) 3-(*N*-morpholino) propanesulfonic acid (MOPS); (iii) tris (hydroxymethyl) aminomethane (TRIS) and (iv) 4-(2-hydroxyethyl)-1-piperazineethanesulfonic acid

(HEPES) in the culture medium. In addition, two other sets of experiments were conducted to understand the fermentability of glucose by *T. neapolitana* in the absence of buffering agents: a first one sparged with CO₂ and a second one sparged with N₂ gas. The effect of the carbon source was studied by using 5 g/L each of arabinose, xylose, glucose, sucrose, laminarin and carboxymethyl cellulose (CMC) in the culture medium as done for the standard medium (d'Ippolito et al., 2010).

Two additional sets of optimization tests were conducted by combining the best performing culture parameters (i.e. salinity level, buffering agent and carbon source) in terms of H₂ and lactic acid production. The culture parameters selected for the optimization tests were: (i) 35 g/L NaCl, (ii) 0.01 M phosphate buffer and (iii) 28 mM of glucose or 33 mM arabinose.

4.2.3 Scale-up experiment

The optimization experiment with glucose was successfully scaled up to a 3 L CSTR and the culture parameters were set as: (i) 35 g/L NaCl, (ii) 0.01 M phosphate buffer and (iii) 28 mM of glucose. The scale-up test was carried out in a jacketed 3 L reactor (Applikon Biotechnology, The Netherlands) containing 0.7 L culture medium and inoculated with wet biomass (6%, v/v), previously washed twice in a 10 g/L NaCl solution. The mixture was sparged with pure CO₂ for 5 min at 30 mL/min. The initial pH of the fermentation mixture was adjusted to 7.5 by titrating with 1 M NaOH. The temperature was kept thermostatically constant at 80 (± 1) °C and the mixture was stirred at 50 rpm using an electro-magnetic stirring unit (Pradhan et al., 2016b). The fermentation was carried out for 24 h with samples taken at the beginning (t = 0 h) as well as at the end (t = 24 h) of the batch test. The test in the CSTR was conducted in triplicate.

4.2.4 Analytical methods

The gaseous metabolites (H₂ and CO₂) were measured by gas chromatography (Focus GC, Thermo Scientific) as described by Dipasquale et al. (2014). The aqueous samples were centrifuged (at 13,000 rpm for 5 min) and the supernatant was stored at -20 °C for further biochemical analyses as described by Dipasquale et al. (2014). The analyses of aqueous metabolites (i.e. acetic and lactic acid) were performed on the supernatants by ¹H Nuclear Magnetic Resonance (NMR) 600 MHz spectrometer (Bruker Avance 600) as described by Dipasquale et al. (2014). Biomass growth was

monitored through optical density measurements ($\lambda = 540 \text{ nm}$) by a UV/Vis spectrophotometer (V-650, Jasco).

The residual glucose concentration was measured by the dinitrosalicylic acid (DNS) method calibrated on a standard solution of 1 g/L of glucose (Bernfeld, 1955). Similarly, the residual arabinose and xylose concentrations were measured by the DNS method calibrated on a standard solution of 1 g/L of xylose. The residual concentrations of sucrose, laminarin and CMC were measured by the phenol/sulfuric acid method calibrated on a standard solution of 0.2 g/L of glucose (Dubois et al., 1956).

4.3 Results

4.3.1 Effect of salinity

The results of the effect of the salinity level on the H_2 and organic acids (i.e. acetic and lactic acid) production are presented in Table 4.1. Over 90% of the substrates were consumed in 72 h of incubation. The H_2 production was increased by 30% when the NaCl concentration increased from 0 to 20 g/L and decreased by 15% when the NaCl concentration was further increased to 35 g/L (Fig. 4.1a). Fig. 4.1b showed a clear link between the biomass growth and the H_2 production. The biomass attained its peak growth rate at 10 g/L NaCl and decreased by 23% at 35 g/L NaCl in the culture medium.

The acetic acid production showed a similar trend to the H_2 production and biomass growth: it increased from 20.7 (± 0.3) mM at no NaCl in the culture medium to 26.1 (± 4.7) mM at 10 g/L NaCl and then decreased to 23.2 (± 0.8) mM at 35 g/L NaCl. However, there is a dramatic increase of over 7.5 fold in the lactic acid production when increasing the NaCl concentration from 0 and 35 g/L NaCl, i.e. from 2.8 (± 0.3) mM to 21.6 (± 6.2) mM lactic acid.

Pradhan et al. (2016b) reported that 29.9 (± 1.3) mM acetic acid, 14.8 (± 0.8) mM lactic acid and 3.3 mol H_2 /mol of glucose, which is comparable to the results of the present study under similar operating conditions at 10 g/L NaCl, i.e. 26.1 (± 4.7) mM acetic acid, 11.6 (± 2.4) mM lactic acid and 3.1 (± 0.8) mol H_2 /mol of glucose. The tests with varying salinity level revealed that the higher the salinity level, the better the fermentation performance with respect to H_2 and lactic acid production, i.e. 2.9 (± 0.4) mol H_2 /mol of glucose and 21.6 (± 6.2) mM lactic acid at 35 g/L NaCl in the culture

medium. The experiments also revealed that *T. neapolitana* can degrade organic substrate with in the absence of NaCl in the culture medium.

Table 4. 1 Effect of varying salinity level (0–35 g/L NaCl) on H₂ and organic acids production via the CLF pathway in tests supplemented with 28 mM glucose (72 h of incubation).

NaCl (g/L)	S (mM)	HPR (mL/L/h)	Y _{H₂/S} (mol/mol)	Ac (mM)	Lac (mM)	Lac/Ac
0	25.6 (± 0.1)	20.8 (± 3.5)	2.4 (± 0.4)	20.7 (± 0.3)	2.8 (± 0.3)	0.1 (± 0.1)
5	26.0 (± 0.1)	22.8 (± 7.6)	2.6 (± 0.9)	24.6 (± 1.0)	6.2 (± 3.3)	0.3 (± 0.1)
10	26.1 (± 0.2)	27.7 (± 7.0)	3.1 (± 0.8)	26.1 (± 4.7)	11.6 (± 2.4)	0.5 (± 0.1)
20	25.9 (± 0.1)	30.3 (± 1.8)	3.4 (± 0.2)	25.6 (± 1.0)	13.4 (± 0.9)	0.5 (± 0.1)
35	25.7 (± 0.3)	25.4 (± 3.4)	2.9 (± 0.4)	23.2 (± 0.8)	21.6 (± 6.2)	0.9 (± 0.3)

Notes: S = Substrate consumed; HPR = H₂ production rate; Y_{H₂/S} = H₂ yield; Ac = Acetic acid; Lac = Lactic acid; Lac/Ac = Lactic acid/Acetic acid ratio; the results are expressed as mean ± standard error (n = 3).

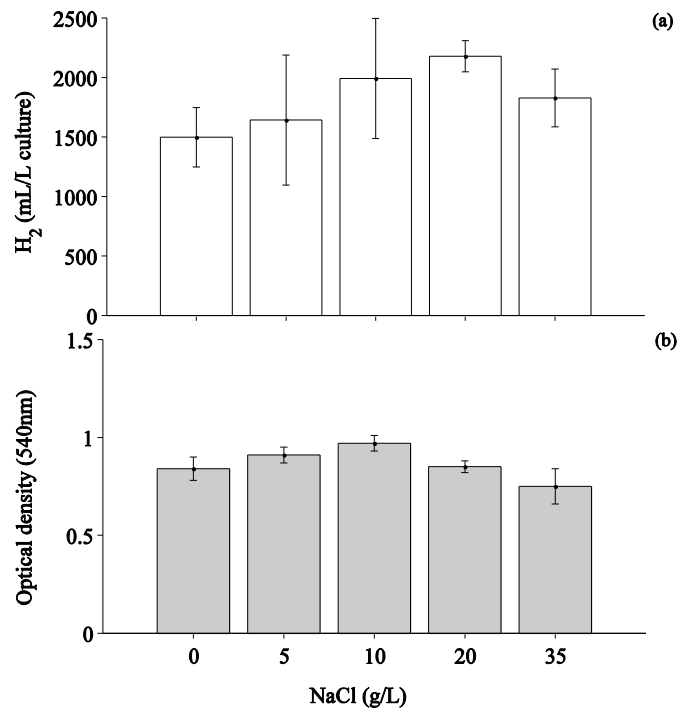


Fig. 4. 1 Effect of salinity level on (a) the H₂ production (mL/L culture) and (b) the biomass growth via the CLF pathway after 72 h of incubation ($n = 3$, error bars = standard error of mean).

4.3.2 Effect of buffering agent

The results of buffering agent tests are presented in Table 4.2. The H₂ yield ranged from 2.0 (± 0.1) to 3.3 (± 0.2) mol H₂/mol of glucose for the tests with various buffering agents. The H₂ production was found to be highest with MOPS buffer as shown in Fig. 4.2a. The biomass growth was found to be the highest for the culture with phosphate buffer and the lowest for the control test (Fig. 4.2b). The highest and lowest acetic acid production were 26.8 (± 0.3) mM and 22.8 (± 0.4) mM for the TRIS buffer and control tests, respectively. The highest value of lactic acid production was 14.9 (± 0.3) mM with phosphate buffer and the lowest (11.3 ± 0.6 mM) in the control test (Table 4.2). The results from buffering agent tests indicate that buffering agents along with CO₂ (or HCO₃⁻) played a crucial role in maintaining the pH, thereby facilitating complete substrate degradation.

Table 4. 2 Effect of the buffering agent (0.01 M) on H₂ and organic acids production via CLF pathway in the tests supplemented with 28 mM glucose (72 h of incubation).

Buffering agents	S (mM)	HPR (mL/L/h)	Y _{H₂/S} (mol/mol)	Ac (mM)	Lac (mM)	Lac/Ac
Control ^a	18.5 (± 0.2)	16.9 (± 0.9)	2.0 (± 0.1)	22.8 (± 0.4)	11.3 (± 0.6)	0.5 (± 0.1)
CO ₂ /HCO ₃ ^{-b}	25.6 (± 0.1)	19.8 (± 4.3)	2.2 (± 0.5)	22.8 (± 0.8)	14.6 (± 3.2)	0.6 (± 0.3)
Phosphate	26.2 (± 0.3)	24.6 (± 4.8)	2.7 (± 0.5)	24.7 (± 0.6)	14.9 (± 0.3)	0.6 (± 0.1)
MOPS	26.4 (± 0.1)	29.8 (± 1.6)	3.3 (± 0.2)	26.7 (± 0.9)	14.2 (± 0.2)	0.5 (± 0.1)
TRIS	25.6 (± 0.1)	27.5 (± 1.0)	3.1 (± 0.1)	26.8 (± 0.3)	12.1 (± 0.9)	0.5 (± 0.1)
HEPES	26.0 (± 0.1)	24.7 (± 4.5)	2.8 (± 0.5)	25.6 (± 0.5)	13.6 (± 0.9)	0.5 (± 0.1)

Notes:

^a culture medium without buffering agents and CO₂ sparging.

^b culture medium without buffering agents but sparged with CO₂.

the results are expressed as mean \pm standard error ($n = 3$).

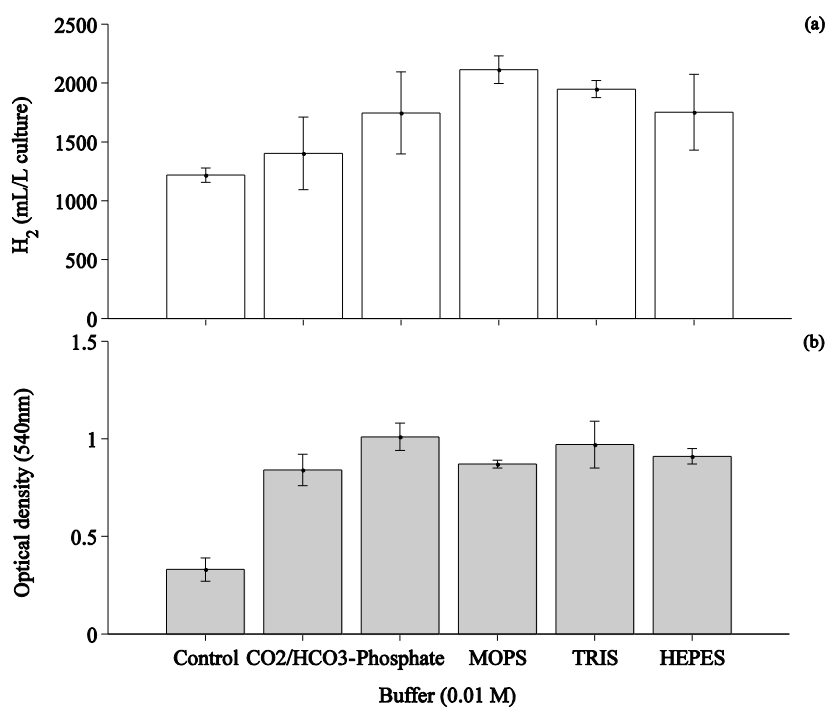


Fig. 4. 2 Effect of buffering agent on (a) the H₂ production (mL/L culture) and (b) the biomass growth via CLF pathway after 72 h of incubation ($n = 3$, error bars = standard error of mean).

4.3.3 Effect of carbon source

T. neapolitana can metabolize both simple and complex organic substrates to produce H₂ and organic acids (Pradhan et al., 2015). The results of H₂ and organic acid production from various types of carbon source are presented in Table 4.3. In addition, the H₂ production and biomass growth are shown in Fig. 4.3a and Fig. 4.3b, respectively. The H₂ yield under CLF conditions from the pentose sugars xylose and arabinose was 3.2 (± 0.1) and 2.8 (± 0.3) mol H₂/mol of pentose sugar, respectively. Similarly, the H₂ yield from glucose, sucrose and laminarin were 3.3 (± 0.1) mol H₂/mol of glucose, 2.6 (± 0.1) mol H₂/mol of glucose equivalent and 3.7 (± 0.2) mol H₂/mol of glucose equivalent, respectively. From CMC, the H₂ yield was 2.1 (± 0.1) mol H₂/mol of glucose equivalent with only 10% of the substrate consumed after 72 h of fermentation. The fermentation with CMC as carbon source indicates that it requires either pre-treatment or a much longer incubation time to complete the fermentation.

The lactic acid production was found to be significantly higher with glucose and sucrose as the carbon source, i.e. 14.8 (± 0.3) and 17.0 (± 1.3) mM, respectively, compared to the other sugars (Table 4.3). The lactic acid to acetic acid (*Lac/Ac*) ratio for both arabinose and glucose was amounted to 0.5 (± 0.1), whereas the highest *Lac/Ac* ratio (0.7 ± 0.1) was observed for sucrose as the carbon source. From the tests with various carbon source, it is evident that both glucose and arabinose performed best with respect to the H₂ yield and lactic acid production. Hence, these were selected for the process optimization experiments.

Table 4. 3 Effect of the different carbon source (5 g/L) on H₂ and organic acids production under CLF conditions.

Carbon sources	S (mM)	HPR (mL/L/h)	Y _{H₂/S} (mol/mol)	Ac (mM)	Lac (mM)	Lac/Ac
Xylose	29.6 (± 0.1)	32.4 (± 0.7)	3.2 (± 0.1) ^c	26.3 (± 0.3)	3.8 (± 0.2)	0.2 (± 0.1)
Arabinose	30.5 (± 0.1)	29.5 (± 3.1)	2.8 (± 0.3) ^c	23.1 (± 0.3)	10.9 (± 0.4)	0.5 (± 0.1)
Glucose	26.3 (± 0.1)	28.8 (± 0.2)	3.3 (± 0.1)	30.3 (± 0.1)	14.8 (± 0.3)	0.5 (± 0.1)
Sucrose	23.3 (± 0.7)	20.2 (± 1.0)	2.6 (± 0.1) ^d	25.1 (± 1.4)	17.0 (± 1.3)	0.7 (± 0.1)
Laminarin	24.7 (± 0.1)	31.1 (± 1.5)	3.7 (± 0.2) ^d	28.8 (± 0.8)	7.6 (± 0.3)	0.3 (± 0.1)
CMC	2.8 (± 0.3)	1.9 (± 0.1)	2.1 (± 0.1) ^d	3.4 (± 0.3)	1.2 (± 0.1)	0.4 (± 0.1)

Notes:

^c mol H₂/mol of pentose sugar.

^d mol H₂/mol of glucose equivalent.

the results are expressed as mean \pm standard error (n = 3).

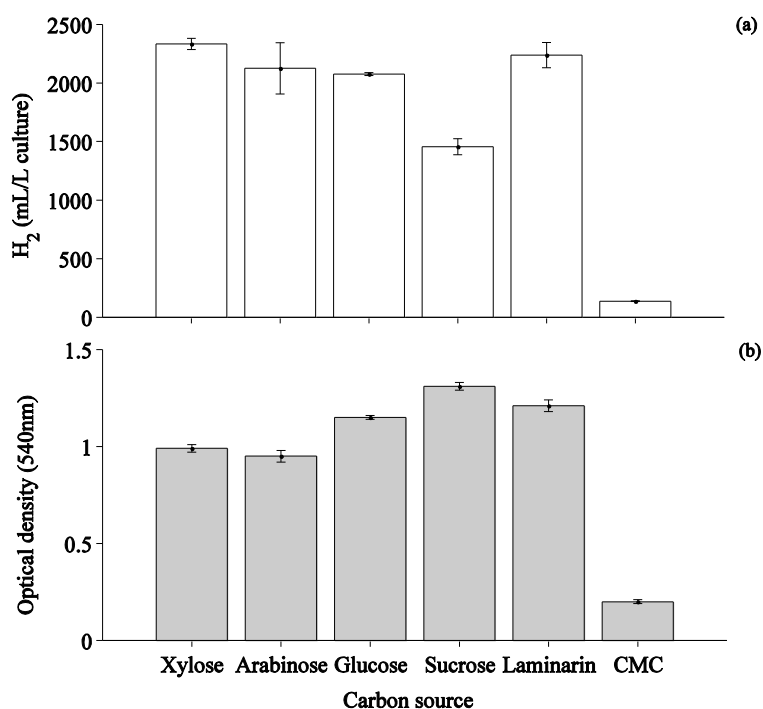


Fig. 4. 3 Effect of carbon source on (a) the H₂ production (mL/L culture) and (b) the biomass growth under CLF condition after 72 h of incubation ($n = 3$, error bars = standard error of mean).

4.3.4 Optimization tests

A salinity level of 35 g/L NaCl, 0.01 M of phosphate buffer and 28 mM of glucose or 33 mM arabinose as carbon source were selected for the culture parameter optimization tests. Table 4.4 shows the results of the optimization tests whereas the H₂ production and biomass growth are presented in Fig. 4.4a and Fig. 4.4b, respectively. About 80% of the substrate was consumed after 72 h of incubation. The H₂ yield from arabinose and glucose amounted to 3.0 (± 0.1) mol H₂/mol of arabinose and 3.1 (± 0.3) mol H₂/mol of glucose. The lactic acid productions from arabinose and glucose fermentation was 5.0 (± 0.1) mM and 12.7 (± 0.5) mM, respectively. The culture parameter optimization experiments showed that a higher quantity of lactic acid was synthesized with glucose as the carbon source compared to arabinose under similar operating conditions.

Table 4. 4 Substrate consumption and major fermentation products via the CLF pathway with 35 g/L NaCl and 0.01 M phosphate buffer after 72 h of fermentation in serum bottles and 24 h of fermentation in a CSTR.

	S (mM)	HPR (mL/L/h)	$Y_{H_2/S}$ (mol/mol)	Ac (mM)	Lac (mM)	Lac/Ac
Arabinose ^e	23.4 (\pm 0.2)	23.7 (\pm 0.7)	3.0 (\pm 0.1)	17.5 (\pm 0.1)	5.0 (\pm 0.1)	0.3 (\pm 0.1)
Glucose ^e	23.6 (\pm 0.4)	29.7 (\pm 2.3)	3.1 (\pm 0.3)	18.9 (\pm 0.6)	12.7 (\pm 0.5)	0.7 (\pm 0.1)
Glucose ^f	25.1 (\pm 2.8)	95.2 (\pm 17.3)	3.1 (\pm 0.2)	22.5 (\pm 2.3)	29.4 (\pm 6.9)	1.3 (\pm 0.3)

Notes:

^e culture parameter optimization experiments in 0.12 L serum bottles.

^f process scale-up experiments in a 3 L CSTR.

the results are expressed as mean \pm error (n = 3).

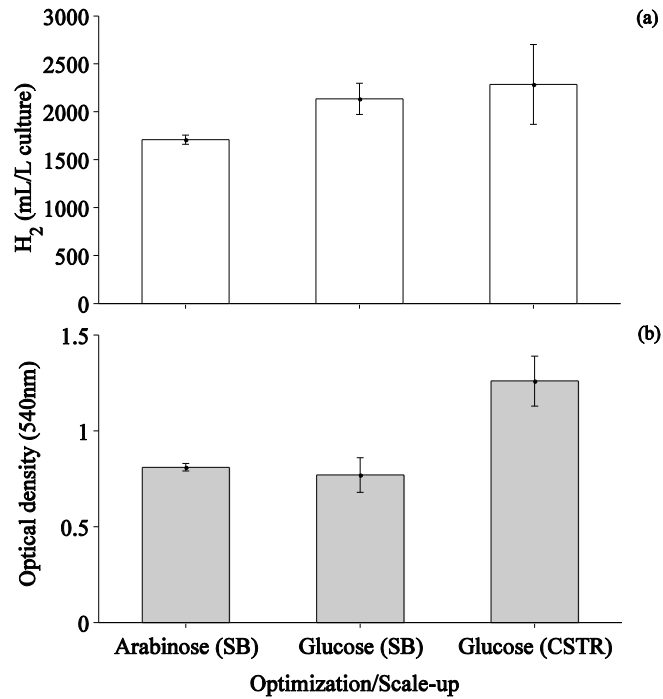


Fig. 4. 4 Effect of culture parameter optimization (serum bottles: SB) and process scale-up (CSTR) tests on (a) the H₂ production (mL/L culture) and (b) the biomass growth via the CLF pathway after 72 h of incubation (n = 3, error bars = standard error of mean).

4.3.5 Process scale-up

To validate the performance of the culture parameter optimization experiments, the experiments were scaled up from 0.12 L serum bottles to a 3 L CSTR containing 35 g/L NaCl, 0.01 M phosphate buffer and 28 mM glucose in the culture medium (Table 4.4). The performance of the culture parameter optimization experiments was further improved with over 90% glucose consumed in 24 h fermentation in the 3 L CSTR compared to 80% (approx.) in the 0.12 L serum bottles after 72 h of incubation. The H₂ yield was 3.1 (± 0.2) mol H₂/mol of glucose, which was comparable to the optimization tests conducted in the serum bottles (Table 4.4 and Fig. 4.4a). The lactic acid production was 29.4 (± 6.9) mM with a *Lac/Ac* ratio of 1.3 (± 0.3) compared to 0.7 (± 0.1) with the serum bottles. The process scale-up experiments not only improved the overall fermentation efficiency, but also enhanced the lactic acid production by 230% compared to the serum bottle experiments with similar culture parameters.

4.4 Discussion

The experimental study reported here has been conducted in three steps: (i) the effect of the three culture parameters (i.e. salinity level, buffering agent and carbon source) on H₂ and lactic acid production under CLF condition was investigated, (ii) the combined effect of culture parameters on the H₂ and lactic acid production through culture parameter optimization experiments and (iii) the culture parameter optimization experiment was up-scaled to a 3 L CSTR.

4.4.1 Optimization of culture parameters for CLF by *T. neapolitana*

4.4.1.1 Effect of salinity

Table 4.1 shows that *T. neapolitana* has a great adaptability on a wide range of salinity levels (also without any NaCl in the culture medium), exhibiting H₂ yield, which was always higher or comparable to *T. neapolitana* fermentation under various operating conditions (Dipasquale et al., 2015; Pradhan et al., 2015). For example, Pierra et al. (2014) studied the effect of the salinity level (9–75 g/L NaCl) on the H₂ production using mixed culture biomass and found that the increasing salinity level increased the lactic acid production. Similarly, in this study the lactic acid production increased over 7 folds when the NaCl concentration in the culture medium increased

from 0 to 35 g/L NaCl. The increasing or decreasing trend of H₂ production (Table 4.1 and Fig. 4.1a) with increasing salinity level could be referred to the available reductant energy, which is channelled out for extrusion of Na⁺ ions outside the cells, thus preventing the Na⁺ ion influx (Boiangiu et al., 2005). This suggests that the increasing salinity level could have further enhanced the recycling of acetic acid to form lactic acid under CLF conditions. However, this needs further investigations at biochemical pathway level.

4.4.1.2 Effect of buffering agent

Experiments with 0.01 M of different buffering agents along with CO₂ sparging showed consistent results based on H₂ and lactic acid production (Table 4.2). Cappelletti et al. (2012) studied different buffering agents of various concentrations and found that 0.1 M of HEPES was the best performing buffering agent under N₂ sparging atmosphere, yielding 1.6 (± 0.1) mol H₂/mol of glucose and 1.1 (± 0.1) mol acetic acid/mol of glucose. In another study by Ngo et al. (2011), 0.05 M HEPES was found to be sufficient in maintaining the buffering capacity of the culture medium and produced 2.7 (± 0.1) mol H₂/mol of glycerol consumed under N₂ sparging atmosphere. In a sharp contrast, Table 4.2 showed that only 0.01 M of buffers (either of Phosphate, MOPS, TRIS and HEPES) under CLF condition provided better results in terms of both H₂ and lactic acid production.

The buffering agent along with dissolved CO₂ in the form of HCO₃⁻ played a major role in maintaining the pH of the culture medium (~ 6.5), which ensured complete substrate degradation and product formation. However, the application of carbon based buffering agents like MOPS, TRIS and HEPES is expensive and could interfere in the quantification of carbon-based metabolites, and are consequently not recommended for large-scale applications. Therefore, the buffering capacity of the culture medium can best be maintained by using non-carbon based buffer like phosphate buffer along with CO₂ sparging (which supplies bicarbonate alkalinity). The phosphate buffer along with CO₂ combination will reduce the overall cost of maintaining the culture pH as well as to improve the overall performance of fermentation (Dipasquale et al., 2015; Pradhan et al., 2016a; Pradhan et al., 2016b).

4.4.1.3 Effect of carbon source

The abilities of *T. neapolitana* to ferment different carbon sources under N₂ sparging atmosphere was investigated by Pradhan et al. (2015). The H₂ yields from xylose, arabinose, glucose, sucrose, laminarin and CMC under N₂ sparging atmosphere were quite similar to the results obtained under CO₂ sparging atmosphere by *T. neapolitana* fermentation in the present study (Dipasquale et al., 2012; Eriksen et al., 2011; Nguyen et al., 2008; Pradhan et al., 2016b). The present study showed that the *Lac/Ac* ratio exceeds 0.5 for all the experiments (Table 4.2), thus the results are quite encouraging when compared to the N₂ sparged culture under similar experimental conditions where the *Lac/Ac* ratios were 0.2 (d'Ippolito et al., 2010) and 0.3 (Pradhan et al., 2016b). A negligible quantity of lactic acid was produced when the experiments were performed under N₂ sparging atmosphere (De Vrije et al., 2009; Frascari et al., 2013; Munro et al., 2009).

The ability of *T. neapolitana* to utilize xylose as carbon source opens a new prospective for handling agriculture-based waste where xylose is one of the main component. Among all the carbon sources tested in this study, the overall performance of fermentation with glucose and arabinose were found to be promising under CLF conditions.

4.4.2 Culture parameter optimization and process scale-up

The process scale-up experiments showed a 2.3 times higher lactic acid production in the 3 L CSTR compared to the experiments with 0.12 L serum bottles under similar operating conditions (see Table 4.4). In addition, a 20%, 50% and 100% higher acetic acid, biomass yield and *Lac/Ac* ratio, respectively, were achieved during 24 h of fermentation compared to the 72 h incubation in serum bottles.

As per the conventional dark fermentation model, the lactic acid production is always associated to a metabolic shift due to a sudden change in the environment parameters (e.g., pH, partial pressure of gases, organic loading rate, hydraulic retention time), indicating that the culture was not adapted to the new environmental condition (Temudo et al., 2007). van Niel et al. (2003) found that 5–10 mM of H₂ accumulation in the gas phase of the culture medium initiated a metabolic shift towards lactic acid synthesis for the extreme thermophile *Caldicellulosiruptor saccharolyticus*. Willquist et al. (2011) also observed that the dissolved H₂ in the culture medium and the osmotic

pressure determined a metabolic shift towards the lactic acid production.

In contrast to the findings by [Temudo et al. \(2007\)](#), [van Niel et al. \(2003\)](#) and [Willquist et al. \(2011\)](#) on *T. neapolitana* fermentation under N₂ sparging atmosphere, the recent studies by [Dipasquale et al. \(2014\)](#) and [d'Ippolito et al. \(2014\)](#) showed a new metabolic pathway where dissolved CO₂ and acetic acid are recycled back to produce lactic acid by a single enzyme, i.e. pyruvate:ferredoxin oxidoreductase (PFOR). Although the redox potential of the *T. neapolitana* cells are known to regulate lactic acid formation under CLF conditions ([d'Ippolito et al., 2014](#)), but the CLF mechanism is not fully understood which requires a detailed investigation into the culture medium along with the metabolic routes for the amino acids in the medium. This study clearly showed that both CO₂ in the form of HCO₃⁻ and Na⁺ ions in the culture medium trigger lactic acid synthesis, probably by using the residual energy (i.e. NADH) available from the amino acid degradation. This new CLF technology can be applied produce lactic acid at industrial scale. In addition, the CLF process has potential to significantly contribute to the global lactic acid production as it has high commercial value because of its application in various fields.

4.5 Conclusions

The feasibility of simultaneous H₂ and lactic acid synthesis by *T. neapolitana* was investigated by varying key culture parameters under CLF conditions. The study clearly depicted that increasing NaCl concentration from 0 to 35 g/L in the culture medium increased the lactic acid production by at least 750% without significant effects on the H₂ yield. The process scale-up experiments showed the scope for applying CLF-based fermentation to valorize organic substrates with higher salinity level. In addition, the process scale-up not only reduced the fermentation time by 66% but also improved the lactic acid production by over 230%. Application of CLF-based processes for industrial biotechnology would be a tangible step towards a novel approach for handling and treating biological recalcitrant organic substrates, such as high salinity wastewaters as well as solid wastes, for resource (H₂ and lactic acid) recovery and value addition.

References

- Bernfeld, P. 1955. Alpha and beta-amylases. *Methods in Enzymology*, **1**, 149-158.
- Boiangiu, C.D., Jayamani, E., Brugel, D., Herrmann, G., Kim, J., Forzi, L., Hedderich, R., Irini, V., Pierik, A.J., Steuber, J., Buckel, W. 2005. Sodium ion pumps and

- hydrogen production in glutamate fermenting anaerobic bacteria. *Journal of Molecular Microbiology and Biotechnology*, **10**, 105-119.
- Cappelletti, M., Bucchi, G., Mendes, J.D.S., Alberini, A., Fedi, S., Bertin, L., Frascari, D. 2012. Biohydrogen production from glucose, molasses and cheese whey by suspended and attached cells of four hyperthermophilic *Thermotoga* strains. *Journal of Chemical Technology and Biotechnology*, **87**, 1291-1301.
- d'Ippolito, G., Dipasquale, L., Fontana, A. 2014. Recycling of carbon dioxide and acetate as lactic acid by the hydrogen-producing bacterium *Thermotoga neapolitana*. *ChemSusChem*, **7**, 2678-83.
- d'Ippolito, G., Dipasquale, L., Vella, F.M., Romano, I., Gambacorta, A., Cutignano, A., Fontana, A. 2010. Hydrogen metabolism in the extreme thermophile *Thermotoga neapolitana*. *International Journal of Hydrogen Energy*, **35**, 2290-2295.
- De Vrije, T., Bakker, R.R., Budde, M.A.W., Lai, M.H., Mars, A.E., Claassen, P.A.M. 2009. Efficient hydrogen production from the lignocellulosic energy crop miscanthus by the extreme thermophilic bacteria *Caldicellulosiruptor saccharolyticus* and *Thermotoga neapolitana*. *Biotechnol. Biofuels*, **2**, 12.
- Dipasquale, L., Adessi, A., d'Ippolito, G., Rossi, F., Fontana, A., De Philippis, R. 2015. Introducing capnophilic lactic fermentation in a combined dark-photo fermentation process: a route to unparalleled hydrogen yields. *Applied Microbiology and Biotechnology*, **99**, 1001-10.
- Dipasquale, L., d'Ippolito, G., Fontana, A. 2014. Capnophilic lactic fermentation and hydrogen synthesis by *Thermotoga neapolitana*: An unexpected deviation from the dark fermentation model. *International Journal of Hydrogen Energy*, **39**, 4857-4862.
- Dipasquale, L., d'Ippolito, G., Gallo, C., Vella, F.M., Gambacorta, A., Picariello, G., Fontana, A. 2012. Hydrogen production by the thermophilic eubacterium *Thermotoga neapolitana* from storage polysaccharides of the carbon dioxide fixing diatom *Thalassiosira weissflogii*. *International Journal of Hydrogen Energy*, **37**, 12250-12257.
- Dubois, M., Gilles, K.A., Hamilton, J.K., Rebers, P.A., Smith, F. 1956. Colorimetric method for determination of sugars and related substances. *Analytical Chemistry*, **28**, 350-6.
- Eriksen, N.T., Riis, M.L., Holm, N.K., Iversen, N. 2011. Hydrogen synthesis from pentoses and biomass in *Thermotoga* spp. *Biotechnology Letters*, **33**, 293-300.
- Frascari, D., Cappelletti, M., Mendes, J.D.S., Alberini, A., Scimonelli, F., Manfreda, C., Longanesi, L., Zannoni, D., Pinelli, D., Fedi, S. 2013. A kinetic study of biohydrogen production from glucose, molasses and cheese whey by suspended and attached cells of *Thermotoga neapolitana*. *Bioresource Technology*, **147**, 553-61.

- Joglekar, H.G., Rahman, I., Babu, S., Kulkarni, B.D., Joshi, A. 2006. Comparative assessment of downstream processing options for lactic acid. *Separation and Purification Technology*, **52**, 1-17.
- Johnston, B., Mayo, M.C., Khare, A. 2005. Hydrogen: the energy source for the 21st century. *Technovation*, **25**(6), 569-585.
- Munro, S.A., Zinder, S.H., Walker, L.P. 2009. The fermentation stoichiometry of *Thermotoga neapolitana* and influence of temperature, oxygen, and pH on hydrogen production. *Biotechnology Progress*, **25**, 1035-1042.
- Nath, K., Das, D. 2004. Improvement of fermentative hydrogen production: Various approaches. *Applied Microbiology and Biotechnology*, **65**, 520-529.
- Ngo, T.A., Kim, M.S., Sim, S.J. 2011. High-yield biohydrogen production from biodiesel manufacturing waste by *Thermotoga neapolitana*. *International Journal of Hydrogen Energy*, **36**, 5836-42.
- Nguyen, T.A.D., Kim, J.P., Kim, M.S., Oh, Y.K., Sim, S.J. 2008. Optimization of hydrogen production by hyperthermophilic eubacteria, *Thermotoga maritima* and *Thermotoga neapolitana* in batch fermentation. *International Journal of Hydrogen Energy*, **33**, 1483-88.
- Pierra, M., Trably, E., Godon, J.J., Bernet, N. 2014. Fermentative hydrogen production under moderate halophilic conditions. *International Journal of Hydrogen Energy*, **39**(14), 7508-7517.
- Pradhan, N., Dipasquale, L., d'Ippolito, G., Fontana, A., Panico, A., Pirozzi, F., Lens, P.N.L., Esposito, G. 2016a. Model development and experimental validation of capnophilic lactic fermentation and hydrogen synthesis by *Thermotoga neapolitana*. *Water Research*, **99**, 225-234.
- Pradhan, N., Dipasquale, L., d'Ippolito, G., Fontana, A., Panico, A., Lens, P.N.L., Pirozzi, F., Esposito, G. 2016b. Kinetic modeling of fermentative hydrogen production by *Thermotoga neapolitana*. *International Journal of Hydrogen Energy*, **41**, 4931-4940.
- Pradhan, N., Dipasquale, L., d'Ippolito, G., Panico, A., Lens, P.N.L., Esposito, G., Fontana, A. 2015. Hydrogen production by the thermophilic bacterium *Thermotoga neapolitana*. *International Journal of Molecular Sciences*, **16**, 12578-12600.
- Temudo, M.F., Kleerebezem, R., van Loosdrecht, M. 2007. Influence of the pH on (open) mixed culture fermentation of glucose: a chemostat study. *Biotechnology and Bioengineering*, **98**, 69-79.
- van Niel, E.W.J., Claassen, P.A.M., Stams, A.J.M. 2003. Substrate and product inhibition of hydrogen production by the extreme thermophile, *Caldicellulosiruptor saccharolyticus*. *Biotechnology and Bioengineering*, **81**, 255-262.
- Willquist, K., Pawar, S.S., van Niel, E.W.J. 2011. Reassessment of hydrogen tolerance in *Caldicellulosiruptor saccharolyticus*. *Microbial Cell Factories*, **10**, 111-121.

Chapter 5

Dark fermentation model

This chapter has been published as:

Pradhan, N., Dipasquale, L., d'Ippolito, G., Fontana, A., Panico, A., Lens, P.N.L., Pirozzi, F., Esposito, G. 2016. Kinetic modeling of fermentative hydrogen production by *Thermotoga neapolitana*. *International Journal of Hydrogen Energy*, 41, 4931-4940.

Chapter 5: Dark fermentation model

Abstract

A kinetic model of fermentative hydrogen (H_2) production was developed for the hyperthermophilic marine bacterium *Thermotoga neapolitana* DSMZ 4359^T using glucose as the substrate. The model was built based on anaerobic digestion model no.1 (ADM1) by IWA using Monod-like kinetic equations. Several series of pH controlled batch fermentation tests were performed under pure CO_2 or N_2 atmosphere in serum bottles to evaluate the growth kinetic parameters. The kinetic parameters were estimated by applying the non-linear least square method to Monod and Michaelis-Menten kinetic equations. The experimentally estimated value of k , k_S , Y and k_d were 0.839 1/h, 1.42 g/L, 0.1204 and 0.0043 1/h, respectively. The kinetic parameters were analyzed for sensitivities and subsequently calibrated and validated by a separate set of experimental results. The model was particularly effective in estimating the biomass growth, substrate consumption, and H_2 production except for acetate and lactate production, due to capnophilic condition (under CO_2 atmosphere).

Keywords: dark fermentation; kinetic model; sensitivity analysis; model calibration; model validation; hydrogen.

5.1 Introduction

Hydrogen (H_2) is one of the cleanest energy carriers and has the potential to mitigate greenhouse gas (GHG) emissions. H_2 is currently produced from fossil resources, such as natural gas, hydrocarbons and coal by pyrolysis and gasification, but it is also obtainable from water and organic substrates by electrolytic, photolytic and biological processes, respectively. Traditionally, the biological H_2 production by photo-fermentation (PF) and dark fermentation (DF) has been considered technically feasible and environmentally friendly (Hallenbeck & Benemann, 2002; Manish & Banerjee, 2008; Nath & Das, 2004). The DF process provides high H_2 production rates with simple technological requirements. The process is also independent of light that, on the contrary, is a crucial technical constraint to configure photo-fermentation processes (Antonopoulou et al., 2011; Nath & Das, 2004).

H_2 production by DF also benefits from the possibility to use a very wide range of organic substrates, including agro-industrial wastes, as starting feedstocks and to operate at various environmental conditions such as pH, temperature, organic loading rate (OLR) and hydraulic retention time (HRT) (Amend & Shock, 2001; Elsharnouby et al., 2013). The significant advantages of using hyperthermophilic bacterial fermentation are as follow: (i) improves hydrolysis of the substrate, (ii) reduces fermentation time, (iii) minimizes contamination level and improves process efficiency by allowing to use a variety of waste streams and (iv) produces clean and few fermentation byproducts (H_2 , CO_2 , acetic acid, lactic acid and alanine) (Pradhan et al., 2015). Furthermore, conversion of the organic substrate into H_2 is associated to the synthesis of various volatile organic acids (VOAs) as byproducts. The qualitative and quantitative composition of VOAs depends on the microbial species, culture conditions and metabolic pathways. The type and quantities of these products are strictly related to the H_2 yield of the chemotrophic processes. DF can be successfully performed with both pure and mixed cultures. Several researchers have shown that pure cultures can yield higher amounts of hydrogen compared to mixed culture biomass (Elsharnouby et al., 2013; Van Ooteghem et al., 2004). In the last decade, some researchers have used pure cultures of *Thermotogales* species to produce hydrogen and have reported 4 mol H_2 /mol of glucose, i.e. the theoretical maximum value of H_2 production under DF (Elsharnouby et al., 2013; Thauer, 1977; Van Ooteghem et al., 2004).

Among the *Thermotogales*, *Thermotoga neapolitana* is a hyperthermophilic marine bacterium extensively used in the DF process to produce up to or above 3.6 mol H₂/mol of glucose consumed (d'Ippolito et al., 2010; Eriksen et al., 2011; Munro et al., 2009). Recently, some of the authors of this paper have shown that under CO₂ atmosphere (i.e. capnophilic condition) the bacterium not only produces H₂, but also synthesizes significant quantities of lactic acid without affecting the overall H₂ yield (Dipasquale et al., 2015; Dipasquale et al., 2014).

In order to transfer the technology from laboratory to industrial scale or commercial application, it is imperative to model, calibrate and optimize the process. From the scientific literature survey, it was found that the majority of the researchers have adapted and modified existing mathematical (or empirical) models to describe their experimental results (Gadhe et al., 2014). The Gompertz empirical model and anaerobic digestion model no. 1 (ADM1) of the international water association (IWA) are popular models that are extensively used to simulate the DF process.

The Gompertz model is based on a sigmoid function that operates on a time series and is commonly used for fermentative H₂ production. This model is particularly used to estimate the maximum H₂ production potential and to determine the lag phase for H₂ production (Gadhamshetty et al., 2010; Khanna et al., 2011; Maru et al., 2013). However, it is difficult to understand the process kinetics from the Gompertz empirical model owing to exclusion of operating conditions (e.g. substrate type and concentration, pH, temperature and partial pressure of gas mixture) that regulate the fermentation reaction. On the other hand, ADM1 is a complete and comprehensive kinetic model based on Monod-like kinetic equations, used to model the anaerobic digestion process in detail (Batstone et al., 2002; Castello et al., 2009; Paulo et al., 2013). Over the last decade, several researchers have adapted ADM1 to model DF reactions (Frasconi et al., 2013; Gadhamshetty et al., 2010; Yu & Drapcho, 2011). The kinetic parameters used in the ADM1 model are estimated from a series of batch and continuous experiments by using Monod (or Michaelis-Menten) kinetic equations (Frasconi et al., 2013; Yu & Drapcho, 2011).

As dark fermentative H₂ production by hyperthermophilic bacteria like *T. neapolitana* is relatively new, the biological kinetic parameters are still not well studied and understood. Furthermore, the conventional kinetic parameters found in the literature

(Batstone et al., 2002) cannot be applied directly to model the *T. neapolitana* fermentation. In this study, we aimed at developing a kinetic model for fermentative H₂ production by a pure culture bacterium *T. neapolitana* according to DF conditions. To achieve this aim, batch fermentation tests were carried out in order to estimate the kinetic parameters for *T. neapolitana* fermentation and then the process was mathematically modeled (i.e. sensitivity analysis, model calibration and model validation) according to the DF principles.

5.2 Materials and methods

5.2.1 Bacterial strain and medium composition

Thermotoga neapolitana DSMZ 4359^T (i.e. laboratory strain ‘TN-CMut’ as in Chapter 3) was purchased from the Deutsche Sammlung von Mikroorganismen und Zellkulturen (Braunschweig, Germany). The bacterium was grown anaerobically according to d’Ippolito et al. (2010) and Dipasquale et al. (2014) in the modified version of the ATCC 1977 culture medium. This culture medium contains (g/L): NaCl 10.0; KCl 0.1; MgCl₂·6H₂O 0.2; NH₄Cl 1.0; K₂HPO₄ 0.3; KH₂PO₄ 0.3; CaCl₂·2H₂O 0.1; cysteine-HCl 1.0; yeast extract 2.0; tryptone 2.0; glucose 5.0; resazurin (redox indicator) 0.001; 10 ml/L of both filter-sterilized vitamins and trace element solutions (DSM medium 141) in 1L distilled H₂O.

5.2.2 Experiments

30 mL of culture medium was poured into 120 mL serum bottles. The dissolved O₂ in the culture medium was removed by heating the serum bottles until the medium was colorless with the presence of the redox indicator resazurin. Similarly, the culture medium for the 3 L continuously stirred tank reactor (CSTR) was prepared and the glucose concentration of the medium was increased to 10 g/L instead of 5 g/L. The serum bottles with culture medium and culture medium for CSTR were sterilized by autoclaving at 110 °C for 15 min. Three different series of batch fermentation tests were carried out at 80 ± 1 °C and under anaerobic conditions. Batch test A and B were conducted in serum bottles under CO₂ and N₂ sparging atmosphere, respectively, to estimate the kinetic parameters. Test C was conducted under CO₂ sparging atmosphere in the 3 L CSTR for model validation purposes.

The serum bottles (tests A and B) were sparged with CO₂ and N₂, respectively, for 3 min and adjusted to approximately pH 7.5 by adding 1 mL of 1 M NaOH. The

bottles were subsequently inoculated with 6% v/v of pure *T. neapolitana* pre-culture and kept in the oven at 80 ± 1 °C. 3 mL, fermentation sample was sampled at the end of each test and the supernatant was stored for further analysis. For test C, the sterilized culture medium (742 mL including 6% v/v pre-culture inoculum) was transferred to a jacketed 3 L CSTR (ezControl Applikon Biotechnology, The Netherlands). For all the batch tests, the culture volume to the headspace ratio was maintained at 1:3. The mixture was sparged with pure CO₂ for 5 min at 30 mL min⁻¹ to create an anaerobic environment. The initial working pH was adjusted to 7.5 with 1 M NaOH and then the pH probe was reset to 6.5 ± 0.1 and maintained by automatic titration with 1 M NaOH for the entire duration of the experiment. The temperature was thermostatically kept constant at 80 ± 1 °C and the mixing rate was set to 50 rpm using an electro-magnetic stirring unit. 3 mL of the fermentation mixture was sampled at regular intervals, centrifuged and stored for further analysis. The fermentation mixture was sparged with CO₂ at each sampling point to remove H₂ trapped in the bulk and in the headspace of the bioreactor.

5.2.3 Analytical methods

Gas (H₂ and CO₂) measurements were performed by a gas chromatograph (Focus GC, Thermo Scientific) equipped with a thermo-conductivity detector (TCD), a 3 m molecular sieve column (Hayesep Q) and nitrogen was used as carrier gas (Dipasquale et al., 2014). All the analyses were performed on the supernatants of the samples previously centrifuged at 13,000 rpm for 5 min.

Acetic acid, lactic acid, and alanine concentrations were detected by a ¹H Nuclear Magnetic Resonance (NMR) 600 MHz spectrometer (Bruker Avance 600) equipped with a cryoprobe and 3.8 mM trime-thylamine hydrochloride (TMA) was used as internal standard (Dipasquale et al., 2014). The residual glucose concentration was measured by the dinitrosalicylic acid (DNS) method calibrated on a standard solution of 2.0 g/L glucose (Bernfeld, 1955).

The biomass growth was monitored through optical density (OD) measurements at $\lambda = 540$ nm by a UV/Vis spectrophotometer (V-650, Jasco). The biomass growth was also monitored as wet and dry cell weight. Before lyophilization, the cells were previously centrifuged at 13,000 rpm for 5 min and washed twice with a NaCl (10 g/L) solution. Correlation between cells dry weight (CDW) measurement and OD_{540nm}

showed a coefficient of regression i.e. $R^2 = 0.98$ and the equation as $CDW \text{ (g/L)} = 0.347 \cdot OD_{540nm} + 0.016$, for the cultures sparged with CO_2 .

5.3 Mathematical modeling

5.3.1 Metabolic pathway and equations

According to the traditional model of H_2 production by chemotrophic bacteria (Fig. 5.1), the theoretical limit of 4 mol H_2 /mol of glucose consumed is possible when acetate is the only fermentation by-product. This process, which is typical in many thermophilic and hyperthermophilic bacteria, is reduced by simultaneous excretion of other fermentation products, e.g. lactic acid, whose synthesis depends on operating factors such as working pH, partial pressure of gases in the headspace and concentration of inhibitory compounds. *T. neapolitana* follows mainly the Embden-Meyerhoff pathway (EMP) for glucose catabolism ($C_6H_{12}O_6 + 4ADP + 4P_i + 2H_2O \rightarrow 2CH_3COOH + 2CO_2 + 4H_2 + 4ATP$) and uses a unique ferredoxin-coupled reaction to oxidize NADH and replenish NAD^+ (d'Ippolito et al., 2010; Dipasquale et al., 2015).

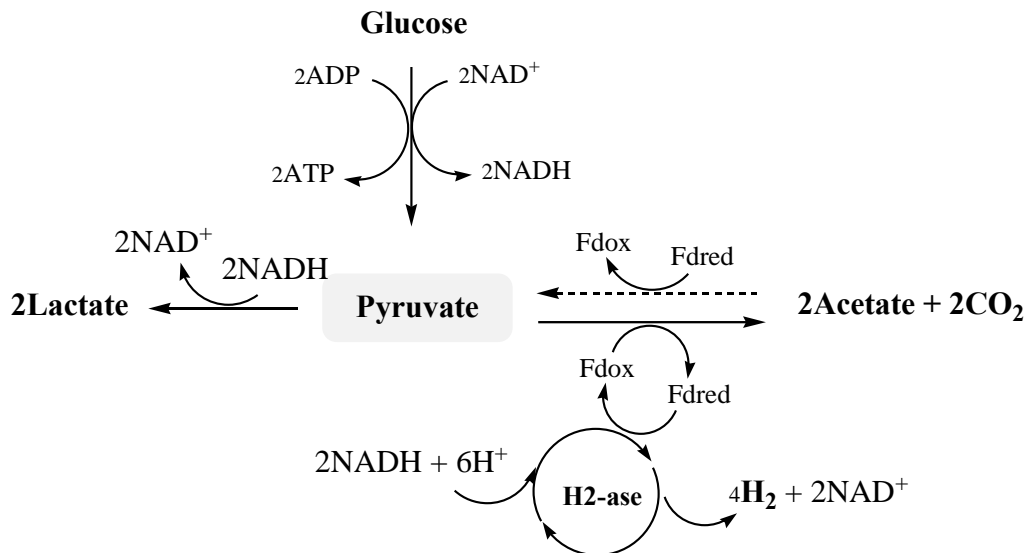


Fig. 5. 1 Simplified biochemical pathway for fermentative hydrogen production by *T. neapolitana* (adapted and modified from Dipasquale et al. (2014)). Dashed arrow indicates the feedback cycle triggered by CO_2 during CLF.

The present kinetic model considers the basic metabolic pathway depicted in Fig. 5.1 to construct the kinetic model for DF. All the differential algebraic equations (DAEs) equations for metabolic reactions were written according to the Monod's kinetic equation and presented in Table 5.1 (Eqs. (5.1)–(5.3)). Eq. (5.4) in Table 5.1 is a pH inhibition equation used to represent the effect on the fermentation reaction due to the variation of pH from the desired value (Batstone et al., 2002). The equations in Table 5.1 were solved by the ordinary differential equations (ODEs) tool (i.e. ode15s) of MATLAB R2010a. The kinetic parameters of the equations were evaluated by a non-linear least square method discussed in sub-section Kinetic parameter estimation and subsequently refined by model calibration (see sub-section Model simulation), whereas the stoichiometric coefficients in the equations were determined from the batch tests (i.e. test A and C). The concentrations of biomass, glucose, acetate, lactate, alanine and hydrogen gas were measured at different time intervals. The experiment A and C were conducted under CO₂ atmosphere so the CO₂ production rate was not measured hence only CO₂ prediction was shown in the model.

Table 5. 1 Kinetic expressions used for the simulation of the experimental data according to ADM1 model.

Process	Equations
Substrate consumption	$\frac{dS}{dt} = -k \left(\frac{S}{k_S + S} \right) X * I_{pH} \quad (5.1)$
Net biomass growth	$\frac{dX}{dt} = -Y \left(\frac{dS}{dt} \right) - (k_d X) \quad (5.2)$
Products formation	$\frac{dS_i}{dt} = -(1 - Y) f_i \left(\frac{dS}{dt} \right) \quad (5.3)$
pH inhibition	$I_{pH} = \frac{1 + 2 * 10^{0.5(pH_{LL} - pH_{UL})}}{1 + 10^{(pH - pH_{UL})} + 10^{(pH_{LL} - pH)}} \quad (5.4)$

Notes: $f_i = f_{ac}, f_{lac}, f_{H2}$ and f_{CO2} are the stoichiometric coefficients of the products.

$S_i = S_{Ac}, S_{Lac}, S_{H2}$ and S_{CO2} .

Ac = Acetic acid (mM); Lac = Lactic acid (mM); CO₂ = Carbon dioxide (mM).

k = maximum specific uptake rate (1/h); k_S = semi-saturation constant (g/L); Y = biomass yield coefficient; k_d = endogenous decay rate (1/h); X = biomass concentration

(g/L); S = substrate concentration (g/L); I_{pH} = pH inhibition factor; pH_{LL} = pH lower limit; pH_{UL} = pH upper limit.

5.3.2 Kinetic parameter estimation

The correlation between the specific uptake rate of substrate consumption and the substrate concentration is given through the Michaelis-Menten kinetics (Eq. (5.5)). Eq. (5.5) is used where the concentration of a single substrate (S) can limit the degradation rate and the accumulation of growth inhibiting compounds are neglected (Nwabanne et al., 2009). A non-linear least square method (Fang et al., 2013; Frascari et al., 2013; Nath et al., 2008) was applied to the Michaelis-Menten kinetic equation for calculating the kinetic parameters (Eq. (5.6)). Eq. (5.6) was integrated using MATLAB software to determine the values of all the kinetic parameters.

$$v = \frac{k S}{k_S + S} \quad (5.5)$$

$$\sum_{i=1}^n e_i^2 = \sum_{i=1}^n (v_i - v_i^{th})^2 = \sum_{i=1}^n \left(v_i - \frac{k S_i}{k_S + S_i} \right)^2 \quad (5.6)$$

where v (1/h) = specific uptake rate, e_j = the error calculated by the difference between experimental (v_j) and predicted (v_j^{th}) values of a dependent variable for each experimental point, S_j value is the variable with respect to n experimental points. The results of batch test A were selected to estimate the kinetic parameters k and k_S using Eqs. (5.5) and (5.6). Similarly, Monod's kinetic equation was applied to Eq. (5.6) to evaluate the kinetic parameter Y and k_d .

5.3.3 Model simulation

MATLAB version 7.10.0 by MathWorks™ was used to run the mathematical model composed of DAEs shown in Table 5.1. The stoichiometric coefficients for the DAEs were in accordance with the test results shown in Table 5.2 (i.e. test A). The input state variables X_0 (biomass concentration at time $t = 0$ h) and S_0 (substrate concentration at time $t = 0$ h) were set to 0.1 g/L and 5 g/L, respectively. A lag phase of 4-6 h was assumed at the beginning of the fermentation test. The model input and output functions were written in a M-file of MATLAB. The simulation cycle was

carried out in 3 key process steps, i.e. sensitivity analysis, model calibration and model validation.

5.3.4 Sensitivity analysis

A sensitivity analysis was performed to determine the most influential kinetic parameters that affect the model output. In this study, a local sensitivity analysis tool was used to check the stability of the model with respect to the input state variables (X, S, H₂, Ac, Lac and CO₂) and kinetic parameters (k , k_S , Y and k_d). The partial derivatives (Eq. (5.7)) of the input state variables with respect to kinetic parameters gave the values for absolute (or local) sensitivities at different time intervals. SENS_SYS, a local sensitivity analysis tool was used to measure the sensitivities of the model parameters to the model output using a set of ordinary differential equation (ODE) functions (Maly & Petzold, 1996; Molla & Padilla, 2002):

$$F(t, y, y', u) = 0 \quad (5.7)$$

where t = time (T), y = input state variables, y' = first derivative of y with respect to t and u = kinetic parameters.

5.3.5 Model calibration

The main aim of the model calibration was to minimize the error between model prediction and measured data until the best fitting of the model prediction curve with the measured data was achieved. The results of batch test A were used for the model calibration, which was conducted as per Esposito et al. (2011) and Janssen and Heuberger (1995) in 4 steps. Kinetic parameters k , Y and k_d were selected for calibration as they mostly affected the model outputs according to sensitivity analysis (see sub-section Sensitivity analysis). In the step 1, a variation range was assigned to the following kinetic parameters: k , Y and k_d . The range was assigned based on the estimated values obtained from the non-linear least square method. In step 2, an array was defined for the kinetic parameters (k , Y and k_d) as shown in Eqs. (5.8)–(5.10). The calculation was performed by taking $m+1$ step values for both Y and k_d between the variation ranges, according to the following equations:

$$k^i = k^{i-1} + \partial k; \quad i = 1 \dots m \quad (5.8)$$

$$Y^i = Y^{i-1} + \partial Y; \quad i = 1 \dots m \quad (5.9)$$

$$k_d^i = k_d^{i-1} + \partial k_d; \quad i = 1 \dots m \quad (5.10)$$

where $k^0 = 1.0$ 1/h and $k^m = 5.0$ 1/h were the lower and upper bounds of the variation range for k , respectively, and δk is the ratio between the length of the range and m . Similarly, $Y^0 = 0.05$ 1/h and $k_d^0 = 0.002$ 1/h were the lower bounds of the variation range, and $Y^m = 0.15$ and $k_d^m = 0.10$ were the upper bounds of the variation range for Y and k_d , whereas δY and δk_d are the ratios between the range length and m , respectively, for Y and k_d .

Firstly, the parameter k was calibrated by keeping the other kinetic parameters constant and then Y and k_d were calibrated with the new value of k , whereas k_s was kept constant throughout the calibration process (see [sub-section Sensitivity analysis](#)). To improve the accuracy of the results, the value of m (number of points) was set to 10. A ‘m x m’ (10 x 10) matrix was built with the different values of Y and k_d and the model was run for each set of Y and k_d values taken from the matrix. In step 3, the output of the calibration process was plotted in a 3-D surface plot for each set of Y and k_d values. Three commonly used regression tools, i.e. Modeling Efficiency (ME), Index of Agreement (IA) and Root Mean Square Error (RMSE) were applied to compare the quality of fitting between predicted and measured data ([Esposito et al., 2011](#); [Janssen & Heuberger, 1995](#)). The Eqs. (5.11)–(5.13) for the regression tools are as follows:

$$ME = 1 - \frac{\sum_{i=1}^n (O_i - P_i)^2}{\sum_{i=1}^n (O_i - \bar{O})^2} \quad (5.11)$$

$$IA = 1 - \frac{\sum_{i=1}^n (O_i - P_i)^2}{\sum_{i=1}^n (|P_i - \bar{O}| + |O_i - \bar{O}|)^2} \quad (5.12)$$

$$RMSE = \sqrt{\frac{\sum_{i=1}^n (O_i - P_i)^2}{n}} \quad (5.13)$$

where n = number of observed values, O_i = observed values, P_i = predicted values, \bar{O} = mean of observed values. In step 4, the best set of values for Y and k_d was determined from the 3-D surface plot by checking the three regression tools and similarly, the best value for k was obtained by analyzing the regression tools.

5.3.6 Model validation

The model validation was carried out using the optimized set of kinetic parameters from the model calibration step and using the results of the 3.0 L CSTR (test C). The input state variables such as X_0 and S_0 were 0.1 g/L and 10 g/L, respectively.

The quality of model fitting was evaluated in terms of ME, IA and RMSE as the way done for the model calibration process (see [sub-section Model calibration](#)).

5.4 Results and discussion

5.4.1 Fermentation of sugar by *T. neapolitana*

[Table 5.2](#) shows the main results from batch tests performed under various conditions. Batch test A and B in [Table 5.2](#) show a similar trend for substrate consumption, biomass growth and product formation as clearly depicted in [Fig. 5.2](#). The H₂ yield for test A was found to be 3.27 mol H₂/mol of glucose consumed, whereas for test B it was 2.32 mol H₂/mol of glucose consumed. The yields of H₂, acetate and lactate for test A were found to be 41%, 15% and 80%, respectively, higher than for test B. For test C, the H₂, acetate and lactate yield was found to be 3.26, 1.16 and 0.89 mol/mol of glucose consumed, respectively. Synthesis of alanine was very low and its contribution to the model was considered negligible.

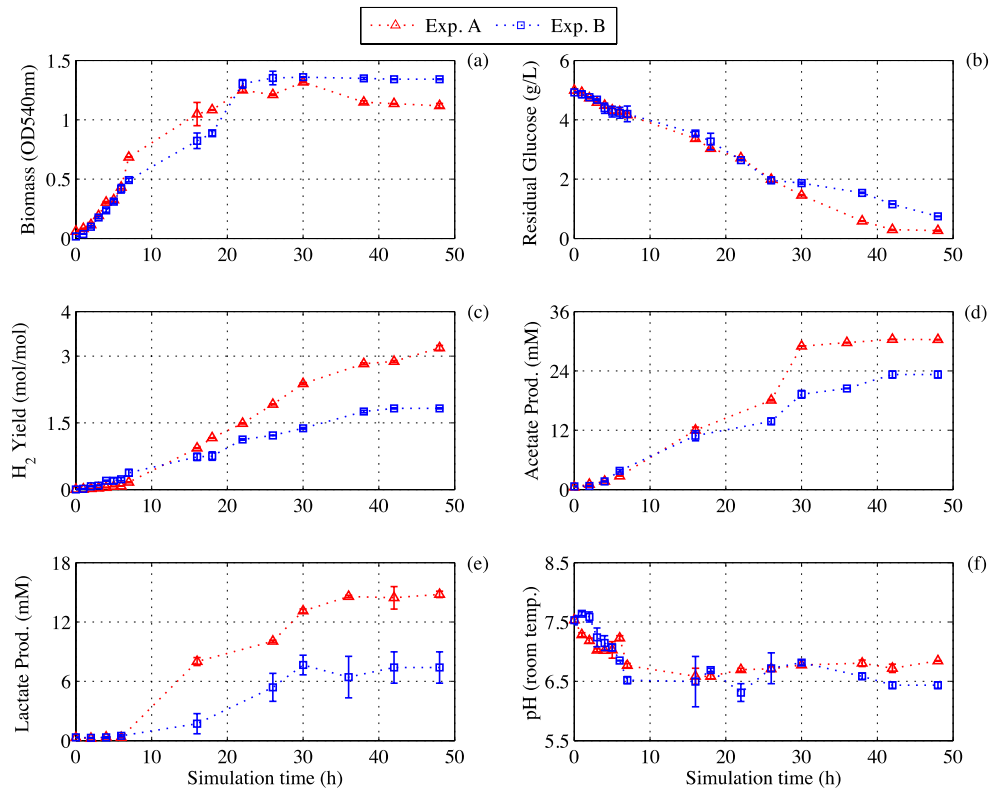


Fig. 5. 2 Biomass growth, substrate consumption and product formation by *T. neapolitana* from tests A and B: (a) biomass growth, (b) residual glucose, (c) H₂ yield, (d) acetate production, (e) lactate production and (f) pH (room temperature).

Table 5. 2 Results from batch fermentation tests by *T. neapolitana* under CO₂ or N₂ atmosphere.

	V ^a : 120 mL, WV ^b : 32 mL		V: 3.0 L, WV:
			740mL
	(CO ₂ , sparged) ^c	(N ₂ , sparged) ^c	(CO ₂ , sparged) ^d
	A	B	C
Time (h)	48	48	52
Glucose input (mM)	27.75	27.75	55.50
Glucose consumed (mM)	26.30±0.03	24.02±0.14	48.99±2.32
Y (g dry cells/g glucose)	0.11±0.02	0.12±0.006	0.078±0.001

f_{H2} (mol/mol)	3.27±0.09	2.32±0.02	3.26±0.15
f_{Ac} (mol/mol)	1.15±0.05	1.01±0.03	1.16±0.07
f_{Lac} (mol/mol)	0.56±0.03	0.31±0.07	0.89±0.19
f_{Ala} (mol/mol)	0.10±0.01	0.16±0.01	0.04±0.01

Notes: test A and B were conducted in duplicates and test C was conducted triplicates.

^a volume of the reactor.

^b working volume.

^c intermittent pH correction.

^d continuous pH correction.

5.4.2 Evaluation of kinetic parameters and model simulation

Applying the non-linear least square method to the results of batch test A, the values of k , k_s , Y , and k_d were found to be 0.839 1/h, 1.42 g/L, 0.1204 and 0.0043 1/h, respectively. The above kinetic parameters were used to develop the model. Fig. 5.3 compares the model results with the experimental values from test A. The regression value for the ME, IA and RMSE for biomass growth, substrate consumption and product formation were found to be > 0.80, > 0.98 and < 0.34, respectively. This proves that the kinetic parameters determined from batch test A were accurate and can be used successfully to simulate other experimental data with similar operating conditions. Hence, a sensitivity analysis was performed on the kinetic parameters to check the most sensitive kinetic parameters that affect the model results.

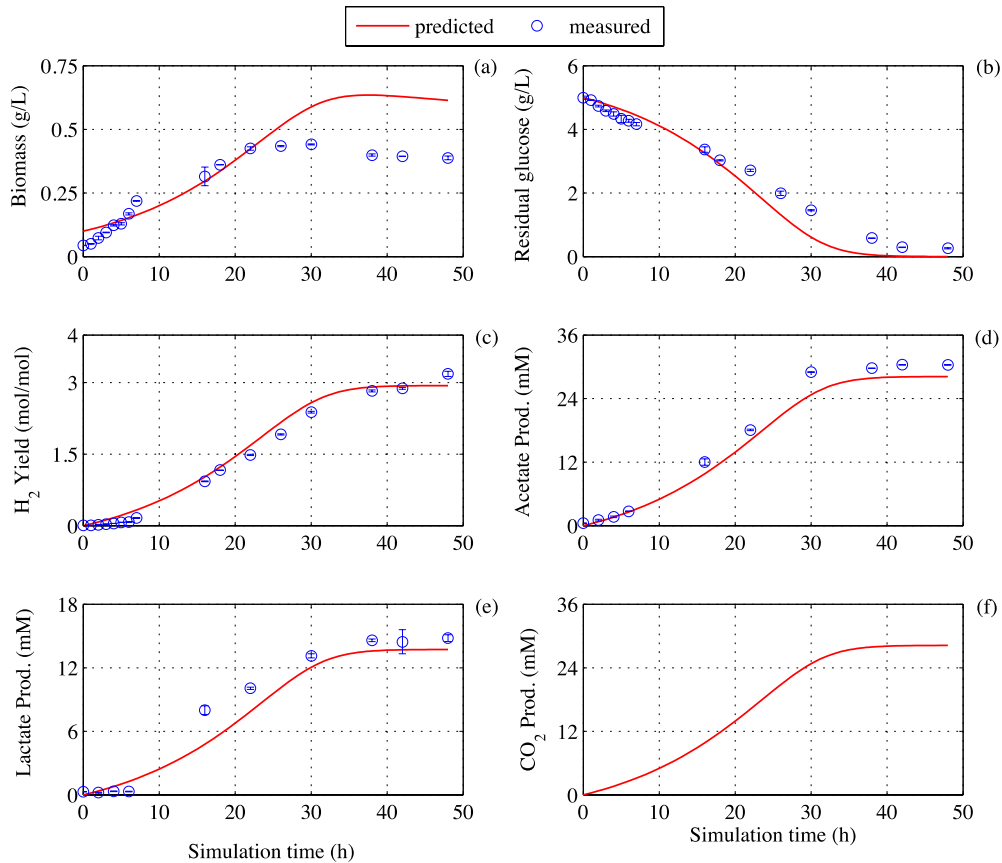


Fig. 5.3 Model simulation for biomass growth and product formation by *T. neapolitana* for batch experiment A: predicted and measured results for (a) biomass growth (cell dry weight), (b) residual glucose, (c) H₂ yield, (d) acetate production, (e) lactate production and (f) predicted CO₂ production.

5.4.3 Sensitivity analysis

Fig. 5.4 shows the absolute sensitivities of the kinetic parameters for the input state variables. The endogenous decay rate (k_d) and biomass yield coefficient (Y) have the highest impact on the model output state variables (Fig. 5.4). The absolute sensitivities for Y and k_d reach their maximum value around 28 h and then decrease. Fig. 5.4 shows that the model prediction is critical around 28 h of fermentation. On the other hand, the maximum specific uptake rate (k) has a minimal impact on the model prediction, whereas the semi-saturation constant (k_S) has no impact on the model prediction. Therefore, k , Y and k_d were sensitive kinetic parameters and were optimized in the model calibration step.

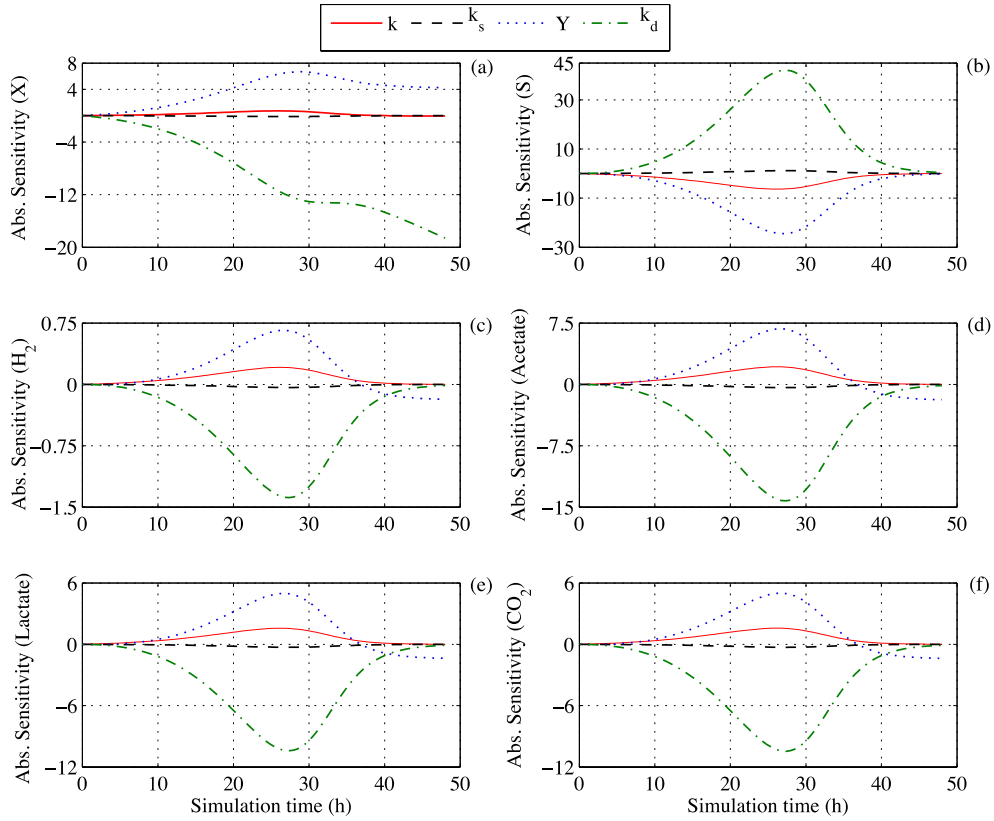


Fig. 5. 4 Absolute (or local) sensitivities of kinetic parameters during the fermentation time for (a) biomass growth, (b) substrate consumption, (c) H₂ yield, (d) acetate production, (e) lactate production and (f) CO₂ production.

5.4.4 Model calibration

Model calibration was performed on the substrate (S) consumption and H₂ production. Fig. 5.5 shows the 3D surface plot for the varying kinetic parameters on S and H₂. Fig. 5.5 shows a region of linear optima for all the parameters hence, a possible set of values for Y and kd along with it's corresponding regression coefficients was extracted and analyzed for best fitting condition. The final set of calibrated kinetic parameters were selected based on the analysis of regression coefficients, i.e. ME > 0.95, IA > 0.99 and RMSE < 0.1. The respective calibrated values of k, Y and k_d were 1.42 1/h, 0.1125 and 0.0525 1/h, respectively. The other kinetic parameters such as maximum specific growth rate ($\mu_{max} = Y*k$) and biomass doubling time ($t_d = \ln(2)/\mu$) for *T. neapolitana* were found to be 0.16 1/h and 4.37 h, respectively. The k_d value for *T. neapolitana* was found to be higher than estimated because of the quick biomass

doubling time (t_d). Apart from this study, two more studies estimated the kinetic parameters of *T. neapolitana* from batch experiments under N₂ sparging atmosphere. [Yu and Drapcho \(2011\)](#) reported that the μ_{max} , k_S and Y for *T. neapolitana* growing on glucose were 0.94 h⁻¹, 0.57 g/L and 0.248, respectively. More recently [Frasconi et al. \(2013\)](#) have studied the kinetic parameters for *T. neapolitana* grown on glucose under N₂ sparging atmosphere. The μ_{max} and k_S values were found to be 0.024 ± 0.005 h⁻¹ and 1.1 ± 0.3 g/L, respectively ([Frasconi et al., 2013](#)).

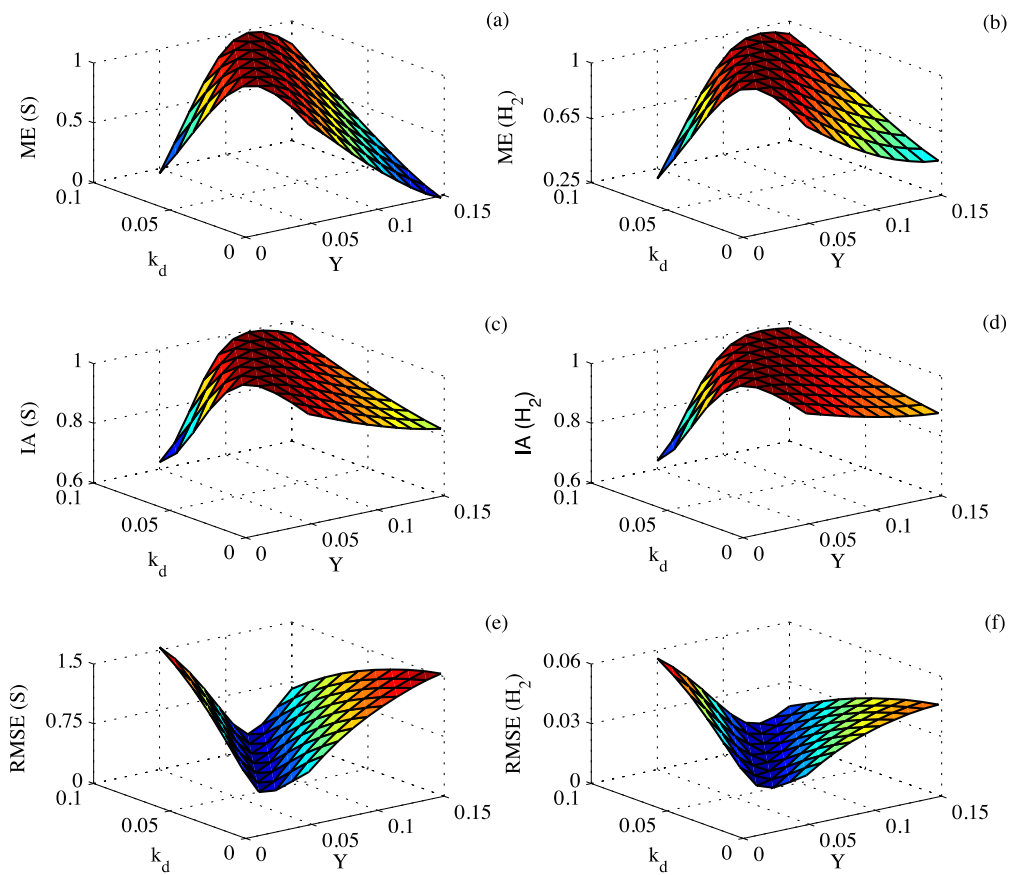


Fig. 5.5 Model calibration for simultaneous changes in biomass yield coefficient (Y) and endogenous decay rate (k_d) with respect to ME for (a) substrate consumption (S) and (b) H₂ production (H₂); IA for (c) S and (d) H₂; and RMSE for (e) S and (f) H₂.

5.4.5 Model validation

The results from batch test C were used to validate the model with the calibrated kinetic parameters, i.e. k , k_S , Y and k_d being 1.42 1/h, 1.42 g/L, 0.1125 and 0.0525 1/h, respectively. The ME and IA for X and H₂ were higher than 0.90 and 0.97, respectively and the RMSE lower than 0.05 (Table 5.3).

From Fig. 5.6b it can be observed that the model prediction for substrate consumption slightly deviated between 30 and 52 h of cultivation. The reason for such a deviation in the prediction for substrate consumption can be understood from Fig. 5.6a, where the biomass growth reaches a peak between 30 and 45 h and hence, more substrate was consumed. Fig. 5.6d and Fig. 5.6e show that the model prediction overestimates the acetate production and underestimates the lactate production and there was a poor model fitting between predicted and measured data and this was possibly due to capnophilic condition. It has been recently noticed that sparging CO₂ to the pure culture of *T. neapolitana* increases the substrate consumption rate as well as the H₂ production rate (Dipasquale et al., 2014). However, it was found that CO₂ sparging or capnophilic conditions led to the simultaneous synthesis of lactate without affecting the overall H₂ yield (Dipasquale et al., 2014). Feeding labeled carbon (¹³CO₂) it was clearly shown that part of the CO₂ is biologically coupled with acetyl-CoA to form lactic acid when the cultures are grown in a CO₂ atmosphere or enriched with sodium bicarbonate (d'Ippolito et al., 2014; Dipasquale et al., 2014; Pradhan et al., 2015). This process recycles part of the acetate via acetyl-CoA to form lactate. It is clear that capnophilic lactic fermentation (CLF) is responsible for the metabolic shift and that the N₂ sparged conditions cannot yield such a large quantity of lactic acid unless the biomass gets inhibited due to a too low or high pH and high H₂ gas partial pressure. Therefore, the conventional DF model is not able to accurately predict the production of acetic and lactic acid under the CLF pathway.

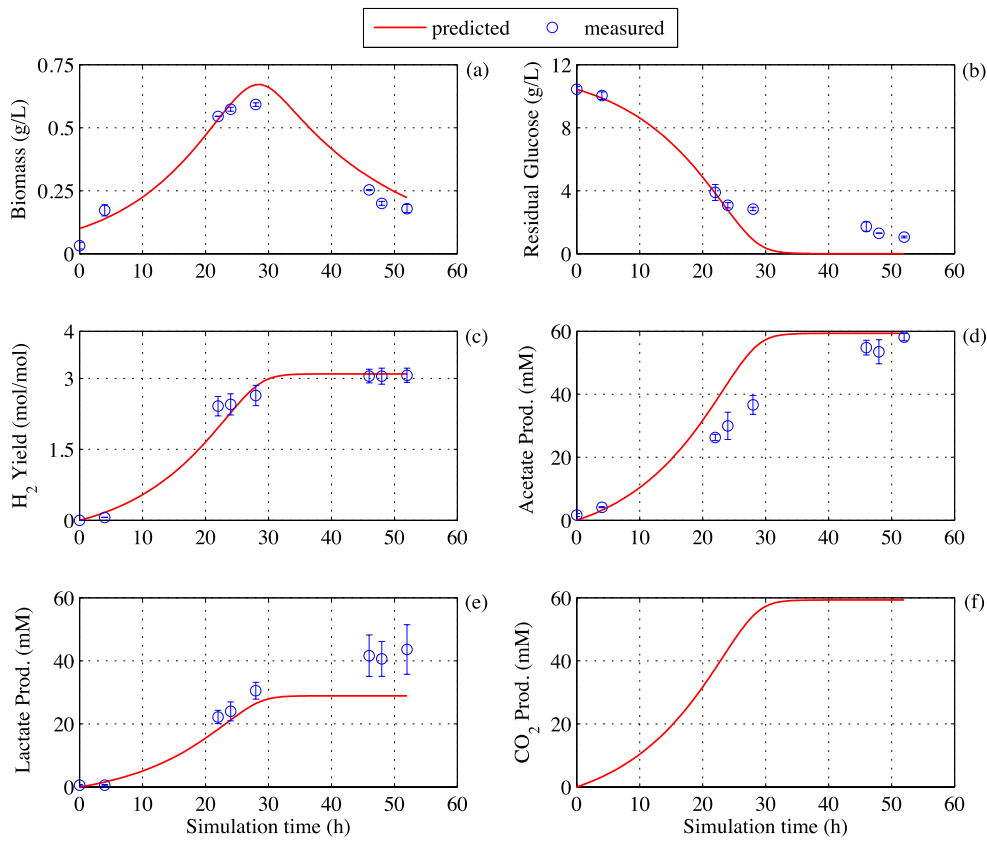


Fig. 5. 6 Model validation for biomass growth and product formation by *T. neapolitana* from batch experiment C: predicted and measured data for (a) biomass growth (cell dry weight), (b) residual glucose, (c) H₂ yield, (d) acetate production, (e) lactate production and (f) CO₂ production.

Table 5. 3 Regression parameters for model validation.

Parameters	ME	IA	RMSE
X	0.9019	0.9751	0.0554
S	0.8653	0.9730	1.0280
H	0.9212	0.9807	0.0295
Ac	0.8066	0.9587	0.4586
Lac	0.6015	0.8467	0.7733

The kinetic parameters estimated under CO₂ or N₂ sparging atmosphere differed from each other due to the operating conditions and techniques applied to perform the

experiments (Frascari et al., 2013). In a DF reaction, if lactate is the only end-product, no H₂ will be produced and vice versa (Fig. 5.1). But, under capnophilic conditions (i.e. CO₂ led fermentation) high amounts of lactate are formed without reducing the molar yield of H₂. The excess lactate production process is triggered by the presence of high concentrations of CO₂ in the fermentation medium. Under equilibrium, the CO₂ and acetate were recycled with the coordinated action between various enzymes to form lactate without affecting the overall yield of H₂ gas (d'Ippolito et al., 2014).

5.5 Conclusions

The optimized kinetic parameters of *T. neapolitana* fermentation, i.e. k , k_s , Y and k_d were 1.42 1/h, 1.42 g/L, 0.1125 and 0.0525 1/h, respectively. The kinetic model based on ADM1 accurately predicts biomass growth, substrate consumption and H₂ production under DF conditions. However, there are significant deviations for lactate and acetate in the model validation under capnophilic conditions, thus suggesting to incorporate CLF pathway to the classic DF model. Further developments of the model with optimization of the growth kinetic parameters under CLF conditions are currently in progress.

References

- Amend, J.P., Shock, E.L. 2001. Energetics of overall metabolic reactions of thermophilic and hyperthermophilic Archaea and Bacteria. *FEMS Microbiology Reviews*, **25**, 175-243.
- Antonopoulou, G., Ntaikou, I., Stamatelatou, K., Lyberatos, G. 2011. *Biological and fermentative production of hydrogen*. Handbook of Biofuels Production: Processes and Technologies.
- Batstone, D.J., Keller, J., Angelidaki, I., Kalyuzhnyi, S.V., Pavlostathis, S.G., Rozzi, A. 2002. Anaerobic digestion model No. 1. *IWA Scientific and Technical Report* **13**.
- Bernfeld, P. 1955. Alpha and beta-amylases. *Methods in Enzymology*, **1**, 149-158.
- Castello, E., Garcia y Santos, C., Iglesias, T., Paolino, G., Wenzel, J., Borzacconi, L., Etchebehere, C. 2009. Feasibility of biohydrogen production from cheese whey using a UASB reactor: Links between microbial community and reactor performance. *International Journal of Hydrogen Energy*, **34**, 5674-5682.
- d'Ippolito, G., Dipasquale, L., Fontana, A. 2014. Recycling of carbon dioxide and acetate as lactic acid by the hydrogen-producing bacterium *Thermotoga neapolitana*. *ChemSusChem*, **7**, 2678-83.
- d'Ippolito, G., Dipasquale, L., Vella, F.M., Romano, I., Gambacorta, A., Cutignano, A., Fontana, A. 2010. Hydrogen metabolism in the extreme thermophile

- Thermotoga neapolitana*. *International Journal of Hydrogen Energy*, **35**, 2290-2295.
- Dipasquale, L., Adessi, A., d'Ippolito, G., Rossi, F., Fontana, A., De Philippis, R. 2015. Introducing capnophilic lactic fermentation in a combined dark-photo fermentation process: a route to unparalleled hydrogen yields. *Applied Microbiology and Biotechnology*, **99**, 1001-10.
- Dipasquale, L., d'Ippolito, G., Fontana, A. 2014. Capnophilic lactic fermentation and hydrogen synthesis by *Thermotoga neapolitana*: An unexpected deviation from the dark fermentation model. *International Journal of Hydrogen Energy*, **39**, 4857-4862.
- Elsharnouby, O., Hafez, H., Nakhla, G., el Naggar, M.H. 2013. A critical literature review on biohydrogen production by pure cultures. *International Journal of Hydrogen Energy*, **38**, 4945-4966.
- Eriksen, N.T., Riis, M.L., Holm, N.K., Iversen, N. 2011. Hydrogen synthesis from pentoses and biomass in *Thermotoga* spp. *Biotechnology Letters*, **33**, 293-300.
- Esposito, G., Frunzo, L., Panico, A., Pirozzi, F. 2011. Model calibration and validation for OFMSW and sewage sludge co-digestion reactors. *Waste Management*, **31**, 2527-2535.
- Fang, F., Mu, Y., Sheng, G.P., Yub, H.Q., Li, Y.Y., Kubota, K., Harada, H. 2013. Kinetic analysis on gaseous and aqueous product formation by mixed anaerobic hydrogen-producing cultures. *International Journal of Hydrogen Energy*, **38**, 15590-15597.
- Frasconi, D., Cappelletti, M., Mendes, J.D.S., Alberini, A., Scimonelli, F., Manfreda, C., Longanesi, L., Zannoni, D., Pinelli, D., Fedi, S. 2013. A kinetic study of biohydrogen production from glucose, molasses and cheese whey by suspended and attached cells of *Thermotoga neapolitana*. *Bioresource Technology*, **147**, 553-61.
- Gadhamshetty, V., Arudchelvam, Y., Nirmalakhandan, N., Johnson, D.C. 2010. Modeling dark fermentation for biohydrogen production: ADM1-based model vs. Gompertz model. *International Journal of Hydrogen Energy*, **35**, 479-490.
- Gadhe, A., Sonawane, S.S., Varma, M.N. 2014. Kinetic analysis of biohydrogen production from complex dairy wastewater under optimized condition. *International Journal of Hydrogen Energy*, **39**(3), 1306-1314.
- Hallenbeck, P.C., Benemann, J.R. 2002. Biological hydrogen production; fundamentals and limiting processes. *International Journal of Hydrogen Energy*, **27**, 1185-1193.
- Janssen, P.H.M., Heuberger, P.S.C. 1995. Calibration of process-oriented models. *Ecological Modelling*, **83**, 55-66.
- Khanna, N., Kotay, S.M., Gilbert, J.J., Das, D. 2011. Improvement of biohydrogen production by *Enterobacter cloacae* IIT-BT 08 under regulated pH. *Journal of Biotechnology*, **152**, 9-15.

- Maly, T., Petzold, L.R. 1996. Numerical methods and software for sensitivity analysis of differential-algebraic systems. *Applied Numerical Mathematics*, **20**, 57-79.
- Manish, S., Banerjee, R. 2008. Comparison of biohydrogen production processes. *International Journal of Hydrogen Energy*, **33**, 279-286.
- Maru, B.T., Bielen, A.A.M., Constanti, M., Medina, F., Kengen, S.W.M. 2013. Glycerol fermentation to hydrogen by *Thermotoga maritima*: Proposed pathway and bioenergetic considerations. *International Journal of Hydrogen Energy*, **38**, 5563-5572.
- Molla, V.M.G., Padilla, R.G. 2002. Description of the MATLAB functions SENS_SYS and SENS_IND. *Universidad Politécnica de Valencia, Spain*.
- Munro, S.A., Zinder, S.H., Walker, L.P. 2009. The fermentation stoichiometry of *Thermotoga neapolitana* and influence of temperature, oxygen, and pH on hydrogen production. *Biotechnology Progress*, **25**, 1035-1042.
- Nath, K., Das, D. 2004. Biohydrogen production as a potential energy resource - Present state-of-art. *Journal of Scientific & Industrial Research*, **63**, 729-738.
- Nath, K., Muthukumar, M., Kumar, A., Das, D. 2008. Kinetics of two-stage fermentation process for the production of hydrogen. *International Journal of Hydrogen Energy*, **33**, 1195-1203.
- Nwabanne, J., Onukwuli, O., Ifeakandu, C. 2009. Biokinetics of Anaerobic Digestion of Municipal Waste. *International Journal of Environmental Research*, **3**, 551-556.
- Paulo, C.I., Di Maggio, J.A., Soledad Diaz, M., Ruggeri, B. 2013. Modeling and Parameter Estimation in Biofuel Discontinuous Production by Hydrogen Forming Bacteria (HFB). *11th International Conference on Chemical and Process Engineering*, **32**, 1033-1038.
- Pradhan, N., Dipasquale, L., d'Ippolito, G., Panico, A., Lens, P.N.L., Esposito, G., Fontana, A. 2015. Hydrogen production by the thermophilic bacterium *Thermotoga neapolitana*. *International Journal of Molecular Sciences*, **16**, 12578-12600.
- Thauer, R. 1977. Limitation of microbial hydrogen formation via fermentatio. *Microbial Energy Conversion*, 201-204.
- Van Ooteghem, S.A., Jones, A., Van Der Lelie, D., Dong, B., Mahajan, D. 2004. Hydrogen production and carbon utilization by *Thermotoga neapolitana* under anaerobic and microaerobic growth conditions. *Biotechnology Letters*, **26**, 1223-32.
- Yu, X., Drapcho, C. 2011. Hydrogen production by the hyperthermophilic bacterium *Thermotoga neapolitana* using agricultural-based carbon and nitrogen sources. *Biological Engineering Transactions*, **4**, 101-112.

Chapter 6

Capnophilic lactic fermentation model

This chapter has been published as:

Pradhan, N., Dipasquale, L., d'Ippolito, G., Fontana, A., Panico, A., Pirozzi, F., Lens, P.N.L., Esposito, G. 2016. Model development and experimental validation of capnophilic lactic fermentation and hydrogen synthesis by *Thermotoga neapolitana*. *Water Research*, 99, 225-234.

Chapter 6: Capnophilic lactic fermentation model

Abstract

The aim of the present study was to develop a kinetic model for a recently proposed unique and novel metabolic process called capnophilic (CO₂-requiring) lactic fermentation (CLF) pathway in *Thermotoga neapolitana*. The model was based on Monod kinetics and the mathematical expressions were developed to enable the simulation of biomass growth, substrate consumption and product formation. The calibrated kinetic parameters such as maximum specific uptake rate (k), semi-saturation constant (k_s), biomass yield coefficient (Y) and endogenous decay rate (k_d) were 1.30 1/h, 1.42 g/L, 0.1195 and 0.0205 1/h, respectively. A high correlation (> 0.98) was obtained between the experimental data and model predictions for both model validation and cross validation processes. An increase of the lactate production in the range of 40–80% was obtained through CLF pathway compared to the classic dark fermentation model. The proposed kinetic model is the first mechanistically based model for the CLF pathway. This model provides useful information to improve the knowledge about how acetate and CO₂ are recycled back by *T. neapolitana* to produce lactate without compromising the overall hydrogen yield.

Keywords: hydrogen; capnophilic lactic fermentation; kinetic model; model calibration; sensitivity analysis; model validation.

6.1 Introduction

Greenhouse gas (GHG) emissions from the burning of fossil fuels are one of the responsible factors for the global warming phenomenon. Initiatives to develop clean and sustainable energy resources have gained major interest to abate the usage of non-renewable energy resources. Hydrogen (H₂) is considered as one of the cleanest sources of biofuels, albeit > 90% of H₂ is still produced from fossil fuels through gasification or pyrolysis, releasing massive amounts of CO₂ into the atmosphere (Nath & Das, 2011). H₂ can also be produced by biological methods from agro-industrial waste, thereby opening a new perspective for the waste management sector (Hallenbeck & Ghosh, 2009; Pradhan et al., 2015). Dark fermentation (DF), photo fermentation and direct or indirect photolysis are the biological methods which can be used to produce H₂ (Nath & Das, 2004).

Dark fermentative H₂ production is of interest to scientific communities thanks to its ease of operation, inexpensive feedstock and environmentally friendly processes compared to other biological H₂ production routes. The recently developed capnophilic (CO₂-requiring) lactic fermentation (CLF) process was tested on a marine hyperthermophilic bacterium *Thermotoga neapolitana*, which yielded a significant quantity of lactic acid without compromising the overall H₂ yield (Dipasquale et al., 2014). The CLF pathway fundamentally differed from the well-established DF principles in terms of acetate and lactate production, however, the overall carbon pool remained the same at the end of the fermentation (d'Ippolito et al., 2014). This indicates a new-branched reverse metabolic pathway is being triggered under capnophilic conditions, leading to the accumulation of lactate by recycling a proportional amount of acetate and dissolved CO₂. This CLF process worked well in the presence of 12-14 mM dissolved CO₂ in the culture medium (Dipasquale et al., 2014) thereby non-photosynthetically recycling CO₂ and acetate (*Ac*) to form lactate (*Lac*) via acetyl-CoA by pyruvate:ferredoxin oxidoreductase (PFOR) enzyme (d'Ippolito et al., 2014). The ability to simultaneously produce lactate and H₂ has tremendous potential for both lactate recovery with a growing need for bio-plastic industries and H₂ gas for clean energy sector applications (Pradhan et al., 2015).

The CLF-based process needs thorough testing with different operating conditions if it has to be used for industrial scale applications. However, several series

of experiments are required to scale up the CLF technology from the laboratory to industrial scale, thus consuming a significant amount of time and resources. Application of mathematical modeling could help to reduce time and resources, as well as improve the process efficiency to a great extent and minimizing errors in the process design and product estimation (Pradhan et al., 2016). Modeling the CLF-based process requires the knowledge of the biomass growth kinetics, which can explain the complex biochemical reactions through simplified mathematical expressions. A kinetic model based on anaerobic digestion model no. 1 (ADM1) of IWA could be used to estimate fermentation products of CLF by *T. neapolitana* (Pradhan et al., 2016). In addition, it could also be used to analyze, design, operate and optimize the fermentation process.

In this study, the previously estimated kinetic parameters (Pradhan et al., 2016) are re-calibrated to fit the experimental results under capnophilic condition. Furthermore, a new kinetic model with mass balance equations is used to describe the kinetics of the formation of the main products (i.e. H₂, lactate and acetate). In addition, the process of lactate production from acetate is evaluated and integrated to the previously developed dark fermentation model. The main objective of this study is to develop a useful mathematical tool for understanding the CLF pathway and consequently designing and operating reactors for biotechnological applications.

6.2 Materials and methods

6.2.1 Bacterial strain and medium composition

Thermotoga neapolitana strain (i.e. laboratory strain ‘TN-CMut’ as in Chapter 3) was purchased from the Deutsche Sammlung von Mikroorganismen und Zellkulturen (Braunschweig, Germany). The bacterium was grown anaerobically in the culture medium according to Dipasquale et al. (2014).

6.2.2 Experiments

All the experiments were carried out in a 3 L continuously stirred tank reactor (CSTR) (ezControl Applikon Biotechnology, The Netherlands) with a working volume of 742 mL. The culture medium was sterilized by autoclaving for 15 min at 110 °C and inoculated with *T. neapolitana* from a pre-culture at 6% (v/v) of the working volume. Three different series of batch fermentation tests, i.e. fed with (i) 55.50 mM (or 10 g/L) glucose to re-calibrate the previously estimated kinetic parameters (named as ‘Glc-10’), (ii) 27.75 mM (or 5 g/L) glucose to validate the model (named as ‘Glc-5’) and (iii)

33.30 mM (or 5 g/L) arabinose to cross validate the model (named as 'Arb-5'), were carried out under CLF conditions. The tests with glucose as carbon source were conducted in triplicate and the test with arabinose as carbon source was conducted in duplicate.

The fermentation mixture was sparged with pure CO₂ for 5 min at 30 mL min⁻¹ to create an anaerobic environment inside the bioreactor. The initial pH was adjusted to 7.5 with 1 M NaOH and then maintained constant at 6.5 ± 0.1 by auto-titrating with 1 M NaOH for the entire duration of the fermentation. The temperature of the medium was maintained at 80 ± 1 °C by thermostatic water circulation system. The agitation speed was maintained at 50 rpm by an electro-magnetic mixing unit. Approximately 3 mL fermentation mixture was withdrawn at different time intervals, centrifuged (at 13,000 rpm for 5 min) and stored (at -20 °C) for the biochemical assays (Pradhan et al., 2016).

6.2.3 Analytical methods

The gas mixture (H₂ and CO₂) in the headspace of the fermenter was analyzed by a gas chromatograph (Focus GC, Thermo Scientific) (Dipasquale et al., 2014). The analyses for aqueous metabolites were performed on the supernatants previously centrifuged and stored. Acetic and lactic acid concentrations were detected using a ¹H Nuclear Magnetic Resonance (NMR) 600 MHz spectrometer (Bruker Avance 600) (Dipasquale et al., 2014). The residual glucose and arabinose concentrations were measured by the dinitrosalicylic acid (DNS) method calibrated on a standard solution of 1 g/L glucose and arabinose, respectively (Bernfeld, 1955). The biomass growth was monitored through optical density measurements at λ = 540 nm by a UV/Vis spectrophotometer (V-650, Jasco) (Dipasquale et al., 2014). Further, the cell dry weight (CDW) was calculated by using a correlative equation for *T. neapolitana* growth (CDW (g/L) = 0.347* λ (540nm) + 0.016) (Pradhan et al., 2016).

6.3 Mathematical model design

6.3.1 Capnophilic lactic fermentation pathway

Theoretically 4 mol of H₂ can be produced from a mol of hexose sugar consumed under DF conditions and similarly 3.3 mol of H₂ per mol of pentose sugar consumed (Thauer et al., 1977). Eqs. (6.1)–(6.2) and Eqs. (6.4)–(6.7) are thermodynamically feasible under standard DF conditions as shown in Table 6.1. Eq. (6.3) is an energetically unfavorable reaction, but the reaction is propelled by accepting

electrons from other physiological reductants under capnophilic conditions (d'Ippolito et al., 2014). Eq. (6.3) can thus be activated only under capnophilic conditions to produce lactate by reductive carboxylation of acetyl-CoA. The enzyme PFOR recycles acetate and dissolved CO₂ to produce lactate as shown in Fig. 6.1 and stoichiometrically explained in Table 6.2 (d'Ippolito et al., 2014). This new CLF metabolic pathway in *T. neapolitana* fermentation was proposed by d'Ippolito et al. (2014) and the pathway was constructed by growing *T. neapolitana* with ¹³C labeled substrates and analyzed by ¹H and ¹³C NMR.

Table 6. 1 Main possible metabolic reactions of glucose and xylose degradation via DF and CLF-based pathways in CSTR system.

Metabolic reactions (glucose and arabinose)	ΔG^0 (kJ/reaction)	Equation
$C_6H_{12}O_6 + H_2O \rightarrow 2C_2H_3O_2^- + 2H^+ + 4H_2 + 2CO_2$	-215.90	(6.1)
$C_6H_{12}O_6 \rightarrow 2C_3H_5O_3^- + 2H^+$	-198.34	(6.2)
$C_2H_4O_2 + CO_2 + 4H^+ + 4e^- \rightarrow C_3H_6O_3 + H_2O$	+160.33	(6.3)
$C_6H_{12}O_6 + (2 - \alpha - \beta)H_2O$ $\rightarrow (\alpha + \beta)C_3H_6O_3$ $+ (2 - \alpha - \beta)C_2H_4O_2 + (4 - 2\alpha)H_2$ $+ (2 - \alpha - \beta)CO_2$		(6.4)
$C_5H_{10}O_5 + 1.67H_2O$ $\rightarrow 1.67C_2H_3O_2^- + 1.67H^+ + 3.33H_2$ $+ 1.67CO_2$	-197.66	(6.5)
$C_5H_{10}O_5 \rightarrow 1.67C_3H_5O_3^- + 1.67H^+$	-182.99	(6.6)
$C_5H_{10}O_5 + (1.67 - \alpha - \beta)H_2O$ $\rightarrow (\alpha + \beta)C_3H_6O_3$ $+ (1.67 - \alpha - \beta)C_2H_4O_2$ $+ (3.33 - 2\alpha)H_2$ $+ (1.67 - \alpha - \beta)CO_2$		(6.7)

Notes: ΔG^0 (kJ/reaction) = Gibbs free energies (at 25°C) for the reactions was calculated from the Gibbs energy of formation of the compounds participating in the

reaction at standard conditions (Thauer et al., 1977).

α and β are stoichiometric yield of lactate via DF and CLF-based pathways, respectively where, $\alpha \geq 0$ and $\beta \geq 0$.

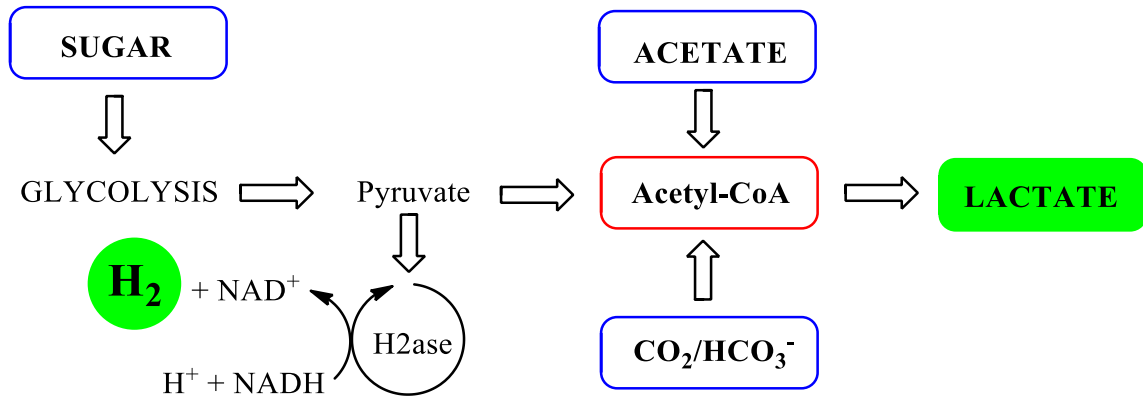


Fig. 6. 1 Simplified CLF-based biochemical pathway for fermentative H₂ and lactic acid production by *T. neapolitana*.

Table 6. 2 The DF and CLF-based model pathway stoichiometries with glucose as the substrate.

Fermentation products	DF pathway			CLF pathway
	Acetate pathway	Lactate pathway	Mixed pathway	
f_{H_2}	4	0	$4 - 2\alpha$	$4 - 2\alpha$
f_{Ac}	2	0	$2 - \alpha$	$2 - (\alpha + \beta)$
f_{CO_2}	2	0	$2 - \alpha$	$2 - (\alpha + \beta)$
f_{Lac}	0	2	α	$\alpha + \beta$

Note: f_{Ac} , f_{H_2} , f_{CO_2} and f_{Lac} are the stoichiometric coefficients of the products.

6.3.2 Bioprocess kinetics

To model the CLF-based pathway, Monod like kinetic equations (Kongjan et al., 2009) (Eqs. (6.8)–(6.13)) were written according to the stoichiometry of microbial fermentation (Xiao & VanBriesen, 2006) as shown in Table 6.3. Substrate consumption, biomass growth and product formation (i.e. acetate, lactate, H₂ and CO₂) were

incorporated in the model. The equations used for modeling the CLF-based pathway were substrate degradation (Eq. (6.8)), net biomass growth (Eq. (6.9)) and product formation (Eqs. (6.10)–(6.13)).

6.3.3 Model simulation

The equations in Table 6.3 were written in the form of differential algebraic equations (DAEs) and were solved by the ordinary differential equations (ODEs) solver (i.e. ode15s) of MATLAB R2010a by MathWorks™ (Pradhan et al., 2016). The stoichiometric coefficients for the DAEs were in accordance with Table 6.2. The model input and output functions were written in a M-file of MATLAB. The simulation cycle was carried out in 3 key process steps, i.e. sensitivity analysis, model calibration and model validation as shown in Fig. 6.2 (Pradhan et al., 2016).

Table 6. 3 The kinetic expressions included in the CLF-based model.

Process	Rate equations	Equation
Substrate consumption	$\frac{\partial S}{\partial t} = -k \left(\frac{S}{k_S + S} \right) X$	(6.8)
Net biomass growth	$\frac{\partial X}{\partial t} = -Y \left(\frac{\partial S}{\partial t} \right) - k_d X$	(6.9)
H ₂ production	$\frac{\partial S_{H_2}}{\partial t} = -(1 - Y) f_{H_2} \left(\frac{\partial S}{\partial t} \right)$	(6.10)
Acetate production	$\frac{\partial S_{Ac}}{\partial t} = -(1 - Y) (f_{Ac} - f_{Lac}) \left(\frac{\partial S}{\partial t} \right)$	(6.11)
CO ₂ production	$\frac{\partial S_{CO_2}}{\partial t} = -(1 - Y) (f_{CO_2} - f_{Lac}) \left(\frac{\partial S}{\partial t} \right)$	(6.12)
Lactate production	$\frac{\partial S_{Lac}}{\partial t} = -(1 - Y) f_{Lac} \left(\frac{\partial S}{\partial t} \right)$	(6.13)

Notes: S_{H_2} , S_{Ac} , S_{CO_2} and S_{Lac} are the concentrations of the products.

Ac = acetic acid (mM); Lac = lactic acid (mM); CO_2 = carbon dioxide (mM). k = maximum specific uptake rate (1/h); k_S = semi-saturation constant (g/L); Y = biomass yield coefficient; k_d = endogenous decay rate (1/h); X = biomass concentration (g/L); S = substrate concentration (g/L).

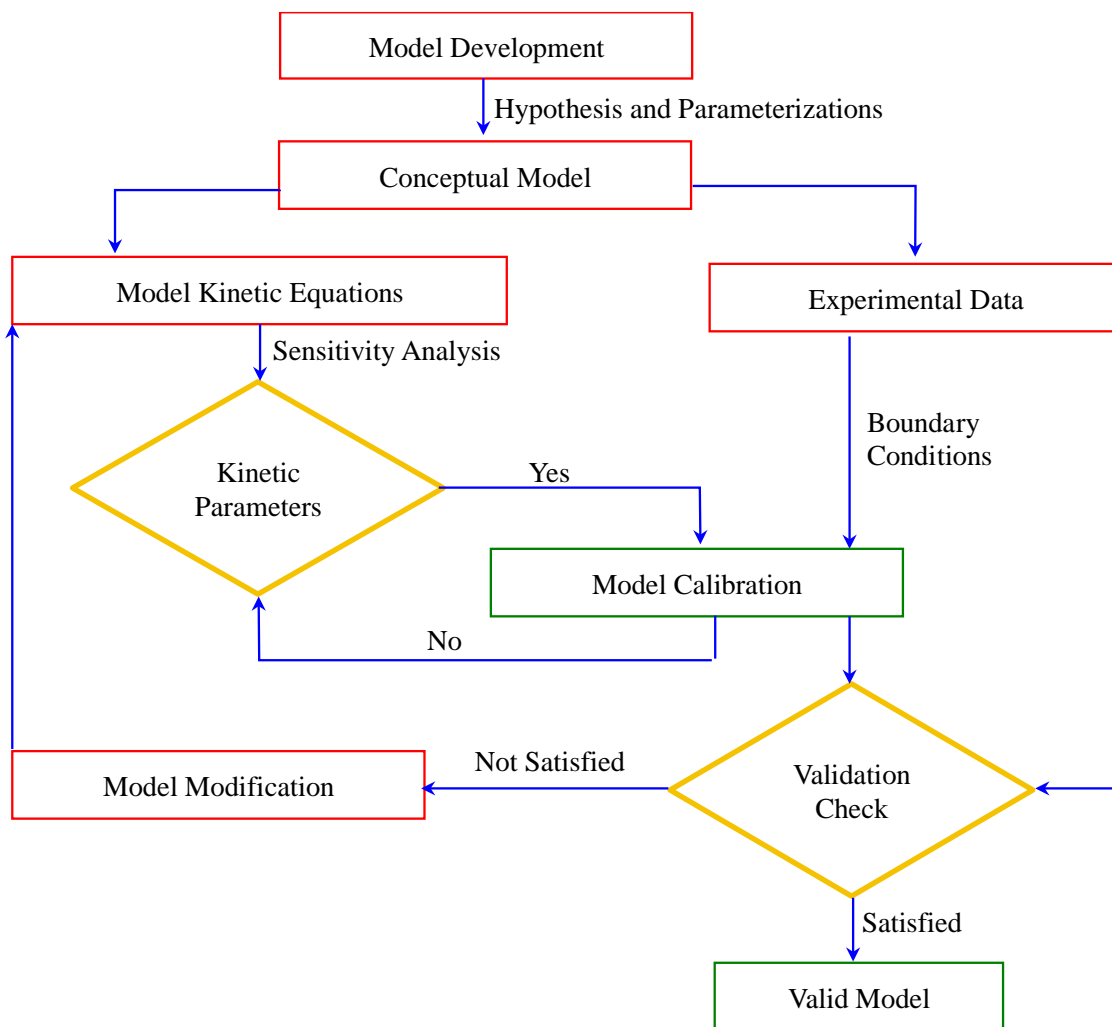


Fig. 6. 2 Simplified model simulation flow chart for sensitivity analysis, calibration and validation.

6.3.4 Sensitivity analysis

The sensitivity analysis (SA) was used to test the model stability and to determine the model parameters that required further optimization. In this model, the SA was applied to explore the perturbation affecting the model output over a time series due to a change in model input parameters, i.e. kinetic parameters, stoichiometry and state input variables (Donoso-Bravo et al., 2011; Wang et al., 2012). In general, a local sensitivity analysis could be applied to biological models by the use of differential analysis of outputs with respect to the model input parameters (Ribes et al., 2004; Tartakovsky et al., 2007). The sensitivity tool applied to this model is an automatic differentiation tool, which predicts local sensitivities. The SA Eq. (6.14) was used to

determine the sensitive kinetic parameters with respect to the model state input variables:

$$F(t, y, y', u) = 0 \quad (6.14)$$

where t = time (h), y = input state variables, y' = first derivative of y with respect to t and u = kinetic parameters.

A SA tool (i.e. SENS_SYS) developed by [Maly and Petzold \(1996\)](#) and [Molla and Padilla \(2002\)](#) was used in conjunction with the ODE solver of MATLAB to perform the sensitivity analysis. The functions in SENS_SYS were extensions of ode15s, which calculated derivatives (or sensitivities) of solutions (i.e. input state variables) with respect to parameters (i.e. kinetic parameters). In addition, the SENS_SYS tool suffers from the limitations of nominal range series as all the kinetic parameters are set to their mean values and the model provides perturbation values on the time series.

6.3.5 Model calibration

In the SA step, the sensitive kinetic parameters for each model output were noted and ranked. The sensitive parameters were chosen for further calibration in order to improve the quality of the model fit ([Nath & Das, 2011](#); [Siegrist et al., 2002](#)). The calibration was conducted by varying the kinetic parameters within a range so that the absolute errors for model predictions compared to experimental data could be minimized. In order to avoid the tedious trial and error approach, various statistical functions have been formulated to optimize the kinetic parameters ([Siegrist et al., 2002](#)).

The results of batch test ‘Glc-10’ were used to calibrate the kinetic parameters. The method for calibration was adopted from [Esposito et al. \(2011\)](#) and [Janssen and Heuberger \(1995\)](#), and carried out in four steps. In step (i), a variation range was assigned to the sensitive parameters, i.e. k , Y and k_d in this case. In step (ii), algebraic Eqs. (6.15)–(6.17) were used to step-by-step vary the parameters between lower and upper bound limits while keeping the other kinetic parameters constant:

$$k^i = k^{i-1} + \partial k; \quad i = 1 \dots m \quad (6.15)$$

$$Y^i = Y^{i-1} + \partial Y; \quad i = 1 \dots m \quad (6.16)$$

$$k_d^i = k_d^{i-1} + \partial k_d; \quad i = 1 \dots m \quad (6.17)$$

A ‘ $m \times m$ ’ matrix was constructed with different values of k^i , Y^i and k_d^i ranging between the lower and upper bound limits. The value of m was set to 10.

In step (iii), the output of the calibration process was plotted on the 3-D surface plot along with three statistical tools, i.e. Modeling Efficiency (ME), Index of Agreement (IA) and Root Mean Square Error (RMSE) described in Eqs. (18)–(20) (Esposito et al., 2011; Janssen & Heuberger, 1995):

$$ME = 1 - \frac{\sum_{i=1}^n (O_i - P_i)^2}{\sum_{i=1}^n (O_i - \bar{O})^2} \quad (6.18)$$

$$IA = 1 - \frac{\sum_{i=1}^n (O_i - P_i)^2}{\sum_{i=1}^n (|P_i - \bar{O}| + |O_i - \bar{O}|)^2} \quad (6.19)$$

$$RMSE = \sqrt{\frac{\sum_{i=1}^n (O_i - P_i)^2}{n}} \quad (6.20)$$

where n = number of observed values, O_i = observed values, P_i = predicted values, \bar{O} = mean of observed values.

Three statistical tools (ME, IA and RMSE) were chosen to evaluate the model fitting for the calibration of the sensitive kinetic parameters based on the bias, large error and mean error. The ME (varies from $-\infty$ to 1, with optimum value of 1) represents the degree of collinearity (or bias) between measured and predicted data, whereas the IA (varies from 0 to 1, with optimum value of 1) is the ratio of the sum of squared errors and the largest potential error with respect to the mean of the measured values. RMSE (varies from 0 to $+\infty$, with optimum value of 0) is an error index for the mean error and indicates the overall agreement between measured and predicted data. In step (iv), the best possible set of k , Y and k_d was estimated from the surface plot by analyzing the regression values.

6.3.6 Model validation

The model validation and cross-validation were conducted using a different series of experimental results (batch tests with glucose and arabinose sugar). The simulation was carried out with the optimized kinetic parameters and same initial conditions used for the model simulation and calibration. The quality of predictive abilities of the kinetic parameters were tested by a set of regression tools (see [subsection Model calibration](#)).

6.4 Results and discussion

6.4.1 Model simulation under DF condition

The model simulation in this section was carried out as per the classic DF principle where the kinetic parameters were not calibrated for CLF conditions (Pradhan et al., 2016). The input state variables X_0 (biomass concentration at time $t = 0$ h) and S_0 (substrate concentration at time $t = 0$ h) were set to 0.1 g/L and 10 g/L, respectively. A lag phase of 4-6 h was assumed at the beginning of the fermentation test to make the biomass adapted to the operating environment. Independent batch experiments were conducted to estimate the growth kinetic parameters by applying the nonlinear least square method to Monod's and Michaelis-Menten kinetic equations (Pradhan et al., 2016). The previously determined kinetic parameters (Pradhan et al., 2016), i.e. k , k_S , Y and $k_d = 1.42$ 1/h, 1.42 g/L, 0.1125 and 0.0525 1/h, respectively, are used for the model simulation. The experimentally determined stoichiometric coefficients, i.e. f_{H_2} , f_{Ac} , f_{CO_2} and f_{Lac} shown in Table 6.4 are used for model simulations. The simulation outputs of the test 'Glc-10' are presented in Fig. 6.3.

As shown in Fig. 6.3a, after the lag phase, the substrate was subsequently consumed rapidly. In agreement with previous studies, the substrate consumption and products formation attained their peak at around 20 h and the accumulation of gaseous (i.e. H_2 and CO_2) and aqueous (i.e. acetate and lactate) by-products was observed towards the end of the exponential growth phase of biomass (d'Ippolito et al., 2010; Pradhan et al., 2016). It can be noted that there is an over and under-estimation of predicted quantities of acetate and lactate, respectively, as shown in Fig. 6.3d and e. The deviation can be attributed to the activation of the CLF pathway, which contributed in the range of 40-80% of the total amount of lactate produced in the process by recycling part of produced acetate and dissolved CO_2 (d'Ippolito et al., 2014). As a result, the classic DF model failed to predict acetate and lactate under CLF condition. The quantity and percentage of lactate produced through the CLF pathway can be ascertained by simple mathematical predictions based on Table 6.2. CO_2 is one of the fermentation by-products, but under the CLF conditions, we did not measure CO_2 and only CO_2 prediction by the model is shown in Fig. 6.3f.

Table 6. 4 Experimental results of glucose and arabinose fermentation by *T. neapolitana* under CLF conditions.

V ^a : 3.0 L, WV ^b : 742 mL				
Batch test	Units	Glc-10 ^c	Glc-5 ^d	Arb-5 ^e
Time	h	52	48	48
<i>S</i>	mM	48.99±2.32	24.96±0.86	29.12±1.05
<i>f_{H2}</i>	mol H ₂ /mol substrate	3.26±0.15	3.57±0.33	2.93±0.03
<i>f_{Ac}</i>	mol Ac /mol substrate	1.16±0.07	1.20±0.09	1.20±0.04
<i>f_{Lac}</i>	mol Lac /mol substrate	0.89±0.19	0.61±0.02	0.42±0.02
<i>Lac/Ac^f</i>		0.83±0.17	0.53±0.03	0.35±0.01

Notes:

^a V = volume of the reactor.

^b WV = working volume.

^c Glc-10 = experiments with 10 g/L of glucose (Pradhan et al., 2016).

^d Glc-5 = experiments with 5 g/L of glucose.

^e Arb-5 = experiments with 5 g/L of arabinose.

^f ratio of lactate (*Lac*) to acetate (*Ac*) in terms of mM to mM.

the results are expressed as mean ± standard error.

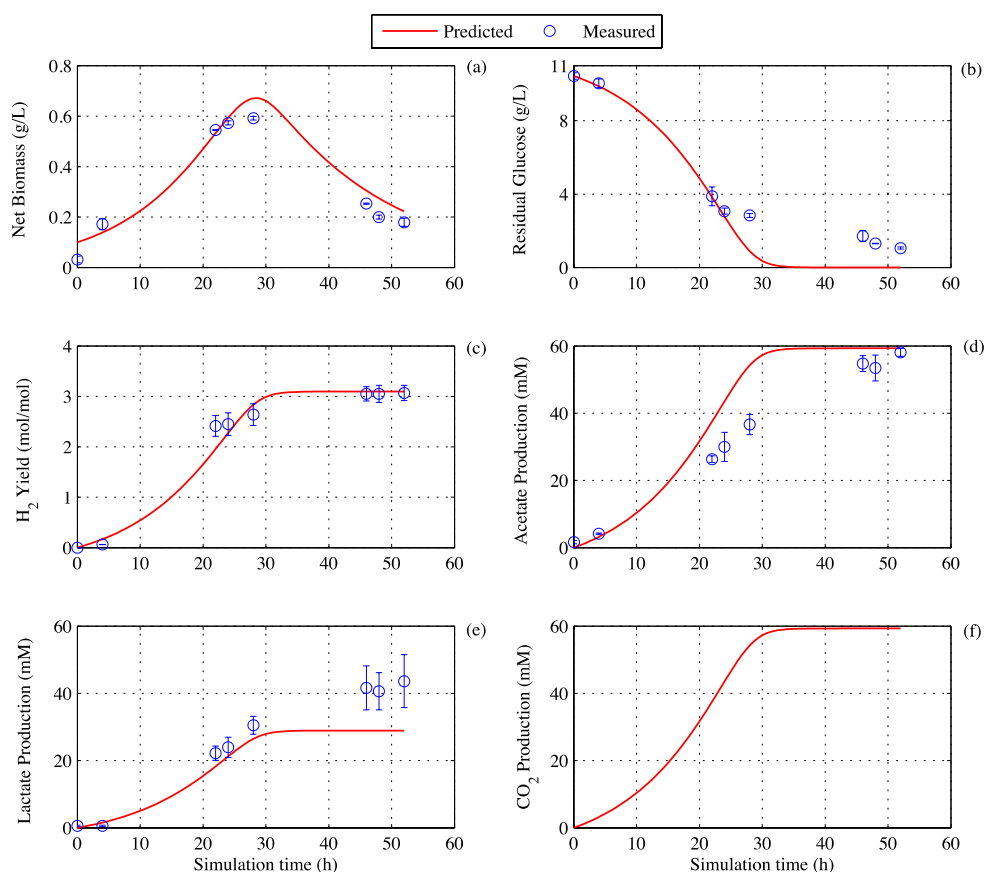


Fig. 6. 3 Model simulation for biomass growth, substrate consumption and products formation by *T. neapolitana*: predicted and measured results for (a) biomass growth in terms of cell dry weight, (b) residual glucose, (c) H₂ yield, (d) acetate production, (e) lactate production and (f) CO₂ production (Pradhan et al., 2016), error bars = standard error of mean (n = 3).

6.4.2 Sensitivity analysis

Fig. 6.4 shows the absolute sensitivities of the kinetic parameters for the input state variables (X , S , H_2 , Ac , CO_2 and Lac as 0.1, 10, 0, 0, 0 and 0, respectively). The derivatives of the input state variables were calculated with respect to kinetic parameters (in this case) as shown in Fig. 6.4. Clearly, the endogenous decay rate (k_d) and biomass yield coefficient (Y) had a profound impact on the model outputs (Fig. 6.4). The absolute sensitivities for Y and k_d attained their peak between 20 and 30 h of fermentation and decreased thereafter. Therefore, the model predictions are critical in that period. On the other hand, the semi-saturation constant (k_s) did not affect the model

output whereas the maximum specific uptake rate (k) had a minimal impact on the model output as observed in Fig. 6.4. The value of k_d was estimated by the least square error method from the batch experiments and the batch experiments do not provide a precise estimation of the k_d value. The accuracy of the k_d value can be increased by performing several series of continuous experiments under different operating conditions. This could be the reason why k_d shows a high degree of sensitivity in the model prediction (Pradhan et al., 2016). Therefore, the kinetic parameters k , Y and k_d were found to be sensitive to the model and considered for further optimization in the model calibration step (see sub-section Model calibration under CLF condition).

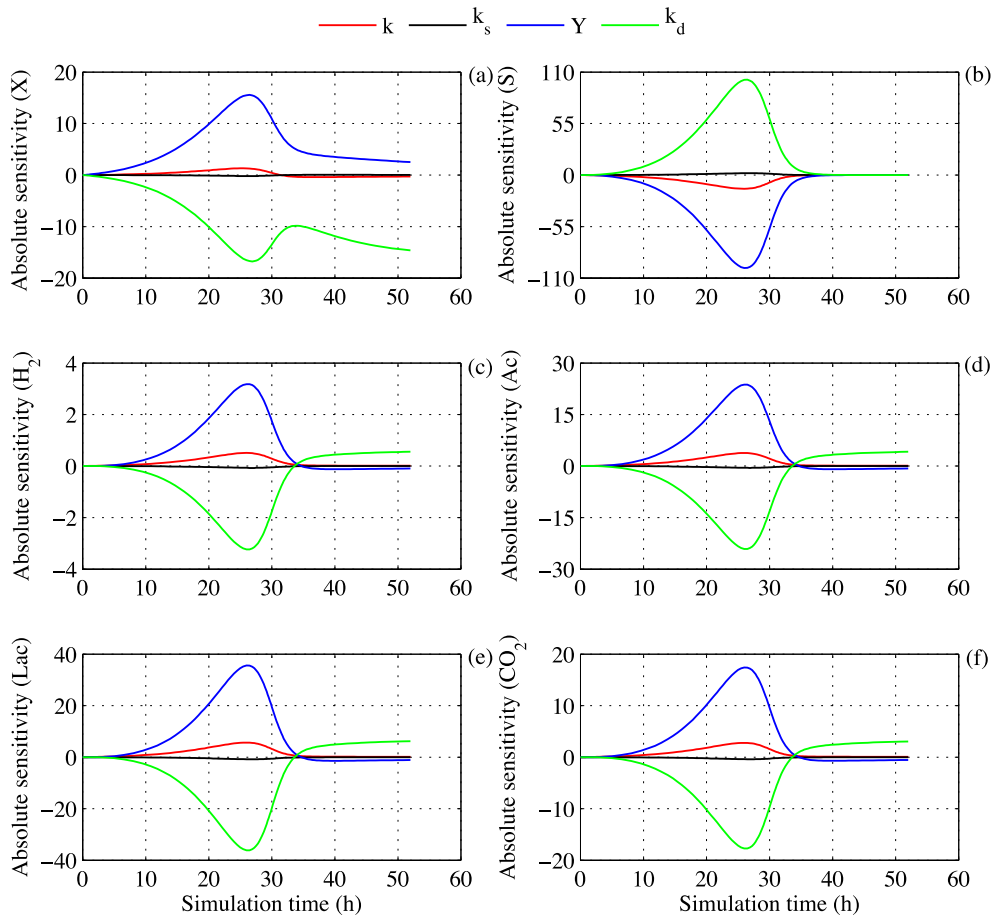


Fig. 6. 4 Absolute (or local) sensitivities of growth kinetic parameters during the simulation time for (a) biomass growth (X), (b) residual glucose (S), (c) H₂ yield, (d) acetate (Ac), (e) lactate (Lac) and (f) CO₂ production.

6.4.3 Model calibration under CLF condition

Experimental results of test ‘Glc-10’ were selected from the previous DF model (Pradhan et al., 2016) to re-calibrate the kinetic parameters for the CLF-based model. An integrated approach was followed to calibrate the sensitive kinetic parameters and minimize the error between model predictions and experimental results. The high sensitivity of the kinetic parameters depicted the reliability of the parameter optimization. A small change in the parameter values yielded a significant impact on the objective functions. This shows that the estimated parameters had a little uncertainty (Fang et al., 2013). In this case, the model calibration was performed on the acetate and lactate production, as they were not in conformity with the classic DF model principles as shown in Fig. 6.4d and e (Pradhan et al., 2016).

The 3-D surface plot (Fig. 6.5) shows the kinetic parameter (Y and k_d) optimization on acetate and lactate with respect to the regression tools, i.e. ME, IA and RMSE. The optimized values of k (figure not shown), Y and k_d were 1.30 1/h, 0.1195 and 0.0205 1/h, respectively. The regression coefficients were predicted from Fig. 6.5 and found to be $ME > 0.99$, $IA = 1$ and $RMSE < 0.01$. The other kinetic parameters such as specific growth rate (μ), maximum specific growth rate ($\mu_{max} = Y*k$) and biomass doubling time ($t_d = \ln(2)/\mu$) for *T. neapolitana* were calculated from the model and the values were 0.16 1/h and 4.37 h, respectively. The k_d value for *T. neapolitana* was found to be high in comparison to other studies because of the quick biomass doubling time (t_d) under capnophilic conditions (Pradhan et al., 2016).

Apart from this study, there are two other studies, which estimated the growth kinetic parameters of *T. neapolitana* from batch tests under N₂ sparging atmosphere. Yu and Drapcho (2011) reported that μ_{max} , k_S and Y for *T. neapolitana* grown on glucose were 0.94 1/h, 0.57 g/L, and 0.248, respectively. More recently, Frascari et al. (2013) studied the kinetic parameters for *T. neapolitana* grown on glucose under N₂ sparging atmosphere and reported that μ_{max} , k_S and k_d values were found to be 0.024 ± 0.005 1/h, 1.1 ± 0.3 g/L and 0.0042 ± 0.003 1/h, respectively. This reiterates that the kinetic parameters estimated and calibrated in this study (under CO₂ sparging atmosphere) were in conformity with previous studies (under N₂ sparging atmosphere).

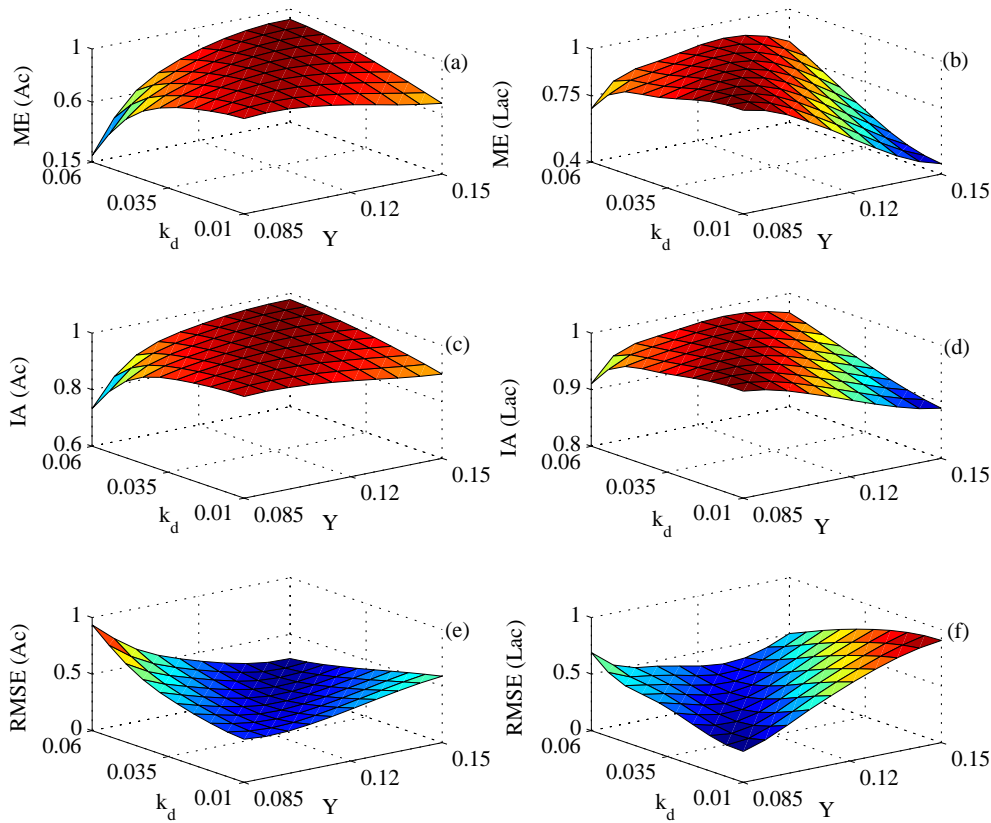


Fig. 6. 5 Model calibration for simultaneous changes in biomass yield coefficient (Y) and endogenous decay rate (k_d) with respect to ME for (a) Acetate (Ac) production and (b) Lactate (Lac) production; IA for (c) Ac and (d) Lac; and RMSE for (e) Ac and (f) Lac.

6.4.4 Model validation and cross validation

The optimized kinetic parameters, i.e. k , k_s , Y and $k_d = 1.30$ 1/h, 1.42 g/L, 0.1195 and 0.0205 1/h, respectively, were used to validate the model. The model simulated experimental results of fermentation by *T. neapolitana* conducted using both glucose (Glc-5) and arabinose (Arb-5) as the substrates. To improve the model validity and acceptability, a hexose (glucose) and pentose (arabinose) sugar were chosen for the model validation and cross validation, respectively. The experimental operating conditions for validating the model were different from those used to calibrate the model. Fig. 6.6 and Fig. 6.7 show predicted and measured data profiles for both the experiments.

A good agreement ($ME > 0.95$, $IA > 0.99$ and $RMSE < 0.154$ for acetate and lactate production in the validation experiment and $ME > 0.95$, $IA > 0.98$ and $RMSE < 0.086$ for acetate and lactate production in the cross validation experiment) was obtained between predicted and measured data, indicating the validity and accuracy of the kinetic parameters. The values of ME, IA and RMSE for substrate degradation, biomass growth and products formation estimated from the model simulation, validation and cross validation are presented in Table 6.5. The model predicted slightly faster conversion of substrate to biomass and products in the lag phase and showed an accurate prediction during the exponential and stationary growth phase of the biomass as observed in the model cross validation (Fig. 6.7a and b).

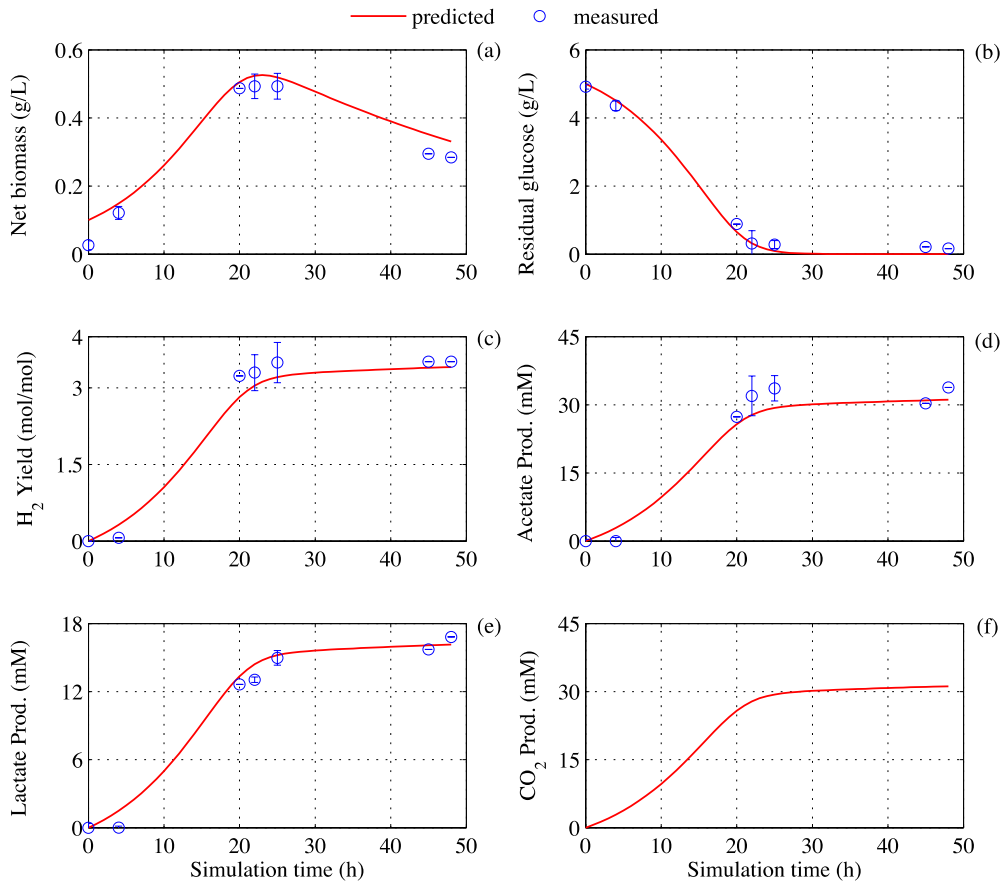


Fig. 6. 6 Model validation for substrate consumption, biomass growth and products formation by *T. neapolitana*: predicted and measured data for (a) biomass growth in terms of cell dry weight, (b) residual glucose, (c) H₂ yield, (d) acetate, (e) lactate and (f) CO₂ production, error bars = standard error of mean (n = 3).

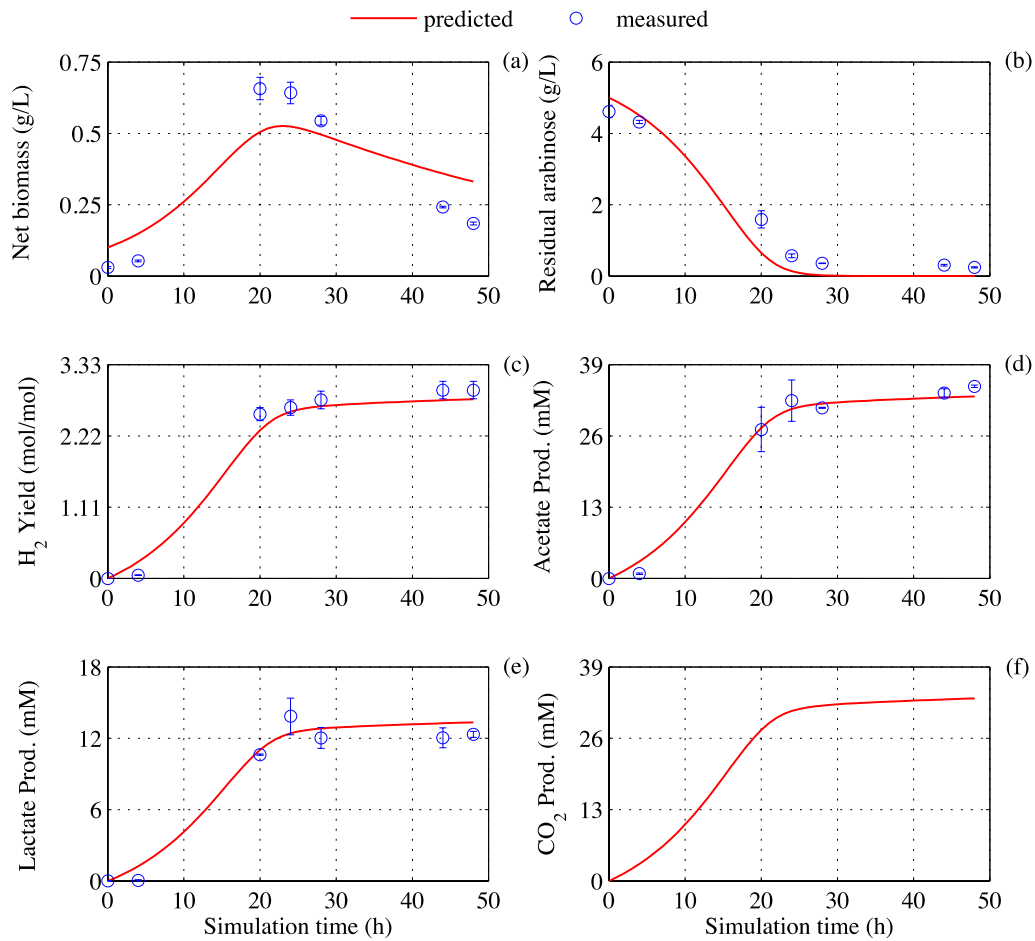


Fig. 6. 7 Model cross validation for substrate consumption, biomass growth and products formation by *T. neapolitana* using arabinose as substrate: predicted and measured data for (a) biomass growth in terms of cell dry weight, (b) residual arabinose, (c) H₂ yield, (d) acetate, (e) lactate and (f) CO₂ production, error bars = standard error of mean (n = 2).

Table 6. 5 Values of regression parameters for model simulation, validation and cross validation.

	Model Simulation			Model Validation			Cross validation		
	ME	IA	RMS E	ME	IA	RMS E	ME	IA	RMSE
X	0.90	0.98	0.055	0.93	0.99	0.035	0.73	0.99	0.113

<i>S</i>	0.87	0.97	1.028	0.98	0.99	0.168	0.92	0.98	0.373
<i>H₂</i>	0.92	0.98	0.029	0.98	0.99	0.011	0.96	0.99	0.012
<i>Ac</i>	0.81	0.96	0.458	0.95	0.99	0.154	0.98	0.99	0.079
<i>Lac</i>	0.60	0.85	0.773	0.98	0.99	0.069	0.95	0.98	0.086

Notes: *X* = biomass concentration; *S* = substrate concentration; *H₂* = hydrogen gas; *Ac* = acetic acid; *Lac* = lactic acid.

ME = modeling efficiency; IA = index of agreement; RMSE = root mean square error.

The new model can simulate monosaccharide-led fermentation tests to describe the substrate degradation, biomass growth and products formation along with a feedback pathway for lactate production via the CLF-based pathway. The purpose of the sensitivity analysis, model calibration and validation was to improve, analyze and predict accurately acetate and lactate production via the CLF-based pathway which was not possible to predict with the classic DF model (Pradhan et al., 2016). Experiments under capnophilic condition accumulated lactate from two different pathways, i.e. through (a) the standard DF pathway and (b) the CLF pathway. This model can effectively predict lactate production from both pathways through simple mathematical integration techniques. An indispensable tool for the model sensitivity analysis, calibration and validation of the CLF-based fermentation was developed. This robust mathematical model, equipped with parameters of clear biological significance and statistically consistent, will help in process optimization, control, design and analysis of CLF based fermentation at industrial scale. Otherwise, it would require complex laboratory experimental setups as well as considerable amount of time and resources to predict the fractions of lactate production via CLF and DF pathways.

With the mathematical model and the data from Table 6.4, it can be predicted that 81% of lactate was produced via the CLF pathway and 19% through the DF pathway for batch test ‘Glc-10’. For the batch test ‘Glc-5’, 97.5% of lactate was produced via the CLF pathway and 2.5% via the DF pathway and similarly for the test with arabinose (Arb-5), 97% of lactate was produced via the CLF pathway and 3% via the DF pathway. The above prediction assumes 12% of the total carbon source was

utilized for biomass growth and maintenance (i.e. assumed from the biomass yield coefficient 0.1195). All the predictions were conducted based on Eq. (6.4) and Eq. (6.7) of Table 6.1 and the fermentation stoichiometry presented in Table 6.2.

The experimental results (Table 6.4) revealed that Monod like kinetic equations can be adopted to describe the *T. neapolitana* metabolism under capnophilic conditions. However, the ADM1-based approach used to develop this model was quite successful in predicting the products formation and has scope to be further improved by applying different kinds of operating conditions. To further improve the model, other substrate inputs (e.g. amino acids), minor metabolites (e.g. alanine) and processes related parameters (e.g. buffering capacity, pH, dissolved CO₂, partial pressure of gases and enzyme kinetics) can be further integrated into this model.

6.5 Conclusions

This paper successfully developed a kinetic model and validated the process for lactate and acetate production under CLF conditions. Monod-like kinetic equations are adopted to improve the fundamental understanding of the CLF-based pathway and quantify the fermentation by-products. The calibrated kinetic parameters k , k_s , Y and k_d = 1.30 1/h, 1.42 g/L, 0.1195 and 0.0205 1/h, respectively, can be applied to *T. neapolitana* fermentation in any CSTR system. A high correlation coefficient (>0.95) for product formation in the model validation indicates the accuracy of the kinetic parameters. The model is equipped to predict lactate either cumulatively or separately produced by the DF and CLF pathway. Furthermore, a cross validation using a pentose sugar also shows a good correlation coefficient (>0.95) between predicted and experimental data. This new model is expected to provide a valuable basis for applying the CLF-based technology to the biotechnological and energy development sectors.

References

- Bernfeld, P. 1955. Alpha and beta-amylases. *Methods in Enzymology*, **1**, 149-158.
- d'Ippolito, G., Dipasquale, L., Fontana, A. 2014. Recycling of carbon dioxide and acetate as lactic acid by the hydrogen-producing bacterium *Thermotoga neapolitana*. *ChemSusChem*, **7**, 2678-83.
- d'Ippolito, G., Dipasquale, L., Vella, F.M., Romano, I., Gambacorta, A., Cutignano, A., Fontana, A. 2010. Hydrogen metabolism in the extreme thermophile *Thermotoga neapolitana*. *International Journal of Hydrogen Energy*, **35**, 2290-2295.

- Dipasquale, L., d'Ippolito, G., Fontana, A. 2014. Capnophilic lactic fermentation and hydrogen synthesis by *Thermotoga neapolitana*: An unexpected deviation from the dark fermentation model. *International Journal of Hydrogen Energy*, **39**, 4857-4862.
- Donoso-Bravo, A., Mailier, J., Martin, C., Rodriguez, J., Aceves-Lara, C.A., Wouwer, A.V. 2011. Model selection, identification and validation in anaerobic digestion: A review. *Water Research*, **45**, 5347-5364.
- Esposito, G., Frunzo, L., Panico, A., Pirozzi, F. 2011. Model calibration and validation for OFMSW and sewage sludge co-digestion reactors. *Waste Management*, **31**, 2527-2535.
- Fang, F., Mu, Y., Sheng, G.P., Yub, H.Q., Li, Y.Y., Kubota, K., Harada, H. 2013. Kinetic analysis on gaseous and aqueous product formation by mixed anaerobic hydrogen-producing cultures. *International Journal of Hydrogen Energy*, **38**, 15590-15597.
- Frasconi, D., Cappelletti, M., Mendes, J.D.S., Alberini, A., Scimonelli, F., Manfreda, C., Longanesi, L., Zannoni, D., Pinelli, D., Fedi, S. 2013. A kinetic study of biohydrogen production from glucose, molasses and cheese whey by suspended and attached cells of *Thermotoga neapolitana*. *Bioresource Technology*, **147**, 553-61.
- Hallenbeck, P.C., Ghosh, D. 2009. Advances in fermentative biohydrogen production: the way forward? *Trends in Biotechnology*, **27**, 287-297.
- Janssen, P.H.M., Heuberger, P.S.C. 1995. Calibration of process-oriented models. *Ecological Modelling*, **83**, 55-66.
- Kongjan, P., Min, B., Angelidaki, I. 2009. Biohydrogen production from xylose at extreme thermophilic temperatures (70 degrees C) by mixed culture fermentation. *Water Research*, **43**, 1414-24.
- Maly, T., Petzold, L.R. 1996. Numerical methods and software for sensitivity analysis of differential-algebraic systems. *Applied Numerical Mathematics*, **20**, 57-79.
- Molla, V.M.G., Padilla, R.G. 2002. Description of the MATLAB functions SENS_SYS and SENS_IND. *Universidad Politécnica de Valencia, Spain*.
- Nath, K., Das, D. 2004. Improvement of fermentative hydrogen production: Various approaches. *Applied Microbiology and Biotechnology*, **65**, 520-529.
- Nath, K., Das, D. 2011. Modeling and optimization of fermentative hydrogen production. *Bioresource Technology*, **102**, 8569-8581.
- Pradhan, N., Dipasquale, L., d'Ippolito, G., Fontana, A., Panico, A., Lens, P.N.L., Pirozzi, F., Esposito, G. 2016. Kinetic modeling of fermentative hydrogen production by *Thermotoga neapolitana*. *International Journal of Hydrogen Energy*, **41**, 4931-4940.
- Pradhan, N., Dipasquale, L., d'Ippolito, G., Panico, A., Lens, P.N.L., Esposito, G., Fontana, A. 2015. Hydrogen production by the thermophilic bacterium *Thermotoga neapolitana*. *International Journal of Molecular Sciences*, **16**, 12578-12600.

- Ribes, J., Keesman, K., Spanjers, H. 2004. Modelling anaerobic biomass growth kinetics with a substrate threshold concentration. *Water Research*, **38**, 4502-10.
- Siegrist, H., Vogt, D., Garcia-Heras, J.L., Gujer, W. 2002. Mathematical model for meso- and thermophilic anaerobic sewage sludge digestion. *Environmental Science and Technology*, **36**, 1113-1123.
- Tartakovsky, B., Mu, S.J., Zeng, J., Lou, S.J., Guiot, S.R., Wu, P. 2007. Anaerobic digestion model No. 1-based distributed parameter model of an anaerobic reactor: II. Model validation. *Bioresource Technology*, **99**, 3676-3684.
- Thauer, R.K., Jungerman, K., Decker, K. 1977. Energy conservation in chemotrophic anaerobic bacteria. *Bacteriological Reviews*, **41**, 100-180.
- Wang, J., Ye, J., Yin, H., Feng, E., Wang, L. 2012. Sensitivity analysis and identification of kinetic parameters in batch fermentation of glycerol. *Journal of Computational and Applied Mathematics*, **236**, 2268-2276.
- Xiao, J., VanBriesen, J.M. 2006. Expanded thermodynamic model for microbial true yield prediction. *Biotechnology and Bioengineering*, **93**, 110-21.
- Yu, X., Drapcho, C. 2011. Hydrogen production by the hyperthermophilic bacterium *Thermotoga neapolitana* using agricultural-based carbon and nitrogen sources. *Biological Engineering Transactions*, **4**, 101-112.

Chapter 7

Starch fermentation model

Chapter 7: Starch fermentation model

Abstract

This study investigated the effect of the salinity level, buffering agent and carbon source on the hydrogen (H₂) and lactic acid production under capnophilic (CO₂-led) lactic fermentation (CLF) by *Thermotoga neapolitana*. Fermentation experiments were conducted either in 0.12 L serum bottles or in a 3 L continuously stirred tank reactor (CSTR). Increasing the salinity level in the culture medium from 0 to 35 g/L NaCl increased the lactic acid production increased by 750% without affecting H₂ yield. A stable H₂ yield (i.e. 3.0 mol H₂/mol of glucose) and lactic acid (i.e. 13.7 mM) synthesis were observed when the culture medium was co-buffered with 0.01 M (diacid/monoacid phosphate, MOPS, TRIS and HEPES) and exogenous CO₂ as the source of bicarbonate. When applying the optimized culture parameters obtained in the 0.12 L serum bottle experiments about 230% higher lactic acid was produced in the process scale-up using a 3 L CSTR. This study shows an alternative strategy to valorize carbohydrate rich organic substrates with different salinity level for simultaneous generation of H₂ and lactic acid by applying CLF-based fermentation techniques.

Keywords: hydrogen; capnophilic lactic fermentation; starch; kinetic model; *Thermotoga neapolitana*.

7.1 Introduction

Hydrogen (H₂) is emerging as one of the clean and alternative energy sources due to its high energy content (120.7 kJ/g) compared to conventional fuels used today. The utilization of H₂ is expected to grow considerably over the coming years with the development of new technologies and also due to the drawbacks of the conventional routes to produce H₂, e.g. steam reforming and gasification, such as massive emissions of greenhouse gases to the atmosphere. The microbial conversion of organic substrates to H₂ and other important organic chemicals (e.g., lactic acid, acetic acid and ethanol) is a promising alternative H₂ production way with a high H₂ yield and low energy requirement (Bao et al., 2012; Vendruscolo, 2014). The major bottlenecks for the commercialization and up-scaling of the dark fermentative H₂ production are the low substrate utilization efficiency (limited to 33%) and high production costs, thus making the process less attractive compared to the physico-chemical or electrolytic processes (Pradhan et al., 2015; Vendruscolo, 2014).

Municipal and agro-industrial organic wastes are rich in carbohydrate, which would enable to reduce the overall production cost of H₂ along with the recovery of commercially valuable organic acids from the fermentation broth. Polysaccharides like starch, cellulose and hemicellulose can be hydrolysed to produce simultaneously H₂ and organic acids after a suitable pre-treatment, i.e. acid or enzymatic hydrolysis. For example, starch is a major component of agro-industrial wastes, i.e. wheat, rice, potato, corn, cassava and sweet potato (Lin et al., 2008). Several studies have reported H₂ production from potato, wheat, rice and cassava starches under mesophilic, thermophilic and hyperthermophilic conditions (Chen et al., 2008; Mars et al., 2010). Essentially, starch is composed of two polymers, i.e. amylose (15–30%) and amylopectin (70–85%), in different proportions according to its source (Alcazar-Alay & Meireles, 2015). Amylose consists of linear chains of glucose into a polymer lined by α (1→4) glycosidic bonds, whereas amylopectin is a highly branched polymer of glucose linked by α (1→6) glycosidic bonds (Vendruscolo, 2014).

Either pure or mixed cultures can be used to produce H₂ from various kinds of organic substrates. Recently, a marine hyperthermophilic bacterium *Thermotoga neapolitana* has been reported to simultaneously synthesize H₂ and lactic acid via a novel metabolic pathway, called the capnophilic (CO₂-requiring) lactic fermentation

(CLF) (d'Ippolito et al., 2014; Dipasquale et al., 2014; Pradhan et al., 2016b). The CLF-based fermentation takes place in the presence of a CO₂ atmosphere. Application of CO₂ gas is well known in the fermentation industries and considered as a cheap sparging gas, which has other important benefits such as positively affecting the buffering capacity and accelerating the fermentation reactions (Pradhan et al., 2015; Willquist & van Niel, 2012).

A study by Willquist and van Niel (2012) found that the lag phase of the biomass growth was decreased by 10 fold when a pure *Caldicellulosiruptor saccharolyticus* culture was sparged with CO₂ gas instead of N₂ gas. A high partial pressure of either CO₂ or H₂ is often linked to either growth inhibition or metabolic shifts in the pure culture of the H₂ producing bacterium (Hallenbeck & Ghosh, 2009; Willquist & van Niel, 2012). In contrast, such effects are not observed or minimal for *T. neapolitana* fermentation at high CO₂/HCO₃⁻ concentrations (~ 14 mM) in the culture medium (Dipasquale et al., 2014).

The bacterium *T. neapolitana* has been widely investigated for H₂ production in different bioreactors with various sugars under different operating conditions (Pradhan et al., 2015). Recently, kinetic models based on the anaerobic model digestion no. 1 (ADM1) (Batstone et al., 2002; Hinken et al., 2014) were developed to model *T. neapolitana* fermentation under N₂ (Pradhan et al., 2016b) and CO₂ enriched atmosphere, i.e. CLF (Pradhan et al., 2016a) in a CSTR system. The complex metabolic pathway was represented by a series of mass balance equations. There were two main goals of this study: (i) to test the fermentability of starches (potato and wheat) for the simultaneous H₂ and lactic acid production using *T. neapolitana* in pH-controlled reactors under CLF conditions and (ii) to apply the CLF-based kinetic model to simulate the experimental results of the starch fermentation in a CSTR system.

7.2 Materials and methods

7.2.1 Bacterial strain and medium composition

T. neapolitana DSZM 4359 strain ((i.e. laboratory strain 'TN-CMut' as in Chapter 3) was purchased from the Deutsche Sammlung von Mikroorganismen und Zellkulturen (DSMZ) (Braunschweig, Germany). The bacterium was grown anaerobically according to d'Ippolito et al. (2010).

7.2.2 Experimental set-up

The experiments were performed either in 120 mL serum bottles for 72 h or in a 3.0 L CSTR (Applikon Biotechnology, The Netherlands) for 48 h with a working volume to headspace ratio of 1:3 (approx.) (Pradhan et al., 2016b). Inoculum cultures were grown overnight (16–18 h) in serum bottles containing glucose as the carbon source as described by d'Ippolito et al. (2010). For starch fermentation, the culture medium was supplemented with 5 g/L of either potato or wheat starch as the carbon source and autoclaved at 110 °C for 15 min.

The sterilized culture medium was sparged with CO₂ for 5 min at 30 mL/min to remove excess oxygen from the bioreactor and then inoculated (6% v/v) with the previously washed (twice with 10 g/L of NaCl) culture of *T. neapolitana*. Subsequently, the pH of the serum bottles was adjusted to ~ 7.5 by adding 1 M NaOH and kept in an oven at 80 °C without shaking. The pH of the CSTR was maintained at 6.5 by auto titrating with 1 M NaOH. The temperature of the CSTR was kept thermostatically constant at 80 (± 1) °C and the stirring speed was set to 50 rpm by an electro-magnetic mixing unit. Samples (3 mL) for biochemical assays were withdrawn at regular time intervals, centrifuged at 13,000 rpm for 5 min and stored at –20 °C for further analyses (Dipasquale et al., 2015).

The experiments were performed in two stages. The first stage, the fermentability of potato starch was investigated in the serum bottles (i.e. potato starch with 10 g/L NaCl in serum bottles (PS10-SB) and potato starch with 35 g/L NaCl in serum bottles (PS35-SB)) at two different salinity levels, i.e. 10 and 35 g/L NaCl. In the second stage, the serum bottle experiments were up-scaled to a 3.0 L pH-controlled (~ 6.5) CSTR (i.e. potato starch with 10 g/L NaCl in a CSTR (PS10-R1), wheat starch with 10 g/L NaCl in a CSTR (WS10-R2) and potato starch with 35 g/L NaCl in a CSTR (PS35-R3)) using both potato and wheat starch.

7.2.3 Analytical methods

The gas samples from the bioreactor headspace were analysed for H₂ and CO₂ concentrations using gas chromatography (Focus GC, Thermo Scientific) (Dipasquale et al., 2014). The analyses for aqueous metabolites (i.e. acetic and lactic acid) were performed on the supernatants by a ¹H Nuclear Magnetic Resonance (NMR) 600 MHz spectrometer (Bruker Avance 600) as per Dipasquale et al. (2014). The residual starch

in the fermenter was measured by the phenol/sulfuric acid method calibrated on a standard solution of 0.2 g/L glucose (Dubois et al., 1956).

The biomass growth was monitored at $\lambda = 540$ nm by a UV/Vis spectrophotometer (DU 730, Beckman Coulter). Further, the cell dry weight (CDW) was calculated using a correlative equation for *T. neapolitana* growth (CDW (g/L) = $0.347 * \lambda (540\text{nm}) + 0.016$) (Pradhan et al., 2016b). The elemental composition of the *T. neapolitana* cells was analysed on lyophilized samples by a CHNS analyser (Thermo Scientific).

7.2.4 Kinetic model and thermodynamic analysis for *T. neapolitana* fermentation

7.2.4.1 Metabolic reactions

To model starch fermentation under CLF conditions, glucose is considered as the model monomer (Eq. (7.1)). H₂, CO₂, acetic acid and lactic acid are the major metabolic by-products of CLF-based fermentation and the biochemical reactions are presented in Table 7.1 (Pradhan et al., 2016a). The biochemical equations are written as per the stoichiometric yields of product formation (Eqs. (7.2)–(7.6)) as shown in Table 7.1 (Donoso-Bravo et al., 2011; Kongjan et al., 2010; Pradhan et al., 2016a; Ribes et al., 2004).

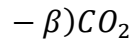
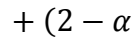
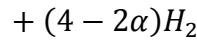
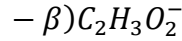
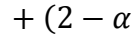
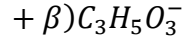
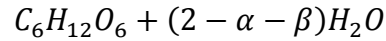
Table 7. 1 Metabolic reactions and Gibbs free energies for the key reactions under CLF conditions.

Metabolic reactions		$\Delta G^0_{298.15\text{K}}$ (kJ/reaction)	$\Delta G^r_{353.15\text{K}}$ (kJ/reaction)	Equation
Hydrolysis of starch to glucose	$(C_6H_{10}O_5)_n + (n - 1)H_2O \rightarrow n(C_6H_{12}O_6)$			(7.1) ^a
Glucose fermentation as per DF model	$C_6H_{12}O_6 + H_2O \rightarrow 2C_2H_3O_2^- + 2H^+ + 4H_2 + 2CO_2$	-215.9	-303.8	(7.2)
CLF mechanism:	$C_6H_{12}O_6 \rightarrow 2C_3H_5O_3^- + 2H^+$	-198.3	-286.2	(7.3)
recycling of acetic acid and dissolved	$C_2H_4O_2 + CO_2 + 4H^+ + 4e^- \rightarrow C_3H_6O_3 + H_2O$	+160.3	+336.1	(7.4)

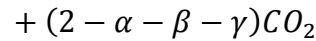
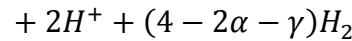
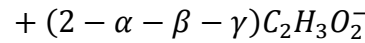
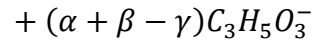
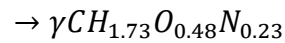
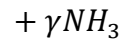
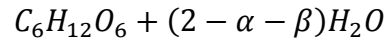
CO₂

Glucose

fermentation as
per CLF model



(7.5)^b



(7.6)^b

Notes:

^a starch hydrolysis.

^b Syntrophic coupled reaction under CLF conditions.

α and β are the stoichiometric yields of lactic acid via DF and CLF-based pathways, respectively where, $\alpha \geq 0$ and $\beta \geq 0$.

γ is the stoichiometric yield of *T. neapolitana*.

ΔG^0 (kJ/reaction) is the standard Gibbs free energy, i.e. reactants and products at 1 M concentration or 1 atm partial pressure (Thauer et al., 1977).

ΔG^r (kJ/reaction) is the Gibbs free energy at pH 6.5, Temperature 80 °C and reactants and products at 1 M concentration or 1 atm partial pressure.

7.2.4.2 Model kinetic parameters and thermodynamics

In this study, the kinetic rate equations previously developed for the CLF-based model were applied (Pradhan et al., 2016a). Three statistical tools are used to evaluate

the degree of model fitting between the predicted and measured data: modeling efficiency (ME), index of agreement (IA) and root mean square error (RMSE) (Pradhan et al., 2016a; Pradhan et al., 2016b). The previously calibrated kinetic parameters, maximum specific uptake rate (k) = 1.30 1/h, semi-saturation constant (k_s) = 1.42 g/L, biomass yield coefficient (Y) = 0.12, and endogenous decay rate (k_d) = 0.02 1/h were used to simulate the results of starch fermentation (Pradhan et al., 2016a).

Thermodynamics play a crucial role in fermentative H₂ production as proton reduction is strongly energy consuming (+79.7 kJ/mol of H₂) (Thauer, 1977). Most of the electron equivalents in the glucose do not accumulate in H₂ but in a range of organic acids (Lee et al., 2008; Yuan et al., 2014). In this study, the Gibbs free energy of a reaction based on the stoichiometric oxidation-reduction equations without the cell biomass synthesis were calculated and discussed (Eq. (7.2)–(7.4)) (Lee et al., 2008). The ΔG^r of a fermentation reaction depends on the pH, operating temperature as well as concentration of products and reactants. For example, the change in ΔG^r for Eq. (7.5) in Table 7.1 can be written as Eq. (7.7):

$$\Delta G^r = \Delta G^0 + RT \ln \left(\frac{[C_3H_5O_3^-]^{(\alpha+\beta-\gamma)} [C_2H_3O_2^-]^{(2-\alpha-\beta-\gamma)} [H^+]^2 [H_2]^{(4-2\alpha-\gamma)} [CO_2]^{(2-\alpha-\beta-\gamma)}}{[C_6H_{12}O_6] [H_2O]^{(2-\alpha-\beta)}} \right) \quad (7.7)$$

where ΔG^0 = Gibbs free energy of the reaction under standard conditions (298.15 K), ΔG^r = Gibbs free energy of the reaction at the operating temperature (353.15 K), $[H^+]$ = proton concentration corresponding to pH value, T = temperature (kelvin) and R = universal gas constant (8.314 J/K/mol).

7.3 Results

7.3.1 Potato starch fermentation in serum bottles

Table 7.2 shows the serum bottle test results of potato starch fermentation under CLF conditions. Nearly 80% of starch was consumed in the serum bottle experiments after 72 h of incubation (Table 7.2). The H₂, acetic acid and lactic acid yields with 10 g/L NaCl were 2.6 (\pm 0.3) mol H₂/mol glucose eq., 0.7 (\pm 0.1) mol acetic acid/mol glucose eq. and 1.4 (\pm 0.1) mol lactic acid/mol glucose eq., respectively. With 35 g/L NaCl, these were 2.8 (\pm 0.3) mol H₂/mol glucose eq., 0.6 (\pm 0.1) mol acetic acid/mol glucose eq. and 0.7 (\pm 0.2) mol lactic acid/mol glucose eq., respectively. The substrate

consumption, H₂ production (HP), H₂ production rate (HPR) and acetic acid production were similar with 10 and 35 g/L NaCl in the culture medium, whereas the lactic acid production with 10 g/L NaCl was 2.2 times higher than that with 35 g/L NaCl in the culture medium.

Table 7. 2 Effect of salinity level on batch fermentation of potato starch by *T. neapolitana* under CLF conditions.

Reactor	NaCl (g/L)	S (mM)	HP (mL/L)	HPR (mL/L/h)	Ac (mM)	Lac (mM)
PS10-SB	10	23.6 (± 1.1)	1645.2 (± 116.9)	22.9 (± 1.6)	17.9 (± 0.5)	37.2 (± 1.1)
PS35-SB	35	22.0 (± 0.4)	1685.4 (± 158.6)	23.4 (± 2.2)	14.1 (± 1.0)	16.9 (± 3.9)

Notes:

SB = serum bottle.

PS10 = potato starch with 10 g/L NaCl.

PS35 = potato starch with 35 g/L NaCl.

S = starch consumed.

HP = H₂ production.

HPR = H₂ production rate.

Ac = acetic acid.

Lac = Lactic acid.

The results are expressed as mean ± standard error (n = 3).

7.3.2 Fermentability of starches in a pH-controlled CSTR

The serum bottle experiments were up-scaled to a 3.0 L CSTR system and tested for the H₂ and lactic acid production potential with potato and wheat starch. An improved starch fermentability and sugar consumption (over 90%) was observed for the CSTR experiments compared to the serum bottle experiments due to better mixing and pH control in the scale-up experiments as shown in [Table 7.3 \(Dipasquale et al., 2014\)](#). The H₂ production (HP) and H₂ production rate (HPR) were the highest for potato starch (PS10-R1) compared to the wheat starch (WS10-R2) fermentation under similar operating conditions. As per some previous studies, the fermentative H₂ production from the starches investigated under thermophilic conditions remained below 2.5 mol

H₂/mol of glucose eq. under N₂ sparging atmosphere (Akutsu et al., 2008; Argun & Kargi, 2010; Chen et al., 2008), whereas, under CO₂ sparging atmosphere the H₂ yield was above 2.5 mol H₂/mol of glucose eq. (Table 7.3). The higher H₂ yield under hyperthermophilic conditions from starch can be explained by in-fermentation hydrolysis of starch due to the higher temperature (i.e. 80 °C) in the reactor (Orozco et al., 2012).

A very interesting trend in the acetic and lactic acid production was observed in the CSTR experiments: the acetic acid produced from the potato starch fermentation is 40% less compared to the wheat starch fermentation with a similar starch consumption. In contrast, the lactic acid produced from the potato starch is 260% higher than that from wheat starch, indicating the activation of the CLF mechanism during the potato starch fermentation. The reduction in the acetic acid concentration during the potato starch fermentation is responsible for the increase in lactic acid concentration (Table 7.3).

Experimental results with the PS10-R1 show a clear correlation between H₂ production, acetic and lactic acid synthesis compared to the WS10-R2 experimental results. According to the classic dark fermentation model (Thauer, 1977), the H₂ production is inversely proportional to the lactic acid production, but the experimental results under CLF conditions were opposite (Dipasquale et al., 2014). A study by d'Ippolito et al. (2014) showed that lactic acid is produced by carboxylation of acetyl-CoA during the fermentation, hence intracellular CO₂ availability is important for high lactic acid synthesis for CLF-based fermentations. Under CLF conditions, the NADH plays a major role by simultaneously supplying energy to the hydrogenases for H₂ production as well as recycling acetic acid to lactic acid, where the extra pool of NADH was assumed to come from the degradation of amino acids, but the exact source still needs to be elucidated (d'Ippolito et al., 2014).

Table 7. 3 Potato and wheat starch fermentation under CLF conditions by *T. neapolitana* in a CSTR system.

Reactor	NaCl (g/L)	S (mM)	HP (mL/L)	HPR (mL/L/h)	Ac (mM)	Lac (mM)
PS10-R1	10	26.8 (± 1.3)	2199.2 (± 187.1)	45.8 (± 3.9)	29.9 (± 1.2)	22.5 (± 10.6)
WS10-R2	10	26.3 (± 0.2)	1820.3 (± 114.6)	37.9 (± 2.4)	38.1 (± 2.2)	8.6 (± 2.9)

PS35-R3 35 26.0 (± 0.3) 1338.0 (± 82.5) 27.9 (± 1.7) 19.4 (± 1.6) 26.3 (± 1.0)

Notes:

PS10-R1 = potato starch with 10 g/L NaCl.

WS10-R2 = wheat starch with 10 g/L NaCl.

PS35-R3 = potato starch with 35 g/L NaCl.

The results are expressed as mean ± standard error.

7.3.3 Kinetic analysis of starch fermentation

Table 7.4 shows the stoichiometric coefficients of the product yield for starch fermentation under CLF conditions. The input state variables for the model simulation were biomass (X) 0.1 g/L, substrate (S) 5 g/L and zero for H₂, acetic acid (Ac) and lactic acid (Lac) as proposed by Pradhan et al. (2016a). The model simulates the starch fermentation experimental results by using previously estimated kinetic parameters (i.e. k , k_s , Y and k_a) of *T. neapolitana* under CLF conditions with glucose as the carbon source (Pradhan et al., 2016a).

Table 7. 4 Stoichiometric yields of main metabolites after 48 h of starch fermentation by *T. neapolitana* under CLF conditions.

Batch test	Units	PS10-R1	WS10-R2	PS35-R3
H ₂ yield	mol H ₂ /mol glucose eq.	3.0 (± 0.2)	2.5 (± 0.2)	2.0 (± 0.3)
Ac yield	mol Ac/mol glucose eq.	0.9 (± 0.2)	1.3 (± 0.1)	0.7 (± 0.1)
Lac yield	mol Lac/mol glucose eq.	0.8 (± 0.3)	0.3 (± 0.1)	0.9 (± 0.1)

Notes:

Ac = acetic acid.

Lac = lactic acid.

The results were normalized with starch to glucose conversion ratio, i.e. 1.11 (Huang et al., 2005).

(Starch hydrolysis: $(C_6H_{12}O_5)_n + (n-1)H_2O \rightarrow n(C_6H_{12}O_6)$)

Conversion factor = $(180 \times n) / ((180 \times n) - (n-1) \times 18)$

as n becomes large, as in the starch molecule, this factor becomes 1.11)

7.3.4 Model simulation of starch fermentation

7.3.4.1 Potato starch fermentation

Fig. 7.1 shows the simulation output for the fermentation results of the PS10-R1 incubation. Fig. 7.1a shows that the model prediction for the biomass growth does not completely agree with the measured data as *T. neapolitana*: apparently *T. neapolitana* grows better in a medium containing starch compared to a medium containing glucose (Pradhan et al., 2016a). The model predictions for the substrate consumption, H₂ yield, acetic and lactic acid production gave a good fitting with the measured data, except for biomass growth, and the fitting parameter values can be seen in Table 7.5. More than 60% of the total amount of lactic acid was produced via the CLF-based pathway by the carboxylation of acetic acid and < 40% via the DF-based pathways, i.e. through direct conversion of pyruvate to lactic acid due to a metabolic shift (Pradhan et al., 2016a). The potato starch fermentation results are promising with respect to H₂ and lactic acid production and can be up-scaled to a pilot scale reactor for the fermentation of starch rich agro-industrial waste.

The Gibbs free energy (ΔG^r) of reactions at different time intervals were calculated and corrected with respect to the *in situ* conditions of *T. neapolitana* fermentation, i.e. pH, temperature as well as partial pressures or concentrations of metabolites (Thauer, 1977). The spontaneity of the reaction depends on the value of the ΔG , if the value is negative the reaction takes place spontaneously, otherwise it requires additional energy for the reaction to proceed. Eqs. (7.2) and (7.3) can proceed spontaneously as the ΔG value is negative, but Eq. (7.4) cannot proceed spontaneously as it requires additional energy. The ΔG values for the potato starch fermentation were calculated from the measured concentrations of the metabolites as well as the prevailing temperature (353.15 K) and pH (varies between 6.5–7.0) (Eq. (7.5)). Fig. 7.1f shows the Gibbs free energy of reaction (ΔG^r) at 353.15 K. The net ΔG^r for the fermentation reaction remained below –300 kJ/reaction, thus favouring the overall *T. neapolitana* fermentation reaction (Eq. (7.5)) to proceed even though the recycled lactic acid pathway remained highly unfavourable as per Eq. (7.4).

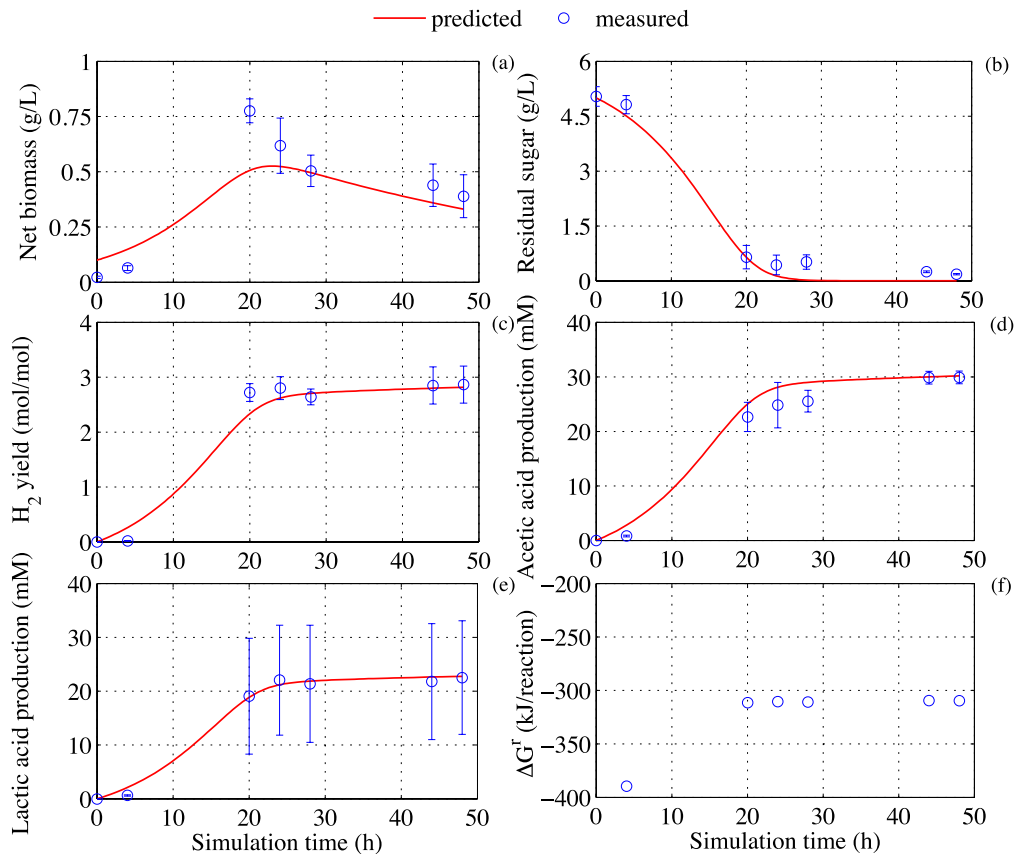


Fig. 7. 1 CLF-based model simulation for catabolism and bioenergetics of the potato starch fermentation by *T. neapolitana*: predicted and measured results for (a) biomass growth in terms of cell dry weight, (b) residual sugar, (c) H₂ yield, (d) acetic acid production, (e) lactic acid production and (f) ΔG^r values calculated from the measured concentrations of products and reactants. Error bars = standard error of mean (n = 4).

7.3.4.2 Wheat starch fermentation

Fig. 7.2 shows the results of fermentation of the wheat starch (WS10-R2) under CLF conditions. The CLF model did not accurately predict biomass growth with the wheat starch and there was a large deviation between the measured and predicted data (Fig. 7.2a). The model slightly overestimated the substrate consumption rate (Fig. 7.2b), H₂ yield (Fig. 7.2c) and acetic acid production (Fig. 7.2d) during the exponential growth phase and underestimated the lactic acid production (Fig. 7.2e). Table 7.5 shows the values of the model fitting parameters between model predictions and measured values. Thus, wheat starch fermentation does not follow the CLF-based pathway and there was no acetic acid recycling to form lactic acid, hence the fermentation followed a

conventional DF pathway. The high amount of acetic acid in the spent medium indicated that the CLF-based recycling of acetic acid did not take place for this fermentation reaction. The net ΔG^r for the fermentation reaction remained below -325 kJ/reaction, thus making the reaction favorable to proceed under hyperthermophilic conditions (Fig. 7.2f).

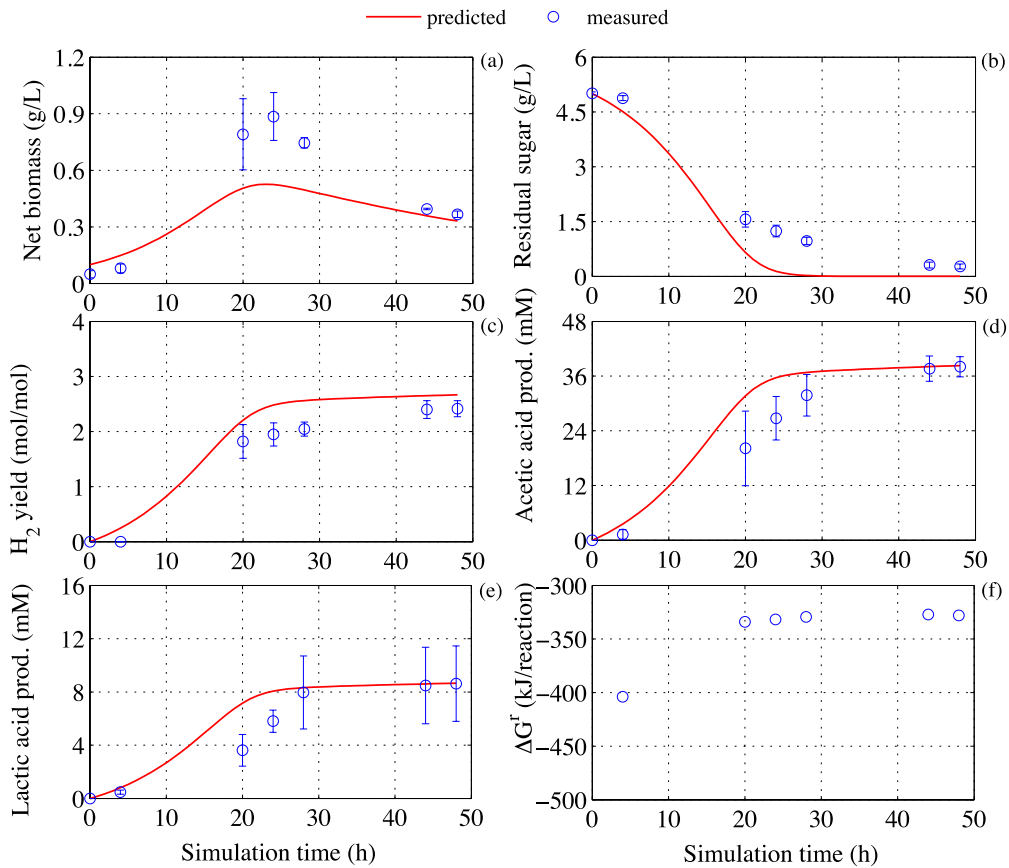


Fig. 7. 2 CLF-based model simulation for the catabolism and bioenergetics of wheat starch fermentation by *T. neapolitana*: predicted and measured results for (a) biomass growth in terms of cell dry weight, (b) residual sugar, (c) H₂ yield, (d) acetic acid production, (e) lactic acid production and (f) ΔG^r values calculated from measured concentrations of products and reactants. Error bars = standard error of mean (n = 2).

7.3.4.3 Potato starch fermentation with 35 g/L NaCl in the culture medium

Fig. 7.3 shows the simulation output for the potato starch fermentation at 35 g/L NaCl in the culture medium (PS35-R3). Except for the biomass growth, the model simulation is coherent with the experimental results of PS35-R3. Table 7.5 shows that

there was a good fitting between the model predictions and the measured data. At a high salinity level (35 g/L NaCl), there was a net decrease in H₂ yield (2.2 ± 0.3 mol H₂/mol glucose eq.) compared to experiments under standard conditions (i.e. with 10 g/L NaCl), which was attributed to the production of significant amounts (~ 70%) of lactic acid via the DF pathway and about 30% of lactic acid via the recycling of acetic acid by the CLF-based pathway as per the mass balance. The net ΔG^r for the experiment is < -400 kJ/reaction, thus making the reaction more spontaneous and favorable at 353.15 K (Fig. 7.3f).

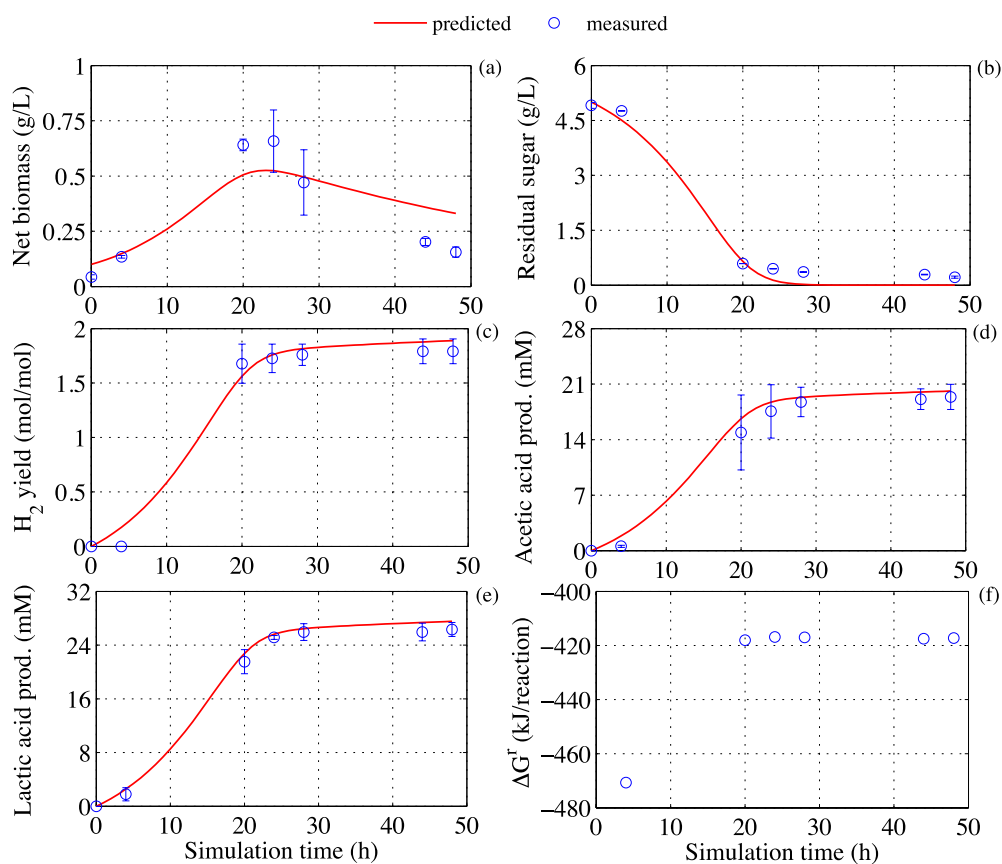


Fig. 7. 3 CLF-based model simulation for the catabolism and bioenergetics of potato starch fermentation supplemented with 35 g/L NaCl by *T. neapolitana*: predicted and measured results for (a) biomass growth in terms of cell dry weight, (b) residual sugar, (c) H₂ yield, (d) acetic acid production, (e) lactic acid production and (f) ΔG^r values calculated from measured concentrations of products and reactants. Error bars = standard error of mean (n = 2).

Table 7. 5 CLF-based model fitting parameters of the starch fermentation.

	PS10-R1			WS10-R2			PS35-R3		
	ME	IA	RMSE	ME	IA	RMSE	ME	IA	RMSE
X	0.70	0.99	0.12	0.58	0.99	0.20	0.65	0.99	0.12
S	0.97	0.99	0.26	0.83	0.96	0.61	0.98	0.99	0.24
H ₂	0.95	0.99	0.01	0.96	0.99	0.01	0.97	0.99	0.01
Ac	0.97	0.99	0.10	0.80	0.95	0.31	0.99	0.99	0.04
Lac	0.99	0.99	0.08	0.73	0.93	0.13	0.99	0.99	0.06

Notes:

X = biomass concentration.

S = substrate concentration.

H₂ = H₂ gas.

Ac = acetic acid.

Lac = lactic acid.

ME = modeling efficiency.

IA = index of agreement.

RMSE = root mean square error.

7.4 Discussion

7.4.1 Analysis of starch fermentation under CLF conditions

This study showed that lactic acid obtained by *T. neapolitana* fermentation of potato starch was the highest reported to date in a CSTR system under CLF conditions. A comparison of the use of potato or wheat starch as a fermentation substrate resulted in contrasting data with respect to the H₂ and lactic acid production (Table 7.4). In this study, the CLF-based kinetic model was applied to the results of potato and wheat starch fermentation by *T. neapolitana* in a CSTR experiments. The kinetic model as well as the experimental results showed that both H₂ and lactic acid production with wheat starch were much lower than with potato starch.

Another comparison between glucose and starch showed that the biomass grew better on starch than that with glucose. By contrast higher H₂ yield was reported when glucose was used as carbon source compared to starch (Pradhan et al., 2016a). Previous studies showed that 3.6 (\pm 0.3) mol H₂/mol of glucose (Pradhan et al., 2016a) and 2.9 (\pm

0.1) mol H₂/mol of arabinose (Pradhan et al., 2016a) were, respectively, produced from glucose and arabinose in comparison to 3.0 (± 0.2) and 2.5 (± 0.2) mol H₂/mol of glucose eq. from, respectively, potato and wheat starch in the present study (Table 7.6). The lactic acid production from glucose and arabinose were 0.6 (± 0.1) mol lactic acid/mol of glucose and 0.4 (± 0.1) mol lactic acid/mol of arabinose, respectively, compared to 0.8 (± 0.3) and 0.3 (± 0.1) mol lactic acid/mol of glucose eq., respectively, with potato and wheat starch in the present study (Table 7.6). Starch fermentation thus offers better performance with respect to lactic acid production compared to glucose and arabinose as carbon source under CLF conditions.

Table 7. 6 Comparative analysis of the present experimental results with the reported data on fermentative H₂ and organic acids production under N₂ and CO₂ (~ 14 mM dissolved CO₂) enriched atmosphere by *T. neapolitana* in a CSTR system supplemented with 5 g/L of carbon source.

Substrate	H2 yield (mol/mol)	Acetic acid yield (mol/mol)	Lactic acid yield (mol/mol)	References
Experiments performed under DF (N ₂ sparging atmosphere) conditions				
Glucose	2.8	1.7 (± 0.1)	0.5 (± 0.1)	Dipasquale et al. (2014)
Xylose	1.4 (± 0.1)	1.1	nd*	Ngo and Bui (2013)
Xylose	2.7 (± 0.1)	1.5 (± 0.1)	0.1	Ngo et al. (2012)
Experiments performed under CLF (CO ₂ sparging atmosphere) conditions				
Glucose	2.8	1.4 (± 0.2)	0.8 (± 0.2)	Dipasquale et al. (2014)
Glucose	3.6 (± 0.3)	1.2 (± 0.1)	0.6 (± 0.1)	Pradhan et al. (2016a)
Arabinose	2.9 (± 0.1)	1.2 (± 0.1)	0.4 (± 0.1)	Pradhan et al. (2016a)
Potato starch	3.0 (± 0.2)	0.9 (± 0.2)	0.8 (± 0.3)	This study
Wheat starch	2.5 (± 0.2)	1.3 (± 0.1)	0.3 (± 0.1)	This study

*nd = not detected.

The data/results are expressed as mean ± standard error.

A 2.6 fold higher lactic acid production was obtained with the potato starch compared to the wheat starch fermentation under similar operating conditions (Table 7.4). About 40% of the acetic acid was recycled back to produce lactic acid for potato

starch fermentation, but the bioconversion seemed absent for the wheat starch fermentation. As per the DF model, 1 mol of glucose can give rise to 4 mol of H₂ and 2 mol each of CO₂ and acetic acid (Thauer, 1977), but under the CLF conditions the imbalance in the H₂ and acetic acid production ratio is due to the activation of the CLF pathway, which has also been reported in the previous studies with glucose and arabinose as substrates (Dipasquale et al., 2015; Dipasquale et al., 2014; Pradhan et al., 2016a; Pradhan et al., 2016b).

7.4.2 Structural analysis of potato and wheat starch

Starches from cereals, roots, tubers and legumes vary in terms of composition and properties (Li et al., 2014). Potato starch has a higher swelling power, solubility and viscosity compared to wheat, corn and rice starches. In addition, potato starch showed a higher tendency towards retrogradation compared with cereal starches (Singh et al., 2003; Waterschoot et al., 2015).

Potato starch has a higher phosphorous content (0.09%) than wheat starch (0.05%) in the form of phosphate monoesters that are covalently bound to amylopectin. The phosphate is ester linked at C-6 (61%), C-3 (38%) and C-2 (1%) positions. The presence of higher phosphate monoesters in potato starch affects its swelling behavior because the negatively charged phosphate group causes repulsion between adjacent amylopectin chains, resulting in rapid hydration and large swelling (Waterschoot et al., 2015). Potato starch has a higher swelling power (168 g/g) at 84 °C compared to wheat starch (swelling power = 40 g/g) (Anggraini et al., 2009; Waterschoot et al., 2015).

Many agro-industrial wastes or wastewaters contain large concentrations of degradable sugars, which are suitable for one-stage processes like fermentation or two-stage sequential processes: a first-stage for H₂ and lactic acid production under the CLF conditions at 80 °C and can be combined with a second methane production stage at mesophilic conditions (Masset et al., 2012; Pradhan et al., 2015). *T. neapolitana* is a tolerant microorganism which can thrive in diverse environmental and operating conditions (Dipasquale et al., 2015). Due to its metabolic flexibility, *T. neapolitana* can be used for simultaneous H₂ and lactic acid synthesis without affecting the H₂ production (Dipasquale et al., 2014).

Renewable energy sources such as starch-based substrates are abundant, cheap and reliable feedstocks found in the agro-industrial residues and food wastes

(Vendruscolo, 2014). Use of starch-based substrates enable for the cost effective H₂ and lactic acid production under CLF conditions. The CLF-based fermentation is a promising technology, however several biological challenges such as clearly understanding the CLF mechanism and adequately the engineering challenges before it becomes a practical reality.

7.5 Conclusions

Fermentation of starch by *T. neapolitana* for the production of H₂ and lactic acid under CLF conditions was investigated. The potato starch fermentation exhibited better performance with respect to H₂ (20% higher) and lactic acid (260% higher) production compared to fermentation of wheat starch under similar operating conditions. The lactic acid production from the potato starch fermentation under CLF conditions is higher and comparable to the previous studies reported till to date using a different type of carbon source, i.e. glucose. In addition, the CLF-based kinetic model simulation and prediction can provide a solid foundation for design and operation of the CLF-based fermentation processes using a variety of carbon sources.

References

- Akutsu, Y., Li, Y.Y., Tandukar, M., Kubota, K., Harada, H. 2008. Effects of seed sludge on fermentative characteristics and microbial community structures in thermophilic hydrogen fermentation of starch. *International Journal of Hydrogen Energy*, **33**, 6541-6548.
- Alcazar-Alay, S.C., Meireles, M.A.A. 2015. Physicochemical properties, modifications and applications of straches from different botanical sources. *Food Science and Technology*, **35**, 215-236.
- Anggraini, V., Sudarmonowati, E., Hartati, N.S., Suurs, L., Visser, R.G.F. 2009. Characterization of cassava starch attributes of different genotypes. *Starch*, **61**, 472-481.
- Argun, H., Kargi, F. 2010. Bio-hydrogen production from ground wheat starch by continuous combined fermentation using annular-hybrid bioreactor. *International Journal of Hydrogen Energy*, **35**, 6170-6178.
- Bao, M., Su, H., Tan, T. 2012. Biohydrogen production by dark fermentation of starch using mixed bacterial cultures of *Bacillus sp* and *Brevumdimonas sp*. *Energy and Fuels*, **26**, 5872-5878.
- Batstone, D.J., Keller, J., Angelidaki, I., Kalyuzhnyi, S.V., Pavlostathis, S.G., Rozzi, A. 2002. Anaerobic digestion model No. 1. *IWA Scientific and Technical Report* **13**.

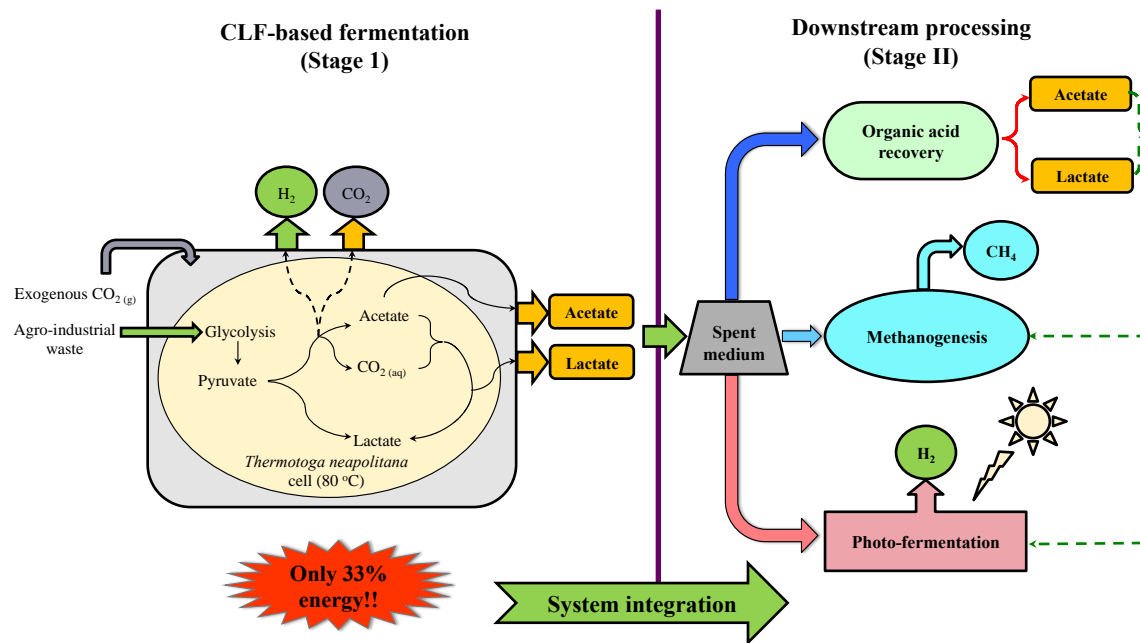
- Chen, S.D., Lee, K.S., Lo, Y.C., Chen, W.M., Wu, J.F., Lin, C.Y., Chang, J.S. 2008. Batch and continuous biohydrogen production from starch hydrolysate by *Clostridium* species. *International Journal of Hydrogen Energy*, **33**, 1803-1812.
- d'Ippolito, G., Dipasquale, L., Fontana, A. 2014. Recycling of carbon dioxide and acetate as lactic acid by the hydrogen-producing bacterium *Thermotoga neapolitana*. *ChemSusChem*, **7**, 2678-83.
- d'Ippolito, G., Dipasquale, L., Vella, F.M., Romano, I., Gambacorta, A., Cutignano, A., Fontana, A. 2010. Hydrogen metabolism in the extreme thermophile *Thermotoga neapolitana*. *International Journal of Hydrogen Energy*, **35**, 2290-2295.
- Dipasquale, L., Adessi, A., d'Ippolito, G., Rossi, F., Fontana, A., De Philippis, R. 2015. Introducing capnophilic lactic fermentation in a combined dark-photo fermentation process: a route to unparalleled hydrogen yields. *Applied Microbiology and Biotechnology*, **99**, 1001-10.
- Dipasquale, L., d'Ippolito, G., Fontana, A. 2014. Capnophilic lactic fermentation and hydrogen synthesis by *Thermotoga neapolitana*: An unexpected deviation from the dark fermentation model. *International Journal of Hydrogen Energy*, **39**, 4857-4862.
- Donoso-Bravo, A., Mailier, J., Martin, C., Rodriguez, J., Aceves-Lara, C.A., Wouwer, A.V. 2011. Model selection, identification and validation in anaerobic digestion: A review. *Water Research*, **45**, 5347-5364.
- Dubois, M., Gilles, K.A., Hamilton, J.K., Rebers, P.A., Smith, F. 1956. Colorimetric method for determination of sugars and related substances. *Analytical Chemistry*, **28**, 350-6.
- Hallenbeck, P.C., Ghosh, D. 2009. Advances in fermentative biohydrogen production: the way forward? *Trends in Biotechnology*, **27**, 287-297.
- Hinken, L., Huber, M., Weichgrebe, D., Rosenwinkel, K.H. 2014. Modified ADM1 for modelling an UASB reactor laboratory plant treating starch wastewater and synthetic substrate load tests. *Water Research*, **64**, 82-93.
- Huang, L.P., Jin, B., Lant, P., Zhou, J. 2005. Simultaneous saccharification and fermentation of potato starch wastewater to lactic acid by *Rhizopus oryzae* and *Rhizopus arrhizus*. *Biochemical Engineering Journal*, **23**, 265-276.
- Kongjan, P., S, O.T., Kotay, M., Min, B., Angelidaki, I. 2010. Biohydrogen production from wheat straw hydrolysate by dark fermentation using extreme thermophilic mixed culture. *Biotechnol Bioeng*, **105**(5), 899-908.
- Lee, H.S., Salerno, M.B., Rittmann, B.E. 2008. Thermodynamic evaluation on hydrogen production in glucose fermentation. *Environmental Science and Technology*, **42**, 2401-2407.
- Li, S., SZhang, Y., Wei, Y., Zhang, W., Zhang, B. 2014. Thermal, pasting and gel textural properties of commercial starches from different botanical sources. *Bioprocessing and Biotechniques*, **4**, 161.

- Lin, C.Y., Chang, C.C., Hung, C.H. 2008. Fermentative hydrogen production from starch using natural mixed cultures. *International Journal of Hydrogen Energy*, **33**, 2445-2453.
- Mars, A.E., Veuskens, T., Budde, M.A.W., van Doeveren, P.F.N.M., Lips, S.J., Bakker, R.R., de Vrije, T., Claassen, P.A.M. 2010. Biohydrogen production from untreated and hydrolyzed potato steam peels by the extreme thermophiles *Caldicellulosiruptor saccharolyticus* and *Thermotoga neapolitana*. *International Journal of Hydrogen Energy*, **35**, 7730–7737.
- Masset, J., Calusinska, M., Hamilton, C., Hiligsmann, S., Joris, B., Wilmotte, A., Thonart, P. 2012. Fermentative hydrogen production from glucose and starch using pure strains and artificial co-cultures of *Clostridium* spp. *Biotechnology for Biofuels*, **5**, 35.
- Ngo, T.A., Bui, H.T.V. 2013. Biohydrogen production using immobilized cells of hyperthermophilic eubacterium *Thermotoga neapolitana* on porous glass beads. *Journal of Technology Innovations in Renewable Energy*, **2**, 231-238.
- Ngo, T.A., Nguyen, T.H., Bui, H.T.V. 2012. Thermophilic fermentative hydrogen production from xylose by *Thermotoga neapolitana* DSM 4359. *Renewable Energy*, **37**, 174-179.
- Orozco, R.L., Redwood, M.D., Leeke, G.A., Bahari, A., Santos, R.C.D., Macaskie, L.E. 2012. Hydrothermal hydrolysis of starch with carbon dioxide and detoxification of the hydrolysates with activated carbon for bio-hydrogen fermentation. *International Journal of Hydrogen Energy*, **37**, 6545-6553.
- Pradhan, N., Dipasquale, L., d’Ippolito, G., Fontana, A., Panico, A., Pirozzi, F., Lens, P.N.L., Esposito, G. 2016a. Model development and experimental validation of capnophilic lactic fermentation and hydrogen synthesis by *Thermotoga neapolitana*. *Water Research*, **99**, 225-234.
- Pradhan, N., Dipasquale, L., d’Ippolito, G., Fontana, A., Panico, A., Lens, P.N.L., Pirozzi, F., Esposito, G. 2016b. Kinetic modeling of fermentative hydrogen production by *Thermotoga neapolitana*. *International Journal of Hydrogen Energy*, **41**, 4931-4940.
- Pradhan, N., Dipasquale, L., d’Ippolito, G., Panico, A., Lens, P.N.L., Esposito, G., Fontana, A. 2015. Hydrogen production by the thermophilic bacterium *Thermotoga neapolitana*. *International Journal of Molecular Sciences*, **16**, 12578-12600.
- Ribes, J., Keesman, K., Spanjers, H. 2004. Modelling anaerobic biomass growth kinetics with a substrate threshold concentration. *Water Research*, **38**, 4502-10.
- Singh, N., Singh, J., Kaur, L., Sodhi, N.S., Gill, B.S. 2003. Morphological, thermal and rheological properties of starches from different botanical sources. *Food Chemistry*, **81**, 219-231.
- Thauer, R. 1977. Limitation of microbial hydrogen formation via fermentation. *Microbial Energy Conversion*, 201-204.

- Thauer, R.K., Jungerman, K., Decker, K. 1977. Energy conservation in chemotrophic anaerobic bacteria. *Bacteriological Reviews*, **41**, 100-180.
- Vendruscolo, F. 2014. Starch: a potential substrate for biohydrogen production. *International Journal of Energy Research*, **39**, 293-302.
- Waterschoot, J., Gomand, S.V., Fierens, E., Delcour, J.A. 2015. Production, structure, physicochemical and functional properties of maize, cassava, wheat, potato and rice starches. *Starch*, **67**, 14-29.
- Willquist, K., van Niel, E.W.J. 2012. Growth and hydrogen production characteristics of *Caldicellulosiruptor saccharolyticus* on chemically defined minimal media. *International Journal of Hydrogen Energy*, **37**, 4925-4929.
- Yuan, X.Z., Shi, X.S., Yuan, C.X., Wang, Y.P., Qiu, Y.L., Guo, R.B., Wang, L.S. 2014. Modeling anaerobic digestion of blue algae: Stoichiometric coefficients of amino acids acidogenesis and thermodynamics analysis. *Water Research*, **49**, 113-123.

7.6 System integration for downstream processing

Dark fermentative pathways can produce at most 4 mol H₂/mol of glucose thereby recovering only 33% of the total energy and the remaining in the form of organic acids or alcohols (Thauer, 1977). Energy can be recovered through different system integrations techniques, each of them has its distinct advantages and disadvantages (Hallenbeck, 2009). The organic feedstocks can be treated by one-stage fermentation (H₂) or two-stage processes (methanogenesis, photo-fermentation and recovery of organic chemicals) (Thi et al., 2016). The important two-stage processes are (i) dark fermentation and recovery of organic chemicals, (ii) dark fermentation and methanogenesis and (iii) dark- and photo-fermentation (Scheme I).



Scheme I. Proposed two-stage systems for complete conversion of substrate through system integration.

A two-stage process is always advantageous compared to a one-stage process in terms of net energy recovery. Anaerobic digestion of organic waste is a cost effective and a matured technology, which has dual benefits as waste valorization and simultaneous energy generation. The photo-fermentative process can give higher H₂ yields compared to the dark fermentative process, but the former one depends on light, thus potentially adding to the extra cost, whereas the yield of the later one is affected due to limited oxidative phosphorylation or thermodynamic barriers (Hallenbeck & Liu, 2016). The

CLF based fermentation process with *T. neapolitana* (Dipasquale et al., 2014; Pradhan et al., 2016a; Pradhan et al., 2016b) offers multiple tail-end system integration options, where the fermentation broth can be used for lactic acid recovery, CH₄ production or photo-fermentation (Scheme I). Several previous studies have investigated methane production and photo-fermentation post treatment process after dark fermentation, so in this study lactic acid recovery was performed as a post treatment process using adsorption and anion exchange mechanisms (Chapter 8).

References

- Dipasquale, L., d'Ippolito, G., Fontana, A. 2014. Capnophilic lactic fermentation and hydrogen synthesis by *Thermotoga neapolitana*: An unexpected deviation from the dark fermentation model. *International Journal of Hydrogen Energy*, **39**, 4857-4862.
- Hallenbeck, P.C. 2009. Fermentative hydrogen production: Principles, progress, and prognosis. *International Journal of Hydrogen Energy*, **34**, 7379-89.
- Hallenbeck, P.C., Liu, Y. 2016. Recent advances in hydrogen production by photosynthetic bacteria. *International Journal of Hydrogen Energy*, **41**, 4446-54.
- Pradhan, N., Dipasquale, L., d'Ippolito, G., Fontana, A., Panico, A., Pirozzi, F., Lens, P.N.L., Esposito, G. 2016a. Model development and experimental validation of capnophilic lactic fermentation and hydrogen synthesis by *Thermotoga neapolitana*. *Water Research*, **99**, 225-234.
- Pradhan, N., Dipasquale, L., d'Ippolito, G., Fontana, A., Panico, A., Lens, P.N.L., Pirozzi, F., Esposito, G. 2016b. Kinetic modeling of fermentative hydrogen production by *Thermotoga neapolitana*. *International Journal of Hydrogen Energy*, **41**, 4931-4940.
- Thauer, R. 1977. Limitation of microbial hydrogen formation via fermentation. *Microbial Energy Conversion*, 201-204.
- Thi, N.B.D., Lin, C.Y., Kumar, G. 2016. Waste-to-wealth for valorization of food waste to hydrogen and methane towards creating a sustainable ideal source of bioenergy. *Journal of Cleaner Production*, **122**, 29-41.

Chapter 8

Lactic acid recovery

This chapter has been submitted as:

Pradhan, N., Rene, E.R., Panico, A., Dipasquale, L., d'Ippolito, G., Fontana, A., Lens, P.N.L., Esposito, G. 2017. Adsorption behaviour of lactic acid on granular activated carbon and anionic resins: Thermodynamics, isotherms and kinetic studies. *Energies*.

Chapter 8: Lactic acid recovery

Abstract

Solid-liquid extraction (adsorption or ion exchange) is a promising approach for the *in situ* separation of organic acids from fermentation broths. In this study, a diluted concentration of lactic acid (< 10 g/L) separation from a model fermentation broth by granular activated carbon (GAC) as well as weak (Reillex[®] 425 or RLX425) and strong (Amberlite[®] IRA-400 or AMB400) base anion exchange resins under various operating conditions was experimentally investigated. Thermodynamic analysis showed that the best lactic acid adsorption performances were obtained at a pH below the pK_a value of lactic acid (i.e. 3.86) for GAC and RLX425 by physical adsorption mechanism and above the pK_a value for the AMB400 resin by an ion exchange mechanism, respectively. The adsorption capacity for GAC (38.2 mg/g) was the highest, followed by AMB400 (31.2 mg/g) and RLX 425 (17.2 mg/g). As per the thermodynamic analysis the lactic acid adsorbed onto GAC and RLX425 through physical adsorption mechanism, whereas the lactic acid adsorbed onto AMB400 with an ion exchange mechanism. The Langmuir adsorption isotherm model ($R^2 > 0.96$) and the pseudo-second order kinetic model ($R^2 \sim 1$) fitted well to the experimental data than the other models tested. Postulating the conditions for the real fermentation broth (pH: 5-6.5 and temperature: 30-80 °C), the resin AMB400 represents an ideal candidate for the *in situ* extraction of lactic acid during fermentation.

Key words: Lactic acid; Adsorption; Kinetics; Isotherms; Thermodynamics; Ion Exchange.

8.1 Introduction

Lactic acid (2-hydroxypropionic acid) is an important commercial chemical due to its application in food, medical, pharmaceutical, packaging and textile industries. In the past decades, the demand for lactic acid has been significantly high, especially for its application in biodegradable polymers, i.e. polylactic acid (PLA), which has a potential to replace traditional commodity plastics. PLA-based plastics have some unique features such as high tensile strength, stiffness and resistance to fats and oils compared to traditional plastic materials; however, they require further improvement in some properties and characteristics such as viscosity, thermal stability and production cost (Hamad et al., 2011). The properties of PLA can be improved by blending with several other synthetic polymers (e.g. polystyrene, polyethylene or polypropylene) and biopolymers (e.g. thermoplastic starch, rubbers or poly(3-hydroxybutyrate)) to obtain novel biodegradable materials with lower cost and higher durability compared to the traditional plastic materials (Hamad et al., 2011; Hamad et al., 2010). However, extraction, purification and continuous supply of lactic acid as raw material from fermentation processes is a major challenge because of its highly hydrophilic structure and the lack of efficient low cost purification techniques (Bayazit et al., 2011).

Lactic acid has a chiral carbon atom and exists in two isomeric forms, i.e. L (+) and D (-). Industrially preferred L (+)lactic acid can be manufactured either by the chemical synthesis of acetaldehyde or by fermentation processes, where the latter accounts for ~ 90% of the global lactic acid production (Joglekar et al., 2006). Traditionally, lactic acid is produced by homolactic fermentation processes using pure cultures of lactic acid bacteria belonging to the genus *Lactobacillus* (Martinez et al., 2013). Recently, a heterolactic fermentation process with a new metabolic pathway named capnophilic (CO₂-led) lactic fermentation (CLF) was found to be present in the hyperthermophilic marine bacterium *Thermotoga neapolitana* (Dipasquale et al., 2014). Under CLF conditions, both hydrogen and lactic acid are synthesized simultaneously unlike in the classic dark fermentation processes (Dipasquale et al., 2014; Pradhan et al., 2016a; Pradhan et al., 2016b; Pradhan et al., 2015). *T. neapolitana* fermentation takes place on a wide range of carbohydrate-rich substrates at 80 °C (353.15 K) and pH 6.5. However, the lactic acid concentration in the *T. neapolitana* fermentation broth is in the lower range (2-10 g/L) compared to lactic acid fermentation (50-150 g/L lactic acid) by

homolactic fermentation processes (Bernardo et al., 2016; Martinez et al., 2013; Sugiyama et al., 2016).

Several downstream processing techniques have been used to recover lactic acid from the fermentation broth, *e.g.* calcium lactate crystallization, ion-exchange, adsorption, esterification-distillation/hydrolysis, membrane extraction and electro-dialysis (Dethe et al., 2006; Takatsuji et al., 1999; Wasewar, 2005; Yi et al., 2008). Among these techniques, adsorption by activated carbon and anionic resins are suitable for fermentation broths with low concentrations of lactic acid, especially from dark- and CLF-based fermentation (Evangelista et al., 1994; Moldes et al., 2003). A wide range of anionic resins are commercially available with various functional groups and support matrices, which makes the adsorption process more flexible under various operating conditions. The adsorption capacity and efficiency are influenced by various factors such as the properties of the adsorbent (porosity, surface area, particle size and functional group), the adsorbate (polarity, pK_a , molecular weight, structure and solute concentration) and the operating conditions (contact time, pH, temperature and mixing speed) (Uslu, 2009; Yousuf et al., 2016).

Several adsorbents such as Amberlite[®] IRA-67 (Yousuf et al., 2016), IRA-92 (Tong et al., 2004), IRA-400 (Cao et al., 2002), IRA-425 (Antonio et al., 2000) and activated carbon (Gao et al., 2011; Yousuf et al., 2016) have been studied for lactic or organic acids adsorption from a fermentation broth at room temperature. Anionic resins are non-toxic to microorganisms and can thus be used directly in the fermenter (Nielsen et al., 2010). Activated carbon has a wider application in the field of water and wastewater treatment due to its highly porous structure with a large surface area (~ 1100 m²/g). Granular activated carbon (GAC) also shows specific affinity towards organic acids like acetic, lactic and butyric acid because of its non-polar nature at different pH conditions (Gao et al., 2011).

In this paper, the effects of contact time, initial pH, adsorbent dose and lactic acid concentration on the adsorption of lactic acid from a model fermentation broth by GAC, as well as weakly-basic (Reillex[®] 425) and strongly-basic (Amberlite[®] IRA-400) anion exchange resins were investigated in batch equilibrium studies. For the first time, the thermodynamic characteristics of lactic acid adsorption onto adsorbents were investigated systematically as a function of temperature. To understand the adsorbate-

adsorbent mechanism and kinetics, the lactic acid adsorption data were analysed using suitable adsorption isotherms and kinetic models. These results enable for the *in situ* extraction of lactic acid during hyperthermophilic *T. neapolitana* or similar dark fermentation processes.

8.2 Materials and methods

8.2.1 Adsorbents

Three types of adsorbents were studied for the extraction of lactic acid: (i) Norit[®] GAC 1240EN with a particle size of 10-40 mesh and a moisture content < 5% (source: www.cabotcorp.com), (ii) Reillex[®] 425 (Poly(4-vinylpyridine)), hereafter referred as RLX425, a weakly basic anion exchange resin cross-linked with 25% divinylbenzene, with pyridine as the functional group, a particle size of 20-50 mesh and a moisture content in the range of 50-75% (source: www.sigmaaldrich.com) and (iii) Amberlite[®] IRA-400 (Cl⁻), hereafter referred as AMB400, a strongly basic anion exchange resin cross-linked with 8% styrene/divinylbenzene (gel), with quaternary ammonium as the functional group, a particle size of 20-25 mesh and a moisture content in the range of 40-47% (source: www.sigmaaldrich.com). The analytical grade anionic resins were purchased from Sigma-Aldrich (Milan, Italy) and used without any pre-treatment.

8.2.2 Batch adsorption tests

The batch equilibrium experiments were conducted in a temperature-controlled (303.15-353.15 K) environment, either on an orbital shaker (INNOVA 2100, New Brunswick Scientific, New Jersey, USA) at a speed of 180 rpm or a shaking thermostatic water bath (GFL1083, GFL, Burgwedel, Germany) as per [Dethe et al. \(Dethe et al., 2006\)](#). The model fermentation broth was prepared from an analytical grade 88% lactic acid stock solution and demineralized water as described by [Moldes et al. \(Moldes et al., 2003\)](#). The initial pH (2.0-6.5) of the bulk solution was adjusted by either adding 6.0 M NaOH or 6.0 M HCl. 25.0 mL serum bottles with screw cap containing 5.0 mL of model fermentation broth (4.5 g/L lactic acid) and 0.5 g adsorbent (or 10% *w/v*) were used for all the batch adsorption studies unless stated otherwise. The adsorbent GAC and RLX425 were studied at pH 2.0, whereas AMB400 was studied at pH 5.0. The model fermentation broth was allowed to equilibrate for 4 h on an orbital

shaker and maintained at 303.15 K. All the batch adsorption experiments were performed in duplicate by employing individual serum bottles for each data point.

8.2.3 Experimental design

The lactic acid adsorption study comprised of 6 different series of experiments, investigating the effect of (i) contact time, (ii) initial pH, (iii) adsorbent dose, (iv) initial lactic acid concentration, (v) temperature and (vi) batch kinetic studies on the adsorption process. The effect of contact time was tested for a period of 24 h by using a model fermentation broth without initial pH (~ 2.35) corrections with samples withdrawn at regular time intervals (0, 2, 4, 6, 8 and 24 h). The adsorption capacity and efficiency (i.e. % lactic acid adsorbed onto the adsorbent) under equilibrium conditions were calculated using Eq. (8.1) and Eq. (8.2), respectively:

$$q_e = \frac{(C_0 - C_e)V}{m} \quad (8.1)$$

$$E = \frac{C_0 - C_e}{C_0} \times 100 \quad (8.2)$$

where q_e = amount of adsorbate in the adsorbent at equilibrium (mg/g), E = lactic acid recovery efficiency (%), C_0 = initial concentration of lactic acid (mg/L), C_e = equilibrium concentration of lactic acid in the solution (mg/L), V = volume of the solution (L) and m = mass of the adsorbent (g).

The effect of the initial pH was tested at 5 different initial pH (2.0, 2.35, 3.86, 5.0 and 6.5) conditions, both above and below the pK_a (3.86) value of lactic acid. The degree of ionization of lactic acid depends on the pH and can be calculated using Eq. (8.3):

$$\%Ionized = \frac{100}{1 + \exp(pK_a - pH)} \quad (8.3)$$

The effect of the adsorbent dose was tested to determine the appropriate adsorbent dose (w/v basis) by varying the dose from 5 to 30% (w/v) with an increment of 5% in each step. The effect of the lactic acid concentration was tested for 9 different lactic acid concentrations, varying between 1.5 and 36.3 g/L. This range was particularly selected to represent the lactic acid production from various homolactic or heterolactic fermentation processes with low concentration of lactic acid in the fermentation broth (Pradhan et al., 2016b; Yousuf et al., 2016).

Lactic acid production takes place at various temperature conditions. The lactic acid adsorption was tested at different temperatures between 303.15 and 353.15 K. The thermodynamic parameters including Gibbs free energy (ΔG^0), enthalpy (ΔH^0) and entropy (ΔS^0) are the indicators of the adsorption process and their values indicate the spontaneity and favourability of the process (Gao et al., 2010; Zhou et al., 2016). The ΔG^0 can be calculated from Eq. (8.4), whereas ΔH^0 and ΔS^0 can be calculated by using the van't Hoff equation from the slope and intercept of the linear plot of $\ln K_L$ versus $1/T$ as shown in Eq. (8.5).

$$\Delta G^0 = -RT \ln K_L \quad (8.4)$$

$$\ln K_L = \frac{-\Delta G^0}{RT} = -\frac{\Delta H^0}{RT} + \frac{\Delta S^0}{R} \quad (8.5)$$

where K_L = Langmuir isotherm constant (L/mol), R = universal gas constant (8.31 J/(mol K)), T = temperature (kelvin), ΔG^0 = Gibbs free energy (kJ/mol), ΔH^0 = enthalpy (kJ/mol) and ΔS^0 = entropy (kJ/(mol K)).

8.2.4 Analytical methods

The initial and final concentrations of lactic acid were measured by ICS-1100 (Dionex, Thermo Fisher Scientific Inc., USA) using an IonPac[®] AS4A-SC (solvent compatible) carbonate-selective anion exchange analytical column (Rich et al., 1980). The mobile phase had 1.7 mM NaHCO₃ and 1.8 mM Na₂CO₃ with a flow rate of 0.5 mL/min. Before analysis, the pH of all the samples was adjusted in the range of 5.0 to 8.0 by using either 6.0 M HCl or 6.0 M NaOH.

8.2.5 Adsorption isotherm and kinetics

8.2.5.1 Lactic acid adsorption isotherms

The batch equilibrium results of different initial lactic acid concentration experiments at 303.15 K were used for the isotherm study. In this study, we chose three commonly used isotherm models (i.e. Langmuir (Eq. (I)), Freundlich (Eq. (II)) and Temkin (Eq. (III))) to describe the lactic acid adsorption process (Gao et al., 2010; Pezoti et al., 2016). The linear and non-linear forms of the isotherm model equations are presented in Table 8.1 (Foo & Hameed, 2010).

The Langmuir adsorption isotherm model assumes homogeneous and monolayer adsorption with no lateral interaction or steric hindrances between the adsorbate molecules (Foo & Hameed, 2010). The nature of adsorption in the Langmuir adsorption isotherm model is represented by a dimensionless constant known as the separation factor (R_L), $R_L = 1/(1 + (K_L \times C_0))$, where K_L = Langmuir isotherm constant (L/mg), C_0 = initial concentration of lactic acid (mg/L), $R_L > 1$ (unfavourable), $R_L = 1$ (linear), $R_L = 0$ (irreversible) and $0 < R_L < 1$ (favourable) (Webber & Chakkravorti, 1974).

On the other hand, the Freundlich isotherm model describes a non-ideal and reversible adsorption process, which is applied to explain the multilayer adsorption onto a heterogeneous adsorbent surface (Chen, 2015). The Temkin isotherm model assumes that the heat of adsorption of all the molecules in the layer would decrease linearly rather than logarithmically (Foo & Hameed, 2010).

Table 8. 1 List of non-linear and linear forms of adsorption isotherm model equations.

Isotherms	Non-linear form	Linear form	Plot	Equation
Langmuir	$q_e = \frac{q_m K_L C_e}{1 + K_L C_e}$	$\frac{1}{q_e} = \frac{1}{q_m} + \frac{1}{K_L q_m C_e}$	$\frac{1}{q_e}$ vs $\frac{1}{C_e}$	(I)
Freundlich	$q_e = K_F C_e^{1/n}$	$\log q_e = \log K_F + \frac{1}{n} \log C_e$	$\log q_e$ vs $\log C_e$	(II)
Temkin	$q_e = \frac{RT}{K_T} \ln A_T C_e$	$q_e = \frac{RT}{K_T} \ln A_T + \frac{RT}{K_T} \ln C_e$	q_e vs $\ln C_e$	(III)

Notes:

q_e = amount of adsorbate in the adsorbent at equilibrium (mg/g), C_e = equilibrium concentration of lactic acid in the solution (mg/L), q_m = maximum monolayer coverage capacities (mg/g), K_L = Langmuir isotherm constant (L/mg), n = adsorption intensity, K_F = Freundlich isotherm constant (mg/g) (L/g)ⁿ, A_T = Temkin isotherm equilibrium binding constant (L/g), K_T = Temkin isotherm constant, R = universal gas constant (8.314 J/(mol K)) and T = temperature (K).

Source: Modified from Foo and Hameed (2010), Pezoti et al. (2016) and Chen (2015).

8.2.5.2 Lactic acid adsorption kinetics

Lactic acid adsorption kinetics were studied for a period of 8 h in order to understand the adsorption mechanism and the binding properties of lactic acid onto the adsorbents. The samples were periodically collected from the serum bottles and analysed for residual lactic acid concentrations. The kinetic models of pseudo-first order (Eq. (A)), pseudo-second order (Eq. (B)) and Elovich (Eq. (C)) were investigated in order to describe the adsorption dynamics of lactic acid onto the GAC, RLX425 and AMB400 (Pezoti et al., 2016). The differential and linear forms of adsorption kinetic equations are shown in Table 8.2 (Shi et al., 2013; Uslu, 2009).

Table 8. 2 List of differential and linear forms of adsorption kinetic model equations.

Kinetic model	Differential form	Linear form	Plot	Equation
Pseudo-first order	$\frac{dq_t}{dt} = K_1(q_e - q_t)$	$\log(q_e - q_t) = \log q_e - \left(\frac{K_1}{2.303}\right)t$	$\log(q_e - q_t) vs t$	(A)
Pseudo-second order	$\frac{dq_t}{dt} = K_2(q_e - q_t)^2$	$\frac{t}{q_t} = \frac{1}{K_2q_e^2} + \frac{1}{q_e}t$ $= \frac{1}{h_0} + \frac{1}{q_e}t$	$\frac{t}{q_t} vs t$	(B)
Elovich	$\frac{dq_t}{dt} = \alpha e^{-\beta q_t}$	$q_t = \beta \ln \alpha \beta + \ln t$	$q_t vs \ln t$	(C)

Notes:

K_1 = pseudo-first order rate constant (1/min), q_e = amount of adsorbate in the adsorbent at equilibrium (mg/g), t = time (min), q_t = adsorption at any given point of time (mg/g), K_2 = pseudo-second order rate constant (mg/g/min), h_0 = initial adsorption rate (1/min), β = desorption constant (g/mg) and α = initial adsorption rate (mg/g/min).

8.3 Results

8.3.1 Effect of contact time, pH, adsorbent dose and lactic acid concentration on lactic acid adsorption

The effect of the contact time on the adsorption of lactic acid by GAC, RLX425 and AMB400 was studied for a period of 24 h with an initial lactic acid concentration of 4.5 g/L without pH (~ 2.35) correction. Fig. 8.1a shows the lactic acid recovery

efficiency at various contact times onto the adsorbents. The uptake of lactic acid by the adsorbents at equilibrium was calculated from the residual lactic acid concentration. The contact time experiments showed that the adsorption reached its equilibrium between 2 to 6 h with lactic acid adsorbed onto GAC (29 mg lactic acid/g adsorbent), RLX425 (18 mg lactic acid/g adsorbent) and AMB400 (10 mg lactic acid/g adsorbent) from an initial concentration of 4.5 g lactic acid/L. From this batch experiment, a contact time of 4 h was selected for the subsequent experiments.

Fig. 8.1b shows the effect of different initial pH values (2.0-6.5) on lactic acid adsorption onto GAC, RLX425 and AMB400. The pH change and the degree of ionization induces the protonation and deprotonation of lactic acid and thus affects the adsorption rate. The recovery efficiency of lactic acid onto GAC decreased significantly from 81.2 (± 1.4)% at pH 2.0 to 24.7 (± 1.9)% at pH 6.5 and a similar trend was also observed for RLX425: the recovery efficiency decreased from 37.9 (± 0.5)% at pH 2.0 to 6.5 (± 0.2)% at pH 6.5 (Fig. 8.1b). In the case of AMB400, the recovery efficiency increased steadily from 19.8 (± 2.7)% at pH 2.0 to 51.1 (± 1.1)% at pH 5.0 and then decreased slightly to 46.6 (± 1.1)% at pH 6.5. The experimental results confirmed that both GAC and RLX425 show selectivity at a pH (2.0) below the pK_a (3.86) value and AMB400 at a pH (5.0) above the pK_a value. The degree of ionization of lactic acid in the bulk solution was calculated from the relation between the pK_a value and the pH of the solution. The degree of ionization was found to be 13.5, 18.1, 24.2 and 6.7% at, respectively, pH 2.0, 2.35, 5.0 and 6.5.

Fig. 8.1c shows the lactic acid recovery efficiency with different adsorbent dose in the range of 5 to 30% (w/v). The increase in GAC dose from 5 to 30% (w/v) increased the lactic acid recovery efficiency from 79.0 (± 0.5) to 90.1 (± 0.3)%. Similarly, for RLX425, the increase of adsorbent dose from 5 to 30% (w/v) increased the lactic acid recovery efficiency from 27.8 (± 0.7) to 62.9 (± 3.9)%. Concerning AMB400, the increase of dose from 5 to 30% (w/v) increased the lactic acid recovery efficiency from 41.7 (± 1.4) to 73.1 (± 1.1)%. The experimental results with different adsorbent dose showed that 10-15% (w/v) adsorbent dose has a good lactic acid recovery (%), and thus, 10% (w/v) adsorbent dose was selected for all the batch adsorption experiments.

The binding capacity of lactic acid was studied by varying the initial lactic acid concentration in the range of 1.5 to 36.3 g/L as shown in Fig. 8.1d. The lactic acid

recovery efficiency decreased from 83.2 (± 0.9) to 38.2 (± 0.2)% for GAC when the lactic acid concentration increased from 1.5 g/L to 36.3 g/L. However, the adsorption capacity (q_e) with GAC increased sharply from 12 mg lactic acid/g adsorbent (at 1.5 g/L lactic acid) to 162 mg lactic acid/g adsorbent (at 36.3 g/L lactic acid). Similarly, for RLX425, the lactic acid recovery efficiency decreased from 41.9 (± 6.6)% (at 1.5 g/L lactic acid) to 19.1 (± 0.5)% (at 36.3 g/L lactic acid) with a maximum q_e value of 79 mg lactic acid/g adsorbent (at 36.3 g/L lactic acid). The recovery efficiency for AMB400 decreased from 58.8 (± 2.6) to 20.2 (± 0.1)%, with an increase in the lactic acid concentration from 1.5 g/L to 36.3 g/L and the maximum q_e value was found to be 73 mg lactic acid/g adsorbent at a lactic acid concentration of 36.3 g/L.

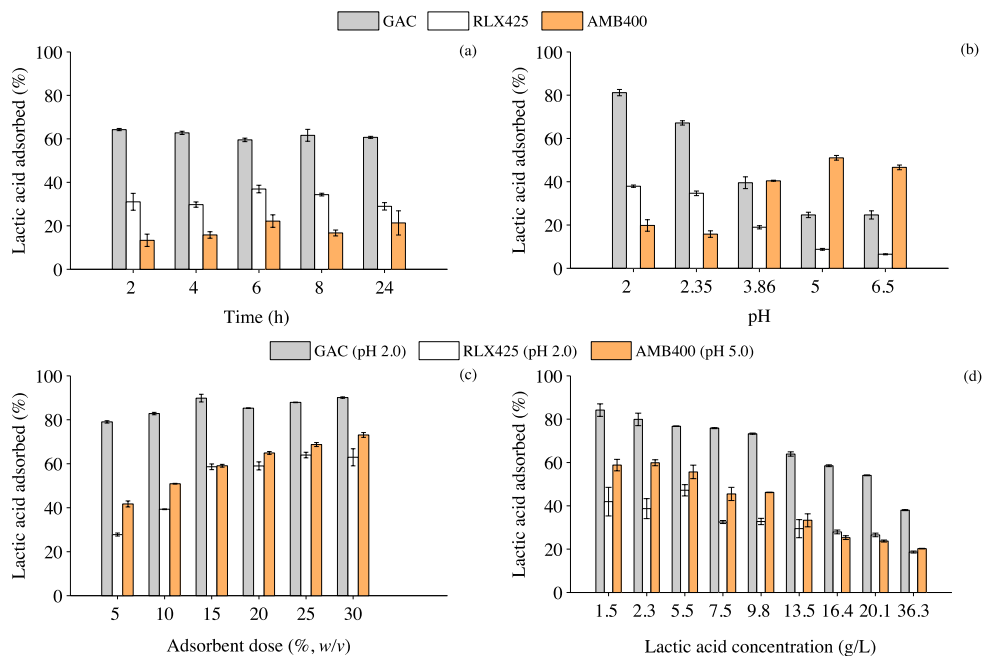


Fig. 8. 1 Effect of lactic acid adsorption onto GAC, RLX425 and AMB400 at 303.15 K. (a) contact time (0-24 h) with 4.5 g/L of lactic acid in the bulk solution without initial pH correction and an adsorbent dose of 10% (w/v), (b) different initial pH (2.0-6.5) with 4.5 g/L of lactic acid in the bulk solution and an adsorbent dose of 10% (w/v), (c) various adsorbent doses (5-30%) with 4.5 g/L of lactic acid in the bulk solution accompanied by initial pH corrections and (d) different initial lactic acid concentrations (1.5-36.3 g/L) accompanied by initial pH correction with an adsorbent dose of 10% (w/v).

8.3.2 Effect of temperature on lactic acid adsorption

The effect of temperature (303.15 to 353.15 K) on lactic acid adsorption onto the adsorbents is shown in Fig. 8.2a. The temperature was raised to 353.15 K to test the effectiveness of the adsorbents to adsorb lactic acid from a model fermentation broth representing *T. neapolitana* fermentation, which operates at 353.15 K (or 80 °C). Both GAC and RLX425 exhibited a decrease in q_e and recovery efficiency values for temperatures higher than 313.15 K. Increasing the temperature from 303.15 to 353.15 K decreased the adsorption capacity of GAC and RLX425 by ~13% and 50%, respectively. When the temperature exceeded 313.15 K, desorption of lactic acid was observed for both GAC and RLX425. In contrast, the q_e (24 mg lactic acid/g adsorbent) and recovery efficiency (~ 51%) of AMB400 remained nearly constant throughout the tested temperature range (303.15-353.15 K), thus making the resin more suitable than GAC and RLX425.

The thermodynamic parameters for lactic acid adsorption were calculated from Fig. 8.2b by using the van't Hoff equation. The thermodynamic model assumed (i) fluid density and viscosity are constant and (ii) isothermal operation during the adsorption of lactic acid. The corresponding ΔG^0 values are shown in Table 8.3. The results clearly show that the adsorption process by both GAC and RLX425 is exothermic (i.e. $\Delta H^0 < 0$ and $\Delta S^0 < 0$) and adsorption by AMB400 is endothermic (i.e. $\Delta H^0 > 0$ and $\Delta S^0 > 0$). The $\Delta G^0 < 0$ for all the tested adsorbents indicate that the adsorption process is favourable (GAC > AMB400 > RLX425) and spontaneous.

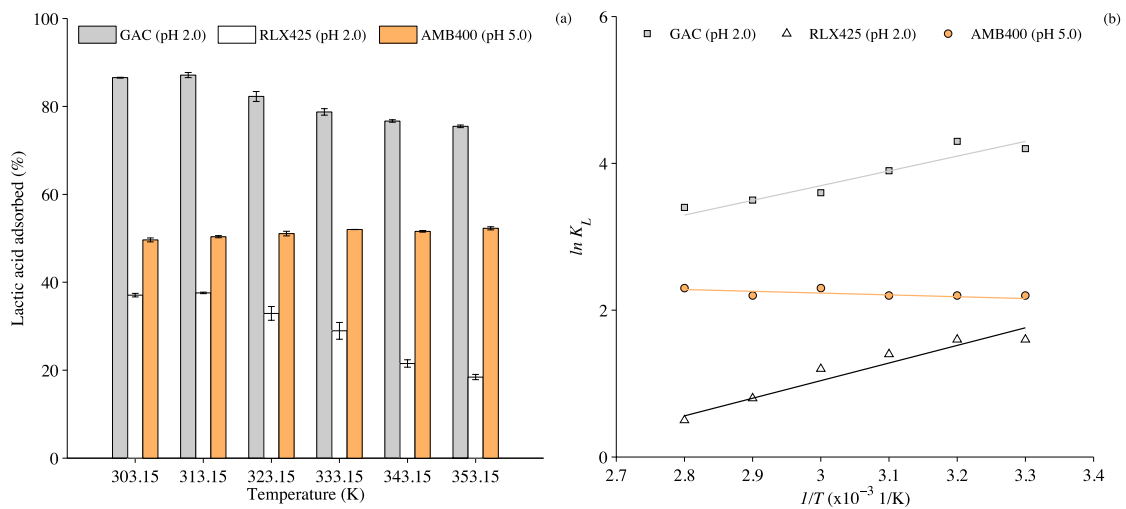


Fig. 8. 2 (a) Effect of temperature (303.15-353.15 K) on the adsorption capacities of the adsorbents with 4.5 g/L of lactic acid in the bulk solution accompanied by initial pH corrections and 10% (w/v) adsorbent dose and (b) plot of $\ln K_L$ versus $1/T$ at a lactic acid concentration of 4.5 g/L in the temperature range of 303.15-353.15 K.

Table 8. 3 Gibbs free energy for adsorption of lactic acid onto GAC, RLX425 and AMB400 at temperature ranges from 303.15 to 353.15 K ($\Delta H^0 = -16.7$ kJ/mol and $\Delta S^0 = -0.02$ kJ/ (mol K) for GAC; $\Delta H^0 = -19.9$ kJ/mol and $\Delta S^0 = -0.05$ kJ/ (mol K) for RLX425; $\Delta H^0 = 2.0$ kJ/mol and $\Delta S^0 = 0.02$ kJ/ (mol K) for AMB400).

Adsorbents	GAC	RLX425	AMB400
Temperature (K)	ΔG^0 (kJ/mol)	ΔG^0 (kJ/mol)	ΔG^0 (kJ/mol)
303.15	-10.9	-4.5	-5.5
313.15	-10.7	-4.0	-5.8
323.15	-10.5	-3.5	-6.0
333.15	-10.4	-3.0	-6.3
343.15	-10.2	-2.4	-6.5
353.15	-9.9	-1.9	-6.8

8.3.3 Lactic acid adsorption isotherms

Fig. 8.3 shows the linearized plots for three different adsorption isotherms (Langmuir, Freundlich and Temkin) of lactic acid adsorption at 303.15 K. **Table 8.4** presents the isotherm parameters and regression coefficients for all the isotherm plots. **Fig. 8.3a** shows the linear fit ($1/q_e$ versus $1/C_e$) of the Langmuir isotherm model. The maximum monolayer adsorption capacity (q_m) value was found to be the highest for GAC (126.6 mg lactic acid/g adsorbent), followed by RLX425 (108.7 mg lactic acid/g adsorbent) and AMB400 (63.5 mg lactic acid/g adsorbent). In addition, the separation factor (R_L) values, calculated to be in the range of 0.05-0.6 for GAC, 0.2-0.9 for RLX425 and 0.2-0.8 for AMB400, indicate a favourable adsorption process. A good agreement ($R^2 > 0.96$) was observed between the experimental data and the Langmuir isotherm model.

Fig. 8.3b shows the plot between $\log q_e$ versus $\log C_e$ for the Freundlich isotherm model. The adsorption intensity (n) was the highest for AMB400, followed by GAC and RLX425 (**Table 8.4**). The slope ($1/n$) in **Fig. 8.3b** ranges between 0 and 1 and is a measure of surface heterogeneity, where the adsorption becomes more

heterogeneous as the $1/n$ value approaches 0 (Foo & Hameed, 2010). Table 8.4 shows $n > 1$ for all the adsorbents investigated, indicating a nonlinearity due to adsorption site heterogeneity.

The Temkin isotherm model shows the adsorption potential of the adsorbent towards the adsorbate. The Temkin isotherm parameters such as A_T and K_T were calculated from the linear plots of q_e versus $\ln C_e$ as shown in Fig. 8.3c. The Temkin isotherm model showed a reasonably good fitting between the experimental results of lactic acid adsorption and the model prediction for all the adsorbents investigated.

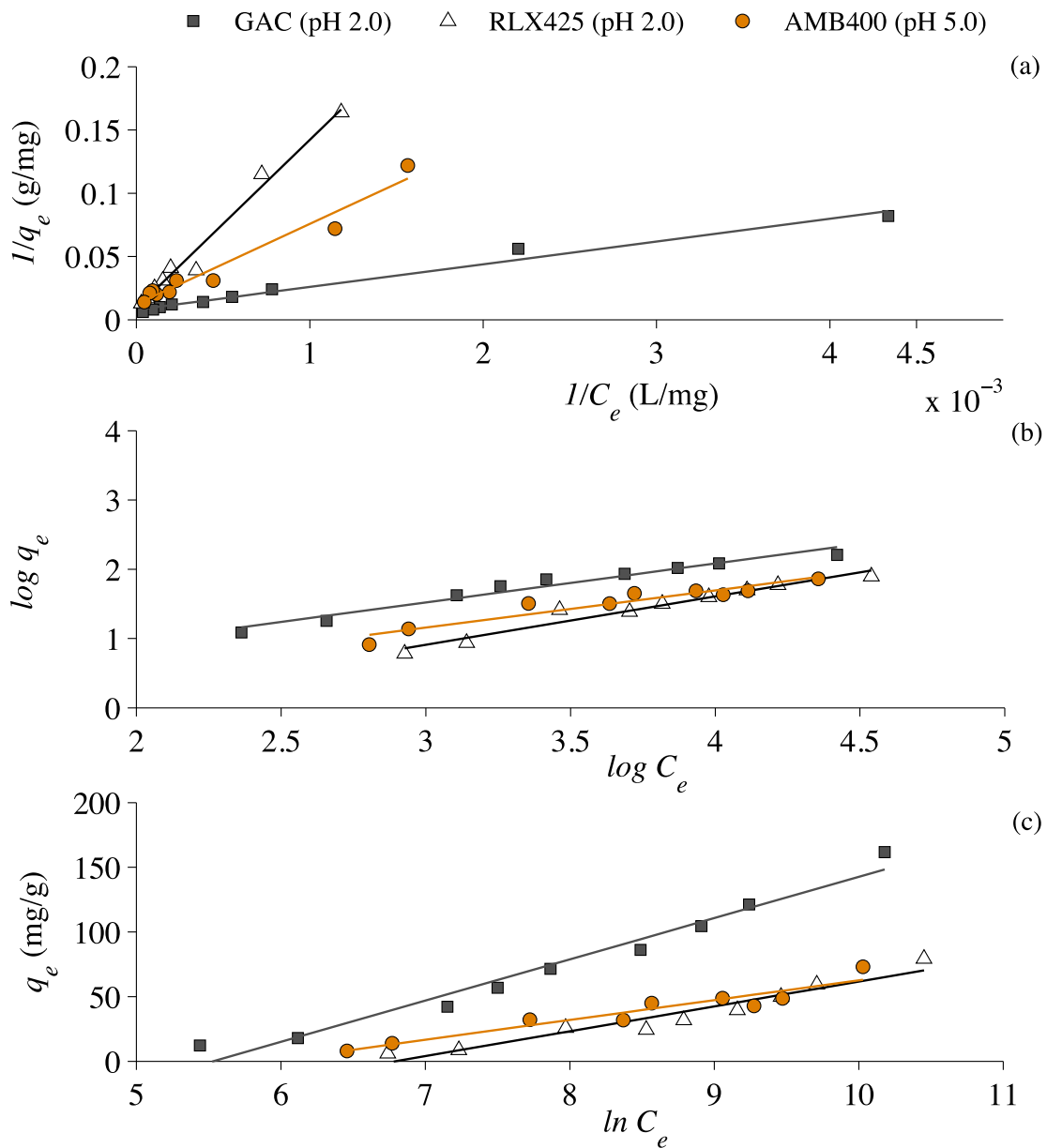


Fig. 8. 3 Linear fits of the (a) Langmuir, (b) Freundlich and (c) Temkin isotherm models for GAC and RLX425 at initial pH 2.0 and AMB400 at initial pH 5.0 with 4.5 g/L of lactic acid in the bulk solution at 303.15 K and an adsorbent dose of 10% (w/v).

Table 8. 4 The Langmuir, Freundlich and Temkin isotherm model parameters obtained from the linear fitting for the three adsorbents (GAC, RLX425 and AMB400).

Isotherms	Coefficients/ Constants	Units	GAC	RLX425	AMB400
Langmuir	q_m	mg/g	126.6	108.7	63.5
	K_L	L/mg	4.4×10^{-4}	6.9×10^{-5}	1.9×10^{-4}
	R^2		0.98	0.98	0.96
Freundlich	n		1.8	1.4	1.9
	K_F	mg/g (L/g) ⁿ	1.2	3.3	1.6
	R^2		0.96	0.95	0.90
Temkin	A_T	L/g	251.7	887.6	371.3
	K_T		31.9	19.2	15.3
	R^2		0.97	0.93	0.91

8.3.4 Lactic acid adsorption kinetics

Among the adsorption kinetic models (i.e. pseudo-first order, pseudo-second order and Elovich) investigated, only the pseudo-second order kinetic model followed the experimental results. Fig. 4 shows the pseudo-first order, pseudo-second order and Elovich kinetic model plots for lactic acid adsorption onto GAC, RLX425 and AMB400, respectively. The pseudo-first order and Elovich kinetic model showed poor fitting between the experimental and model predicted results (data not shown), and hence these models failed to explain the experimental results.

The straight-line plot (Fig. 4b) between t/q_t versus t was used to calculate the pseudo-second order kinetic constants, namely q_e and K_2 as shown in Table 5. Fig. 4b shows a good correlation ($R^2 \sim 1$) between the experimental data and the model predictions for the three adsorbents tested. The initial adsorption rate (h_0) was the highest for AMB400 (142.9 1/min), followed by GAC (31.5 1/min) and RLX425 (13.6 1/min). The q_e value was the highest for GAC (38.2 mg lactic acid/g adsorbent), followed by AMB400 (31.2 mg lactic acid/g adsorbent) and RLX425 (17.2 mg lactic acid/g adsorbent).

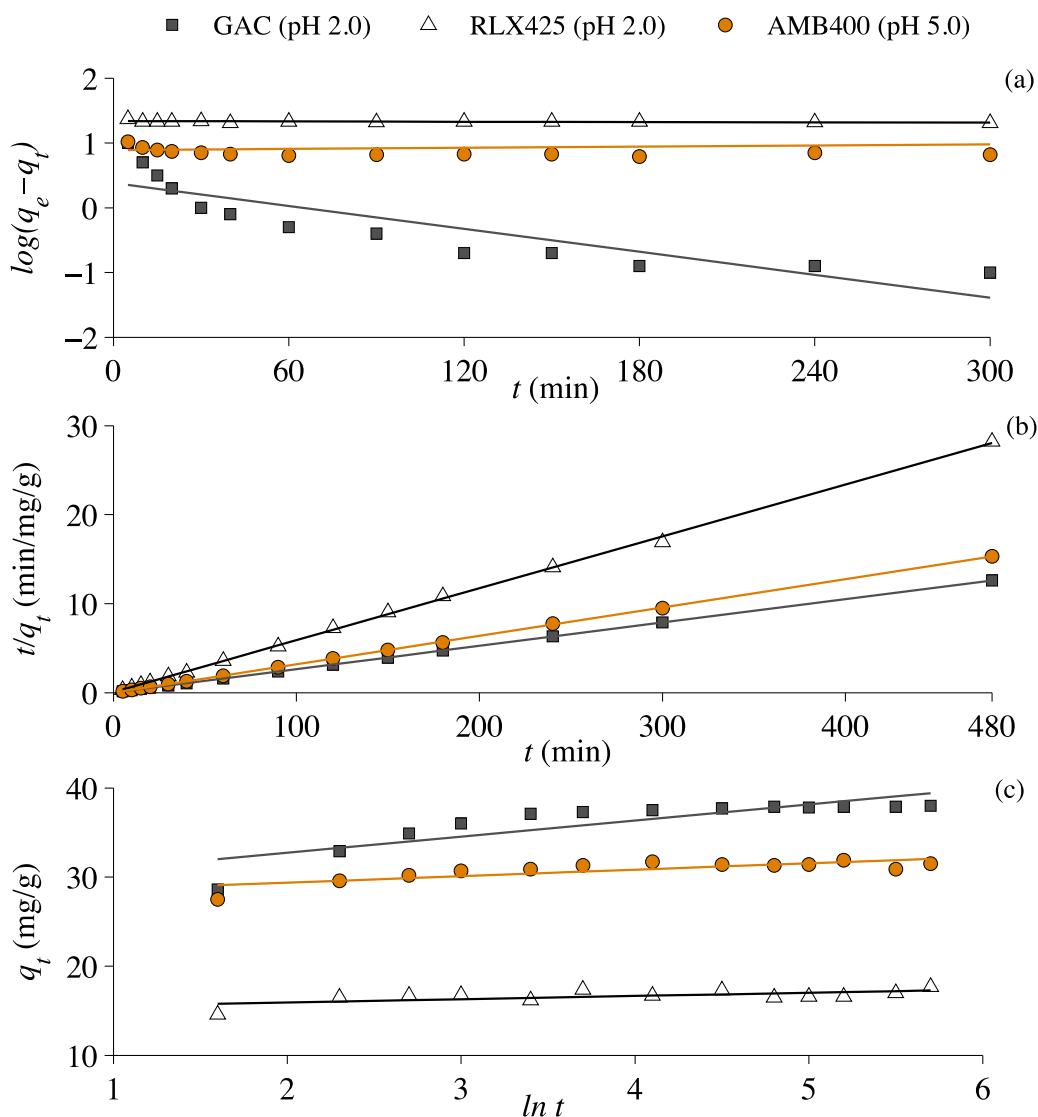


Fig. 8. 4 Adsorption kinetics of lactic acid by the three adsorbents GAC, RLX425 and AMB400 at 303.15 K. (a) Pseudo-first order, (b) pseudo-second order and (c) Elovich kinetic models at an initial lactic acid concentration of 4.5 g/L and an adsorbent dose of 10% (w/v).

Table 8. 5 Pseudo-second order model kinetic parameters for the three adsorbents (GAC, RLX452 and AMB400) at 303.15 K and with 4.5 g/L of lactic acid in the bulk solution.

Kinetics	Coefficients/ constants	Units	GAC	RLX425	AMB400
Pseudo-	q_e	mg/g	38.2	17.2	31.2

second	K_2	mg/g/min	0.02	0.05	0.15
order	h_o	1/min	31.5	13.6	142.9
	R^2		1	0.99	0.99

8.4 Discussion

8.4.1 Influence of operating parameters of lactic acid adsorption onto GAC and anionic resins

8.4.1.1 Effect of the pH on the lactic acid adsorption mechanisms

The study shows that GAC, RLX425 and AMB400 can be used to adsorb lactic acid from a model fermentation broth used for *T. neapolitana* fermentation that typically contains lower (< 5 g/L) concentration of lactic acid. The adsorption capacity for GAC (38.2 mg lactic acid/g adsorbent) was found to be the highest, followed by AMB400 (31.2 mg lactic acid/g adsorbent) and RLX425 (17.2 mg lactic acid/g adsorbent) with 10% (*w/v*) adsorbent dose and an initial lactic acid concentration of 4.5 g/L at 303.15 K. This study also showed that the lactic acid recovery efficiency is better for the GAC and AMB400 resin compared to the efficiencies reported by previous studies (Table 8.6).

Both GAC and the weakly basic anion exchange resin (RLX425) were effective in adsorbing lactic acid at a pH below the pK_a (3.86) of lactic acid, whereas the strongly basic anion exchange resin (AMB400) was effective at a pH above the pK_a value (Fig. 8.1b). The results show that GAC and RLX425 are effective at pH 2.0 and AMB400 is effective at pH 5.0 (Fig. 8.1b). The adsorption of lactic acid onto GAC is due to a physical adsorption process and depends on electronic polarizability, the decreased physical adsorption of lactic acid at high pH is due to decreased dipole-dipole interactions (Gao et al., 2011).

Lactic acid is usually recovered from the fermentation broth via hydrophobic interactions with a neutral poly(styrene-*co*-DVB) resin at pH 2.0, as reported by Thang and Novalin (2008). In addition, Nielsen et al. (2010) found that the adsorption of organic acids onto GAC or weakly basic anionic resins like Amberlite® IRA-67 is dominated at a pH below the pK_a value of the acids, which was also observed for the RLX425 resin in this study (Fig. 8.1b). RLX425 is a weakly-basic resin that has a pyridine functional group and the lone electron pair of the nitrogen atom allows it to

form hydrogen bonds with the lactate ion (Wasewar, 2005). Both GAC and the RLX425 resin are effective at a low pH (2.0); hence, they cannot be used directly in the fermenter as most of the dark fermentation experiments are performed between pH 4.5 and 6.5 (Gao et al., 2010; Yousuf et al., 2016). A strongly basic adsorbent like AMB400, which is effective at pH 5.0, is often recommended for *in situ* extraction of lactic acid from a fermenter (Cao et al., 2002). The results from this study were further corroborated by the observations from previous studies, where GAC as well as the weakly basic resins were effective in adsorbing lactic acid at a pH 2.0 (Evangelista et al., 1994; Gao et al., 2011; Gao et al., 2010; Yousuf et al., 2016) and strongly basic resins were effective at a pH 5.0 (Cao et al., 2002; Quintero et al., 2016).

AMB400 is a strongly basic resin that has a quaternary ammonium as functional group with a positive charge and can thus form ionic bonds with the lactate ion. The binding of lactic acid to AMB400 predominantly occurs as: $R_{rm}^+Cl^- + L^- \leftrightarrow R_{rm}^+L^- + Cl^-$, where L^- is the lactate ion and R_{rm} is the resin matrix with a functional group (Bishai et al., 2015). The Cl^- form of the quaternary ammonium of the AMB400 resin has a weak basic property. This facilitates lactic acid adsorption through Lewis acid-base interactions with the partially positively charged hydroxyl (OH^-) and acidic protons (H^+) of lactic acid (Dethe et al., 2006; Wasewar, 2005). The low recovery efficiency (~50%) of lactic acid with the AMB400 resin is attributed to the positively charged quaternary ammonium functional group which cannot be approached by the partial negatively charged oxygen of the acid due to the steric hindrance provided by the bulk alkyl groups on the nitrogen as well as due to competing counter ion species (i.e. Cl^- and L^-) (Dethe et al., 2006). The lactic acid adsorption by the AMB400 resin occurs through an ion exchange mechanism (Sodsai & Sookkumnerd, 2013).

The quaternary ammonium functional group can adsorb both molecular lactic acid and the lactate ion, however, further studies are required to demonstrate the competition between molecular lactic acid and the lactate ion. In addition, other organic components found in the real fermentation broth (*e.g.* acetic acid, alanine, glucose, tryptone, yeast extract *etc.*) are likely to impact the adsorption capacity and recovery efficiency due to composite uptake. The composite adsorption depends on the relative adsorption affinity, which is further linked to the polarity strength of the solute in the solution (*e.g.* acetic acid > ethanol > glycerol > glucose) (Zhou et al., 2013).

Table 8. 6 Lactic acid recovery from the model fermentation broths using GAC, RLX425 and AMB400 in batch adsorption experiments (adsorbent dose 10% *w/v*).

Resin/ adsorbent	Initial pH	Temperature (K)	Initial lactic acid concentration (g/L)	q_e (mg lactic acid/g adsorbent)	E (%)	References
GAC	2	303.15	50	175	35	(Gao et al., 2011)
	2	298.15	7	48	69	(Yousuf et al., 2016)
	2	303.15	22	121	54	This study
	2	303.15	4.8	38	81	This study
	2	353.15	4.7	35	76	This study
	2.83	303.15	5.7	32	56	(Evangelista et al., 1994)
RLX425	2	303.15	22	60	27	This study
	2	303.15	4.8	17	35	This study
	2	353.15	4.7	9	18	This study
AMB400	4	303.15	100	350	35	(Rampai et al., 2016)
	5	298.15	88.7	197	22	(Cao et al., 2002)
	4.85	303.15	60	160	27	(Moldes et al., 2003)
	5	298.15	34	107	31	(Quintero et al., 2016)
	5	303.15	18	48	24	This study
	5	303.15	5.4	31	57	This study
	5	353.15	4.7	25	52	This study

8.4.1.2 Effect of adsorbent dose on lactic acid adsorption

In addition to pH, adsorbent dose (Fig. 8.1c) and temperature (Fig. 8.2a) also play a major role in the absorption of lactic or organic acids. The increase in adsorbent

dose from 5 to 30% (*w/v*) increased the recovery efficiency for GAC by 10% and by 50% for, respectively, RLX425 and AMB400 resins (Fig. 8.1c). However, an adsorbent dose of 10% (*w/v*) was found to be suitable for all the adsorbents at 303 K with an initial lactic acid concentration of 4.5 g/L (Fig. 8.1c) as also reported by other authors (Gao et al., 2011; Gao et al., 2010; Yousuf et al., 2016). Yousuf et al. (2016) studied the effect of adsorbent (Amberlite® IRA-67 and activated carbon) dose (2-20%, *w/v*) on the lactic acid recovery efficiency and found that 10% (*w/v*) was the most appropriate adsorbent dose at 298 K with an initial lactic acid concentration ranging between 6.7 and 7.0 g/L. Gao et al. (2010) also studied the effect of the adsorbent (Amberlite® IRA-67) dose (5-17.5%) on the lactic acid recovery efficiency and reported that 10% (*w/v*) is the best performing adsorbent dose for initial lactic acid concentrations varying between 21.0 and 99.5 g/L, at 323 K. In contrast, Gao et al. (2011) found that 30% (*w/v*) activated carbon dose was suitable for lactic acid recovery from an initial lactic acid concentration of 50.0 g/L at 303 K when tested on adsorbent doses ranging between 10 and 50% (*w/v*).

8.4.1.3 Effect of temperature on lactic acid adsorption

The effect of temperature (303.15 to 353.15 K) shows an interesting trend for lactic acid adsorption from the model fermentation broth (Fig. 8.2a). Increasing the temperature from 303.15 to 353.15 K decreased the adsorption capacity of GAC and RLX425 by ~ 13% and ~ 50%, respectively. Among the adsorbents tested in this study, the AMB400 resin was the most efficient adsorbent for lactic acid recovery, because of its operational flexibility at varying temperature ranges. Gao et al. (2010) reported that the lactic acid adsorption capacity decreased by ~ 20% for the Amberlite® IRA-67 resin when the temperature increased from 293 to 323 K with an initial lactic acid concentration of 42.5 g/L. In another study, the adsorption capacity of the lactic acid onto Zeolite molecular sieves decreased from 10.5 mg/g to 3.6 mg/g when the temperature increased from 299 K to 339 K with an initial lactic acid concentration varying between 14.2 and 16.1 g/L (Aljundi et al., 2005). The decrease in lactic acid adsorption at higher temperatures is mainly due to weak interactions between the active sites of the adsorbent and adsorbate molecules (Ye et al., 2014). The extraction of acids by GAC and amine groups is shown to be exothermic and decreases with increase in the temperature due to the following reasons: (i) decrease in the adsorption affinity towards

adsorbate molecules, (ii) shifting the equilibrium towards the liquid phase and (iii) promoting desorption as the reactions are exothermic in nature (Farhadpour & Bono, 1996).

8.4.2 Thermodynamics analysis of lactic acid adsorption

The negative values of ΔG^0 (-9.9 to -10.9 kJ/mol) and ΔH^0 (-16.7 kJ/mol) revealed that the lactic acid adsorption onto GAC was spontaneous and exothermic between 303.15 K and 353.15 K (Table 8.3). Similarly, the negative values of ΔG^0 (-4.5 to -1.9 kJ/mol) and ΔH^0 (-19.9 kJ/mol) assures that the lactic acid adsorption onto the RLX425 resin was spontaneous and exothermic between 303.15 and 353.15 K (Table 8.3). On the contrary, the negative values of ΔG^0 (-5.5 to -6.8 kJ/mol) and positive values for ΔH^0 (+2.0 kJ/mol) showed that the lactic acid adsorption onto AMB400 resin was spontaneous, but endothermic between 303.15 K and 353.15 K due to ion exchange mechanisms (Table 8.3). Gao et al. (2010) calculated the thermodynamic parameters for the lactic acid adsorption onto a weakly basic anionic (Amberlite® IRA-67) resin between 293 K and 323 K. In that study, the ΔH^0 value for lactic acid adsorption onto Amberlite® IRA-67 was -32.8 kJ/mol and the adsorption process was exothermic between 298 K and 323 K. Aljundi et al. (2005) reported that the ΔH^0 value for the lactic acid adsorption onto Zeolite molecular sieves was +29 (± 17) kJ/mol and the adsorption process was endothermic between 299 K and 339 K.

The negative values of ΔG^0 descending with the increase of temperature indicated a decrease in lactic acid adsorption from the bulk solution at elevated temperatures (> 313.15 K) for both GAC and RLX425. On the other hand, the negative values of ΔG^0 ascending with temperature increase indicated an increase in lactic acid adsorption with the AMB400 resin, but the increase was not large. The study by Gao et al. (2010) showed that the ΔG^0 (-8.8 to -6.7 kJ/mol) decreased with an increase in the temperature between 298 and 323 K for lactic acid adsorption onto the Amberlite® IRA-67 resin.

The negative ΔS^0 value (-0.05 kJ/(mol K)) for the weakly-basic resin (RLX425) shows decreased randomness at the adsorbent-adsorbate interface during the adsorption of lactic acid onto the active sites of the resin, which was further validated by the negative ΔS^0 (-0.8 kJ/(mol K)) value found in a previous study on a weakly-basic resin (Amberlite® IRA-67) (Gao et al., 2010). In addition, the positive value of ΔS^0 (0.02

kJ/(mol K)) indicates the increased randomness at the adsorbent-adsorbate interface during the adsorption of lactic acid onto the active sites of the AMB400 resin. From the adsorption results at varying temperature, the increase in temperature decreased the recovery efficiency for both GAC and RLX425 (Fig. 8.2a), which was further validated by the ΔG^0 values in Table 8.3 as the reaction spontaneity was found to decrease with an increase in the temperature (Zhou et al., 2016).

Generally, the adsorption enthalpy for physical adsorption (or electrostatic interaction between adsorption sites and the adsorbate species) ranges between -20 and 40 kJ/mol (Lian et al., 2009) and for chemisorption between -80 and -400 kJ/mol, respectively (Gao et al., 2010; Kolodynska, 2012; Zhou et al., 2016). The ΔH^0 (-16.7 kJ/mol for GAC and -19.9 kJ/mol for RLX425) values obtained in this study were within the range of physical adsorption. Hence, the adsorption experiments with GAC and anionic resins indicated a physical adsorption process for lactic acid adsorption. In a related study, adsorption of acetic, propionic and butyric acid onto activated carbon and a weak base anionic resin (Puralite A133S) showed a physical adsorption (i.e. ΔH^0 between -20 and 40 kJ/mol) process based on the thermodynamic analysis and the favourability: butyric > acetic > propionic acid (da Silva & Miranda, 2013). The amount of lactic acid adsorbed via ion exchange (AMB400) was slightly lower than that adsorbed by physical adsorption (GAC and RLX425) (Sodsai & Sookkumnerd, 2013).

8.4.3 Lactic acid adsorption isotherms and kinetics

Among the isotherms investigated, the Langmuir isotherm was found to be more suitable in explaining the adsorption mechanism compared to the Freundlich and Temkin isotherms. The Dubinin-Radushkevich isotherm and intraparticle diffusion kinetic model were investigated in this study for lactic acid adsorption, but none of these two models were able to explain the experimental results of lactic acid adsorption (data not shown). The understanding on lactic acid adsorption mechanism can be improved by applying Redlich-Peterson isotherm (a hybrid isotherm featuring both Langmuir and Freundlich) and a multilayer adsorbent-adsorbate interface Brunauer-Emmett-Teller (BET) isotherm model to fixed bed column experiments (Foo & Hameed, 2010).

In a similar study, adsorption of formic acid onto Amberlite® IRA-67 followed the Langmuir isotherm under similar operating conditions (Uslu, 2009). In contrast, Gao

et al. (2010) showed that the lactic acid adsorption onto Amberlite® IRA-67 was fitted by the Freundlich isotherm model. The plot (Fig. 8.3a) from the Langmuir isotherm shows that the lactic acid was adsorbed as a monolayer and homogeneously distributed over the surface of the adsorbent with restricted interaction between the adsorbate (i.e. lactic acid) molecules (Table 8.4). In addition, the Langmuir isotherm also suggests that adsorption of lactic acid onto the GAC, RLX425 and AMB400 is favourable ($0 < R_L < 1$). From the adsorption kinetic studies, the pseudo-second order kinetic model showed a strong correlation ($R^2 \sim 1$) between the experimental results and the model predictions for all the adsorbents tested.

8.4.4 Practical implications

Desorption of lactic acid from the adsorbents is an important factor that needs to be examined as a downstream processing strategy. According to previous studies, the adsorbed lactic acid onto GAC and anionic resins can be desorbed by various chemicals, depending on the pH, temperature and functional groups present on the adsorbents as well as the nature of the desorbent, i.e. acetone, methanol, 1 M NaCl, NaOH (2-4%), NH₄OH (2-4%), Na₂CO₃ (4-8%) and 1 M H₂SO₄ (Dethe et al., 2006; Gao et al., 2011; Gao et al., 2010). In addition to desorption studies, it is important to scale-up the batch experiments with fixed-bed adsorption columns along with analysis of the lactic acid adsorption breakthrough curves in order to evaluate the most economical and feasible adsorbents for *in situ* lactic acid removal from fermentation broth.

The optical purity of the lactic acid can be achieved > 99% by desorbing it with organic solvents (e.g. acetone and methanol) (Gao et al., 2011). The optical purity of the lactic acid will slightly decrease when it is desorbed with HCl, NaOH and NaCl. In addition, the optical purity of the acid will be impacted by the presence of other constituents in the model or real fermentation broth. The contamination can be reduced by filtration or acid/base treatments.

8.5 Conclusions

GAC as well as weak and strong base anion exchange resins were successfully applied for the separation of lactic acid from a model *T. neapolitana* fermentation broth at a pH above and below the pK_a (3.86) value of lactic acid. The temperature experiments showed that increasing the temperature from 303.15 to 353.15 K decreased the lactic acid recovery efficiency by 50% and 13% for RLX425 resin and GAC,

respectively, whereas the recovery efficiency remained unchanged for the AMB400 resin. From the thermodynamic analysis, the lactic acid adsorption onto the adsorbents suggests a physical adsorption mechanism for both GAC and RLX 425 and ion exchange for the AMB400 resin. The equilibrium adsorption data for the lactic acid were adequately explained by the Langmuir isotherm model, indicating a monolayer adsorption process. Lactic acid recovery was found to be well represented by pseudo-second order kinetics. Among the different adsorbents tested, the strongly basic resin (AMB400) showed good lactic acid recovery from the model fermentation broth in terms of adsorption kinetics, adsorption capacity and thermodynamic feasibility.

References

- Aljundi, I.H., Belovich, J.M., Talu, O. 2005. Adsorption of lactic acid from fermentation broth and aqueous solutions on Zeolite molecular sieves. *Chemical Engineering Science*, **60**, 5004-5009.
- Antonio, G.R., Vaccari, G., Dosi, E., Trilli, A., Rossi, M., Matteuzzi, D. 2000. Enhanced production of L-(+)-lactic acid in chemostat by *Lactobacillus casei* DSM 20011 using ion-exchange resins and cross-flow filtration in a fully automated pilot plant controlled via NIR. *Biotechnology and Bioengineering*, **67**, 147-156.
- Bayazit, S.S., Inci, I., Uslu, H. 2011. Adsorption of lactic acid from model fermentation broth onto activated carbon and amberlite IRA-67. *Journal of Chemical and Engineering Data*, **56**, 1751-1754.
- Bernardo, M.P., Coelho, L.F., Sass, D.C., Contiero, J. 2016. L-(+)-Lactic acid production by *Lactobacillus rhamnosus* B103 from dairy industry waste. *Brazilian Journal of Microbiology*, **47**, 640-646.
- Bishai, M., De, S., Adhikari, B., Banerjee, R. 2015. A platform technology of recovery of lactic acid from a fermentation broth of novel substrate *Zizyphus oenophlia*. *3 Biotech*, **5**, 455-463.
- Cao, X., Yun, H.S., Koo, Y.M. 2002. Recovery of l-(+)-lactic acid by anion exchange resin Amberlite IRA-400. *Biochemical Engineering Journal*, **11**, 189-196.
- Chen, X. 2015. Modeling of experimental adsorption isotherm data. *Information*, **6**, 14-22.
- da Silva, A.H., Miranda, A.E. 2013. Adsorption/desorption of organic acids onto different adsorbents for their recovery from fermentation broths. *Journal of Chemical & Engineering Data*, **58**, 1454-1463.
- Dethe, M.J., Marathe, K.V., Gaikar, V.G. 2006. Adsorption of lactic acid on weak base polymeric resins. *Separation Science and Technology*, **41**, 2947-2971.
- Dipasquale, L., d'Ippolito, G., Fontana, A. 2014. Capnophilic lactic fermentation and hydrogen synthesis by *Thermotoga neapolitana*: An unexpected deviation from

- the dark fermentation model. *International Journal of Hydrogen Energy*, **39**, 4857-4862.
- Evangelista, R.L., Mangold, A.J., Nikolov, Z.L. 1994. Recovery of lactic acid by sorption: resin evaluation. *Applied Biochemistry and Biotechnology*, **45-46**, 131-144.
- Farhadpour, F.A., Bono, A. 1996. Sorptive separation of ethanol-water mixtures with a bi-dispersed hydrophobic molecular sieve, silicalite: Determination of the controlling mass transfer mechanism. *Chem Eng Process*, **35**, 141-155.
- Foo, K.Y., Hameed, B.H. 2010. Insights into the modeling of adsorption isotherm systems. *Chemical Engineering Journal*, **156**, 2-10.
- Gao, M.T., Shimamura, T., Ishida, N., Takahashi, H. 2011. pH-uncontrolled lactic acid fermentation with activated carbon as an adsorbent. *Enzyme and Microbial Technology*, **48**, 526-530.
- Gao, Q., Liu, F., Zhang, T., Zhang, J., Jia, S., Yu, C., Jiang, K., Gao, N. 2010. The role of lactic acid adsorption by ion exchange chromatography. *PLoS one*, **5**, e13948.
- Hamad, K., Kaseem, M., Deri, F. 2011. Melt rheology of poly(lactic acid)/low density polyethylene polymer blends *Advances in Chemical Engineering and Science*, **1**, 208-2014.
- Hamad, K., Kaseem, M., Deri, F. 2010. Rheological and mechanical properties of poly(lactic acid)/polystyrene polymer blend. *Polymer Bulletin*, **65**, 509-519.
- Joglekar, H.G., Rahman, I., Babu, S., Kulkarni, B.D., Joshi, A. 2006. Comparative assessment of downstream processing options for lactic acid. *Separation and Purification Technology*, **52**, 1-17.
- Kolodynska, D. 2012. Adsorption Characteristics of chitosan modified by chelating agents of a new generation. *Chemical Engineering Journal*, **179**, 33-43.
- Lian, L., Guo, L., Guo, C. 2009. Adsorption of Congo red from aqueous solutions onto Ca-bentonite. *Journal of Hazardous Materials*, **161**, 126-131.
- Martinez, F.A.C., Balciunas, E.M., Salgado, J.M., Gonzalez, J.M.D., Converti, A., Oliveira, R.P.S. 2013. Lactic acid properties, applications and production: A review. *Trends in Food Science & Technology*, **30**, 70-83.
- Moldes, A.B., Alonso, J.L., Parajo, J.C. 2003. Recovery of lactic acid from simultaneous saccharification and fermentation media using anion exchange resins. *Bioprocess and Biosystems Engineering*, **25**, 357-363.
- Nielsen, D.R., Amarasiriwardena, G.S., Prather, K.L.J. 2010. Predicting the adsorption of second generation biofuels by polymeric resins with applications for in situ product recovery (ISPR). *Bioresource Technology*, **101**, 2762-2769.
- Pezoti, O., Cazetta, A.L., Bedin, K.C., Souza, L.S., Martins, A.C., Silva, T.L., Junior, O.O.S., Visentainer, J.V., Almeida, V.C. 2016. NaOH-activated carbon of high surface area produced from guava seeds as a high-efficiency adsorbent for amoxicillin removal: Kinetic, isotherm and thermodynamic studies. *Chemical Engineering Journal*, **288**, 778-788.

- Pradhan, N., Dipasquale, L., d'Ippolito, G., Fontana, A., Panico, A., Pirozzi, F., Lens, P.N.L., Esposito, G. 2016a. Model development and experimental validation of capnophilic lactic fermentation and hydrogen synthesis by *Thermotoga neapolitana*. *Water Research*, **99**, 225-234.
- Pradhan, N., Dipasquale, L., d'Ippolito, G., Fontana, A., Panico, A., Lens, P.N.L., Pirozzi, F., Esposito, G. 2016b. Kinetic modeling of fermentative hydrogen production by *Thermotoga neapolitana*. *International Journal of Hydrogen Energy*, **41**, 4931-4940.
- Pradhan, N., Dipasquale, L., d'Ippolito, G., Panico, A., Lens, P.N.L., Esposito, G., Fontana, A. 2015. Hydrogen production by the thermophilic bacterium *Thermotoga neapolitana*. *International Journal of Molecular Sciences*, **16**, 12578-12600.
- Quintero, J., Acosta, A., Mejia, C., Rios, R., Torres, M. 2016. Purification of lactic acid obtained from a fermentative process of cassava syrup using ion exchange resins. *Rev Fac Ing Univ Antioquia N*, **65**, 139–151.
- Rampai, T., Thitiprasert, S., Boonkong, W., Kodama, K., Tolieng, V., Thongchul, N. 2016. Improved lactic acid productivity by simultaneous recovery during fermentation using resin exchanger. **21**, 193-199.
- Rich, W., Johnson, E., Lois, L., Kabra, P., Stafford, B., Marton, L. 1980. Determination of organic acids in biological fluids by Ion Chromatography: plasma Lactate and pyruvate and urinary vanillylmandelic acid. *Clinical chemistry*, **26**, 1492-1498.
- Shi, Y., Kong, X., Zhang, C., Chen, Y., Hua, Y. 2013. Adsorption of soy isoflavones by activated carbon: Kinetics, thermodynamics and influence of soy oligosaccharides. *Chemical Engineering Journal*, **215-216**, 113-121.
- Sodsai, W., Sookkumnerd, T. 2013. Modeling of lactic acid adsorption isotherm by anion exchange resin Amberlite IRA-96. *KMITL Science and Technology Journal*, **13**, 82-86.
- Sugiyama, M., Akase, S., Nakanishi, R., Kaneko, Y., Harashima, S. 2016. Overexpression of ESBP6 improves lactic acid resistance and production in *Saccharomyces cerevisiae*. *Journal of Bioscience and Bioengineering*, **122**, 415-420.
- Takatsuji, W., Nakauchi, M., Yoshida, H. 1999. Removal of salt and organic acids from solution used to season salted Japanese apricots (*ume*) by electrodialysis, precipitation and adsorption. *Journal of Bioscience and Bioengineering*, **88**, 348-351.
- Thang, V.H., Novalin, S. 2008. Green biorefinery: separation of lactic acid from grass silage juice by chromatography using neutral polymeric resin. *Bioresource Technology*, **99**, 4368-4379.
- Tong, W.Y., Fu, X.Y., Lee, S.M., Yu, J., Liu, J.W., Wei, D.W., Koo, Y.M. 2004. Purification of l(+)-lactic acid from fermentation broth with paper sludge as a cellulosic feedstock using weak anion exchanger Amberlite IRA-92. *Biochemical Engineering Journal*, **18**, 89-96.

- Uslu, H. 2009. Adsorption equilibria of formic acid by weakly basic adsorbent Amberlite IRA-67: Equilibrium, kinetics, thermodynamic. *Chemical Engineering Journal*, **155**, 320-325.
- Wasewar, K.L. 2005. Separation of lactic acid: Recent advances. *Chemical and Biochemical Engineering Quarterly*, **19**, 159-172.
- Webber, T.W., Chakkravorti, R.K. 1974. Pore and solid diffusion models for fixed-bed adsorbers. *AIChE Journal*, **20**, 228-238.
- Ye, C., Wang, X., Wang, H., Wang, Z. 2014. Effects of counter anions on the adsorption properties of 4-methylimidazolium-modified silica materials. *Journal of the Taiwan Institute of Chemical Engineers*, **45**, 2868-2877.
- Yi, S.S., Lu, Y.C., Luo, G.S. 2008. Separation and concentration of lactic acid by electro-electrodialysis. *Separation and Purification Technology*, **60**, 308-314.
- Yousuf, A., Bonk, F., Oyanedel, J.R.B., Schmidt, J.E. 2016. Recovery of carboxylic acids produced during dark fermentation of food waste by adsorption on Amberlite IRA-67 and activated carbon. *Bioresource Technology*, **217**, 137-140.
- Zhou, J., Wu, J., Liu, Y., Zou, F., Wu, J., Li, K., Chen, Y. 2013. Modeling of breakthrough curves of single and quaternary mixtures of ethanol, glucose, glycerol and acetic acid adsorption onto a microporous hyper-cross-linked resin. *Bioresource Technology*, **143**, 360-368.
- Zhou, Q., Chen, F., Wu, W., Bu, R., Li, W., Yang, F. 2016. Reactive orange 5 removal from aqueous solution using hydroxyl ammonium ionic liquids/layered double hydroxides intercalation composites. *Chemical Engineering Journal*, **285**, 198-206.

Chapter 9

General discussion and recommendations

Chapter 9: General discussion and recommendations

9.1 General overview

Non-renewable energy has been the key driving force for the rapid industrialization and urbanization in the past centuries. Fossil derived fuels contribute to global warming and a major challenge in contemporary energy and environmental management. The quest for alternative energy has inspired the innovation of several sustainable neo-carbon-neutral technologies especially through biological routes. To that end, microbes including bacteria, fungi and microalgae play a vital role in the carbon cycle by transforming organic carbon into fuel (hydrogen and methane) and fuel precursors (methanol and ethanol) through biocatalysis. There are several microbial technologies available for biological hydrogen (H₂) production, but due to thermodynamic constraints it is not possible to achieve complete energy recovery by applying a single-stage process. Here, the research work explicitly proposes a novel approach by applying the capnophilic lactic fermentation (CLF) to a hyperthermophilic marine bacterium *Thermotoga neapolitana* to develop processes for environmentally sustainable energy generation.

The main objective of this research was to study and investigate the engineering techniques for improving simultaneous synthesis of H₂ and lactic acid from various feedstocks under CLF conditions using *T. neapolitana* as model bacterium. This includes phenotypic and genotypic characterizations of *T. neapolitana* (wild-type and laboratory) strains along with culture parameter optimization (i.e., salinity level, carbon source and buffering agent), growth kinetic parameter estimation and mathematical model development in a continuous stirred-tank reactor (CSTR) system and recovery of lactic acid from a model fermentation broth by adsorption. Fig. 9.1 shows the general overview of the thesis and the aspects of CLF-based fermentation in a CSTR system.

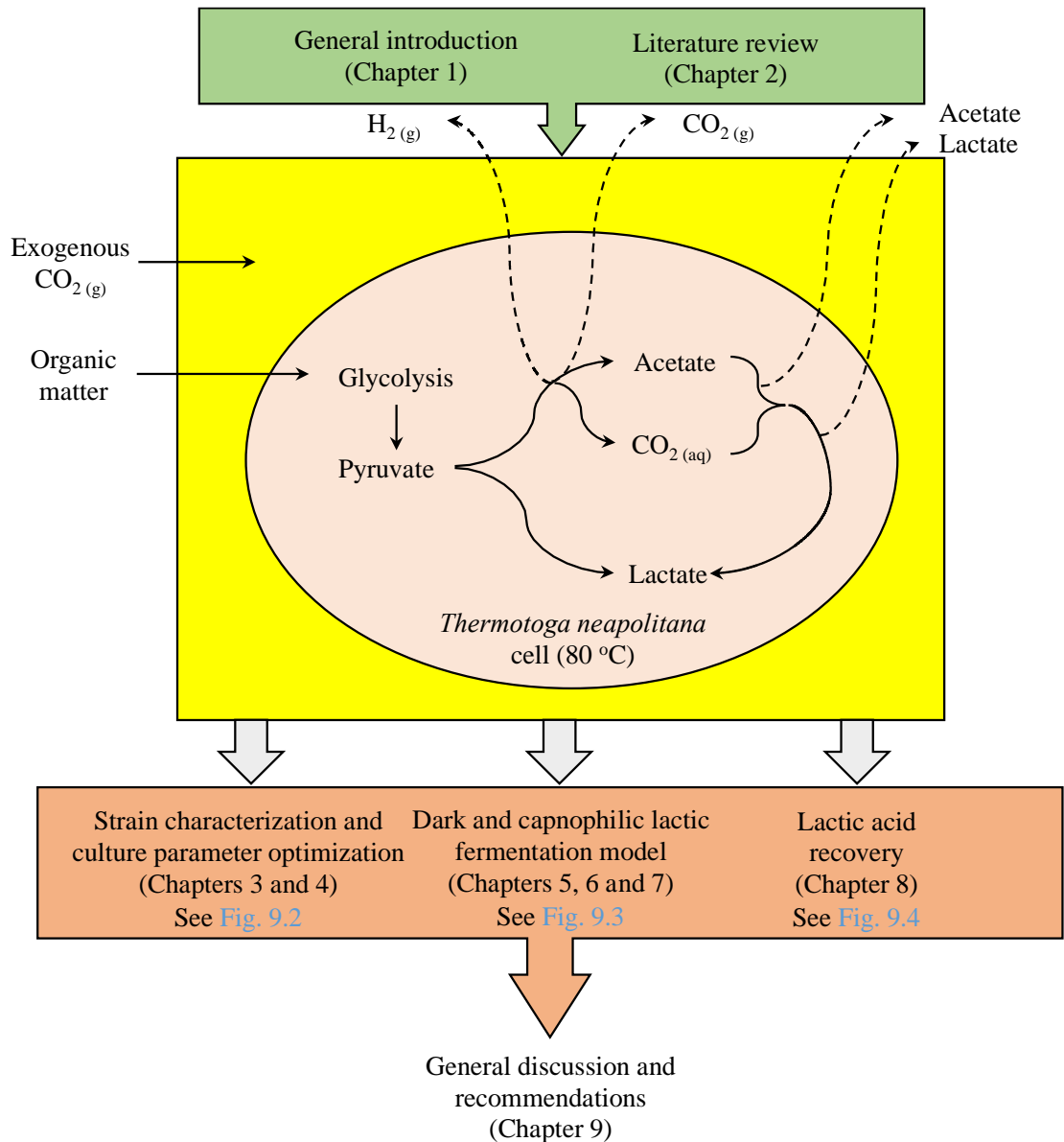


Fig. 9. 1 Overview of the thesis structure and the aspects of CLF-based fermentation in a CSTR system.

9.2 Microbial fermentation: wet-lab experiments

9.2.1 Genotypic and phenotypic characterization of *T. neapolitana* strains

The lab strain (mutant) of *T. neapolitana* maintained in CO₂ enriched atmosphere showed a unique ability to produce lactic acid under CLF conditions (Dipasquale et al., 2014; Pradhan et al., 2016a), compared to the experiment with N₂ enriched atmosphere (d'Ippolito et al., 2010; Dipasquale et al., 2012; Nguyen et al., 2010). As per Clemente et al. (2007) and Derrick et al. (2015), the susceptibility of

microorganisms to mutations has often been associated with the influence of natural environments on the DNA integrity. The genotypic comparison was performed between the mutant and the parent isolate of *T. neapolitana* (Chapter 3). It revealed a DNA homology of 88.1 (\pm 2.4)%, which was well above the 70% similarity that is the gold standard threshold for species boundaries (Schumann & Maier, 2014). The genotyping by RiboPrint[®] and matrix assisted laser desorption ionization time-of-flight mass spectrometry (MALDI-TOF MS) analyses showed a genetic differentiation beyond species level for both strains (Soro-Yao et al., 2014).

The phenotypic characterization (with respect to growth temperature, growth rate, substrate preference, salinity, hydrogen rate and yield) supported a high correlation between the two strains except for the lactic acid production. The lab strain produced in the range of 10–90% higher lactic acid concentrations than the parent isolate under similar operating conditions without affecting the H₂ yield (Fig. 9.2). The difference between the two strains is more prominent with respect to lactic acid under standard operating conditions (at 80 °C). Based on the genotypic and phenotypic characterization, the lab strain (*T. neapolitana* subsp. nov.) is proposed as a new subspecies in the genus *Thermotoga* with the name *T. neapolitana* subsp. *lactica* referring to its ability to over produce lactic acid.

9.2.2 Effect of culture parameters on *T. neapolitana* fermentation

The H₂ and lactic acid production of *T. neapolitana* by changing the culture parameters (salinity, buffering agents and substrates) was investigated under CLF conditions either in 0.12 L serum bottles or in a 3 L CSTR (Fig. 9.2). Increasing salinity levels from 0 to 35 g/L NaCl increased the lactic acid production by 750% (2.8 (\pm 0.3) to 21.6 (\pm 6.2) mM lactic acid), whereas the average H₂ yield remained about 2.9 mol H₂/mol of glucose. For example, Pierra et al. (2014) studied the effect of the salinity level (9–75 g/L NaCl) on H₂ production using mixed culture biomass and found that the increasing salinity level increased lactic acid production.

A stable H₂ yield (i.e. 3.0 mol H₂/mol of glucose) and lactic acid (i.e. 13.7 mM) production were observed when the culture medium was co-buffered with 0.01 M concentration of different buffering agents (i.e. phosphate, MOPS, TRIS and HEPES) under CLF conditions. For example, Cappelletti et al. (2012) studied different buffering agents of various concentrations and found that 0.1 M of HEPES was the best

performing buffering agent under N₂ sparging atmosphere yielding 1.6 (± 0.1) mol H₂/mol of glucose and 1.1 (± 0.1) mol acetic acid/mol of glucose. In an another study by [Ngo et al. \(2011\)](#), 0.05 M HEPES was found to be sufficient in maintaining the buffering capacity of the culture medium and produced 2.7 (± 0.1) mol H₂/mol of glycerol consumed under N₂ sparging atmosphere. In a nutshell, it was proposed that the phosphate buffer along with CO₂ atmosphere will reduce the overall cost of maintaining the culture pH as well as to improve the overall performance of the fermentation.

The H₂ yields from xylose, arabinose, glucose, sucrose, laminarin and carboxymethyl cellulose (CMC) under N₂ sparging atmosphere were quite similar to the results obtained under CO₂ sparging atmosphere by *T. neapolitana* fermentation in the present study ([Dipasquale et al., 2012](#); [Eriksen et al., 2011](#); [Nguyen et al., 2008b](#); [Pradhan et al., 2016b](#)). Among all the sugars tested, CMC had a low utilization ability for both H₂ and lactic acid production and thus required pre-treatment assisted fermentation as per [De Vrije et al. \(2009\)](#). Glucose as carbon source gave the best H₂ yield (3.3 mol H₂/mol glucose) and lactic acid (0.6 mol lactic acid/mol glucose) production among the carbon sources tested. A negligible quantity of lactic acid was produced when the experiments were performed under N₂ sparging atmosphere ([De Vrije et al., 2009](#); [Frascari et al., 2013](#); [Munro et al., 2009](#)). Further, the scale-up (3.0 L CSTR) tests (35 g/L NaCl, 0.01 M phosphate buffer and glucose as carbon source) produced 230% more lactic acid compared to the serum bottle experiments under similar operating conditions.

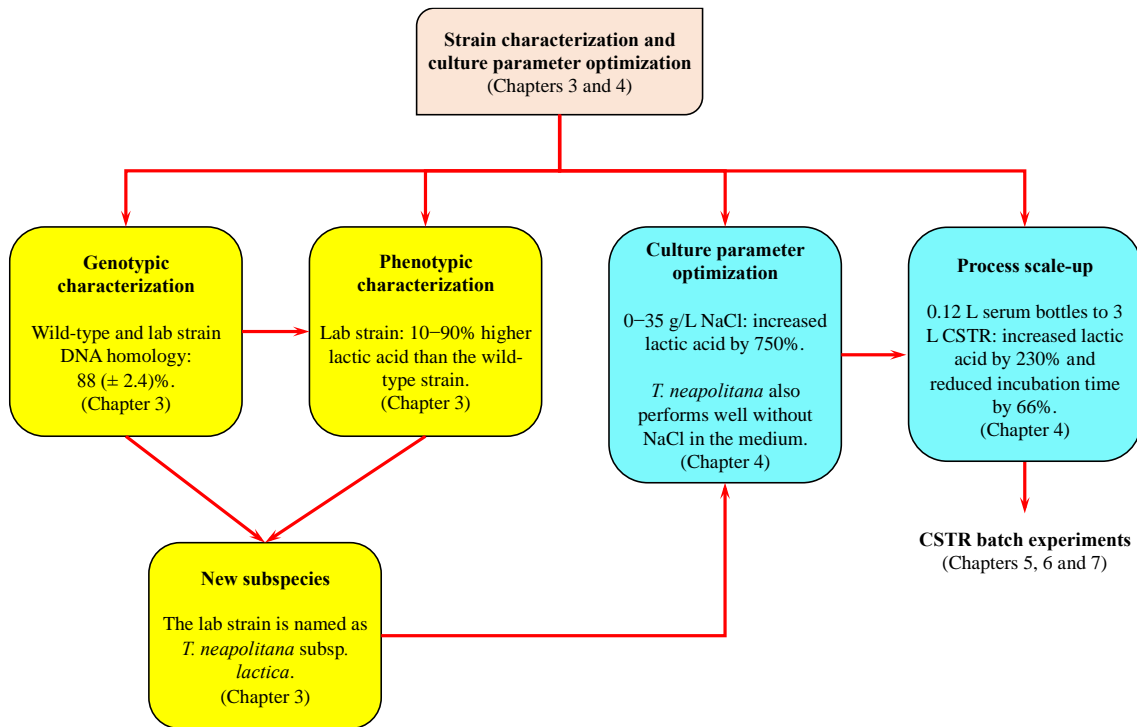


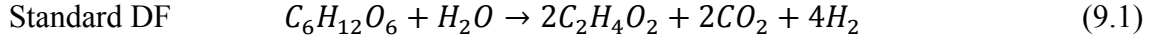
Fig. 9. 2 Overview of the results of this thesis concerning *T. neapolitana* strain characterization and culture parameters optimization under CLF conditions.

9.3 Process modeling for *T. neapolitana* fermentation

To transfer the fermentation technologies from the laboratory scale reactors to industrial or commercial scale reactors, it is important to know the biological growth kinetic parameters. The growth kinetic parameters are essential to model, design, optimize and control the fermentation reactors (Fig. 9.3). As the CLF-based fermentation for *T. neapolitana* is a new process, batch kinetic experiments were performed using glucose as carbon source under CO₂ enriched atmosphere (Pradhan et al., 2016b). The kinetic parameters were estimated by applying the non-linear least square method to Monod -type kinetic equations (Fang et al., 2013; Frascari et al., 2013). The experimentally estimated kinetic parameters, i.e. maximum specific uptake rate (k), semi-saturation constant (k_s), biomass yield coefficient (Y) and endogenous decay rate (k_d) were 0.84 1/h, 1.42 g/L, 0.12 and 0.004 1/h, respectively (Pradhan et al., 2016b).

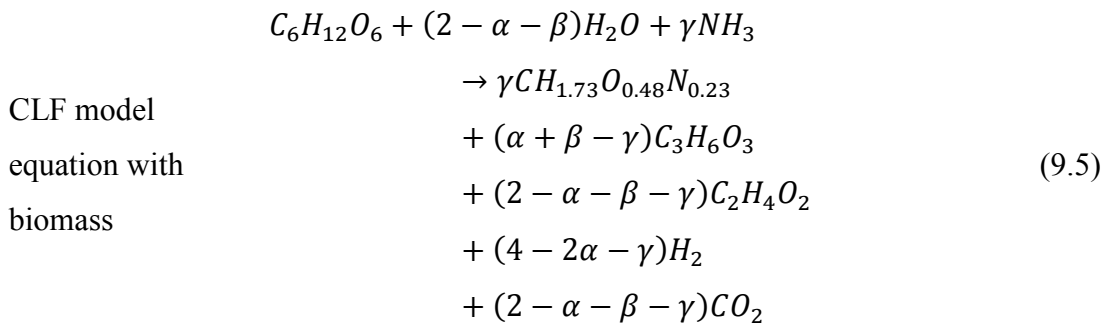
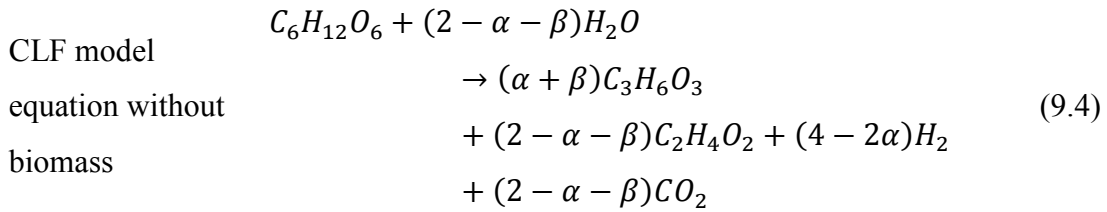
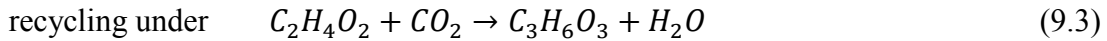
The anaerobic digestion model no.1 (ADM1) was used to develop a model for *T. neapolitana* fermentation in a CSTR system (Eqs. (9.1) and (9.2)) (Batstone et al., 2002; Pradhan et al., 2016b). The ADM1 principle was applied to write Monod-type kinetic

equations in order to represent the *T. neapolitana* fermentation metabolic pathway based on the reactants and products (Batstone et al., 2002; Castello et al., 2009; Pradhan et al., 2016a; Pradhan et al., 2016b). Further, the kinetic parameters were analysed for their sensitivity (Maly & Petzold, 1996; Molla & Padilla, 2002), calibrated (Esposito et al., 2011) and validated by a separate set of experimental data (Pradhan et al., 2016a; Pradhan et al., 2016b).



In the first stage of the model development, it was observed that the model overestimated acetic acid and underestimated lactic acid production since the model was developed based on the dark fermentation principle, where the acetic acid and H_2 production are inversely proportional to the lactic acid production (Pradhan et al., 2016b). In the second stage, the model kinetic parameters were recalibrated based on the CLF principle (Eqs. (9.3)–(9.5)) (i.e. simultaneous synthesis of H_2 and lactic acid), the calibrated kinetic parameters k , k_s , Y and k_d were 1.30 1/h, 1.42 g/L, 0.12 and 0.02 1/h, respectively (Pradhan et al., 2016a). Finally, the CLF model was validated with the pentose, hexose and polysaccharide sugar fermentation results under CLF conditions.

Acetic acid



Apart from this study, there are two other studies, which also estimated the growth kinetic parameters of *T. neapolitana* under N₂ sparging atmosphere (Frascari et al., 2013; Yu & Drapcho, 2011). Yu and Drapcho (2011) reported that μ_{max} , k_S and Y values for *T. neapolitana* grown on glucose were 0.94 1/h, 0.57 g/L, and 0.25, respectively. More recently, Frascari et al. (2013) reported that μ_{max} , k_S and k_d values were 0.024 (\pm 0.01) 1/h, 1.1 (\pm 0.3) g/L and 0.004 (\pm 0.01) 1/h, respectively. The kinetic parameters found under CO₂ sparging atmosphere are quite similar to those obtained under N₂ sparging atmosphere.

The previous studies show that 3.6 (\pm 0.3) mol H₂/mol of glucose and 2.9 (\pm 0.1) mol H₂/mol of arabinose, respectively, were produced from glucose and arabinose in comparison to 3.0 (\pm 0.2) and 2.5 (\pm 0.2) mol H₂/mol of glucose equivalent from potato and wheat starch, respectively, in the present study (Pradhan et al., 2016a). Whereas, the lactic acid production from glucose and arabinose were 0.6 (\pm 0.1) mol lactic acid/mol of glucose and 0.4 (\pm 0.1) mol lactic acid/mol of arabinose, respectively, in comparison to 0.8 (\pm 0.3) and 0.3 (\pm 0.1) mol lactic acid/mol of glucose equivalent, respectively, with potato and wheat starch in the present study (Pradhan et al., 2016a).

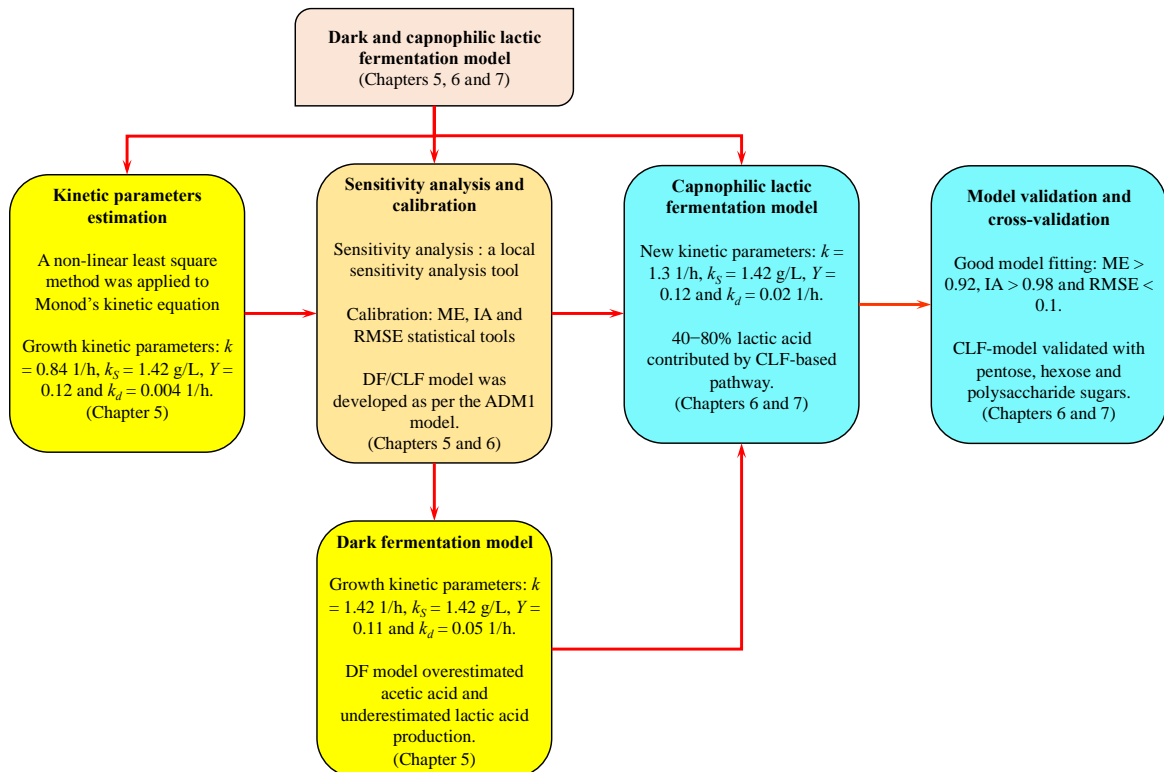


Fig. 9. 3 Overview of the results of this thesis concerning DF and CLF-based model for *T. neapolitana* fermentation.

9.4 Downstream processing of lactic acid

There is an increasing need for biodegradable polymers like polylactic acid (PLA), which are renewable, cheap and recyclable compared to synthetic polymers (Heydarifard et al., 2016). Globally > 90% of the lactic acid is produced by fermentative processes (Joglekar et al., 2006). The extraction, purification and continuous supply of lactic acid as raw material from the fermentation processes is a major challenge due to lack of efficient low-cost purification techniques (Bayazit et al., 2011). There are several downstream processing techniques used to recover lactic acid: crystallization, adsorption, distillation/hydrolysis, membrane extraction and electro-dialysis (Dethe et al., 2006; Wasewar, 2005). Adsorption is most suitable for the low concentration (< 10 g/L) lactic acid fermentation broths (Evangelista et al., 1994).

Several adsorbents such as Amberlite IRA-67 (Yousuf et al., 2016), IRA-92 (Tong et al., 2004), IRA-400 (Cao et al., 2002), IRA-425 (Antonio et al., 2000) and activated carbon (Gao et al., 2011; Yousuf et al., 2016) were studied for lactic or organic acids adsorption from the fermentation broth. In the present study, granular activated carbon (GAC) and polymeric resins (weakly- and strongly basic) were investigated for the lactic acid recovery from a model fermentation broth representing *T. neapolitana* fermentation (Fig. 9.4). The adsorption capacity for the GAC (38.2 mg lactic acid/g adsorbent) is the highest, followed by Amberlite IRA-400 (31.2 mg lactic acid/g adsorbent) and Reillex 425 (17.2 mg lactic acid/g adsorbent) with 10% (w/v) adsorbent dose and a feed lactic acid concentration of 4.5 g/L at 30 °C. Like in the previous studies, the experimental results also showed that both GAC and Reillex 425 were effective at pH 2.0 due to its weakly basic characteristics (Gao et al., 2011; Yousuf et al., 2016) and Amberlite IRA-400 was effective at pH 5.0 due to its strongly basic characteristics (Cao et al., 2002; Quintero et al., 2016).

The lactic acid adsorption capacity decreased by 13% and 50%, respectively, for GAC and Reillex 425, whereas the adsorption capacity remained unchanged for the Amberlite IRA-400 resin when the temperature was increased from 30 to 80 °C. The results found are in consistent with previous studies, where the lactic acid adsorption

capacity decreased by ~ 20% for the Amberlite IRA-67 resin, when the temperature increased from 20 to 50 °C with a feed lactic acid concentration of 42.5 g/L (Gao et al., 2010). Based on the thermodynamic analysis, the adsorption experiments with GAC and polymeric resins (Reillex 425 and Amberlite IRA-400) indicate a physisorption process for the lactic acid. In a related study, adsorption of acetic, propionic and butyric acid onto activated carbon and weak base anionic resin (Puralite A133S) showed a physisorption process (da Silva & Miranda, 2013).

Among the isotherms (the Langmuir, Freundlich and Temkin) investigated, the Langmuir isotherm was found to be more suitable ($R^2 > 0.96$) in explaining the adsorption mechanism compared to the Freundlich and Temkin isotherms, thus confirming a monolayer adsorption onto a homogeneous surfaces (Gao et al., 2010; Uslu, 2009). From the adsorption kinetic studies, the pseudo-second order kinetic model shows a strong correlation ($R^2 \sim 1$) between the experimental results and the model predictions for all adsorbents (Gao et al., 2010; Uslu, 2009). Among the adsorbents tested, the strongly basic resin (Amberlite IRA-400) in chloride form shows a favorable behavior for lactic acid extraction from the model fermentation broth, in terms of kinetics, adsorption capacity and thermodynamic feasibility under various operating conditions.

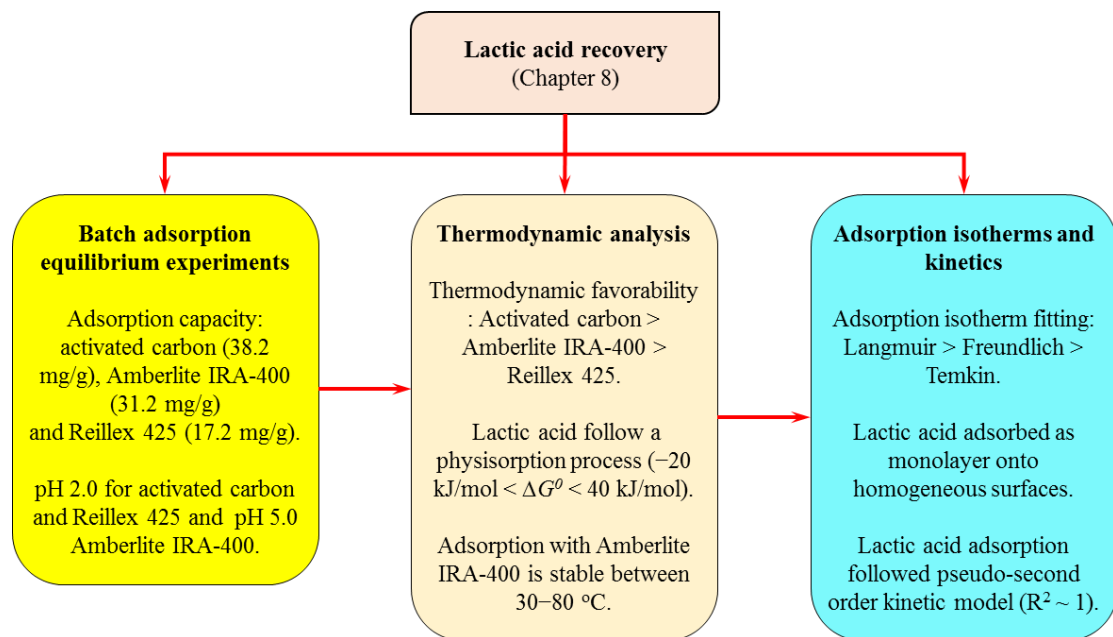


Fig. 9. 4 Overview of the results of this thesis concerning lactic acid recovery from a model *T. neapolitana* fermentation broth by adsorption.

9.5 Outlook and recommendations for future work

The research findings are optimistic and encouraging with respect to fermentation under CLF conditions, thus taking the technology a step closer to process scale-up. However, there are ample scopes for further development by improving the understanding of the CLF mechanisms. A comprehensive study is required to understand the bioenergetics of CLF mechanisms along formulation of suitable strategies to recycle 100% acetic acid to lactic acid. Further, applications of real organic waste from various sources along with bringing in suitable modifications to the bioreactor technology are required. Apart from the lactic acid recovery, other possible options must be explored to maximize energy recovery in order to make the process more attractive with respect to techno-economic feasibility.

9.5.1 Role of proteins or amino acids for the CLF-based fermentation

Nitrogen in the form of proteins/amino acids is essential for biomass growth. There are conflicting reports on the effect of protein lysates on the biomass growth and H₂ production for *T. neapolitana* fermentation (d'Ippolito et al., 2010; Maru et al., 2012). Maru et al. (2012) reported that reduced levels of yeast extract negatively affects biomass growth as well as H₂ production. Cappelletti et al. (2012) showed that part of the H₂ production is contributed from the metabolism of tryptone soy broth but the contribution from yeast extract is absent. On the other hand, d'Ippolito et al. (2010) and Eriksen et al. (2011) showed that metabolism of peptone, tryptone and yeast extract contributed in the range of 10–15% to the total H₂ production. For CLF-based fermentation, it is also believed that part of NADH required for lactic acid synthesis comes from protein metabolism. However, there is little evidence to prove the claim and further investigations are required. So, the role of proteins/amino acids in the culture medium must be established clearly especially for the hyperthermophilic fermentations.

9.5.2 Role of biofilms and EPS

Extracellular polymeric substances (EPS) are sticky and highly hydrated matrices, which results from microbial cells excretion under stress conditions, cell lysis as well as absorption of molecules from the culture medium. Like other bacteria, *T. neapolitana* also form EPS during fermentation. It will be interesting to characterize

EPS in order to understand the (i) cell aggregation process, (ii) biofilm formation, (iii) substrate diffusivity and (iv) extracellular enzymatic activity. So, a comprehensive study must be done on the *T. neapolitana* EPS in order to understand its properties with respect to biofilm formation.

9.5.3 Application of cellulosic feedstocks and algal biomass

Use of food sources (i.e. pure sugars) for the H₂ and lactic acid production is controversial, so large scale H₂ and lactic acid production initiatives must use non-food based feedstocks, such as agricultural waste, industrial waste, municipal food waste, trees, perennial grasses, forest residues and algae. Previously, some studies have reported to use cellulosic feedstocks as well as algal biomass with some exciting results with respect to H₂ production (Dipasquale et al., 2012; Nguyen et al., 2008a). However, the cellulosic feedstocks cannot be used directly for fermentation, hence a low-cost thermo-chemical or enzymatic pre-treatment technique must be devised prior to its fermentation.

9.5.4 Validation of CLF principle with other anaerobic bacteria

The innovation of the CLF process for simultaneous H₂ and lactic acid synthesis is a milestone in the field of biotechnology and biofuels development. The present research work has laid a foundation for the CLF process with respect to substrate utilization, culture parameter optimization, growth kinetic parameter estimation and model development for *T. neapolitana* fermentation. However, the validity of the CLF principle should be extended beyond *T. neapolitana* fermentation, to other anaerobic pure or mixed cultures at mesophilic, thermophilic and hyperthermophilic conditions.

9.5.5 Bioreactor selection and design

In this research work, experiments were either performed with 0.12 L serum bottles or in a 3 L CSTR system. To meet the engineering standards for bioprocess developments, the experiments in the serum bottles were successfully reproduced with comparable phenomena in the CSTR system with respect to biomass growth, substrate consumption and product formation. The efficiency in substrate utilization and H₂ production have improved due to reengineering of bioreactor technologies and process parameter optimization. Nonetheless, it is possible to further improve and optimize the CLF technology for simultaneous H₂ and lactic acid production by bringing in suitable

engineering modifications to the bioreactor design, based on the understanding the growth kinetics of *T. neapolitana* in batch reactors (Pradhan et al., 2016a; Pradhan et al., 2016b).

The measurements for pH, dissolved CO₂ and cellular energetics are key factors for the success of the CLF-based fermentations. In addition, hyperthermophilic fermentations can be made more lucrative only if the reactors can handle high organic loading rates (OLR) with a short hydraulic retention time (HRT). A high OLR and short HRT is unlikely for a CSTR system due to poor biomass density and retention capacity, which can be improved either by using immobilized biomass or by applying other bioreactor configurations such as packed bed reactor (PBR) or fluidized bed reactor (FBR).

9.5.6 The economics of biological H₂ production

Biological H₂ production is a promising prospect and probably the way forward for the future energy security. However, the benefits of biological H₂ production cannot be realized until and unless the fundamental issues with economics are solved. Today, the cost of production, storage and utilization of H₂ are extremely high compared to fossil fuels. So, a comprehensive value chain assessments with respect to biological H₂ technologies, comparison with other biofuel (*e.g.*, ethanol, methanol and methane) production technologies and mapping feedstocks availability are essential to understand the economics of H₂ production. The economic model for the biological H₂ production will help to implement and commercialize the technology.

9.5.7 Lactic acid recovery and purification

Lactic acid is an industrial chemical of high commercial value. The traditional methods for lactic acid production, recovery and purification are changing to cope up with the market requirements. New heterolactic fermentation methods (*i.e.* DF and CLF) along with lactic acid recovery by anionic resins will reduce the cost of lactic acid purification. Further studies are required to focus on: (i) selection of more anionic resins (*e.g.*, Amberlite IRA-67, 96 and 900) with an aim to extract ~ 100% lactic acid from the model fermentation broth, (ii) the competitive uptake of other components in the real fermentation broth, (iii) maintaining the desorption efficiency $\geq 99.5\%$ and (iv) optimizing process parameters for fixed-bed adsorption columns.

References

- Antonio, G.R., Vaccari, G., Dosi, E., Trilli, A., Rossi, M., Matteuzzi, D. 2000. Enhanced production of L-(+)-lactic acid in chemostat by *Lactobacillus casei* DSM 20011 using ion-exchange resins and cross-flow filtration in a fully automated pilot plant controlled via NIR. *Biotechnology and Bioengineering*, **67**, 147-156.
- Batstone, D.J., Keller, J., Angelidaki, I., Kalyuzhnyi, S.V., Pavlostathis, S.G., Rozzi, A. 2002. Anaerobic digestion model No. 1. *IWA Scientific and Technical Report* **13**.
- Bayazit, S.S., Inci, I., Uslu, H. 2011. Adsorption of lactic acid from model fermentation broth onto activated carbon and amberlite IRA-67. *Journal of Chemical and Engineering Data*, **56**, 1751-1754.
- Cao, X., Yun, H.S., Koo, Y.M. 2002. Recovery of l-(+)-lactic acid by anion exchange resin Amberlite IRA-400. *Biochemical Engineering Journal*, **11**, 189-196.
- Cappelletti, M., Bucchi, G., Mendes, J.D.S., Alberini, A., Fedi, S., Bertin, L., Frascari, D. 2012. Biohydrogen production from glucose, molasses and cheese whey by suspended and attached cells of four hyperthermophilic *Thermotoga* strains. *Journal of Chemical Technology and Biotechnology*, **87**, 1291-1301.
- Castello, E., Garcia y Santos, C., Iglesias, T., Paolino, G., Wenzel, J., Borzacconi, L., Etchebere, C. 2009. Feasibility of biohydrogen production from cheese whey using a UASB reactor: Links between microbial community and reactor performance. *International Journal of Hydrogen Energy*, **34**, 5674-5682.
- Clemente, I.M., Matthew, R.J., Chung-Jung, C., Shannon, B.C., Sarah, G.G., Sabrina, T., Jason, D.N., Robert, M.K. 2007. Responses of wild-type and resistant strains of the hyperthermophilic bacterium *Thermotoga maritima* to chloramphenicol challenge. *Applied and Environment Microbiology*, **73**, 5058-5065.
- d'Ippolito, G., Dipasquale, L., Vella, F.M., Romano, I., Gambacorta, A., Cutignano, A., Fontana, A. 2010. Hydrogen metabolism in the extreme thermophile *Thermotoga neapolitana*. *International Journal of Hydrogen Energy*, **35**, 2290-2295.
- da Silva, A.H., Miranda, A.E. 2013. Adsorption/desorption of organic acids onto different adsorbents for their recovery from fermentation broths. *Journal of Chemical & Engineering Data*, **58**, 1454-1463.
- De Vrije, T., Bakker, R.R., Budde, M.A.W., Lai, M.H., Mars, A.E., Claassen, P.A.M. 2009. Efficient hydrogen production from the lignocellulosic energy crop miscanthus by the extreme thermophilic bacteria *Caldicellulosiruptor saccharolyticus* and *Thermotoga neapolitana*. *Biotechnol. Biofuels*, **2**, 12.
- Derrick, L.L., Jaspreet, S.N., Sanjeev, K.C., Andrew, J.L., Gina, L.L., Michael, W.W.A., Robert, M.K. 2015. A mutant ('lab strain') of the hyperthermophilic archaeon *Pyrococcus furiosus*, lacking agella, has unusual growth physiology. *Extremophiles*, **19**, 269-281.

- Dethe, M.J., Marathe, K.V., Gaikar, V.G. 2006. Adsorption of lactic acid on weak base polymeric resins. *Separation Science and Technology*, **41**, 2947-2971.
- Dipasquale, L., d'Ippolito, G., Fontana, A. 2014. Capnophilic lactic fermentation and hydrogen synthesis by *Thermotoga neapolitana*: An unexpected deviation from the dark fermentation model. *International Journal of Hydrogen Energy*, **39**, 4857-4862.
- Dipasquale, L., d'Ippolito, G., Gallo, C., Vella, F.M., Gambacorta, A., Picariello, G., Fontana, A. 2012. Hydrogen production by the thermophilic eubacterium *Thermotoga neapolitana* from storage polysaccharides of the carbon dioxide fixing diatom *Thalassiosira weissflogii*. *International Journal of Hydrogen Energy*, **37**, 12250-12257.
- Eriksen, N.T., Riis, M.L., Holm, N.K., Iversen, N. 2011. Hydrogen synthesis from pentoses and biomass in *Thermotoga* spp. *Biotechnology Letters*, **33**, 293-300.
- Esposito, G., Frunzo, L., Panico, A., Pirozzi, F. 2011. Model calibration and validation for OFMSW and sewage sludge co-digestion reactors. *Waste Management*, **31**, 2527-2535.
- Evangelista, R.L., Mangold, A.J., Nikolov, Z.L. 1994. Recovery of lactic acid by sorption: resin evaluation. *Applied Biochemistry and Biotechnology*, **45-46**, 131-144.
- Fang, F., Mu, Y., Sheng, G.P., Yub, H.Q., Li, Y.Y., Kubota, K., Harada, H. 2013. Kinetic analysis on gaseous and aqueous product formation by mixed anaerobic hydrogen-producing cultures. *International Journal of Hydrogen Energy*, **38**, 15590-15597.
- Frasconi, D., Cappelletti, M., Mendes, J.D.S., Alberini, A., Scimonelli, F., Manfreda, C., Longanesi, L., Zannoni, D., Pinelli, D., Fedi, S. 2013. A kinetic study of biohydrogen production from glucose, molasses and cheese whey by suspended and attached cells of *Thermotoga neapolitana*. *Bioresource Technology*, **147**, 553-61.
- Gao, M.T., Shimamura, T., Ishida, N., Takahashi, H. 2011. pH-uncontrolled lactic acid fermentation with activated carbon as an adsorbent. *Enzyme and Microbial Technology*, **48**, 526-530.
- Gao, Q., Liu, F., Zhang, T., Zhang, J., Jia, S., Yu, C., Jiang, K., Gao, N. 2010. The role of lactic acid adsorption by ion exchange chromatography. *PLoS one*, **5**, e13948.
- Heydarifard, S., Nazhad, M.M., Xiao, H., Shipin, O., Olson, J. 2016. Water-resistant cellulosic filter for aerosol entrapment and water purification, Part I: production of water-resistant cellulosic filter. *Environmental Technology* **37**, 1716-1722.
- Joglekar, H.G., Rahman, I., Babu, S., Kulkarni, B.D., Joshi, A. 2006. Comparative assessment of downstream processing options for lactic acid. *Separation and Purification Technology*, **52**, 1-17.
- Maly, T., Petzold, L.R. 1996. Numerical methods and software for sensitivity analysis of differential-algebraic systems. *Applied Numerical Mathematics*, **20**, 57-79.

- Maru, B.T., Bielen, A.A.M., Kengen, S.W.M., Constanti, M., Medina, F. 2012. Biohydrogen production from glycerol using *Thermotoga* spp. *Energy Procedia*, **29**, 300-307.
- Molla, V.M.G., Padilla, R.G. 2002. Description of the MATLAB functions SENS_SYS and SENS_IND. *Universidad Politécnica de Valencia, Spain*.
- Munro, S.A., Zinder, S.H., Walker, L.P. 2009. The fermentation stoichiometry of *Thermotoga neapolitana* and influence of temperature, oxygen, and pH on hydrogen production. *Biotechnology Progress*, **25**, 1035-1042.
- Ngo, T.A., Kim, M.S., Sim, S.J. 2011. High-yield biohydrogen production from biodiesel manufacturing waste by *Thermotoga neapolitana*. *International Journal of Hydrogen Energy*, **36**, 5836-42.
- Nguyen, T.A.D., Han, S.J., Kim, J.P., Kim, M.S., Oh, Y.K., Sim, S.J. 2008a. Hydrogen production by the hyperthermophilic eubacterium, *Thermotoga neapolitana*, using cellulose pretreated by ionic liquid. *International Journal of Hydrogen Energy*, **33**, 5161-68.
- Nguyen, T.A.D., Han, S.J., Kim, J.P., Kim, M.S., Sim, S.J. 2010. Hydrogen production of the hyperthermophilic eubacterium, *Thermotoga neapolitana* under nitrogen sparging condition. *Bioresource Technology*, **101**, 38-41.
- Nguyen, T.A.D., Kim, J.P., Kim, M.S., Oh, Y.K., Sim, S.J. 2008b. Optimization of hydrogen production by hyperthermophilic eubacteria, *Thermotoga maritima* and *Thermotoga neapolitana* in batch fermentation. *International Journal of Hydrogen Energy*, **33**, 1483-88.
- Pierra, M., Trably, E., Godon, J.J., Bernet, N. 2014. Fermentative hydrogen production under moderate halophilic conditions. *International Journal of Hydrogen Energy*, **39**(14), 7508-7517.
- Pradhan, N., Dipasquale, L., d'Ippolito, G., Fontana, A., Panico, A., Pirozzi, F., Lens, P.N.L., Esposito, G. 2016a. Model development and experimental validation of capnophilic lactic fermentation and hydrogen synthesis by *Thermotoga neapolitana*. *Water Research*, **99**, 225-234.
- Pradhan, N., Dipasquale, L., d'Ippolito, G., Fontana, A., Panico, A., Lens, P.N.L., Pirozzi, F., Esposito, G. 2016b. Kinetic modeling of fermentative hydrogen production by *Thermotoga neapolitana*. *International Journal of Hydrogen Energy*, **41**, 4931-4940.
- Quintero, J., Acosta, A., Mejia, C., Rios, R., Torres, M. 2016. Purification of lactic acid obtained from a fermentative process of cassava syrup using ion exchange resins. *Rev Fac Ing Univ Antioquia N*, **65**, 139-151.
- Schumann, P., Maier, T. 2014. MALDI-TOF mass spectrometry applied to classification and identification of bacteria. *Methods Microbiol*, **41**, 275-306.
- Soro-Yao, A.A., Schumann, P., Thonart, P., Dje, K.M., Pukall, R. 2014. The use of MALDI-TOF mass spectrometry, ribotyping and phenotypic tests to identify lactic acid bacteria from fermented cereal foods in Abidjan (Côte d'Ivoire). *The Open Microbiology Journal*, **8**, 78-86.

- Tong, W.Y., Fu, X.Y., Lee, S.M., Yu, J., Liu, J.W., Wei, D.W., Koo, Y.M. 2004. Purification of l(+)-lactic acid from fermentation broth with paper sludge as a cellulosic feedstock using weak anion exchanger Amberlite IRA-92. *Biochemical Engineering Journal*, **18**, 89-96.
- Uslu, H. 2009. Adsorption equilibria of formic acid by weakly basic adsorbent Amberlite IRA-67: Equilibrium, kinetics, thermodynamic. *Chemical Engineering Journal*, **155**, 320-325.
- Wasewar, K.L. 2005. Separation of lactic acid: Recent advances. *Chemical and Biochemical Engineering Quarterly*, **19**, 159-172.
- Yousuf, A., Bonk, F., Oyanedel, J.R.B., Schmidt, J.E. 2016. Recovery of carboxylic acids produced during dark fermentation of food waste by adsorption on Amberlite IRA-67 and activated carbon. *Bioresource Technology*, **217**, 137-140.
- Yu, X., Drapcho, C. 2011. Hydrogen production by the hyperthermophilic bacterium *Thermotoga neapolitana* using agricultural-based carbon and nitrogen sources. *Biological Engineering Transactions*, **4**, 101-112.

Curriculum Vitae

Nirakar PRADHAN

Soro | Balasore | Odisha | India | 756045

Cell: +91-828-092-6398 | Email- nirakar.pradhan@gmail.com

EDUCATION DETAILS

Ph.D. in Environmental Technology

2016 **University of Paris-Est – France, University of Cassino and Southern Lazio – Italy and UNESCO-IHE, Institute for Water Education – Netherlands.**

Dissertation: “Hydrogen and lactic acid synthesis through capnophilic lactic fermentation by *Thermotoga neapolitana*”.

Promoter: Prof. Giovanni Esposito

M.Eng. in Environmental Engineering and Management

2012 **Asian Institute of Technology – Thailand, CGPA: 3.98/4.**

Thesis: “Cumulative effects assessment of impacts on a lake catchment area case study of Inle lake, Myanmar”.

Promoter: Prof. Oleg V. Shipin

B.Tech. in Agricultural Engineering

2007 **Orissa University of Agriculture and Technology – India, CGPA: 8.26/10.**

SKILLS

- Excellent computer skills
- Statistical analysis and interpretation
- Monitoring and supervision
- Design of Experiments (DoE)
- Interdisciplinary research
- Developing scientific research proposals
- Environmental planning and implementation

WORK HISTORY

07/2012 to 09/2013 **Environmental Engineer at Utility Business Alliance Co. Ltd. – Thailand**
• Developed conceptual designs for industrial and municipal wastewater treatment plants.

- Planned laboratory-based experiments to confirm feasibility of new processes and technologies for wastewater and sludge treatments.
- Assessed vendor products and maintained positive vendor relations along with attended and organized trade shows, conferences and seminars.

Research Associate at Asian Institute of Technology – Thailand

05/2012 to 06/2012 • Conducted studies on the applicability of integrated water resources management (IWRM) for select Afghanistan river basins.

- Environmental impact assessment, cumulative effects assessment and environmental modeling for Inle lake wetland.
- Prepared technical reports, manuscripts, proposals and technical manuals.

Program Officer at Centre for People's Forestry – India

06/2009 to 07/2010 • Led a multidisciplinary program that served the poor people in the rural areas of Odisha, Telengana, Andhra Pradesh and Jharkhand states of India.

- Spearheaded and led several teams and developmental projects, including watershed development, water resource conservation, rural sanitation and public health, bioenergy development, rain water harvesting, organic farming and non-pesticide management.
- Monitored team performance, including developing performance improvement plans and recommending achievement awards.

Project Officer at Foundation for Ecological Security – India

09/2007 to 05/2009 • Implemented rural livelihood projects with a special focus on bioenergy, forest conservation, sustainable agriculture and watershed development across 8 states of India.

- Designed projects to promote ecological protection, including water reclamation facilities, soil conservation measures and operations converting waste to energy in semi-arid regions of India.
- Research and analysis along with preparation of environmental reports for wider publications.

RESEARCH AND TEACHING INTERESTS

- Waste to energy
- Industrial biotechnology
- Natural resource management
- Environmental governance
- Environmental policies
- Energy economics
- Water and wastewater treatment
- Solid waste management
- Life cycle assessment
- Environmental impact assessment
- Climate change and adaptation
- Community development

TECHNICAL SKILLS

- Computer applications: Proficient in use of the Internet and window based computer applications (MS word, MS excel, MS PowerPoint and Lotus Notes).

FELLOWSHIPS/AWARDS

- Erasmus mundus joint doctorate fellowship to conduct doctoral research, European Union, 2013.
- Most outstanding academic performance, The Robert B. Banks Prize, AIT, Thailand, 2012.
- K-water global internship program, South Korea, 2011.
- ADB-JSP scholarship to pursue Masters at AIT, Thailand, 2010.
- Merit scholarship to pursue bachelor degree at OUAT, India, 2003.

REFEREED JOURNAL ARTICLES

- **Pradhan, N.,** Dipasquale, L., d'Ippolito., G., Fontana, A., Panico, A., Lens, P.N.L., Pirozzi, F., Esposito, G. 2016. Model development and experimental validation of capnophilic lactic fermentation and hydrogen synthesis by *Thermotoga neapolitana*. *Water Research*, 99, 225-234.
- **Pradhan, N.,** Dipasquale, L., d'Ippolito., G., Fontana, A., Panico, A., Lens, P.N.L., Pirozzi, F., Esposito, G. 2016. Kinetic modeling of fermentative hydrogen production by *Thermotoga neapolitana*. *International Journal of Hydrogen Energy*, 41, 4931-4940.
- **Pradhan, N.,** Dipasquale, L., d'Ippolito., G., Panico, A., Lens, P.N.L., Esposito, G., Fontana, A. 2015. Hydrogen production by the thermophilic bacterium *Thermotoga neapolitana*. *International Journal of Molecular*

Sciences, 16, 12578-12600.

- **Pradhan, N.**, Habib, H., Venkatappa, V., Ebberts, T., Duboz, R., Shipin, O. 2015. Framework tool for a rapid cumulative effects assessment: case of a prominent wetland in Myanmar. *Environmental Monitoring and Assessment*, 187, 341-359.
- **Pradhan, N.**, Dipasquale, L., d'Ippolito., G., Panico, A., Lens, P.N.L., Esposito, G., Fontana, A. 2016. Hydrogen and lactic acid synthesis by the wild-type and a laboratory strain of the hyperthermophilic bacterium *Thermotoga neapolitana* DSMZ 4359 under capnophilic lactic fermentation condition. *International Journal of Hydrogen Energy*. (Under review).
- **Pradhan, N.**, Eldon, R.R., Panico, A., Dipasquale, L., d'Ippolito., G., Lens, P.N.L., Fontana, A., Esposito, G. 2016. Adsorption behaviour of lactic acid on granular activated carbon and anionic resins: Thermodynamics, isotherms and kinetic studies. *Energies*. (Under review).
- **Pradhan, N.**, Dipasquale, L., d'Ippolito., G., Panico, A., Lens, P.N.L., Esposito, G., Fontana, A. 2017. Simultaneous synthesis of lactic acid and hydrogen from sugars via capnophilic lactic fermentation pathway: a new direction for biotechnology. *Applied Energy*. (To be submitted).
- **Pradhan, N.**, Dipasquale, L., d'Ippolito., G., Panico, A., Lens, P.N.L., Fontana, A., Esposito, G. 2017. Kinetic modeling and starch fermentation for hydrogen and lactic acid production via capnophilic lactic fermentation pathway. *Biotechnology and Bioengineering*. (To be submitted).
- **Pradhan, N.**, Eldon, R.R., Lens, P.N.L. 2017. Microbial fermentation: A prospective for energy security. *Trends in Biotechnology*. (To be submitted).
- **Pradhan, N.**, Angelo, P., Eldon, R.R., Angela, S., d'Ippolito., G., Lens, P.N.L., Fontana, A., Pirozzi, F. 2017. Lactic acid recovery by anionic resins in a fixed bed reactor. *Chemical Engineering Journal*. (Under preparation).

CONFERENCE PROCEEDINGS

- **Pradhan, N.**, Dipasquale, L., d'Ippolito., G., Fontana, A., Panico, A., Lens, P.N.L., Pirozzi, F., Esposito, G. 2015. Fermentative hydrogen production by the hyperthermophilic bacterium *Thermotoga neapolitana*. *European Fuel Cell Technology and Applications Conference*.

- **Pradhan, N.**, et al., 2011. Surface water quality and risk analysis in a Peri-urban area, Thailand, *International Symposium on Southeast Asian Water Environment*, Vol.9, (part 1).

BOOK CHAPTERS

- Deb, P., **Pradhan, N.** 2016. Reservoir inflows in a tropical humid climate: Thailand. In Panigrahi, B. and Goyal, M. R. (Eds.), *Soil and Water Engineering: Principles and Applications of Modeling*. Apple Academic Press.
- Loc, H.H., Irvine, K.N., **Pradhan, N.** 2016. Social-based exploratory assessment of sustainable urban drainage systems (SUDS). In Panigrahi, B. and Goyal, M. R. (Eds.), *Modeling Methods and Practices in Soil and Water Engineering*. Apple Academic Press.
- Ding, Z., **Pradhan, N.**, Verstraete, W. 2016. Enhanced Anaerobic Digestion by Inoculation with Compost. In Goyal, M. R. (Eds.), *Emerging Technologies in Agricultural Engineering*. Apple Academic Press.